Newcastle University

Institute for Ageing

Institute for Cell & Molecular Biosciences

Does a senescence-like phenotype in neurons contribute to brain ageing and neurodegeneration?

Edward Peter Fielder

A thesis submitted for the degree of Doctor of Philosophy

Supervisors:

Dr Diana Jurk

Dr João Passos

Prof. Thomas von Zglinicki

May 2018

Table of Contents

List of figures

List of tables

List of abbreviations

53BP1	p53 Binding Protein 1
AD	Alzheimer's Disease
ATM	Ataxia-telangiectasia, mutated
BBB	Blood brain barrier
CA	*Cornu Ammonis*
CCL	Chemokine (C-C motif) ligand
CDK	Checkpoint Kinase
COX-2	Cyclooxygenase-2
DAPI	4',6-Diamidino-2-phenylindole
DCX	Doublecortin
DDR	DNA Damage Response
DG	Dentate Gyrus
DNA	Deoxyribonucleic acid
DNA-PK	DNA-dependent Protein Kinase
DQ	Dasatinib and Quercetin
DSB	Double strand break
EC	Entorhinal Cortex
FISH	Fluorescent in situ hybridisation
GABA	γ-Aminobutyric acid
GADD45	Growth Arrest and DNA Damage
H2A.X	Histone variant H2A.X
γH2A.X	Phosphorylated histone variant H2A.X
HDAC	Histone Deacetylase
HMGB1	High Mobility Group Box 1 protein
Iba1	Ionized calcium-binding adapter molecule 1
IKK	IκB kinase
IL	Interleukin
LPS	Lipopolysaccharide

LPF	Local Field Potential
MCI	Mild cognitive impairment
MCP	Monocyte chemoattractant protein
M-CSF	Macrophage colony-stimulating factor
MDC1	Mediator of DNA Damage Checkpoint Protein 1
NADPH	Nicotinamide adenine dinucleotide phosphate
NEMO	NF-κB Essential Modulator
NeuN	Neuronal nuclei antigen
NF-κB	Nuclear factor kappa-light-chain-enhancer of activated B cells
NHEJ	Non Homologous End Joining
NOR	Novel Object Recognition
NSAID	Early Non-Steroidal Anti-Inflammatory Drug
p16	Cyclin-dependent kinase inhibitor 2A, alternatively p16INK4a
p21	Cyclin-dependent kinase inhibitor 1A, alternatively p21CIP1/WAF1
p38MAPK	p38 mitogen-activated protein kinases
p53	Tumour protein p53
PCNA	Proliferating Cell Nuclear Antigen
PI3KK	Phosphatidylinositol-3-OH-Kinase-like Kinases
pRb	Phosphorylated Retinoblastoma
RANTES	Regulated on activation, normal T cell expressed and secreted
RNA	Ribonucleic acid
RNAISH	Ribonucleic acid in situ hybridisation
ROS	Reactive Oxygen Species
SASP	Senescence associate secretory phenotype
Sen-β-Gal	Senescence associated Beta Galactosidase
TAF	Telomere associated foci
TNF	Tumour Necrosis Factor
TRF-2	TTAGGG repeat binding factor 2

Acknowledgements

Tremendous thanks to all my friends for making my time in Newcastle and CAV such a great experience. I would like to thank *The International Cookers*, past and present. To James, Nik, Luis, Julia, Anne, Amy, Ellie, Josh and Heinz for their support, and the countless days and nights that I'll either never forget, or never remember; to Xanthe for failing to teach me the difference between Zoet and Zout; to G-bear for not mocking my cycling abilities *too* much.

I would like to thank my friends and lab members; to Melanie for her friendship, support and proof-reading, Antho for making sure I actually ran that marathon; Mikołaj, for his invaluable knowledge and assistance, Olena for teaching me to tango, Clara for all her help and patience in those first years, Glyn for everything about optics and brewing, Satomi for teaching me the ways of the mitochondria, Hannia for teaching me about quinoa, and to Jodie, Stella, James, Graham and more for the good times. And thanks to everyone in CAV, to Abbas and Tengfei for late nights in the office, Dan and his never-ending knowledge of neuroscience, Brigit, Sandra, Neil, Gabi, and many more. I would like to thank Clare and Fiona for their fantastic help and advice, and the entire 'Darkside' crew (especially Felix and his fantastic pub-quizzes) for making my time in IoN an absolute pleasure.

I would also like to thank my supervisors; to Diana and Joao for their advice, assistance and teaching me the virtues of olive oil, and Thomas for his assistance and advice. To my progression team, I'd like to thank Viktor for his ability to drink us all under the table, and Johannes for first suggesting I travel this long road.

To my parents, thank you for your unfaltering support and assistance. And providing many meals long after I nominally moved out. To my brother and closest friend, I would like to officially state that my room *is* better than your room.

To *The Old Heatonians*; Danny, Helen, Rosh, Louise, Mai, Joey, Scraffers, Erin, Jane, Kirkby and all the rest - thank you for the decades of nonsense.

Alas! The fleeting years slip by

Abstract

Senescent cells accumulate in the body with age, and drive organismal ageing and tissue dysfunction. Senescence is not a simple growth arrest, but is accompanied by a host of phenotypic changes, including the generation of pro-inflammatory molecules, and is maintained by a network of auto- and paracrine reinforcement. Senescence is now also understood to occur in post-mitotic cells, including neurons – contrary to the former definition of senescence occurring exclusively in proliferating cells. This is called the senescent-like phenotype. While senescent cells can be seen to increase with age, little is known about their relation to cognitive function with age or pathological states such neuro-inflammation.

Using a model of chronic inflammation, the *nfkb1*$^{-/-}$ mouse, I investigated neuro-inflammation, cognitive function and the frequency of senescent-like neurons with age and treatment with the COX-2 inhibitor ibuprofen. Increasing microglial proliferation and neuro-inflammation could be observed, together with deficits in spatial memory. This was accompanied by an increase in the numbers of senescent-like neurons. Increased accumulation of persistent DNA damage in pyramidal neurons, and a deficit in the generation and propagation of Carbachol induced gamma frequency oscillations, could be seen in the CA3. COX-2 appears to have a role in mediating these effects, as treatment with ibuprofen was effective in ameliorating levels of neuro-inflammation, cognitive dysfunction and senescent-like neurons.

Ageing INK-ATTAC mice were given pharmacogenetic and pharmacological treatments to investigate if these could clear senescent-like neurons. Pharmacological clearance (Dasatinib and Quercetin) was effective in reducing the numbers of senescent like neurons, and these mice showed an improvement in cognitive function, while pharmacogenetic treatment had a lesser effect.

The data presented in this thesis implicate the senescence and the senescent-like phenotype in neuro-inflammation and ageing, and in driving the accompanying declines in cognitive function.

1.0: Introduction

1.1 – Brain ageing and cognitive deficits

There is an unprecedented demographic shift from young to old occurring in many countries around the world. As the population ages, there are increased difficulties in dealing with age associated conditions; namely frailty and chronic diseases. These conditions increase the burden on health-services and contribute towards economic withdrawal of not only those affected, but the family members who must care for them. These are serious human and economic threats that must be effectively countered to ensure the progress of civilisation. As such, understanding the biological mechanisms underlying the ageing process, and seeking effective therapies, is of paramount importance.

Cognitive deficits are a common feature in ageing, but are not universal and present with differing symptoms, rates of onsets and pathologies [1]. Even 'mild' changes can be distressing and damage self-image and self-reliance. The onset of neurodegenerative conditions, such as Alzheimer's Disease (AD), is especially devastating. These changes not only rob people of their memories and identity, but are one of the leading causes of death. In the UK, Dementia and AD are the leading cause of death in women over 80, and second in men over 80. As the majority can now expect to live to this age, cognitive impairment and dementias represent a major source of disability in the population. It is important to understand what processes contribute towards this during ageing, and if existing knowledge and therapies in the Biology of Ageing field can be applied.

1.1.1 – Changes in the brain with age

Despite significant incidence of neurodegenerative conditions, the majority will not suffer from dementia; however, they will experience some age-associated cognitive decline – primarily presenting as defects in memory, navigation, and executive capacity [2, 3]. Ageing does not show a uniform decrease across all types of memory; generally, while the speed of memory recall without a verbal or object cue is delayed, recognition and memory following a cue remains stable [2]. The ability to recall the source of learned information and remembering to perform a future action declines, but the actual memory of how to do a task and chronological order remain stable [2]. Cognitive speed and memory, reasoning and spatial visualisation capacity decline, while other factors such as vocabulary improve with age, peaking at age 60 [4]. As a rule, while sum knowledge increases, efficiency decreases.

Given that declines in cognitive function occur in normal ageing, and the frequency of neurodegenerative diseases increases with age, one might assume that neurodegeneration presents a form of accelerated ageing. However, this is not supported by the evidence, as clinical diagnosis of cognitive impairment and dementia do not show a linear relationship with the presence of the associated pathology [5, 6]. Neuropathological assessment of cognitively unimpaired aged individuals from 50 to 102 has shown a great deal of variability in the protein pathologies of 'normally' ageing brains [5]. These brains frequently contain protein aggregates associated with neurodegenerative conditions, such as amyloid plaques, hyper-phosphorylated tau and alpha-synuclein aggregates, often in combination, but with a great degree of variability between lesions and areas affected [5]. A study of individuals age 90 and above, with and without dementia, reported a strong association between multiple protein pathologies and dementia; however, in non-demented individuals they also found at least one form of pathology in 49% of brains and mixed pathologies in 14% of individuals, suggesting a complex interplay of mechanisms in causing clinically diagnosable dementia [6].

There are changes in brain volume with age. In humans, total grey matter declines from early life, initially in the pre-frontal cortex, and there are age-related reductions in the hippocampus [7, 8]. Cerebrospinal fluid volume, found primarily in the ventricles, increases linearly with age; while white matter shows an inverse U-shaped progression, peaking at age 40-50 before declining again [8]. Similar patterns are observed in mice, with a slight reduction in total brain volume and the volume of the hippocampus at 12 months, but with increases in ventricular size [9]. However, whether volume is an important measure is difficult to establish. Meta-analysis of studies has suggested that a larger volume of brain structures such as the hippocampus is often correlated with improved performance in cognitive parameters in 'healthy' aged individuals [10]. Most commonly these showed a correlation in the hippocampal formation and global cognition and memory, and with executive function in the frontal formation [10].

Declines in brain volume and cognitive impairment in neurodegenerative diseases are associated with neuronal cell-death and apoptosis [11-13], but the rates of cell death in normally aged brains is less clear [14-16]. Certainly, there are some reductions in brain mass with aged cognitively healthy humans; with a ~5-15% reduction between those aged 50-59 years old and those over 90 [5]. In mice, while there are declines in the mass of sub-structures, including the hippocampus [17], the actual gross brain weight appears to remain fairly constant throughout ageing [15]. Yet, examination of neuron numbers in healthy aged humans aged 56 to 103 has shown no significant loss in actual number - despite the presence of age-related atrophy [14]. The same can be seen in mice, with a lack of significant cell death with age [15, 16].

Instead, the loss of volume in 'healthy' ageing may be related to changes in neuronal morphology [3], rather than gross loss of neurons [14, 18, 19]. With ageing, some loss of complexity in axonal and dendritic processes of neurons appears to occur [19-21]. Early reports suggested a drastic deterioration of dendritic branch length and complexity in areas such as the hippocampus [22]. Yet these included demented individuals along with the cognitively healthy and later analysis has reported that these changes are not as severe [19, 23]. No great loss of dendritic length appears to occur in aged neurons across the brain [24, 25] Instead the changes appear more subtle, with some declines in spine density and size in normally aged mice, but not in all regions [26].

Many neurochemical changes have been observed within synapses, with shifts in receptor densities and types [27, 28] and a decline in pre-synapse receptor density in human brains with age [29]. Synapses are highly dynamic structures that undergo complex regulation cascades and can be formed or pruned, their activity potentiated or reduced through stimulus. Accelerated ageing models show reductions in synapse numbers and apical dendrites [30], however, in normally aged wild-type mice this is less clear. In fact, studies have reported no age-related loss in synapse number in normally aged mice [31]. However, when cognitive function was assessed, there was a significant association with performance in memory tasks, such as the Morris water maze, and synapse number [31]. Levels of neuro-transmitter in these synapses do decline with age [32], however, no relation was found between these levels and performance in the tasks. Instead, an association was found between performance in memory tasks and increased levels of synaptic structural stability proteins and decreased activity-dependent signalling factors [32]. These changes suggest that a decreased ability to alter synapses in response to stimuli (synaptic plasticity), rather than raw synapse number [31], differentiates cognitive decline in ageing.

Changes in plasticity can be seen on both a network and individual cell level in the brain with ageing [23]. Cognitively impaired aged animals show altered synaptic plasticity, especially in areas such as the hippocampus [33-35]. In electrophysical parameters, while basal parameters are similar, young rodents maintain increased synaptic strength following high-frequency stimulation for longer than aged animals, which show an almost immediate decline [36]. This matches their performance in spatial tasks such as the Barnes Maze, with comparable performance to younger controls in spatial parameters during early training, and no divergence until after repeated trials [36]. Increased after-hyperpolarisation has been observed with ageing that might increase the threshold to induce the long-term potentiation cascade [37] or interfere with activity-dependent network dynamics, such as gamma-frequency oscillations [38], that influence spatial navigation and retention. Yet in physiological

conditions, neuron firing rates either remain the same, or even exhibit hyper-excitability and increased firing rates depending on region [39].

1.1.2. Ageing in specific brain structures

While both 'normal' ageing and neurodegenerative conditions share vulnerable circuits, the effects that lead to the dysfunction are seemingly different. The brain is an incredibly complex overall structure, with a complex interplay of neuronal circuits running between populations and broken down into definable structures, with complex and differing roles. There is much variation in the effects of ageing between different brain regions and sub-populations therein; as such it is necessary to focus on key areas affected with age, and to discuss these in more depth (Figure 1.1.2.3A).

1.1.2.1 – Ageing in the Hippocampus

First described as a flexible structure with shape of a 'Hippocampus, that being a small sea-horse' [40], the Hippocampus plays an important role in cognition for episodic and working spatial memory [41, 42]. These functions can either be through direct firing of hippocampal neurons and through the binding and co-ordination of inputs from other areas; indeed it has strong connections to many regions of the brain and its correct functioning supports global cognition [41].

1.1.2.1.1 – Hippocampal structure

The hippocampus is a highly structured formation, with distinct subfields with different connections, cell-types and functions that form a uni-directional circuit [43-45]. In the tri-synaptic model, the perforant pathway connects layer II of the Entorhinal Cortex (EC) to the Dentate Gyrus (DG), which projects mossy fibres to the *stratum lucidum* of the *Cornu Ammonis (CA)* 3 (Figure 1.1.2.3B). CA3 neurons connect to other neurons in the CA3 and project Shaffer collaterals to CA1 *stratum radiatum* (and to the CA1 in the contralateral hippocampus), which then projects to the subiculum. This model simplifies affairs somewhat; the EC layer II connects to the CA3, layer III also connects to the CA1 and subiculum, while CA1 and the subiculum feed back into the EC, completing the circuit, but also project to other brain areas directly [43]. Further, the CA2 is often excluded from studies due to its small size, but is now beginning to be re-examined with differences in connectivity, gene expression and soma size being observed [44, 45]; CA2 receives input from both the DG at the *stratum lucidum* and CA3 at *stratum radiatum*, but in contrast to CA3 it projects to the *stratum oriens* of CA1, as well as to the CA3 *stratum oriens* to a smaller degree [44, 45].

Damage to the Hippocampus in rodents results in a hyperactive response to new environments, and defects to both spatial memory and learning [46, 47]. Although, there still debate over spatial navigation and its integration with other hippocampal roles [48]; it was initially proposed that the hippocampus forms an internal map of the surrounding world with pyramidal layer 'Place cells' holding the self's location [49]. Since then, data has suggested that these place cells are perhaps not a cohesive group that gives a location, but instead work as arrays of 'grid', 'head direction' and 'boundary' cells that act encoding different cues, events and stimuli together to form a spatial map [42, 48, 50].

The CA1 and CA3 have distinct roles with the learning of new environments and remembering spatial cues. When exposed to a new environment, both the CA1 and CA3 are active, but the CA3 shows much more distinct changes in firing when alterations are made to local and distal cues [51]. The CA3 is highly interconnected and generates the synchronous firing of neuronal populations, termed neuronal oscillations; these ensure that specific arrays of cells fire in response to stimuli [52]. They are generated by the excitatory and inhibitory firing of pyramidal neurons and interneurons (Figure 1.1.2.3C) and are categorised by the frequency of their firing [53].

The CA3 appears to be key in learning new spatial environments and the location of a target together with CA1, encoding a representation of this information, and ensuring its retention, in the CA1 array [54]. The CA3, working together with the DG, is important for pattern separation, which is the storing of similar representations into distinct memories and the retrieval of the correct information in response to similar external stimuli [55]. The CA3 co-ordinates the specific firing of CA1 neurons through the generation of gamma frequency neuronal oscillations, and this activity allows for the retrieval of spatial memories [52]. Together, this firing encodes spatial representations of an environment [56], stores information about it into short-term memory, and allows for the retrieval of the correct information when required [52, 54, 55, 57].

1.1.2.1.2 – Ageing in hippocampal pyramidal neurons

The hippocampus shows a number of age-related macro changes, with a reduction in hippocampal volume and weight [9, 17], but little to no loss of neurons in the pyramidal and granule cells in healthy human and aged C57Bl/6 mice, even in those showing cognitive impairment [13, 31, 58, 59]. Defects in learning the spatial-location of targets and recall can be observed when relying purely on non-target spatial cues, such as markers or objects outside of a maze [36, 60-62], but performance is comparable when the target is visible directly [60]. Meaning there appears to be little defect in the ability to remember that there is a target, or the need to move to it, in normal ageing, but the capacity to remember and relate its precise location within an internal spatial map does suffer.

There are differences in the pattern of degeneration and dysfunction with age between regions of the hippocampus. The CA1 and subiculum often receive attention, as there is widespread loss of neurons and shrinkage in these regions in Alzheimer's disease [63] and, as the main output point of the hippocampus, defects here can have severe effects on cognition [43]. Yet, while these areas are heavily affected in early Alzheimer's, the CA3 and DG are both comparatively preserved from neuronal death [43, 64]. However, in ageing these two regions show significant changes [39, 64, 65].

Interestingly, the CA1 remains comparatively stable with age [39, 66, 67]. There are some changes in morphology, with reduced dendritic spine number [26], but many other parameters remain comparable to those in the young. The basic electrical firing properties of CA1 neurons remain comparatively constant with age [39, 66, 67] and synapse number does not shift extensively [31]. Studies have shown comparable induction of long-term potentiation and depression in aged and young rodent CA1 neurons [39, 67]. They also retain their ability to adapt their response when exposed to familiar and novel environments with age, suggesting that there are not great declines in their plasticity [39].

The vulnerability of the CA3 in ageing, and the biological mechanisms underpinning it, are now receiving more attention [39, 68]. With age, CA3 neurons show increased basal rates of firing, termed hyper-excitability [39, 68]. When aged rats are exposed to novel changes to the environment, CA3 neurons fail to adjust their firing, unlike young animals [39]. Hyper-excitability in the CA3 has the capacity to affect other regions, as it may interfere with its ability to bind arrays of CA1 neurons to encode spatial information, store it in short-term memory and retrieve the correct information [52, 54, 55, 57]. The failure to adjust firing when exposed to changes in the environment suggests a decreased capacity for pattern separation [39]. This is in line with human data, which finds that healthy aged people with deficits in pattern separation have increased activity by fMRI in the CA3/DG compared to intact controls [69]. Hyper-activity in the CA3 has been suggested as a marker for age-related cognitive impairment [70], and treatment with anti-epileptics that reduce this hyper-activity show improvement in patients with mild cognitive impairment [71].

1.1.2.2 – The Cerebellum

The cerebellum, meaning 'little brain', appears to respond differently with normal ageing and shows a higher vulnerability to age-related changes than most other structures. The cerebellum plays a key role in regulating motor and sensory behaviours, taking in multiple complex inputs such as the signals for muscle movements, and integrating them into a coordinated and cohesive response. It receives

input from the cerebral cortex and outputting, via the thalamus, to the frontal lobe areas controlling cognitive, motor and language functions [72].

Input from outside the cerebellum comes through the pre-cerebellar nucleus cells, which extend mossy fibres to innervate granule cells (Figure 1.1.2.3D) [72]. Granule neurons are the most populous neuron in the brain (making up to 75% of all neurons) and extend parallel fibres into the molecular layer of cerebellum, innervating Purkinje cell's apical dendrites. They also innervate basket and stellate cells, which make inhibitory connections onto Purkinje cells and each other. Purkinje cells reside in a layer between the molecular layer and the granule layer, and receive and integrate input from a wide range of cells and cell-types. They are the sole output from the cerebellar cortex and inhibit deep cerebellar nuclei. These receive their excitatory innervation from mossy and climbing fibre pathways and output information from the cerebellum to the premotor cortex [72].

The Purkinje cell is one of the most recognisable cells in the brain and are often studied due to their large size and ease of identification. Mouse models which display significant defects in Purkinje cells provide insights into the function of the cerebellum. Transgenic 'Lurcher' mice, named after their lurching gait, show significant loss of Purkinje cells during development and present with severe defects in their movement, with a poor coordination, staggered gait and a resting tremor [73]. The loss of Purkinje and granule cells leads to early onset of deficits in motor learning and ability with age [74], and suggest a minor, or indirect, role in spatial learning [73]. 'Staggerer', also named after their gait, mice show significant morphological abnormalities, and earlier onset and exaggerated loss of Purkinje neurons with age [75].

In ageing humans there is a 26% reduction in cerebellar white matter and in total, a 16% decrease in total cerebellar volume [76]. Purkinje cells appear especially sensitive to damage and ageing, seeing a number of age-related changes in both their morphology and function [77]. Yet, unlike the hippocampus, the cerebellum, in particular the anterior lobe, shows a 40% reduction in both Purkinje and granule cell numbers in late age, although, while volume loss is global the neuronal loss is largely restricted to this region [76]. Similar is seen in C57Bl/6 mice, where Purkinje neurons are one of the few neuronal populations that show actual age-related loss [78].

With age, Purkinje cells undergo a number of morphological alterations. Soma size reduces progressively after adulthood in humans [76] and rodents [79]. They also appear to show atrophy in their dendritic processes, with decreased dendrite thickness and the loss of distal connections [77]; which may limit their ability to receive and integrate incoming signals. Studies in rodents have

indicated that Purkinje cells lose up to a third of their synapses on the dendrites [80]. In rodents, age associated declines in a broad range of electrophysical characteristics can be observed, with a reduced activation threshold and increased inhibitory thresholds [81]. These age-related changes typically occur at a younger age than in the hippocampus, with deficits in long-term depression occurring as early on as 8 months [82].

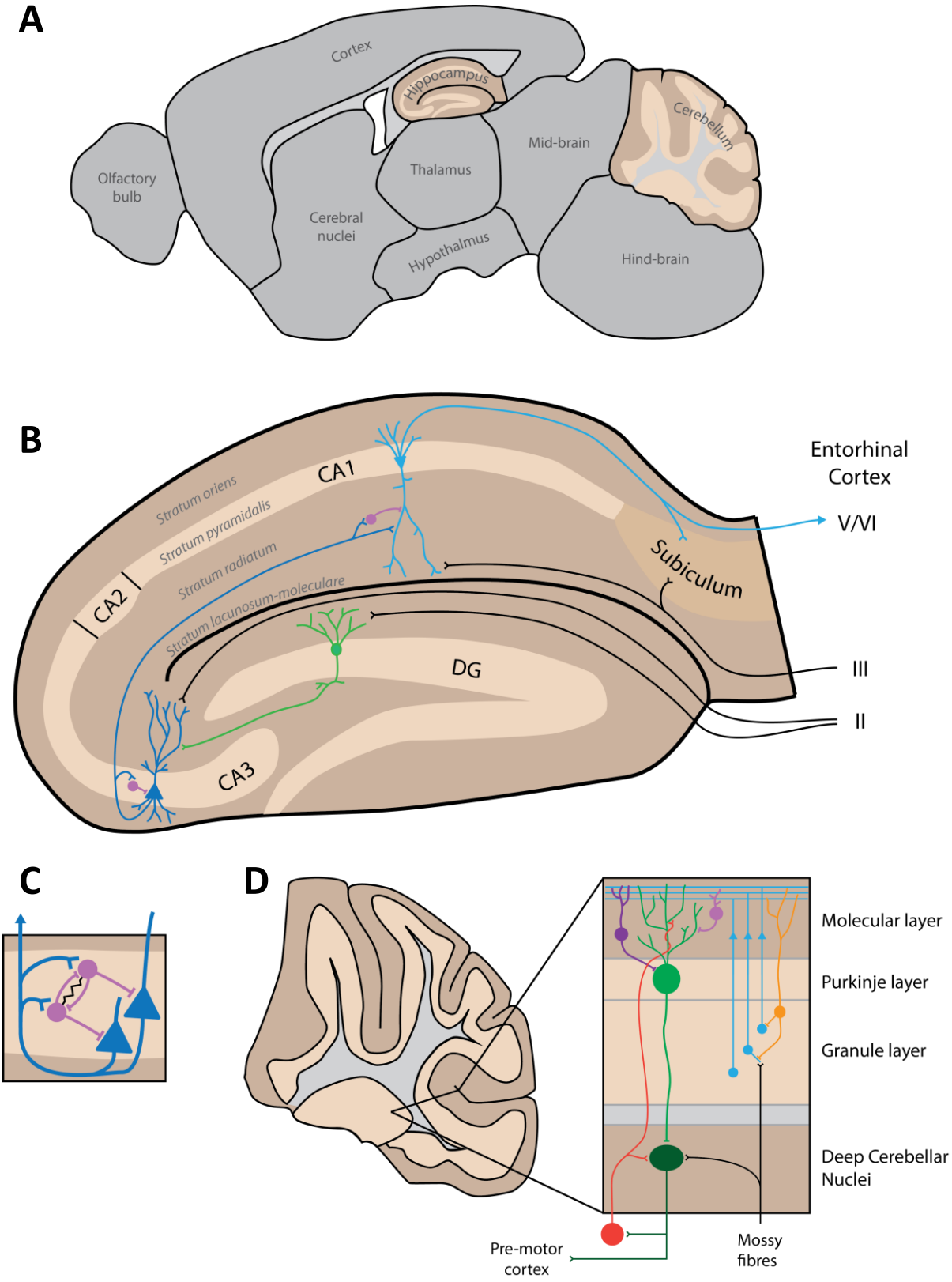
A
Cortex
Hippocampus
Cerebellum
Mid-brain
Olfactory bulb
Thalamus
Cerebral nuclei
Hypothalmus
Hind-brain
B
Entorhinal Cortex
V/VI
Stratum oriens
CA1
Stratum pyramidalis
Stratum radiatum
CA2
Stratum lacunosum-moleculare
Subiculum
DG
III
II
CA3
C
D
Molecular layer
Purkinje layer
Granule layer
Deep Cerebellar Nuclei
Pre-motor cortex
Mossy fibres

Figure 1.1.2.3: Structure and circuitry of the hippocampus and cerebellum

A) Sagittal view of the mouse brain, with both the hippocampus and cerebellum highlighted. B) An overview of the basic hippocampal circuitry. Input from layer II of the Entorhinal cortex via the perforant pathway excites neurons (>-) in the *dentate gyrus* and CA3. Neurons in the *dentate gyrus* can excite neurons in the CA3 via mossy fibre projections. Pyramidal neurons in the CA3 (dark blue) project to neurons in the CA1 via the Schaffer collateral, where they excite both CA1 pyramidal neurons (light blue). In addition, they can excite and inhibitory interneurons (purple) within the CA3 and CA1, which inhibit (⊢) pyramidal neurons in turn. Pyramidal neurons in the CA2 (omitted here) can also excite neurons in the CA3 and CA1, via projections along the *stratum oriens*. Pyramidal neurons in the CA1 additionally receive input from layer III of the entorhinal cortex, and themselves project to the subiculum and layers V and VI of the entorhinal cortex. C) Excitatory pyramidal neurons (blue) and inhibitory interneurons (purple) form feedback loops of excitation and inhibition. Electrical gap junctions between interneurons shown in black. D) Overview of cerebellar circuitry. Excitatory mossy fibres project into the cerebellum and excite the deep cerebellar nuclei (dark green) and granule cells (blue). Deep cerebellar nuclei neurons are also excited by climbing fibre projections from neurons in the inferior olive nucleus (red), and excites these in turn, as well as projecting to the pre-motor cortex. Granule cells project into the molecular layer where they excite golgi cells (orange), which in turn inhibit granule cells, stellate (light purple) and basket cells (dark purple) and purkinje neurons (light green). Purkinje neurons are also excited by neurons in inferior olive nucleus, and inhibited by stellate and basket cells. Purkinje neurons themselves provide inhibitory input to the deep cerebellar nuclei.

1.1.3 – Inflammation and brain ageing

Inflammation and immune regulation with age can be summarised thusly: there is a decline in the adaptive immune system and its capacity to mount an appropriate response to specific threats (Immuno-senescence) [83], but a shift towards increased non-specific inflammation in the tissue micro-environment. This is characterised by increased levels of specific cytokines such as Interleukin-6 (IL-6), TNF-α (Tumour Necrosis Factor-α), and the release of reactive oxygen species (ROS) [83, 84], and has been linked more to cellular level ageing, the regulation of inflammation and 'Cellular senescence' [85, 86] which will be discussed in depth later.

1.1.3.1 – Inflammation induces cognitive deficits

Neuro-inflammation is a prominent aspect of many neurodegenerative diseases, it is linked to ageing associated cognitive impairment [87]. Increased levels of pro-inflammatory cytokines are often observed in patients with cognitive decline [88]. The brain can be affected by both systemic and localised inflammatory insults, and drives inflammation and ageing elsewhere in the body [89, 90]. Inflammatory factors such as cytokines, chemokines, complement and acute phase proteins can transfer from systemic circulation across the blood brain barrier; in turn, the brain can regulate the immune-system via endocrine signalling, and the stimulation of lymphoid cells via the Hypothalamic Pituitary Adrenal axis [89, 90]. Ageing mice brains show shifts in gene expression, with elevated expression of inflammatory and pro-oxidative genes, combined with reduced neurotrophic and anti-oxidant gene expression [91].

Inflammation induces cognitive impairments in a number of different domains. Short-term cytokine overexpression, such as IL-1β in the hippocampus leads to mild learning impairment, activation of glial cells and increased expression of other pro-inflammatory cyto- and chemokines[92]. Lipopolysaccharide (LPS) administration to the ventricles leads to impairments in working memory, increased numbers of microglia and elevated expression of IL-1β, IL-6 and TNF-α in the hippocampus, with the largest effects seen in the neuron dense granule-cell and pyramidal layers [93]; These effects are exacerbated in the older animals, with young animals showing relatively little impairment in spatial learning and memory.

Indeed, most research concentrates on the role of secondary inflammatory insults, as age appears to prime the brain, leading to a much more significant inflammatory and cognitive effect. Older people experience greater declines in cognitive function following insults, such as infection [94] and surgery

[95, 96], while also being more likely to experience them. These see significant inflammatory responses, with perioperative inflammation believed to be the underlying cause of post-operative cognitive dysfunction [95]. Indeed, the driving risk factor for long-term cognitive impairment after surgery is age [96]. The same can be observed in rodents, where peripheral infections produce retrograde amnesia and anterograde deficits in long-term memory in aged rats, but not young rats [97]. Further, following surgery, aged but not young rats, show persistent deficits in spatial reversal-learning with upregulation of cytokines, such as IL-1β and IL-6, and glial activation in the hippocampus [98].

These effects seem to be regulated by a number of processes. Even a single inflammatory insult can lead to reduced expression of genes associated with memory and learning, and increased pro-inflammatory gene expression after 24 hours [99]. It impacts further on a broad range of neuronal functions, reducing neurogenesis following cranial radiation exposure [100], cytokine exposure can increase hyper-active firing in neurons [101] and chronic exposure impairs neuro-plasticity in the hippocampus [102].

1.1.3.2 – Sources of inflammation within the brain

This inflammation is heavily mediated through the brains native and most numerous immune cell, the microglia. These cells constantly monitor the micro-environment to detect signs of damage and pathology, and have complex patterns of activation and response [103]. In response to detecting microbial antigens, cell death or altered neuronal function; they can scavenge extra-cellular debris, kills cells where needed, recruit further immune cells and promote tissue repair [103]; microglia normally rest in a 'quiescent' state with long dendritic processes that sense the micro-environment, but can become 'primed'. This state sees a shift in cell morphology, with the shortening of dendritic processes, and the increased expression of pro-inflammatory genes (IL-1β, TNFα and IL-6), as well as anti-inflammatory genes (IL-10) [103, 104]. Microglia can enter an activated state, which sees the retraction of their dendritic branches and swelling of the cell-body, and an increased inflammatory profile [104, 105].

There appears to be no great change in the numbers of microglia with age in male populations of C57Bl/6 mice [106], although increased numbers can be seen in female C57Bl/6 mice [107]. Instead the increased pro-inflammatory environment that accompanies ageing appears to come from a shift towards primed and activated microglia with age (Note: it can be difficult to distinguish these two states by morphology alone) [108, 109]; with this mediating the exaggerated size and duration of the

inflammation in response to challenge. Aged microglia have elevated basal pro-inflammatory gene expression, and following LPS exposure express elevated levels of pro-inflammatory genes (IL-1β, TNFα and IL-6) and anti-inflammatory genes (IL-10) [104]. A greater proportion of microglia isolated from aged animals were positive for IL-6, and increased IL-6 levels are present in the Cerebellum, cortex and hippocampus of aged mice [108]. The inhibition of microglial activation has shown some improvements in age-associated reductions in long-term potentiation [110].The increased frequency of activated and primed microglia with age likely contributes to general ageing related declines; and the exaggerated response to secondary insult by aged microglia underlies the greater cognitive decline with inflammatory insult.

One of the mechanisms underlying the age-related changes in cell morphology, function and the secretion of inflammatory factors seen in mitotic tissues is Cellular Senescence [86, 111]. A similar phenotype has recently been observed in neurons, and may be a contributing factor in some of the changes outlined above [112]. Below, I analyse the mechanisms underlying cellular senescence and, potentially, the senescent-like phenotype.

1.2 – Cellular Senescence

1.2.1 – Cellular senescence – an overview

Sub-apoptotic DNA damage at a sufficient level in mitotic cells also induces a cell-cycle arrest [111]. However, if this arrest is stable and DDR signalling persists, then the cell can become permanently 'locked in' to this arrest and undergoes a number of phenotypic changes. This is referred to as 'Cellular Senescence' - in addition to roles in development, anti-cancer action and wound healing - it is now regarded as one of the key drivers of organismal and systems ageing in many tissue types. Cellular senescence is perhaps a prime example of Antagonistic Pleiotropy in ageing, where processes that is beneficial in the young, have a deleterious effects in the old, either through direct action or off-target activation [113].

In 2012 our lab observed the hallmarks of this phenotype in post-mitotic neurons in mice, termed a 'Senescence-like Phenotype' [112]. This showed that with age, neurons bore many of the same markers that are typically associated with cellular senescence in mitotic cell types. However, in order to understand the potential relevance of this, it is first it is necessary to describe what senescence in mitotic tissues is.

Cellular Senescence was initially described by Hayflick and Moorhead in the early 1960s as the permanent loss of replicative ability, in cultured cells, that occurred after a reproducible number of cell divisions [114]. Prior to this, cells were widely regarded as being functionally immortal once isolated from the soma, and only lost due to poor cell-culture technique - primarily due to the popularised work of Alexis Carrel and his maintenance of long-lived embryonic chicken heart derived cell cultures. However, while Carrel's work was difficult to replicate, Hayflick and Moorhead's could be replicated. This suggested that the cessation of division was not a mere side-effect of poor technique killing the cells; indeed, these cells remained alive for long durations once they had stopped dividing. Yet no matter the nutrients or cell-density, they did not restart division.

This is now recognised as replicative senescence, one of many forms of Senescence that can be induced. Senescence can be induced by many different stressors, including telomere shortening and uncapping, exposure to ROS and genotoxic DNA damage, chromatin modifications, amongst others [111]. Multiple mechanisms have now been described as triggering cellular senescence, and the phenotype is now understood to consist not of just mere growth arrest, but is characterised by a wide and deep range of phenotypic changes [86]. Changes in cell morphology are often observed in cultured senescent cells, with swelling of the cell body and the altered expression of genes and proteins. Many

of these relate to the cell-cycle, inhibitors are present in increased levels, while cell-cycle activators are typically lower, but seemingly not wholly absent [115, 116]. Increases in the Cyclin Dependent Kinase Inhibitors p21 and p16 can be observed, largely due to the activation of p53 and phosphorylated Retinoblastoma (pRb) [117], and are induced in senescence by multiple mechanisms [118]. Shifts in population level gene expression are seen in senescent cells, leading to a general increase in the expression of inflammatory cyto- and chemo-kines, growth factors and extra-cellular matrix factors [119, 120]. The expression and release of these factors is termed the Senescence Associated Secretory Phenotype and appears to contribute to tissue integrity and inflammation [121]. This secretion of bio-active molecules (in particular the pro-inflammatory cytokines and ROS) into the micro-environment appears to have paracrine effects, ideally recruiting immune cells to clear the damaged cells, but is also causing DNA damage, activating the DDR and inducing senescence in surrounding cells [122].

Yet on an individual cell level, the changes in gene expression are highly variable, even amongst genes often associated with senescence [121]; SASP factor genes show a great deal of variability, with subsets of inflammatory genes clustered at genomic loci accounting for much of the population level increases, and this further complicates the difficult task of finding specific markers of senescence, as even the most accurate markers show less than 90% accuracy, meaning that multiple markers, such as p21 and HMGB1, should be used simultaneously [121].

Senescent cells are observed *in vivo* and appear key in driving the ageing process [123, 124]. Senescence has previously been speculated to have a role in organismal ageing due to the loss of functional cells and the damaging side effects of excreted factors [125], but the lack of specific *in vivo* markers made their presence difficult to analyse. The frequency of senescent cells increases with age, as first observed in skin fibroblasts [126] and subsequently in many organs and cell-types, including the brain [112]. The rate of accumulation in tissues linearly predicts lifespan in accelerated ageing models of mice [127] and targeting these cells with specific drugs and interventions has shown promise in slowing the rate of ageing and delaying the onset of numerous age-related conditions [123, 124].

1.2.2 – DNA Damage and the DNA Damage Response

There are myriad exogenous and endogenous sources that can lead to DNA Damage. The brain demands a lot of energy, accounting for close to a quarter of the body's glucose usage, and requires high levels of Oxygen [128]. This in turn exposes neurons to oxidative damage. Base alteration and single-stranded damage may lead to interference with the transcription of proteins, while double strand breaks are potent activators of the DDR and may lead to apoptosis or the induction of

senescence-like pathways [112, 129]. With damage such as single-strand breaks potentially occurring at a rate of tens of thousands per neuron, per day, effective repair mechanisms must be maintained. Indeed, defects in such mechanisms result in severe neurodegenerative conditions [11, 129].

Radiation is encountered consistently throughout an organism's life-span, from sources such as 'background radiation', medical procedures and sun exposure. Background radiation is a catch-all term covering sources as diverse as radon gas released from the ground or from cosmic sources - which varies by geographic location and altitude, with long-term exposure being a particular concern for space travel. Medical treatments such as cranial radiation and chemotherapeutics that have DNA damaging actions are of interest, as these are associated with memory impairments and neurodegeneration [130, 131]. In mice this irradiation is associated with both reductions in neurogenesis and alterations to neuronal morphology, with loss of dendritic branch complexity and pre-synaptic synaptophysin expression in the hippocampus [130]. Drugs that induce DNA damage, such as chemotherapeutics are often accompanied by neurological side-effects, with memory impairment and neuro-degeneration [131, 132]. This DNA damage has been implicated in the pathology of brain ageing, injury and neurodegenerative conditions [133-135].

1.2.2.1 – Double Stranded Breaks are potent triggers of the DDR

Double stranded breaks (DSBs) are regarded as one of the most cell-lethal types of DNA damage, and act as a potent inducer of DDR signalling; a comparatively small number of breaks are capable of inducing senescence or apoptosis within Eukaryotic cells [136, 137]. The 'choice' between these two outcomes is dependent on not only the level of damage, but the pattern of downstream induction (Figure 1.2.2.4).

DSBs can been seen to accumulate in the cells of various mitotic and post-mitotic tissues in ageing mice, and are observed in cultured senescent cells [138, 139]. These breaks are generated through a number of multiple mechanisms and from many different sources, both internal and external to the cell and organism. Radiation, especially in the X to γ-ray range can cause damage through the direct ionisation of DNA bases, or through the generation of free radicals from H_2O that then react with the sugar backbone [140]. If breaks in both strands are generated within close proximity, typically within 10 base-pairs of each other, then the strand is liable to break [141]. The generation of ROS can have a strong toxic effect with damage to the DNA and other macromolecular structures, it can generate double strand breaks in both the euchromatic and heterochromatic DNA of cells in G_0 and G_1 in a similar way to irradiation induced breakages [142]. The exact formation of these breaks varies considerably both by the length of single-stranded overhang and the chemical composition of the DNA

end points [143], and even low doses can lead to the accumulation of poorly repaired DNA damage [144].

The replication of DNA is largely absent in neurons and the majority of DSBs are repaired through Non Homologous End Joining (NHEJ) [145, 146]. However, as rodent neurons age, the levels of NHEJ proteins and repair efficiency is reduced, which may also contribute to the accumulation of damage and increased DDR signalling [147-149].

1.2.2.2 – Sensing DNA Damage

As mentioned previously, the chemical structure of DSBs is diverse, therefore the DDR must have the flexibility to recognise these different break forms and then mobilise the DDR in an appropriate way, and ideally process the ends in such a way that they can be repaired [145]. Breaks are sensed by complexes with are capable of binding to differential, but overlapping break formations [150]. The initial DSB sensors are the Ku70-80 heterodimer, which recognises and binds to double-stranded DNA ends [151], and the MRN complex, whose subunits can tether linear DNA ends, as might occur in the case of long DNA overhangs [152]. The MRN complex (also referred to as the Mre11 complex) is formed of 3 proteins – Mre11, Rad50 and Nbs1 – and binds to DSBs immediately after damage [153] and can tether break sites in proximity [154]. These can then further recruit and activate Phosphatidylinositol-3-OH-Kinase-like Kinases (PI3KK), such as DNA-dependent Protein Kinase (DNA-PK) and Ataxia-telangiectasia, mutated (ATM) to the break-site leading to the recruitment of DDR factors to form DDR protein foci that can span a large region [145].

DNA-PK is complex consisting of a Ku70-80 hetero-dimer bound by DNA-PK catalytic subunit (DNA-PKcs). The Ku70-80 hetero-dimer forms a ring, which wraps double-stranded DNA and binds sterically to the major and minor grooves of two full DNA turns proximal to the break-site; which supports the DNA end for processing and aligns it into the correct angular phase during repair [155]. Once DNA-PKcs is bound to Ku70-80 its DNA end binding affinity increases [156], this DNA binding is required as a co-factor for the protein's Serine/Threonine kinase activity. Once activated, this activity signals the recruitment and activation of downstream factors (DNA Pol, Artemis, XRCC4, LigIV) to join the DSB, with variations in the order and proteins recruited able to lead to multiple resolutions of the same breaks. Differential phosphorylation of DNA-PKcs allows for the processing and end-ligation, auto-phosphorylation is important for allowing physical access to the DNA for ligation, while ATM mediated phosphorylation allows for the recruitment of repair factors such as Artemis [157].

Like DNA-PK, ATM is a serine/threonine kinase and plays an important role in dictating downstream

effects of the DDR, regulating not only repair, but end-stage outcomes such as apoptosis and senescence. ATM acts together with the MRN complex in responding to the DNA damage, which mediates the initial break detection and ATM's activation [158]. The MRN complex binds to DSBs independently of ATM [153] and promotes ATM dimer dissociation [154]. Following radiation damage ATM is auto-phosphorylated, this promotes ATM dimer dissociation and it is these monomers that constitute the active form [159]. Once the complex is bound to the DNA, Nbs1 can recruit ATM to the site [160] and individual elements of the MRN complex can then be phosphorylated by the active ATM, which then mediates ATM's further phosphorylation of MRN and downstream DDR targets [161].

ATM was initially identified in relation to its name-sake, the autosomal-recessive neurodegenerative condition Ataxia-telangiectasia [162]. This presents with cerebellar ataxia and multiple system disruption, altered neuronal development and decreased neuronal survival later in life. This reduced ATM function leads to radio-sensitivity, defects in DNA repair, genome instability and loss of cell-cycle control. In neuronal development, this results in the persistence of damaged neurons that would otherwise apoptose via ATM-p53 activation in normal development; and in later life leads to neuronal dysfunction and cell loss, with prominent cerebellar ataxia and motor dis-coordination [163]. Defects in the individual subunits of the MRN complex lead to similar phenotypes with increased radio-sensitivity and neurological effects, such as Mre11 hypomorphic mutations (which leads to Ataxia-telangiectasia-like Disorder, displaying with cerebellar atrophy) [164] and Nbs1 hypomorphic mutations (which leads to Nijmegen Breakage Syndrome, with developmental microcephaly) [165].

1.2.2.3 – Downstream DDR Signalling

DNA-PK and ATM quickly phosphorylate Histone variant H2A.X at the break site, and up to several megabases away, after damage [166, 167]. The concentration and size of these foci differs, depending on the initial response and ATM involvement is required for more distal H2A.X phosphorylation [167]. H2A.X is phosphorylated at the Serine 139 site, and once phosphorylated at this site, it is referred to as γH2A.X [168]. H2A.X is highly conserved between species; however, levels vary with age and cell type. In cortical rat neurons, the levels of H2A.X on histones increase rapidly by day 30 postnatal, before plateauing and then very slightly increases with age. At equilibrium, H2A.X variant represents ~15% of total H2A histones [169].

This phosphorylation mediates the recruitment of chromatin remodelling proteins (including p400 and Tip60), which help relax the chromatin to allow access for DDR proteins [170, 171]. Mediator of DNA Damage Checkpoint Protein 1 (MDC1) is recruited, MDC1 secures ATM at the foci, allowing for H2A.X

to be phosphorylated continuously [172]; together MDC1 and γH2A.X act to form a scaffold that allows for the recruitment of more MRN to the site and more DDR proteins, including p53 Binding Protein 1 (53BP1), BRCA1 and RAP-80 which then allows for increased ATM activation [173, 174]. The activation of diffusible downstream kinases, including Checkpoint Kinases 2 (CDK2) [173, 175], propagates and amplifies the DDR signal from the initial DSB and engages downstream effectors such as p53 and cyclin-dependent kinase (Cdk) inhibitor p21 [112, 176, 177].

The mode of activation of p53 in the DDR acts as an important decider of the cell fate following DNA damage, and can be altered to affect its stability and pattern of activation [178]. Stabilisation of active p53 can induce the expression of p21, which has a number of roles in relation to the DDR. p21 can silence Cdk2 expression and inhibit Cyclin E-Cdk2 and Cyclin A-Cdk2, preventing transition into S-phase by ensuring that Retinoblastoma protein (Rb) is hypo-phosphorylated and remains in inhibitory binding to E2F1 [88, 89]. In S-phase, it can displace polymerases from Proliferating Cell Nuclear Antigen (PCNA) and block DNA synthesis from occurring [179, 180], and in this role is important in promoting nucleotide and base excision repair [181]. When localised to the cytoplasm it can block the activity of pro-caspase 3 and the apoptotic cascade [181]. p21 undergoes further regulation and modification, both at the mRNA level, such as by RNA-binding proteins such as HuR after damage [182], and through phosphorylation by kinases at specific motifs, which blocks or allows cleavage of p21 by caspase-3 in apoptosis [183]. p53 is phosphorylated by ATM, and via the ATM-directed interaction with other proteins; these modifications effect both its gene trans-activation and its affinity to the inhibitory binding protein Mdm2 [184], which blocks the trans-activation domain of p53 and targets it for degradation [185].

1.2.2.4 – Outcome of the DDR – A choice between survival or apoptosis

The outcome after genotoxic stress is generally between damage repair and survival, or apoptosis. This is dependent on the level of damage and the duration of the insult, which leads to differential modification of DDR factors leading to different outcomes. One of the most obvious outcomes to heavy damage is the loss of the neuron, with this being readily visible in scans and *post-mortem* histology following major traumas, such as ischæmia, and in neurodegenerative conditions such as Alzheimer's disease. A major cause of cell death is apoptosis, an organised programme that removes cells that are deemed too damaged or whose survival is no longer required [186-188]. DNA damage plays a major regulatory role in the apoptotic pathway, through direct transcriptional inhibition [189] and through the DDR [190].

Much of the DDR's role in apoptosis is regulated through p53, which integrates multiple upstream inputs to regulate the transactivation of differential transcriptional cassettes to favour repair and survival, or apoptosis [178, 191]. This is regulated through the complex interactions of a number of factors; the total protein levels of p53 and relative levels of p53 binding proteins, the p53 binding sites in gene promotors and post-translational modifications to p53.

Post-translational modifications to p53 effect not only its interactions with other proteins in the pathway, but the susceptibility of other p53 motifs to alteration, and its affinity for p53 DNA binding sites [191, 192]. For example, Acetylation of lysine 320 blocks the phosphorylation of NH2-terminal serines and switches p53 to binding to high-affinity p53 binding sites in genes, activating transcription of pro-survival genes such as p21 [191]. Cooperation between the DNA binding sites of tetrameric p53 helps binding to low-affinity promotor p53 binding sites in pro-apoptotic genes [193]. Post-translational modifications to p53 lead to regulation of this cooperation, thus regulating the binding to low- or high-affinity p53 binding sites and expression of pro- or anti-apoptotic genes [191]. Direct action on p53 at binding sites can also occur, with DNA-PKcs binding directly to p53 bound to the p21 promotor site, thus blocking p21's transcription and pro-survival effects [194].

Whether p53 activation is pro- or anti-apoptotic is complicated and ultimately involves a 'threshold' effect dependent not only on absolute levels, but duration and mode of p53 activation [195]. Both high and low levels of p53 can trigger pro-apoptosis or pro-arrest gene expression, but prolonged high-level expression is required to trigger actual apoptosis, with the absolute threshold alterable through modulation of the ratio of pro- and anti-apoptotic signals such as Bcl-2 type protein levels [195]. Alterations to the DDR and p53, as well as levels and duration of activation, act together to generate specific p53 regulated transcriptional cassettes with very different outcomes.

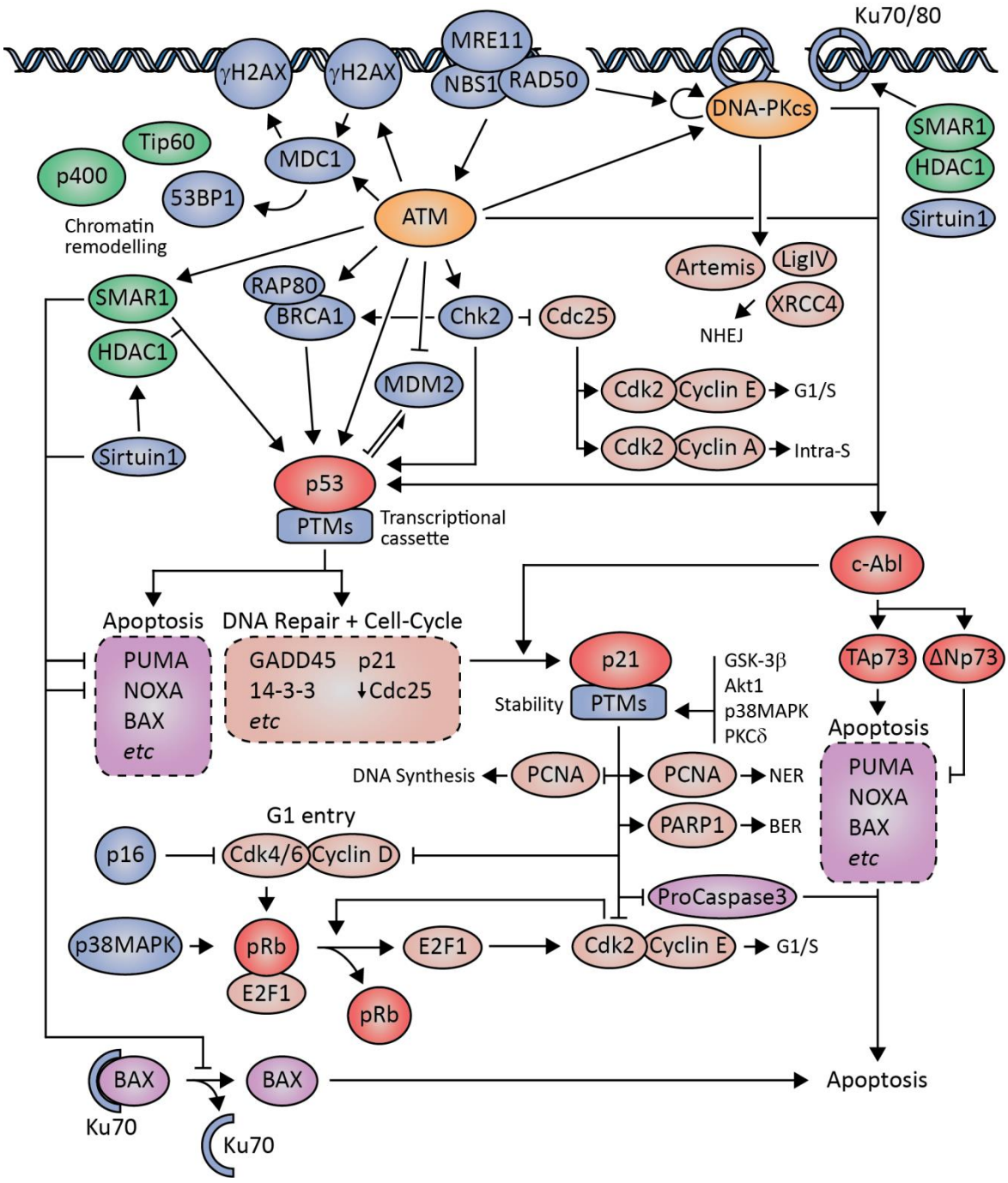

Figure 1.2.2.4: Overview of DDR pathways showing interactions with gene transcription, cell-cycle machinery, and factors promoting survival or apoptosis

Recognition of DNA damage by sensor proteins (yellow) like PI-3K kinases ATM and DNA-PK leads to activation of effector proteins (red) such as p53, p21 and c-Abl that regulate downstream responses, specifically apoptosis (purple) and cell cycle arrest/repair (pink). The balance of the response is altered through chromatin remodelling factors (green), and numerous other intermediatory and regulating factors (blue). Post-Translational Modifications (PTM) of proteins such as p53 and p21 have significant effects on their function. These can shift activation of p53 between transcriptional cassettes and affect the stability of p21, shifting their roles between apoptosis, and survival and repair. Reproduced from Fielder *et al.* 2017 [196].

1.2.2.5 - A persistent DDR can induce Cellular Senescence in mitotic cells

Replicative senescence is primarily induced through the degradation of telomere repeat sequences at the end of DNA during replication [174]. The telomere is protected by a shelterin complex, which is a group of proteins that bind to the telomere and acts to inhibit repair mechanisms that might otherwise recognise the chromosome end as a double-stranded break [197, 198]. If the end of the DNA is recognised as a double-strand break, then it not only triggers DDR signalling (Telomere Induced Foci), but it is vulnerable to the erroneous activity of DNA repair pathways such as NHEJ, resulting in chromosome fusion [199, 200]. The end of the DNA is protected physically through the formation of a DNA 't-loop', mediated by TTAGGG repeat binding factor 2 (TRF-2), which loops the DNA over and round onto itself, 3' overhanging strand is then inserted into the double-stranded helix of the upstream DNA in the loop, forming a 'd-loop' [201]. With the loss of telomere repeats and the 3' overhanging strand, the stability of this loop is decreased and the chance of it collapsing and exposing the DNA end increases [202, 203].

Yet this inhibition of repair molecules can have adverse effects; stress induced senescence is at least partially induced and maintained by persistent DDR signalling [119, 177]. DNA damage can still occur at telomere sites, and while its repair is inhibited, it is still capable of DDR signalling [119, 177]. Senescence is not instant, and often takes 10 days to occur and stabilise in cultured cells; the persistent DDR innervation that comes from this Telomere-Associated Foci (TAF) contributes towards the induction and stabilisation of senescence following DNA damage [119, 177].

DNA damage and the activation of the DDR, and its activation of stress induced senescence can be seen in the tissues of ageing mice [204]. Of interest is that the number of TAF in mice tissues increases with age, regardless of telomere length in the tissues. This is important evidence against the argument at the time that laboratory mice were not a suitable model for senescence, on the basis of their active telomerase and longer telomeres [205]; and is relevant for post-mitotic tissues, as these cells do not undergo telomere extension through telomerase, or loss through replication.

TAF and DNA damage foci located along the genome are similar in their induction of the DDR and associated downstream pathway activation [197]. However, non-TAF are repaired at a comparatively fast rate and total levels of damage inside cells vary considerably [206-208]. This can be as part of the circadian rhythm [206], and from physiological roles such as gene expression, where it allows access to promotors, as in hippocampal neurons [207, 208]. This can limit the use of total foci counts in the assessment of cellular senescence, while the longer life-span of TAF acts as a temporal buffer and

provides a better estimate of the rates of cellular senescence [209]. This has a role in the induction of senescence, as senescence requires a persistent DDR in order to stabilise the phenotype after induction. This appears to be the case, as Hewitt et al. have shown that in stress-induced senescence, up to half of DNA damage foci were co-localised with telomeres *in vitro*, regardless of the telomerase activity in the cells [209].

The DDR continues signalling throughout senescence [210] and it appears that the damage signalling is provided, in part, through these persistent foci [209, 211]. New damage is also constantly generated through the induction of downstream pathways, forming a positive feedback loop [177]. Yet disrupting the DDR alone is not sufficient to reverse senescence once it has become fully established [137]. A number of auto- and paracrine feedback loops act to 'lock in' the phenotype [212, 213]. These develop typically over a number of days and include the production of SASP factors and ROS generation [119, 120].

1.2.3 – Senescence is enforced by positive feedback loops

1.2.3.1 – Mitochondria and ROS

Many of the initial steps in fortifying the transient arrest into senescence are mediated through the production of ROS [214-216]. A major source of ROS in senescence is from mitochondrial dysfunction [215], termed Senescence-Associated Mitochondrial Dysfunction, and without this mitochondrial alteration senescent cells do not develop their morphological, pro-oxidant and pro-inflammatory characteristics [217]. Mitochondrial dysfunction, ROS generation and the reinforcement of senescence can be mediated by the DDR [177, 216, 217]. In turn, mitochondria induce changes in the expression of nuclear genes [218, 219]. This occurs through the mitochondrial retro-grade response following the loss of membrane potential [218, 219]. It both enforces the cell-cycle arrest through blockade of S-phase entry via INK-FOXO mediated activation of Cdk Inhibitors, and through AMPK-p53 signalling [220].

Following DNA damage, an increase in mitochondrial mass occurs in senescent cells [217]. The level of increase is dependent on the level of damage and is mediated independently through p53 and activated Rb [217, 221]. This is downstream of ATM activity and triggers the downstream effectors Akt and mTOR, through the cell-cycle inhibitors p21 and p16 [177, 216, 217, 222]. Signalling from the DDR via p21 promotes GADD45A-mediated p38MAPK activation and TGFβ, resulting in increased ROS generation that causes further DNA damage [177]. In addition to p16's roles in Cdk4/6 inhibition and

activation of Rb, p16 can activate Protein Kinase δ (PKCδ) through ROS, which in turn generates further ROS forming a positive feedback loop [216]. After DNA damage PKCδ can translocate to the mitochondria, where it leads to loss of membrane potential, and activates NF-κB and its pro-survival effects [223, 224]. This results in a collapse of membrane potential in the mitochondria, and the release of ROS into the intracellular environment [221]. Activation of the Akt and mTOR phosphorylation cascades has a number of effects on mitochondria, firstly reducing their degradation by mitophagy, and promoting mitochondrial biogenesis [217, 225]. Together, this promotes the generation of further DNA damage, contributing to persistent DNA damage foci generation and stimulation of the DDR, enforcing the senescent phenotype [177]. Indeed, if mitochondria are completely removed from senescent cells, they lose their typical characteristics, including ROS generation, the SASP and their altered morphology [217].

1.2.3.2 – NF-κB signalling and inflammation in senescence – The Senescence Associated Secretory Phenotype

The SASP is activated downstream of the DDR, and is one of the key features of senescence [119]. On a population level, it results in the release of pro-inflammatory cytokines, chemokines and metalloproteinases, including IL-6, IL-8 and TNF-α [119]. The production of these pro-inflammatory factors and ROS can lead to the reinforcement of senescence via autocrine pathways [212, 213, 226], and can be released into the extra-cellular environment, having paracrine effects on surrounding cells [122, 213]. The release of SASP factors, especially cytokines and chemokines attracts and stimulates immune cells, which should clear senescent cells [227, 228]. However, its paracrine effects induce damage in surrounding cells, and the release of SASP factors by senescent cells appears to be a major cause of increased chronic, sterile inflammation and associated pathology with age [127, 229, 230]. The production of SASP factors is driven by, and drives DNA damage [119, 226], with persistent DDR signalling triggering the SASP [119]. ATM-dependent activation of Chk2, and activation of p21 and Akt through p53, trigger the production of the cytokines such as IL-6 and IL-8 [119, 222].

ATM also triggers the transcription factor NF-κB following DNA damage [231]. NF-κB is a transcription factor and one of the primary regulators of inflammatory gene-expression, including many interleukins and cytokines [232]. Increased NF-κB activity is strongly associated with ageing in multiple tissues with age in humans and mice, and continued signalling through NF-κB appears to drive tissue ageing [233]. Increased NF-κB signalling in mice can drive accelerated ageing and increased rates of senescent cells through chronic inflammation and oxidative damage [127]. It is also a key regulator of the SASP in senescence and regulates more genes than both Rb and p53 [232]. Activation of senescence leads to

a large up-regulation of NF-κB activity and SASP genes, which is necessary for both the establishment and stabilisation of senescence [232, 234].

NF-κB is not a single protein, instead the name covers a family of proteins that form hetero- and homo-dimers from a pool of five Rel proteins - p50/p105, p52/p100, p65 (Rel-A), Rel-B and c-Rel. Each of these has a Rel homology domain allowing dimerization and DNA binding [235, 236]. Rel-A, Rel-B and c-Rel contain transcriptional activation domains located at the c-terminus, which allows them to bind to DNA and promote gene transcription. Both p105 and p100 can be additionally processed to their active subunit forms p50 and p52, respectively, by phosphorylation and subsequent ubiquitination, leading to proteasomal processing; while these lack transcriptional activation domains, they can promote transcriptional activation through forming a dimer with Rel proteins, or inhibit activation through the formation of inhibitory dimers such as p50:p50 [235].

In their inactive form, NF-κB dimers are predominantly localised to the cytoplasm thus rendering the dimers inactive, primarily due to complexing with inhibitory proteins [235, 237]. These include the typical Inhibitor of κB (IκB) proteins (IκBα, IκBβ, IκBε), the atypical IκB proteins (Bcl-3 and IκBζ), and the precursors p105 and p100 [235]. The IκB proteins contain ankyrin repeat sequences that bind Rel homology domains and mask nuclear localisation sequences of the subunits of NFkB dimers. In the binding of IκBα to Rel-A:p50, IκBα can mask the nuclear localisation sequence of Rel-A, however, it does not mask the nuclear localisation sequence of p50 [237]. IκB proteins can contain nuclear export sequences and combined with the masking of one of the localisation sequences leads to shuttling between the nucleus and cytoplasm that heavily favours the cytoplasm [235, 238]. BCL-3 instead contains a transactivation domain, and is primarily localised to the nucleus, where binds strongly to NF-kB homo-dimers of p50 and p52 as a co-activator of transcription [235]. The precursor proteins p105 and p100 can regulate transcriptional activity of NF-κB; their rate of processing of these regulates the levels of p50 and p52, and thus their availability to form active dimers. Additionally, they contain ankyrin-like repeat domains similar to those in IκB proteins at the C termini and can mask nuclear localisation signal [239, 240]. Both p105 and p100 form high molecular weight heterogeneous complexes containing multiple NF-kB subunits with IκB function (IκBγ and IκBδ respectively) that may act as a buffer for levels of active NF-kB dimers [241]. They can also inhibit active NF-kB dimers, such as p100 disrupting the binding of RelA:p50, and form dimers by binding to Rel homology domains in NF-kB subunits and ankyrin domains in IκB [235].

NF-κB is activated by a variety of stimulating factors and pathways through the activation of IκB Kinase (IKK), leading to the phosphorylation and subsequent proteosomal degradation, or processing, of

inhibitory proteins and the nuclear localisation of NF-kB dimers [235]. These can be categorised as occurring via the canonical and non-canonical pathways. Canonical signalling is mediated by dimers containing p50 and Rel-A, or c-Rel, and can be triggered by a range of pro-inflammatory cytokines, such as TNFα and IL-1β, oxidative damage, and bacterial and viral antigens, such as LPS [235]. Binding of these to cell receptors triggers rapid phosphorylation of the IKK complex; in canonical signalling this protein complex contains a heterodimer of 2 catalytic subunits (IKKα and IKKβ) and the regulatory protein NF-κB Essential Modulator (NEMO), also known as IKKγ [235]. Phosphorylation, primarily at the subunit IKKβ, activates IKK which mediates the phosphorylation of IκBα bound to NF-κB dimers (such as RelA:p50), and its subsequent ubquitination and proteasomal degradation. This unmasks the nuclear localisation sequence, allowing the dimer to translocate to the nucleus and bind to DNA [235]. DNA damage signalling can trigger canonical NF-κB signalling through ATM's interaction with NEMO, the regulatory subunit of IKK [231]. ATM can phosphorylate NEMO following DSB formation, leading to its ubiquitin-dependent export from the nucleus, while in turn NEMO promotes export of ATM into the cytoplasm where it triggers IKK activation via the IKK regulatory subunit ELKS [231]. This phosphorylates IκBα leading to its dissociation from Rel-A:p50 dimers, which allows them to translocate to the nucleus and activate the expression of target genes [231, 235]. The inhibition of IKK activity in *ercc1*$^{-/-}$ and *ercc*$^{1/\Delta}$ mice models deficient in DNA repair reduces the incidence of cellular senescence, and oxidative damage to DNA and proteins [242].

Additionally, there is the non-canonical pathway, which is activated by binding of cytokines and ligands to TNF receptor family proteins, and the processing of the precursor protein p100. The activation of TNF receptor signalling leads to the stabilisation of NF-kB inducing kinase protein levels, which is typically degraded rapidly by the E3 ubiquitin ligase complex, which is then disrupted by TNF receptor activation [243]. The increased levels of NF-kB inducing kinase leads to the phosphorylation of IKKα, which in turn phosphorylates p100, leading to ubiquitination and processing to the active p52 form [244]. This allows active dimers containing p52, such as Rel-B:p52 to translocate to the nucleus and promote gene transcription. This has been implicated in senescence, where it can act to suppress senescence in fibroblasts at lower basal levels of p53, with the subunit p100/p52 regulating the expression of Cdk4 and 6, and Rel-B regulating the stability of p21 and p53 [245]; however, again this likely depends on the level of p53 expression, as higher p53 levels following DNA damage, can switch p52 from binding to Bcl-3 to HDAC1, switching from gene expression to repression [246].

1.2.4 – Senescent cells are resistant to apoptosis

Once senescence has been induced, cells show a decreased vulnerability to apoptosis through p53 [247] and oxidative stress [248, 249]; even at higher doses than would be survivable prior to induction [249]. The p53 axis is an important part of senescent cell's apoptotic resistance, with the level of damage and post-translational modifications made to p53 affecting whether it promotes pro- or anti-apoptotic gene cassettes [191-195]. When exposed to p53-mediated and p53-dependent apoptotic stimuli, non-senescent cells undergo apoptosis [247]. However, senescent cells are unable to undergo p53-mediated apoptosis, but are capable of undergoing necrosis [247]. However, rather than just switching the type of cell death, senescence also provides resistance to cell death caused by p53-mediated stimuli, such as high doses of H_2O_2 [250], and p53-independent stimuli, such as Staurosporine, which can stimulate caspase-3 activation [251]. p53 is persistently active in senescent cells and maintained in the nucleus through its association with FOXO4, and provides apoptotic resistance through the regulation of downstream factors [252].

Much of this protective effect comes through alterations in the regulation of 'Bcl-2 family' proteins, which block PUMA/NOXA-regulated apoptosis following stress, rather than a reduction in pro-apoptotic factors [248, 253, 254]. Bcl-2 type proteins can be divided three main classes, depending on the type and topology of the four types of 'Bcl-2 Homology Domains' (BH1-4) present [255].The first of these groups is the 'anti-apoptotic Bcl-2' proteins, defined by their 'Bcl-2 core pocket', which consists of BH3, BH1 and BH2 [255]. This includes Bcl-2 itself, Bcl-W, Bcl-X_L and a number of other variants. These prevent apoptosis through the inhibition of the second class, pro-apoptotic BAX/BAK which promote permeabilisation of mitochondria's outer membranes, the release of Cytochrome C and an apoptotic caspase cascade [256]. The third class contains only the BH3 domain and includes PUMA and NOXA [255]. These act to integrate apoptotic signalling by directly activating BAX and inactivating anti-apoptotic Bcl-2 class proteins [255]. The apoptotic resistance in senescent cells was initially thought to be due to the up-regulation of Bcl-2 and the down-regulation of pro-apoptotic genes [253]. But down-regulation of Bcl-2 and increased levels of PUMA and BIM have been reported in senescent cells [252]. Instead, more recent studies have suggested that the anti-apoptotic effects come instead from the upregulation of other Bcl-2 type proteins, namely Bcl-W and –X_L [257].

Furthermore, continued presence and activity of cell-cycle inhibitors also confers apoptotic resistance up-stream of Bcl-2 family protein activation [258, 259]. One of these cell-cycle inhibitors promoted by p53's anti-apoptotic response is p21 [258, 259]. Furthermore, in senescent cells, it feeds back and inhibits p53 mediated pro-apoptotic signalling following DNA damage [258, 259]. Nuclear p21 inhibits

Cyclin A-Cdk2 normally as a part of the cell-cycle inhibition, but also prevents the pro-apoptotic effects of Cdk2; which is required for chromatin condensation and cell-shrinkage in apoptosis, following activation by caspases [260]. In addition to blocking this caspase-activated activity in the nucleus, p21 can interact with caspases directly [261, 262]. By direct binding to the cleavage domain of pro-caspase 3, p21 can block the initial steps of the caspase cascade [262]. However, it is itself vulnerable to cleavage, by activated caspase-3, as can be seen in cardiomyocytes following hypoxia, leading to Cdk2 activity and apoptosis [263].

Additionally, cytokines released by the SASP can confer apoptotic resistance by stimulating pro-survival genes [264-267]. IL-6 can protect against p53-mediated apoptosis [264, 265], not by regulating p53 activity, but through the separate up-regulation of anti-apoptotic genes, such as Bcl-2 type proteins and IκB type protein Bcl-3, and the down-regulation of pro-apoptotic genes such as Gadd45 and BAX [266, 268]. NF-κB is also protective against apoptotic stimuli, including TNF-α and UVB radiation [269, 270].

1.3 – A Senescence-like Phenotype exists in ageing neurons

While a great deal is known about senescence and its associated characteristics in mitotic cells, little is known about their role in post-mitotic cells. Post-mitotic senescence was initially met with a degree of scepticism, as the senescence phenotype is primarily known in relation to its permanent cell-cycle arrest, and why would a cell that is already post-mitotic undergo such a phenotype? After reviewing the literature, several key points appear [196]; Firstly, significant DNA damage occurs and accumulates with neurons with age, stimulating the DDR. Secondly, re-entry into the cell-cycle and some DNA replication can occur in neurons. However, this is not a complete cycle, but instead leads to apoptosis. The activation of cell-cycle arrest proteins in these neurons provides protection against apoptosis. Thirdly, the time between re-entry and cell death can be considerable, in the range of months to years. This suggests that these neurons are undergoing a protracted or permanent period of active cell-cycle arrest. And finally, the observation of senescence-associated markers is observed in neurons, with increasing levels in ageing mice. [112]

This suggests that while cell cycle re-entry does lead to apoptosis eventually, it is possible to arrest this re-entry for a considerable time, either prior to S-phase or even after DNA replication. If the DDR is persistently stimulated, then it may play a role in maintaining this arrest through its actions on the cell-cycle. This raises a number of questions; firstly, is there evidence of persistent DDR in brain areas known to undergo age related changes. Secondly, does a persistent DDR trigger the same downstream cell-cycle factors in neurons as it does in mitotic cells?. Thirdly, does this trigger the same downstream pathways, feedback loops and changes as senescent cells? And finally, does this correspond to *in vivo* functional changes?

If this is true, it would indicate that a senescence-like phenotype in post-mitotic cells is due to the presence of persistent DNA damage. In addition, there is a mechanism that may contribute to functional declines in neuronal function, either in individual neurons and/or affecting surrounding cells. Furthermore, it presents a novel target for interventions that have not previously been considered.

Mice show increased frequencies of multiple senescence associated markers in neurons with age [112]. This includes Senescence associated Beta Galactosidase activity, activation stress associated kinases such as p38, lipid peroxidation, heterochromatinisation and presence of SASP associated cytokines such as IL-6. These are consistent with the activation of downstream DDR signalling and the SASP, and have been observed in the brain. Senescence associated Beta Galactosidase activity has

been observed in Purkinje cells, cortical neurons and in pyramidal CA3 neurons of the hippocampus in ageing rodents [112, 271]. Activated p38-MAPK observed in neurons may come from the activation of p21 via the DDR, which in senescent cells triggers the production of TGF-B2 and ROS generation [177]. Additionally, neurons have been observed to produce and secrete IL-6 in response to axonal damage [272] and membrane depolarisation [273]. IL-8 induces the expression of SASP factors in cultured neurons, including matrix metalloproteinases and induces cyclin activity, followed by eventual cell death [274]. Elevated levels of these cytokines have negative effects on neuronal networks, with impairments in learning and synaptic transmission [275]. DNA damage and the induction of downstream DDR markers such as p53 and p16 have been observed in Alzheimer's Brains [276, 277]. Activation of p21 follows inflammatory insult from Lipopolysaccharide injection in mice [278] and co-localises with nitric oxide synthases expression in AD [279].

1.3.1 – The Neuronal Senescence-like Phenotype may be activated through the DDR

There is evidence that this phenotype is linked to the induction of the DDR from studies in mice with dysfunctional telomeres and knock-out of p21 [112]. Terc knockout mice lack functional telomerase and are unable to extend their telomeres, leading to uncapping and telomere dysfunction, this worsens with each generation, with increased DNA damage and progeria until they are unable to reproduce at all. Late generation knockout mice showed increased DSBs, p38MAPK activation as well as IL-6 production and oxidative protein damage [112]. Yet, when p21 is knocked out the levels of these markers is reduced [112]. There are two, not mutually exclusive, interpretations for this result; firstly, that with DNA damage generation neurons, much like mitotic cells, develop downstream markers of senescence through p21 activation [177]. Heterozygote *terc*$^{+/-}$ mice maintain their telomere length and do not show the same DNA damage and progeria, when p21 is knocked out in these mice, there is no change in DNA damage levels, but a reduction in factors such as oxidative protein damage and p38MAPK in Purkinje cells, suggesting that this may be regulated through p21 [112]. Secondly, the loss of p21 in neurons may leave them unable to restrain the cell-cycle from progressing, and with the high levels of DNA damage in late generation *terc*$^{-/-}$ mice, neurons that would develop senescence features simply continue progression to the point of apoptosis. p21 has a number of roles in the DDR, regulating cell-cycle activity, and in establishing senescence [177]. Its expression in hippocampal pyramidal neurons is co-localised with the expression of p16, suggesting that activation of both the p16 and p21 sides of the DDR are active in these neurons [279]. p21 is neuro-protective in cultured neurons when exposed to neuro-toxins [280] and when lost allows progression of the cell-cycle and apoptosis [281]. It is neuro-protective in the Dentate Gyrus of the hippocampus following acute systemic inflammation,

but restrains the growth of progenitor cells and is accompanied by increased IL-6, IL-1B and TNF-a [282].

The consequences of the activation of senescence-associated features in neurons is not known currently. Neurons undergoing a DDR show disruption of insulin and Wnt signalling [283] and are associated with early AD and cognitive impairment [284]. The release of SASP factors might stimulate glial responses and contribute to inflammatory feed-back loop, in addition to the roles of factors such as IL-6 on network function and synaptic plasticity [275]. Disruption of mitochondrial homeostasis through p21 [177] would likely have effects on calcium metabolism and disrupt the cellular metabolism required to maintain neuronal function.

1.3.2 – Damage induces neuronal cell-cycle re-entry

Much of the apparent deviation in the DDR between mitotic and post-mitotic tissues relates to its heavy involvement in cell-cycle regulation. In mitotic cells, many of the downstream effects of the DDR feed into the cell-cycle, arresting in order to repair damage and not pass mutations to daughter cells [285]. Post-mitotic cells, such as neurons on the other hand, are often regarded as having permanently exited the cell cycle; however, this is an overly simplistic interpretation and they are not entirely free of the influence of cell-cycle regulators and cell-cycle progression events.

The presence of cell-cycle related proteins has been observed in post-mitotic cells [286], most commonly relating to neurodegenerative conditions, such as Alzheimer's Disease and CNS damage, such as after stroke [287], ischæmia [288] and traumatic brain injuries [289]. Here the expression of cell-cycle proteins such as Cyclin D, Cyclin B, cdc2 can be observed with an association between the loss of neurons to apoptosis and increased presence of cell-cycle related proteins [290-292].

It would be incorrect to describe this as a full re-entry into the cell-cycle and is better described as an aberrant cell-cycle re-entry. This is not mere mis-expression of cell-cycle proteins, but appears to be a coordinated re-activation of cell-cycle machinery; as DNA has been fully, or partially, replicated in neurons in vulnerable brain areas, such as the hippocampus and basal forebrain in AD suggesting they are capable of completing S-phase [293]. While this is mostly observed in the early cell-cycle, at G1 or S phase [291, 293, 294], later markers more commonly associated with G2 such as CDK1 and Cyclin B1 have also been noted [294-296].

A proper entry into M-phase does not appear to occur and given the morphological complexity of neurons would likely end in a mitotic catastrophe, instead this cell-cycle appears to either hold or lead

to apoptosis before this stage is reached [297, 298]. This was initially observed by attempts to induce neuron replication in the early 90s through expression of simian virus 40 large tumour antigen coupled to cell-specific promotors in rod photoreceptors [299] and Purkinje cells [300]; this initiated the cell-cycle, but lead to photoreceptor degeneration in the first case, and cerebellar ataxia and loss of granule cell cohesion in the second.

This is supported by experiments in ATM knockout mice. ATM double knockout mice present with the none-CNS symptoms of Ataxia-telangiectasia but not the characteristic cerebellar ataxia. However, both double-knockout and heterozygote mice show evidence of cell-cycle re-entry and DNA replication in the cerebellar Purkinje and granule cells at day 30 post-natal, unlike wild-type mice [301]. While they do not show ataxia or reductions in neuronal number, this may be due to the lifespan of the mice. The mice die at 3 to 4 months, and in humans the ataxia is not present until later (appearing before 5 years of age), which supports the theory that cycled neurons are capable of surviving for at least this long and that something is preventing the completion of the cycle and immediate cell death, instead requiring an additional 'hit'.

This additional 'hit' that results in neuronal death may, in fact, come from reduced, rather than increased, DDR signalling; this is not necessarily a decrease in DNA damage, but rather a loss of capacity in the DDR to respond to the damage. The DDR pathway acts to arrest the cell-cycle in many situations through the action of proteins such as p21 and its inhibition of cyclin-cdks and PCNA's polymerase activity in S-phase synthesis [302]. A reduction in ATM signalling has been observed in late Alzheimer's Disease areas experiencing neuronal cell-death, together with cell-cycle proteins [303]. This is seen with other DDR factors such as BRCA1, which is reduced in pyramidal and granule neurons of the hippocampus in AD and MCI [304]. Given that these cell-cycle proteins initially appear early in disease pathology and in mild-cognitive impairment [294], it may be a later loss of the DDR's arrestive action on the cell-cycle that allows for further cycling to the point of cell death.

1.3.3 – Arresting the neuronal cell-cycle is protective against apoptosis

While high-levels of DNA damage can cause cell-cycle re-entry and apoptosis through the ATM-p53 axis [305], it can also promote a protective cell-cycle arrest [306]. In the first instance the loss of ATM was protective against etoposide induced cell-cycling and apoptosis, but in the second the knockout of ATM and p53 increased the rates of cell-cycling. There are differences in these experiments, the first is done in isolated cortical neurons using etoposide - which targets topoisomerase II that is used in neurons to generate breaks in order to regulate neuronal early response gene expression [207] - and may represent a severe form of damage. The second is in tau transgenic Drosophila with an

entirely different stressor. There hasn't been a study yet, as far as I'm aware, that has looked for a threshold effect of damage and cycling specifically in neurons; however, as discussed previously, in mitotic cells there is a threshold effect with p53 that affects whether the response promotes cell-cycle arrest or apoptosis depending on factors such as mode and duration of activation [195].

Protecting against this cell-cycle re-entry through inhibitors in neurons does appear to be effective in reducing rates of neuronal cell-death following insults such as traumatic brain injury, ischæmia and excitotoxicity [289, 307]. The use of flavopiridol reduces the expression of Cyclin D1, in culture this can reduce re-entry and neuronal death in primary cortical cultures from genotoxic [289] and excitotoxic stress [307] in the cortex and hippocampus, and treatment proves protective against both neuronal cell death and reactive gliosis following traumatic brain injury in rodents [289]

However, a degree of re-entry into G1 also appears to be of use in actually repairing DNA damage in neurons [281, 308]. *In vitro*, high levels of ROS induce neuronal apoptosis, however, lower levels induced DNA damage without apoptosis, but with G1 entry via Cyclin-C-pRb activation [281]; this appears to be a requirement for NHEJ, as blocking entry through either Cyclin C or Cdc25A [281] or Cdk4/6 inhibition also blocks repair [308]. At the same time, forcing entry via suppressing p21 activity leads to the activation of NHEJ machinery without DNA damage, however, unless further progression is restrained by knocking down Cdk2, the neurons die by apoptosis within 24 hours [281].

The same appears to occur in vivo following exposure to ionising radiation [309]. Sub-lethal irradiation induces DNA damage in mice brains and transient transcription inhibition, but not widespread immediate apoptosis [309]. This is coupled with the expression of Cyclin D and p21 soon after insult, and still present and gradually diminishing, respectively, at later time points; suggesting that at these doses G1 entry does happen to perhaps enable repair, but the activation of p21 is sufficient to prevent further cycling and apoptosis [309]. Likely the degree of damage affects the balance of cell-cycle inhibition and progression. If low level damage is below the level sufficient to induce outright apoptosis, but is persistently generated or unable to be repaired, then it may activate the same downstream DDR pathways that occur in mitotic cells.

1.3.4 – Cell-Cycle re-entry in neurons is associated with cognitive impairment and neurodegenerative diseases

Neurons with cell-cycle reactivation are found at lower rates in non-diseased brain areas of neurodegenerative patients and control patients without cognitive impairment [310]. In fact the presence of this re-entry can be can be observed in patients with mild cognitive impairment (MCI), prior to any progression to clinical Alzheimer's diagnosis (MCI does not imply that they will progress

to AD, merely there is an increased likelihood); the frequencies of these neurons vary between 5 and 10% of pyramidal neurons (and less than 1% in non-demented controls) by *in situ* hybridisation of chromosomes [293], and by immune-histochemical staining of cell-cycle proteins [292].

This, as Yang *et al.* suggest, may mean that the re-entry to the cell cycle is not an event that occurs immediately prior to apoptosis. Given the known rates of neuronal loss in neurodegenerative disease, if this process occurred immediately prior to death, the chance of observing a neuron in this process at the time of fixation would be incredibly small. As the actual observed frequencies in fixed brains are much higher; this process must occur a considerable time before cell death, possibly months or years prior [293].

Neurons with replicated DNA are found at much lower rates in young wild-type mice, forming approximately 0.1-0.2% of neurons in the motor cortices and olfactory bulb of two-month old mice, as measured by X and Y-chromosome fluorescence *in situ* hybridisation (FISH) [311]. Many of these neurons appeared to maintain distal axonal connections, measured through FluoroGold retrograde tracer (10 to 50% depending on area). Immediate early gene expression is often taken as a measure of neuron activity, and a subset of these hyperploid neurons showed expression for gene products of Egr-1 and C-Fos. This suggests that these neurons are at least somewhat capable of function, at least at younger ages, which may explain why it is evolutionarily not preferable to immediately dispose of these neurons.

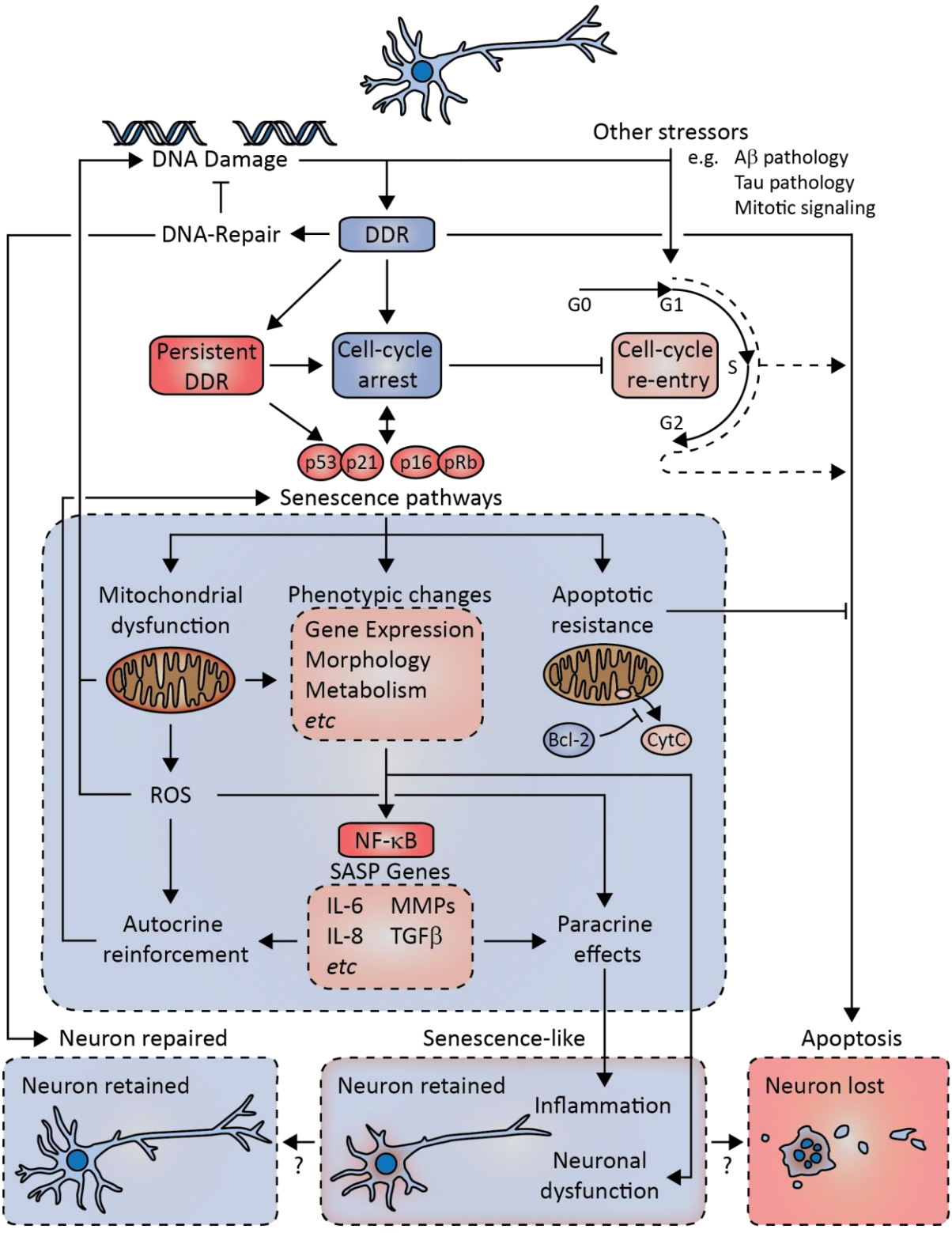

Figure 1.3.4.1: DDR in neuronal cell-fate decision and potential place of the senescence-like phenotype. The potential role of activation of a senescence-like phenotype in response to a DDR, and its relation to the decision between repair, cell-cycle re-entry and arrest, and apoptosis is shown. Replicated from Fielder et al. [196].

1.4 – Approaches for treating and targeting senescent and senescent-like cells

1.4.1 – Targeting the DDR

There are multiple strategies for targeting the DDR and senescence, and given that induction of the DDR and associated features can be seen in neurons, there may be cross-over between existing anti-ageing and anti-cancer treatments [Fielder 2017]. However, it can be a double edged sword, for example while too heavy a DDR can trigger apoptotic response, it also regulates pro-survival mechanisms. Indeed, ATM activation can protect against neuronal apoptosis through its suppression of cyclin D1 following damage [312], and using inhibitors actually promotes aberrant re-entry into the cell-cycle and neuronal death [313]. The same is true with p53; in line with this, the use of small-molecule inhibitors of p53, such as Pifithrin-beta *in vitro*, is effective in protecting neurons from exposure to Aβ fragments at low drug doses, but at higher doses is neuro-toxic [314]. This is potentially due to higher levels of inhibition blocking p53's pro-survival signalling, as p53 inhibitors have not been effective *in vivo* in reducing damage after ischæmia [314].

More *in vivo* success has been had with CdK inhibitors that block apoptotic cell-cycle re-entry [315] [316-318]. Anti-cancer drugs targeting the cell-cycle, such as the non-selective CdK Inhibitor Flavopiridol, have shown promising results in animal models [315]. These have shown promise in blocking cell-cycle re-entry in neurons in response to specific insults, such as neurotoxic colchicine [316], traumatic [317] and ischæmic brain injury [318]. This likely blocks the initial apoptosis and allows time for the levels of damage to be repaired, or reduced to a non-apoptotic level. Selective-inhibitors of CDKs, such as the E2F1-Cdk1 inhibitors have also reduced neuronal cell-death and activation of glia in the hippocampus following traumatic injury [319, 320] and have shown promise *in vitro* by reducing levels of Aβ production [321, 322].

1.4.2 – Treating Inflammation and COX-2

One of the major risks from senescent cells is due to their release of pro-inflammatory factors and spread through bystander action. The release of cyto- and chemo-kines should stimulate immune clearance of senescent cells through T-cell and macrophage action [228], however, with age it becomes increasingly difficult to keep the rate of clearance in line with the rate of accumulation. This is partially due to immunosenescence, and also from the 'run-a-way' effects of the bystander effect. The bystander effects can be blocked through the suppression of the SASP and ROS generation [122, 323]. The SASP is one of the most damaging aspects of DDR activation to the tissue micro-

environment. With both p16 and p53-p21, and activation of NF-κB, contributing to it [121, 265, 324, 325].

COX-2 is a downstream mediator of inflammation and is activated by DNA damage through p53 signalling [324], and pro-inflammatory cytokines via activation of NF-κB and JNK [326, 327]. COX-2 converts arachidonic acid into precursors for pro-inflammatory protanoids, such as Prostaglandin E2 [328]. The enzyme is not typically expressed in most tissues until inflammatory insult and is important in the mediation of inflammation and inflammatory cytotoxicity [329]. However, COX-2 expression is important for regular neurological functions such as neuro-transmission and long-term potentiation [330], while over-activity has pro-inflammatory effects and is linked to neurodegeneration [331]. Elevated levels of COX-2 have been observed in neurons together with phospho-Rb at early Braak stages in AD, prior to peak astrocyte and microglia expression [332, 333]. Further, COX-2 has been seen to co-localise with Cyclin D1 and Cyclin E expression in neurons in AD [334]. Together this suggests that COX-2 may be an important target in neurons that might be in a senescent-like state, and may prime or trigger glial activation.

In normal non-inflamed rodent brains, COX-2 expression is only really seen in small populations of excitatory neurons in the cortex, hippocampus and amygdala and is compartmentalised within these cells to post-synaptic dendrites [329]. However, with stress, such as neuro-inflammation and ischæmia, the levels of COX-2 and downstream products increase across the brain with neuronal damage, such as excito-toxicity, which can be reduced with the administration of COX-2 inhibitors such as NS-398 [331, 335]. Over-expression of COX-2 can induce oxidative stress in neurons and eventually apoptosis, additionally it has been associated with age-dependent declines in spatial memory, and anxiety [336].

COX-2 activity is associated with ROS production; however, oxygen radical species are not directly present in the catalytic pathways of COX-2, with production of other radical species, such as reactive carbon-centred radicals featuring instead [337]. Carbon-centred radicals produced by COX-2 can lead to lipid oxidation such as attack of Phosphatidylserine (a cytosolic cell-membrane Phospholipid), an effect that is countered through NS-398 administration [337]. COX-2 inhibition also counters the formation of the radical Dopamine-quinone [338], which is formed from Dopamine and is capable of attacking sulf-hydryl groups on glutathione and cysteine residues of proteins [339].

Early Non-Steroidal Anti-Inflammatory Drug (NSAID) studies suggest reduced risk of AD in later life [340, 341] and a possible protective effect in PD [342]. Chen *et al.* have investigated the incidence of

PD with NSAID use in approximately 150,000 people across 8 years [343]. The use of Ibuprofen resulted in a relative risk of 0.65 (95% CI: 0.46-0.88) for new cases of PD, showing little difference in the level of protection with sex, age or smoking. The level of risk reduction also appeared to depend on the dosage, increasing from a 30% reduction in risk with 2 tablets per week to 40% reduction in risk with every-day use. However, this effect appeared to be specific to Ibuprofen and they found no differences with other NSAIDs, such as Aspirin and Paracetamol. While generally showing improvements, the evidence for an exact effect is still mixed, with one study even finding that long-term non-aspirin NSAID appeared to be beneficial only in males, with the relative risk actually increasing in females [344].

1.4.3 – Killing senescent cells – Senolytics

If senescence-like neurons are contributors to cognitive impairment and neurodegeneration; then the emerging therapies that target cellular senescence in other tissue-types may be potential therapeutic candidates for these conditions. Many of these therapies are targeted primarily at alleviating the negative aspects of senescence such as the SASP while retaining the cell-cycle arrest [345], but others instead target and eliminate senescent cells themselves [346].

Even if these therapies have only limited direct effects on neurons, then the countering of senescence in glial and progenitor cell populations [347] should provide a positive benefit to cognitive function. Additionally, reductions in the whole-body senescent load should improve the circulatory environment [123, 124, 127] and reduce the infiltration of inflammatory molecules and immune-cells. This is particularly important in ageing, where the blood-brain barrier shows increased permeability (See Farrall & Wardlaw for meta-analysis [348]).

However, there are risks. Neurons are complex and far reaching structures, and any loss can have further effects via glial reactions and the release of intra-cellular factors, which may induce further damage. Yet, if the effect of these neurons is negative on the surrounding environment (promoting inflammation, mis-folding proteins, or inducing apoptosis in surrounding cells) and forms inflammatory feedback loops, then it may be worth this cost - akin to burning a fire-line to fight a forest fire.

1.4.3.1 – Pharmacogenetic clearance of senescent cells: The INK-ATTAC Mouse – Clearing senescent cells through transgenic kill-genes

The initial studies showing the role of cellular senescence in the ageing have relied on the pharmacogenetic targeting of senescent cells in transgenic mice [123, 124]. Although there isn't a true

universal marker of senescence, p16 is positive in many senescent cells and increases in multiple mouse tissues in aged mice, including areas such as the heart and cortex [349]. Additionally, the expression of p16 in the brain has been noted previously in neurons in Alzheimer's Disease [277, 279, 291]. Research so far has not been focused on the brain, and no cognitive deficits, or improvements, following senolytic clearance have been reported.

This pharmacogenetic approach [123, 124] involves replacing the promotor of dimerising caspase (a fusion protein consisting of the membrane bound dimersing protein, FK506-binding-protein and fused caspase 8, with a promotor region of p16 that is activated in senescent cells, together with eGFP under the same promotor control to visualise these cells (Termed INK-ATTAC). When a drug (AP20187) is added, which promotes the dimerization of FK506-binding-protein, the two caspase-8s are also brought together. This activates them and promotes apoptosis in cells where this is expressed. Thus, addition of the drug should selectively promote the apoptosis of cells expressing high levels of p16.

That the elimination of senescent cells can improve age-related declines in function was first shown by Baker *et al* in 2011 using INK-ATTAC mice bred on a prematurely ageing mouse, $BubR1^{H/H}$ [123]. $BubR1^{H/H}$ mice have a defect in BubR1, a protein kinase that is involved in the spindle checkpoint [350]. These mice present progressive aneuploidy and a number of 'premature ageing' phenotypes including a much reduced life-span, sarcopenia, reduced wound healing, dermal thinning and cataracts. p16 positive cells accumulate in tissues associated with these conditions in BubR1 mice [351]; knockout of p16 mildly improved life-span in BubR1 mice (but not wild-types), as well as ageing-associated phenotypes, including sarcopenia, cataracts and dermal thinning [351]. However, it also increased the rate of lung cancers, likely in relation to senescence and p16's role as a tumour suppressor.

Treatment with AP20187 after weening delayed onset of age-related pathologies previously associated with p16, such as sarcopenia and cataracts [351]. This delayed onset correlated with the burden of senescent cells. While treatment later in life was not particularly effective at resolving pathology already acquired, it did help to delay further degeneration. Interestingly there was no real effect in life-span after treatment, but they suggest this is accounted for by the mice dying primarily from cardiac failure (a common cause of death in the model), which was not affected by p16 removal.

While this shows that senescent cells drive accelerated ageing related pathology and that clearance is effective in what is essentially a severe disease condition, it did not answer if senescent cells truly drive 'natural' ageing. This has since been repeated in INK-ATTAC mice bred on a wild-type background, which showed an extension of median life-span and health-span [124]

1.4.3.2 – Pharmacological clearance of Senescent Cells

While highly promising, there is little prospect of implanting humans with such kill-genes, as identifying small molecule compounds that target senescent cells with a good degree of specificity is vital [346]. These drugs must be able to target and eliminate senescent cells, while not killing proliferating, quiescent or terminally differentiated cells. A number of these have been tested, targeting varying aspects of the senescent signalling pathway [252, 257, 346].

Transcript analysis of irradiation induced senescent cells by Zhu et al. 2015 identified a complex network of pro-survival and anti-apoptotic pathways active in senescent cells [346]. Many of these pathways centred around several key proteins, including p21, BCL-X_L and PI3Kδ. These were first targeted with silencing RNAs *in vitro* to suppress this activity. siRNAs for p21 and PI3KCD showed selective toxicity in senescent adipocytes, without significant harm to cell-viability or survival in non-senescent cells. However, siRNA for BXL-xL showed little effect in these cells, but was more toxic in senescent human umbilical vein cells (HUVECs), while p21 and PI3KCD were not. This showed that senescent cells could be targeted with a degree of specificity.

In vitro screening was performed with 46 compounds and identified Dasatinib, and Quercetin, as two promising senolytics. These are both already approved for human use in the United States by the FDA. Dasatinib is a Src family kinase and tyrosine kinase inhibitor used to treat cancer [352]. Dasatinib was able to selectively target pre-adipocytes in culture, but was not as effective against HUVEC cells. In contrast, Quercetin, a flavonol PI3K kinase inhibitor [353] reduced the viability of senescent HUVECs selectively at lower doses (0-10μM), with effects on proliferating cells beginning at higher doses (>20 μM), but with no effect on pre-adipocytes. Dasatinib and Quercetin combination therapy (DQ) proved effective in reducing the viability of both cell types. Short-term and single treatments have showed effectiveness *in vivo* in reducing the levels of cells with senescent markers in normally aged mice in the liver and fat, and also muscle of those exposed to acute irradiation of the leg. Furthermore, there was a degree of improvement in cardiac function (predominantly made up of post-mitotic cardiomyocytes) of aged mice and in the leg motor function of the irradiated mice. Long-term administration showed improvements in the healthspan of ercc1 mice, which have defective DNA repair, progeria and motor neuron degeneration [346].

Since then long-term DQ administration has shown promise in treating age-related diseases [354, 355]. Slight improvements in vascular function in aged mice and significant improvements in diseased hypercholesterolemic mice were observed, which matched the same pattern as in pharmacogenetic clearance in INK-ATTAC mice [354]. Additionally, early intervention in bleomycin-induced idiopathic pulmonary fibrosis with DQ and INK-ATTAC has been shown to improve lung-function and health

[355]. Other compounds such as ABT263 Navitoclax, a specific inhibitor of Bcl-2 and Bcl-xL [356, 357] have since been identified and tested *in vitro* and *in vivo*. Like Quercetin, Navitoclax has shown effectiveness *in vitro* against HUVECs, but not pre-adipocytes [356]. *In vivo*, it has shown effectiveness in reducing senescence in bone marrow and muscle stem-cell niches, and countering the premature ageing effects of total body irradiation [357].

The targeting of senescent cells via transgenic and chemotherapeutic mechanisms has shown great promise in delaying, preventing and alleviating diseases associated with senescence, and ageing itself [124, 354, 358]. However, there are a number of questions that remain to be answered in relation to the use of genetic and chemotherapeutic senolytic therapies in the brain. If senolytic treatments can target senescent-like neurons has yet to be established. INK-ATTAC models targeted against p16 may have some effect, as p16 activity has been observed in the neurons of patients with AD [277, 291, 359].

It is not yet clear if the senescent-like phenotype is simply a protective mechanism by the neurons to prevent cell-cycle related death, or if it can trigger negative effects through senescence-associated pathway induction. Indeed, p16 is capable of preventing neuronal cell death from elevated Cyclin D1 expression [360] and neurons with aneuploidy (which might have resulted through ACCR that has presumably since been arrested) are active to a degree, and maintain axonal connections to distant brain areas [311]. If they are still integrated and not harmful to network connectivity and function, then instead of trying to counter the negative effects of senescence-pathways, such as the production of SASP factors, would be preferential. So far, treatments in other post-mitotic tissues such as skeletal and cardiac muscle have shown improvements in function [123, 124], although whether this is through the clearance of senescent-like cells or through improvements to stem cell niches is not yet known.

1.5 - Aims and Objectives

Although an increase in senescent-like neurons can be seen with age, little is known about its role in brain ageing, inflammation or cognitive deficits. The general aim of this thesis is to understand the potential theoretical underpinnings of the senescent-like phenotype, and to understand if there is a link between senescent-like neurons and deficits in cognitive function.

Specific aims:

1) To characterise if ageing and chronic inflammation induce telomere dysfunction and the senescent-like phenotype in neurons, and if this is associated with the onset of neuro-inflammation and cognitive deficits.
2) To investigate if the clearance of senescent-like neurons could be achieved using pharmacogenetic and pharmacological methods that have shown efficacy in clearing traditionally senescent cells, and if this was associated with improved cognitive performance.

2.0 - Materials and methods

2.1 - Reagents and antibodies

Reagent	Supplier	Catalogue number
Aluminium potassium sulphate dodecahydrate >98%	Sigma	7210
Bovine Serum Albumin, >99.9	Sigma	A3059
Calcium chloride, Mw 147.02	VWR	10035-04-08
Citric acid, Mw 192.12	Sigma	C2404
De-ionised Formamide	Amresco	606
Formamide, Mw 45.04	Sigma	F-7508
Glacial acetic acid, 100%	BDH UK	1001CU
Glycerin	Sigma	G2289
Haematoxylin, Mw 302.28	Sigma	H3136
Halt Protease & phosphatase inhibitor cocktail (100X)	Thermofisher	78442
Histoclear 100%	LAMB UK	HS-200
Hydrogen peroxide, 30%	Fisher Scientific	H/1800/15
M.O.M. Kit	Vector UK	PK-2200
Magnesium chloride, Mw 203.30	BDH UK	101494V
Magnesium sulfate >99.9%	Sigma	203726
Maleic acid, Mw 116.07	BDH UK	103944L
NovaRed Substrate Kit	Vector UK	PK-2800
Paraformaldehyde 100%	Sigma	P6148
PBS 10x	Sigma	D1408
Potassium chloride, >99%	Sigma	P9541
Potassium Phosphate monobasic, Mw 136.09	Sigma	P5655
Roche blocking reagent	Roche	11 096 176 001
Sodium bicarbonate, Mw 84.01	Sigma	S5761
Sodium iodate, Mw 197.89	Sigma	S4007
Sodium phosphate monobasic, Mw 119.98	Sigma	S0751
Sucrose >99.5%, Mw 342.30	Sigma	S0389
Tris base, Mw 121.14	Sigma	T6066
Trisodium citrate, Mw 294.1	Sigma	S4641
Triton X100 100%	Sigma	T-9284
Vestastain Elite ABC (Rabbit IgG)	Vector UK	PK-6101
Xylazine hyrdochloride >99%	Sigma	X1251

Table 2.1.1: Reagents and suppliers

1° Antibody					2° Antibody		3° Antibody, Development Kit
Antigen	Provider		Species	Conc.	Info	Conc.	
γH2AX / P-Histone H2A.X (S139)	Cell Signalling	#9718	Rabbit	1:250	Goat Anti-rabbit, biotinylated	1:200	DCS-fluorescein (Vector Lab)
NeuN	Abcam	ab104224	Mouse	1:500	Goat Anti-mouse, Alexa 647	1:500	n/a
HMGB1	Abcam	ab18526	Rabbit	1:400	Goat Anti-rabbit, biotinylated	1:200	ABC kit (Horseradish Peroxidase), NovaRed (Vector Lab)
Iba1	Abcam	ab5076	Goat	1:400	Horse Anti-goat, biotinylated	1:200	ABC kit (Horseradish Peroxidase), NovaRed (Vector Lab)
Doublecortin/ DCX	Abcam	ab18723	Rabbit	1:250	Goat Anti-rabbit, biotinylated	1:200	ABC kit (Horseradish Peroxidase), NovaRed (Vector Lab)

Table 2.1.2: Antibodies and development systems

2.2 – Stock solutions

Solution	Ingredients
Citric Acid Buffer (0.01M) pH6.0	29.41g Trisodium Citrate, 1L Milli-Q H_2O. Kept at x10 stock at 4°C
Immuno-FISH hybridisation buffer	2.5µl 1M Tris pH 7.2, 21.4µl Magnesium chloride buffer, 175µl De-ionised Formamide (Amresco), 1µl Cy-3 CCCTAA peptide nuclei acid probe (Applied Biosystems), 12.5µl Blocking buffer (1:9 Roche Blocking re-agent in Autoclaved Maleic Acid) and 33.6µl deionised H_2O
Haematoxylin	5g Haematoxylin (Sigma), 300ml Glycerin (Sigma), 50g Aluminium potassium sulphate (Sigma), 0.5g Sodium iodate (Sigma), 40ul Glacial acetic acid (Sigma) in 700ml Milli-Q H_2O. Filtered before use.
Homogenate TRIS Buffer, pH7.4	6.61g Tris-HCl, 0.97 TRIS base in 500ml Milli-Q H_2O stock. Add 0.5% Triton X100 and 1% Protease inhibitor cocktail (Thermofisher; Halt Protease + Phosphatase Inhibitor cocktail) before use.
Magnesium chloride buffer pH7.0	25mM Magnesium Chloride, 9mM Citric acid, 82mM Potassium phosphate in Milli-Q H_2O
Maleic acid buffer pH7.5	100 mM Maleic acid, 150 mM NaCl in Milli-Q H_2O
Modified Artificial Cerbrospinal Fluid	10mM Glucose, 252mM Sucrose, 24mM $NaHCO_3$, 3mM KCl, 2mM $CaCl_2$, 2mM $MgSO_4$, 1.25mM NaH_2PO_4
Roche Blocking re-agent	Dissolved in maleic acid buffer to 10% (w/v). Stored at 4°C for use. Long-term storage at -20°C.
FISH Wash Buffer	70ml Formamide, 30ml 2xSSC
2xSSC pH7.0	0.3M NaCl, 0.03M Sodium Citrate, in Milli-Q H_2O
TRIS Buffer pH7.0	1M Tris base in Milli-Q H_2O

Table 2.2.1: Buffers and solutions used during this research

2.3 - Animals

Experiments in Chapter 4 were performed on male *nfkb1*$^{-/-}$ mice on a C57Bl/6 background and pure C57Bl/6 wild-type controls. Pure background C57Bl/6 mice were a gift from Jorge Caamano, (Birmingham University, UK). Mice were housed at the pathogen-fee barrier area of the Newcastle Animal House (Centre for Comparative Biology). Mice were observed regularly and euthanized when they showed tumours or morbidity, in accordance with the Guidelines for Humane Endpoints for Animals Used in Biomedical Research. *Nfkb1*$^{-/-}$ mice were genotyped by our collaborators according

the Jackson laboratory protocol for *nfkb1*$^{-/-}$ mice. Each mouse was weighed and measured once a week. Mice were housed in cages (56x38x18 cm, North Kent Plastics, Kent, UK) of groups of 4–6 that did not change from weaning. Mice were provided with saw dust and paper bedding and had adlib access to water. Mice were housed at 20±2 C under a 12 h light/12 h dark photoperiod with lights on at 07:00 hours.

For 8 month time-point mice, mice received Ibuprofen via pump (mini-osmotic pump, Alzet, model 2004) for a period of 2 months starting at 6 months of age. Ibuprofen was dissolved in PEG and DMSO (50:50) to a daily dosage of 50mg per kg. A small incision was made on the right flank and a mini-pump was inserted subcutaneously and the wound was repaired with 7mm clips. After 28 days a replacement was implanted. Under general anaesthesia, pumps were surgically removed and a wound repair was performed. A small incision was made on the left flank and a new mini-pump was inserted subcutaneously and the wound was repaired with 7mm clips. Mice were given Ibuprofen mixed in their food to a daily dosage of 50mg per kg (mouse) per day. For 18 month time-point mice, treatment was started at 9 months of age.

For the mice in the clearance of senescent cells on ageing and cognition study, INK-ATTAC transgenic mice were generated and genotyped, as previously described by Baker *et al.* [123]. INK-ATTAC mice were housed in groups of 2-5 at Mayo Clinic, Rochester, Minnesota. Mice were housed at 22±0.5C under a 12 h light/12 h dark photoperiod. INK-ATTAC transgenic mice were genotyped by our collaborators at Mayo clinic. Mice at 25-30 months of age were randomly assigned to vehicle, AP20187 and D&Q treated groups. These drugs are administered by different vectors. DQ (Dasatinib 5mg/kg, Quercetin (10mg/kg)) is given via oral gavage, while AP20187 (10mg/kg) is administered by intra-perineal injection. As such, all mice were given oral gavage and intra-perineal injection, and the appropriate treatment or vehicle (60% Phosal, 10% ethanol, and 30% PEG-400). Vehicle mice were treated with vehicle by both oral gavage and IP. DQ treated mice were given DQ by oral gavage, and vehicle by intra-perineal injection. AP20187 mice were treated with vehicle by oral gavage, and AP20187 by intra-perineal injection. Mice were treated intermittently, with 3 treatments in 1 week, every 2 weeks, for 2 months.Ethical approval was granted by the LERC Newcastle University, UK and IACUC at Mayo Clinic (Protocols A26415, A26713, A40312). All experiments were undertaken in compliance with UK Home Office legislation under the Animals (Scientific Procedures) Act 1986. Organs were either fixed in 4% paraformaldehyde or frozen in liquid nitrogen. Fixed tissues were processed and embedded in paraffin. All sections were cut at a thickness of 3 µm or 10µm.

2.4 – Mouse Cytokine/Chemokine array MD31

Brain tissue was frozen in liquid nitrogen at the time of harvest, and stored at -80°C was ground manually to a fine powder using a steel mortar and pestle. This was wiped clean between samples with 70% EtOH and cooled in liquid nitrogen. Powdered sample was stored at -80°C till homogenate preparation. 0.5ml Homogenate TRIS Buffer was added to powdered sample in a ceramic mortar and pestle, cooled in liquid nitrogen. They were manually ground together, and mixed until they formed a paste, then liquid. This was spun for 30 minutes at 16100 rpm. Supernatent was taken and stored at -80°C. This was adjusted to 5µg/ml and shipped to Eve Technologies Corporation, Calgary, Canada for mouse cytokine/chemokine array MD31 using a Multiplexing LASER Bead Assay.

2.5 - Behavioural Testing

2.5.1 - Y-Maze, Forced Alternation Protocol

A forced alternation Y-Maze set up was used. I built a symmetrical Y-maze using white plastic cut to measure. Each arm was 40 cm long, 8 cm wide, and 15 cm high with a curved lip to make it more difficult for the mouse to climb out. The end of each arm was marked with a black icon (+,▪, o). The home cage was moved into the room for one hour prior to testing to allow mice to acclimatise.

In acquisition, one of the arms (▪ or o) was blocked off by a white barrier. The mouse is placed in the home arm (+) and given 10 minutes to explore the two open arms of the maze (home and familiar). After this, the mouse was returned to the home cage for a 1 hour inter-trial period. Between runs, the maze was cleaned thoroughly with 70% EtOH between trials to remove odors. Up to 5 mice could be tested at a time.

After 1 hour, the mouse was placed in the home arm, with all 3 arms open and allowed to explore for 2 minutes. If the mouse climbs out of the maze, it was returned to the abandoned spot. Latency to novel arm, primary arm choice and time spent in each arm were recorded. Arm Discrimination Index was scored as the time spent in the novel arm, divided by the total time spent in both the familiar and novel arms.

2.5.2 - Barnes Maze

The maze consists of an open circular surface (diameter = 92cm), with a series of 20 holes (diameter = 5 cm) along the border and four visual markers at 0, 90, 180 and 270° positions (Square, Cross, Triangle or Circle) (Figure 2.5.2.1A). Theses visual markers are placed on the walls around the maze and the maze is elevated so that mice cannot exit via the sides (Figure 2.5.2.1B). Under one of these holes is attached the 'target box', which the mouse can enter and provides refuge from the bright and exposed open surface top (Figure 2.5.2.1C). The experiment requires the subject to learn the spatial position of this escape box relative to a number of visual cues positioned on the surrounding walls [361] (Figure 2.5.2.1D).

The mouse is placed in an opaque pipe (diameter = 11cm, height = 15 cm), in the centre of the maze and allowed 10 seconds to calm. The pipe is removed and the timer started. An over-head camera, linked to a DVD recorder and monitor, allows the performance of the mouse to be observed and recorded.

Each mouse is assigned one to one the four visual markers, under which the escape box will be placed during training (Figure 2.5.2.1E). In initial run, naïve mice are guided to the escape hole and allowed to rest inside for 2 minutes to acclimatise. The 'Acquisition phase' follows this, with mice running 4 trials per day, for 4 days. In each trial, the mouse is given 3 minutes to find and enter the escape hole. If the mouse does not find the hole in the allotted time then it is again guided to the escape hole. The mouse is allowed to rest in the target box for 1 minute. Between trials the board and escape box are wiped with 70% EtOH to remove odour trails.

As reported elsewhere [362], mice do not always enter the target hole after finding it and may proceed to either further explore the maze or sit at the entrance hole. To account for this, measurements were taken of the strategy, time and number of errors till first finding the target hole as suggested by Harrison *et al.* [361], these are referred to as the 'primary' parameters.

Primary errors, total errors, primary latency to find hole, total latency to enter hole, and search strategy were recorded. Errors were defined as head deflection and nose-pokes into 'false holes'. Search strategy was defined as 1) Direct – Moving directly to the target hole, or an adjacent hole prior to entry. 2) Serial – Finding the target hole after visiting at least two adjacent holes moving round the maze in a clockwise or counter-clockwise fashion. 3) Mixed – Search pattern involved moving across the centre of the board or seemingly random selection of search areas.

Short-term memory was tested on the fifth day in a 90s trial, without the target box present (Figure 2.5.2.1E). Long-term retention is tested in the same fashion on the twelfth day with no training between these trials (Figure 2.5.2.1E). Location and frequency of visited holes, site of initial visit and time spent in target quadrant were additionally recorded in short and long-term tests.

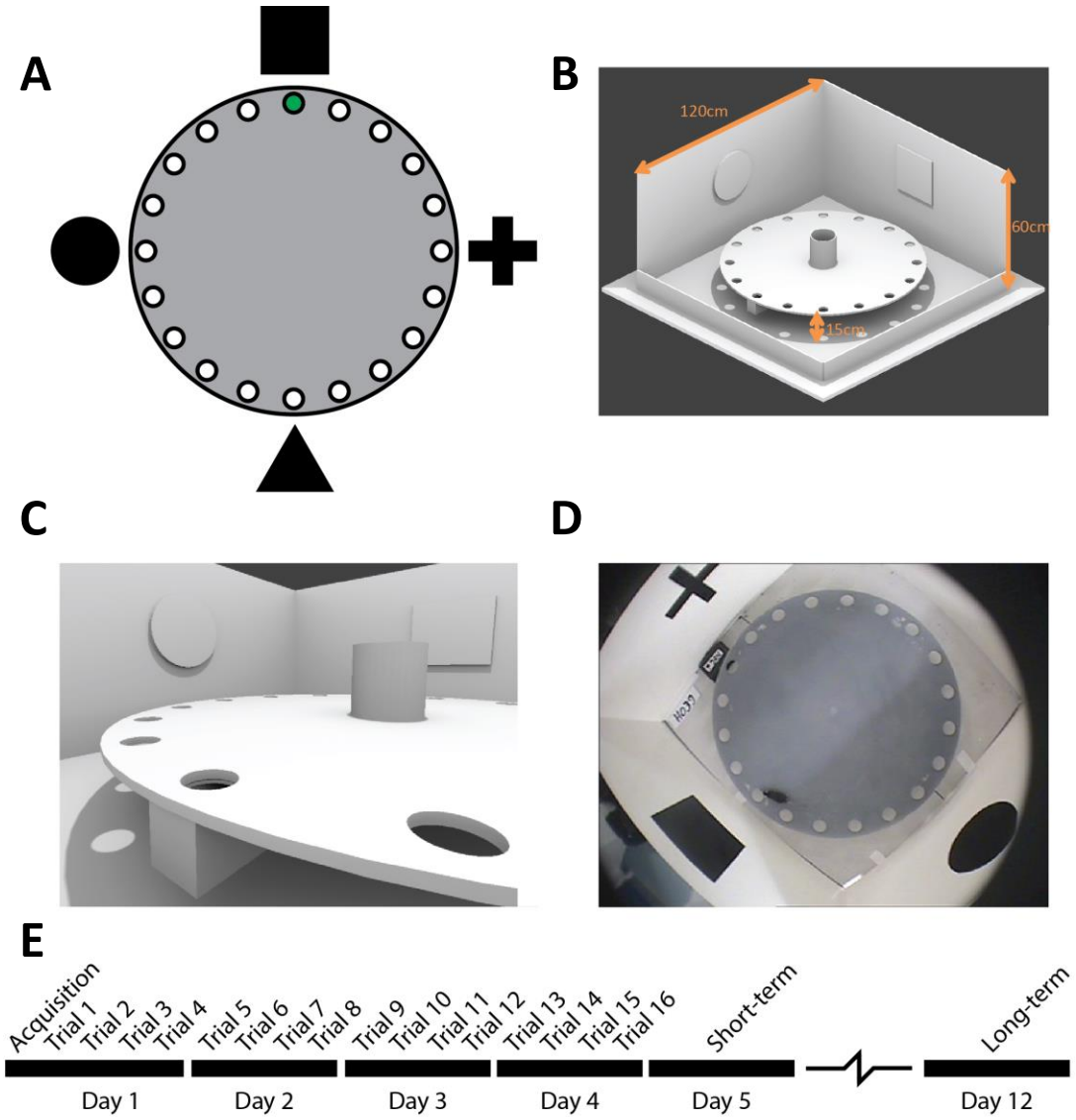

Figure 2.5.2.1 : Barnes Maze set-up and training parameters.

A) Graphical representation of the Barnes maze, showing the positions of visual reference points. **B)** Dimensions of the Barnes maze, walls are 120cm long and 60 cm high and the maze is 92cm in diameter and raised 15cm from the ground. The two closet walls are not rendered to show inside the maze. **C)** Positioning of escape box under target hole, and placement tube in centre of maze. **D)** Still capture from video of mouse in maze. **E)** Training and testing regime as divided by day. Training trials consist of 180 seconds to find and enter the target hole. Once entered, the box is closed and the mouse allowed to rest 2 minutes, it is re-trialled 1 hour late. During memory trials, the target box is removed and the mouse given 90 seconds to explore.

2.6 - Immunohistochemistry

2.6.1 – Immunohistochemistry protocol

Tissues were de-paraffinated and hydrated using two washes of Histoclear, followed by step-down series of ethanol (100%, 90%, 70%) and then twice in distilled H_2O, each step being 5 minutes per wash. Antigen retrieval was performed by incubation in 0.01M Citrate Buffer, microwaved for 4 minutes at 800W, then 10 at 450W, and allowed to cool to room temperature, before being washed in water.

Endogenous Peroxidase activity was blocked with 0.9% H_2O_2 for 30 minutes at RT. Samples were transferred to Phosphate-Buffered Saline (PBS) and drawn around with an immunopen. Blocking of non-specific binding was performed with 70µl per section of freshly prepared Normal Goat Serum (NGS) 1:60 in 0.1% Bovine Serum Albumin (BSA)/ PBS, for 30 minutes at room temperature in a humidified chamber (used for all subsequent incubations). This was followed by Avidin, Biotin blocking (each for 15 minutes, followed by PBS wash). Sections were then incubated over-night with primary antibody diluted in NGS/BSA/PBS at 4°C.

Sections were washed in PBS 3 times and incubated with biotinylated secondary anti-mouse goat antibody in NGS/BSA/PBS for 30 minutes, then washed 3 times in PBS. ABC complex was prepared to manufacturer's instructions 30 minutes prior to use. Sections were washed 3 times in PBS and incubated in freshly prepared NovaRed solution prepared to manufacturer's instructions.

Sections were then rinsed in distilled H_2O, placed in Haematoxylin to counterstain, rinsed thrice in distilled H_2O, placed in hot non-distilled H_2O for 30 seconds, then washed in distilled H_2O. Sections were dehydrated in 2x30 second 95% Ethanol, 2x30 second 100% Ethanol, 2x5min Histoclear and mounted with DPX.

2.6.1.1 - Staining specific modifications

For Iba1 and DCX stainings the following alterations were made. 10µm sections Paraffin embedded sections were used, rather than 3µm sections. Antigen retrieval was performed by incubation in 0.01M Citrate Buffer heated by 4 minutes at 800W, then 6 minutes at 450W, and allowed to cool to room temperature. This reduced separation of sample from the slide while preserving good signal to noise ratio. For goat primary antibodies locking solution used for blocking, primary and secondary antibody was freshly prepared 5% normal serum (of the secondary biotinylated antibody species) in PBS, for 30

minutes at room temperature. For Iba1 this was 5% Normal Horse Serum in PBS. For p21 staining, antigen retrieval time at 800W was increased to 30 minutes to increase antigen unmasking.

2.6.5 - Microscopy

Microscopy for Immunohistochemistry was performed with a Nikon Eclipse E-800 Brightfield Camera. Tile-scan images from the E-800 were stitched using Microsoft Image Composite editor, if required. For analysis of iba1^{+} cells a Leica DMi-8 in Brightfield mode was used for a x40 tile-scan of the hippocampus. This was split into CA3, CA1 and DG. The number of iba1^{+} in each area was recorded, and the area of each area. The final count was expressed as number of iba1^{+} cells per mm^2 in a 10µm slice. DCX^{+} cells were counted along the DG blade, and the length of the DG blade at the sub-granular zone recorded in mm. Final count was expressed as number of DCX^{+} cells per mm. For the wild-type and *nfkb1*$^{-/-}$ study, p21 immunohistochemistry was counted as positive for strong nuclear staining, or moderate to no staining. HMGB1 cells were quantified as positive or negative. These were expressed as a percentage of cells counted.

2.7 – Immunofluorescence

2.7.1 - γH2A.X Immuno-Fluorescence in situ Hybridisation

Tissues were de-paraffinated and hydrated using two washes of Histoclear, followed by step-down series of ethanol (100%, 90%, 70%) and then twice in distilled H_2O, each step being 5 minutes per wash. Antigen retrieval was performed by incubation in 0.01M Citrate Buffer, microwaved for 4 minutes at 800W, then 10 at 450W, and allowed to cool to room temperature, before being washed in water and transferred to Phosphate-Buffered Saline (PBS).

Blocking of non-specific binding was performed with 70µl per section of freshly prepared Normal Goat Serum (NGS) 1:60 in 0.1% Bovine Serum Albumin (BSA)/ PBS, for 30 minutes at room temperature. Sections were then incubated over-night with 1:500 mouse neural antibody NeuN (Abcam) in NGS/BSA/PBS at 4°C. From here all steps were performed in dark conditions to minimise sample bleaching. Sections were washed in PBS and incubated with secondary anti-mouse goat antibody (Alexa, 647nm) at 1:1000 in NGS/BSA/PBS for 30 minutes. Following PBS washes, non-specific blocking was performed for 30 minutes at room temperature with NGS/BSA/PBS, and Avidin, Biotin blocking (each for 15 minutes, followed by PBS wash). Sections were incubated in 1:250 primary rabbit γ-H2A.X antibody (Cell Signalling), NGS/BSA/PBS overnight at 4°C.

Sections were washed with PBS 3 times, and incubated in 1:200 biotinylated secondary goat anti-rabbit antibody (Vector laboratories) in NGS/BSA/PBS for 30 minutes at room temperature. Following PBS wash, Avidin DCS (Vector laboratories, 1:500 in PBS) was applied to the sections for 30 minutes then washed again in PBS. Cross-linking was performed using 4% Para-Formaldehyde/PBS for 20 minutes. Sections were washed in PBS and dehydrated using sequential 3 minute ice cold EtOH ethanol washes (70%, 90%, 100%) and then allowed to air-dry. 10µl of Hybridisation mix (2.5µl 1M Tris pH 7.2, 21.4µl Magnesium chloride buffer, 175µl De-ionised Formamide, 1µl PNA probe (Applied Biosystems), 12.5µl Blocking Buffer 1:9 Roche Blocking re-agent in Autoclaved Malic Acid and 33.6µl deionised H_2O) was applied and a cover-slip placed upon the slide, after which DNA denaturation was performed by placing sections in an 80°C oven for 10 minutes. Sections were placed in humidified chamber for 2 hours at room temperature. Sections were then washed in 70% Formamide/2xSSC for 10 minutes, 2xSSC 10 minutes, PBS 10 minutes on a mixing tray. Sections were mounted using VectorShield with DAPI (Vector laboratories).

2.7.1.1 - γH2A.X quantification

Microscopy for Immuno-fluorescent stainings was performed with a wide-field fluorescent microscope; a Leica DM-5500-B, fitted with a Leica DFC-360-FX camera, and attached to a desktop running Leica LASAF-2.1.0. Focal plane selection in fluorescence was selected using the DAPI channel, with z-stack bounds based on telomere probe focus. Images were stored as unaltered .lif for later measurement. Measurement of number of γH2A.X foci per cell, and number co-localising with telomeres was conducted under blinded conditions, with both the age and genotype of the animal masked. Neurons in the hippocampus were differentiated from glial cells based on location, morphology in the DAPI channel and by positive staining for the neuronal Abcam NeuN antibody, and Purkinje neurons by location, morphology and low intensity in the DAPI channel within the Cerebellum (as these cells do not express NeuN).

2.7.2 - Paraffin-Fixed Tissue Auto-fluorescence

Auto-fluorescence measurement was performed on paraffin-embedded slides from the brains of wild-type versus *nfkb1*$^{-/-}$ knockout mice. Slides were selected, where possible, based on the presence of the areas of interest, namely the Cerebellum, Hippocampus and Cortex. Unprocessed slides were used for Purkinje cells, due to their large soma. The smaller size of Hippocampal neurons necessitated the use of de-waxed and mounted slides to discern individual foci. Microscopy imaging of the slides was performed, using identical settings for lamp intensity, gain, lens aperture and f-stop between slides, with single image capture, at x20 magnification for Purkinje neurons and A4 filter cube (Band Pass

360/40nm, Barrier Filter Band Pass 470/40nm), and x40 for Hippocampal neurons. Imaging was performed in equivalent morphological locations within the areas of interest between slides.

Measurement was performed blinded of age and genotype; In hippocampal neurons, mean number of auto-fluorescent foci was counted per cell. In Purkinje neurons average image fluorescence was measured using a 'Region of Interest' tool to select cells of interest in Fiji (Image J derivative). Signal increases linearly with slide and wax thickness, small differences between sittings can occur due to differing lamp intensity even if exposure is kept standard. To account for this, the signal:noise ratio is used. Noise, or 'Background', correction is performed by taking multiple readings from the edge of the tissue, where only paraffin is present and dividing the signal by this value to obtain the ratio.

2.8 - RNA *In situ* hybridization (RNA*ISH*)

RNA*ISH* performed to specification using Formalin-Fixed Paraffin-Embedded Sample Preparation Pre-treatment Guide User Manual, Part 1 (Catalog No. 322452-USM) and RNAscope® 2.5 HD Detection Kit (RED) User Manual, Part 2 (Catalog No. 322360-USM). HybEZ Oven, with all required ACD reagents were used, with the following alteration. Slides were deparaffinised and hydrated using two washes of Histoclear, followed by step-down series of ethanol (100%, 90%, 70%) and then twice in distilled H_2O, each step being 5 minutes per wash. This was performed by Dr. Diana Jurk. Imaged and quantified by myself.

Sections were imaged at x40 using a Nikon Eclipse E-800 Brightfield Camera. Tile-scan images from the E-800 were stitched using Microsoft Image Composite Editor. The number of cells with positive foci, and total number of cells in each area (CA3 *pyramidale*, CA1 *pyramidale* and DG granular layer) was recorded. Cells with a glial morphology and dark neurons were excluded.

2.9 - Electrophysiology

2.9.1 - Isolated Hippocampus Slice Preparation

On the day of procedure a single mouse was separated from cage-mates and was transported by car to the preparation area. Animals were given 30 minutes to recover and anesthetised with inhaled isoflurane prior to intramuscular injection of Ketamine (≥100 mg kg^{-1}) and xylazine (≥10 mg kg^{-1}).

When all responses to noxious stimuli had ceased, the mice were intra-cardially perfused with ~25ml Modified Artifical CerbroSpinal Fluid (ACSF) [10mM Glucose, 252mM Sucrose, 24mM NAHCO3, 3mM

KCl, 2mM CaCl2, 2mM MgSO4, 1.25mM NaH2PO4]. Once perfused, the brain was removed and Cerebellum and Brainstem separated and stored in 4%PFA. The brain was sectioned using a Leica VT1000s into 450µM sections. These sections were trimmed to isolate the Hippocampus and transferred to a holding chamber were they rested for 1 hour at ~33°C, supplied by ACSF and humidified 95% O_2/5% CO_2. Brain removal and slice preparation was performed by Clare Tweedy, with assistance from myself.

2.9.2 - Oscillation Recording and analysis

For extra-cellular recordings, electrodes are filled with modified ACSF (resistance 2-5 MΩ). Recordings for gamma-frequency oscillation build up were taken in CA3 in the *stratum radiatum* (Figure 2.9.2.1A), with up to two electrodes per recording rig (Figure 2.9.2.1B). These were inserted by Clare Tweedy, while I monitored the rigs and recorded data. Administrating Carbachol, a cholinergic agonist, to isolated hippocampal slices stimulates synchronous low gamma-frequency neuronal oscillations originating primarily in CA3 and propagating to CA1 *stratum radiatum* [363, 364]. These oscillations persist for a number of hours, and in healthy slices will build in power and amplitude before stabilising at approximately 3-4 hours post-Carbachol administration. Carbachol was administered into the bath solution, and 60 second recordings were taken at set intervals for 3 hours (Figure 2.9.2.1C), and then until gamma oscillations stabilised (defined as 3 recordings in succession within 10% of each other, at or after 3 hours post-Carbachol administration). 1 second extract from Figure 2.9.2.1C can be seen in Figure 2.9.2.1D, showing oscillation). After the oscillations were stable, simultaneous measurements were taken between CA3 in CA1 of the same slice, in both *stratum radiatum* and *stratum lacunosum moleculare*. Propagation of the signal to CA1 was recorded

Recordings were taken with an Axoclamp-2B amplifier (AxonInstruments Inc., Union City, CA, USA). Extracellular recordings were filtered at 0.001–0.4 kHz using Bessel filters. Noise from the mains electricity was subtracted from the signal using a Humbug (Digitimer, Welwyn Garden City, Herts, UK). Data were re-digitized at 10 kHz using an ITC-16 interface (Digitimer, Welwyn Garden City, UK). Data were recorded and analysed using Axograph software (Axon Instruments Inc., Union City, CA, USA).

60 second recordings of activity were passed through a Fast Fourier transformation in Axograph to provide power spectra (Figure 2.9.2.1E). Area power for slow gamma oscillations was defined as area under the curve between 15 and 45Hz. Frequency was defined at the peak of the oscillation. Oscillations were determined as stable at or after 3 hours, when within ±10% for three consecutive measurements of 10-15 minute intervals. Once slices stabilised, further measurements were taken in radiatum and pyramidal layer of CA3 and CA1. The rhythmicity of the oscillation was measured by

correlating the generated gamma frequency oscillations to a time-lagged version of itself, which shows how consistent the repeated oscillation is. Oscillation rhythmicity was measured from auto-correlations performed in MATLAB 2012, with the peak was normalised to 1. Cross-correlations compared simultaneously recorded oscillations in CA3 and CA1, recorded by moving two electrodes to the same slice, and placing one in each area.

Data were analysed in Sigmaplot v12.5. P of <0.05 is taken as significant. Build-up data was assessed with 2-way repeated measures analysis of variance, with time and group (wild-type, *nfkb1*$^{-/-}$ untreated, *nfkb1*$^{-/-}$ treated) as factors. Differences between genotype and treatment were assessed by 2-way ANOVA without interactions. If the P-value indicated a significant difference, a Holm-Sidak post-hoc test was used to determine which parameters likely varied.

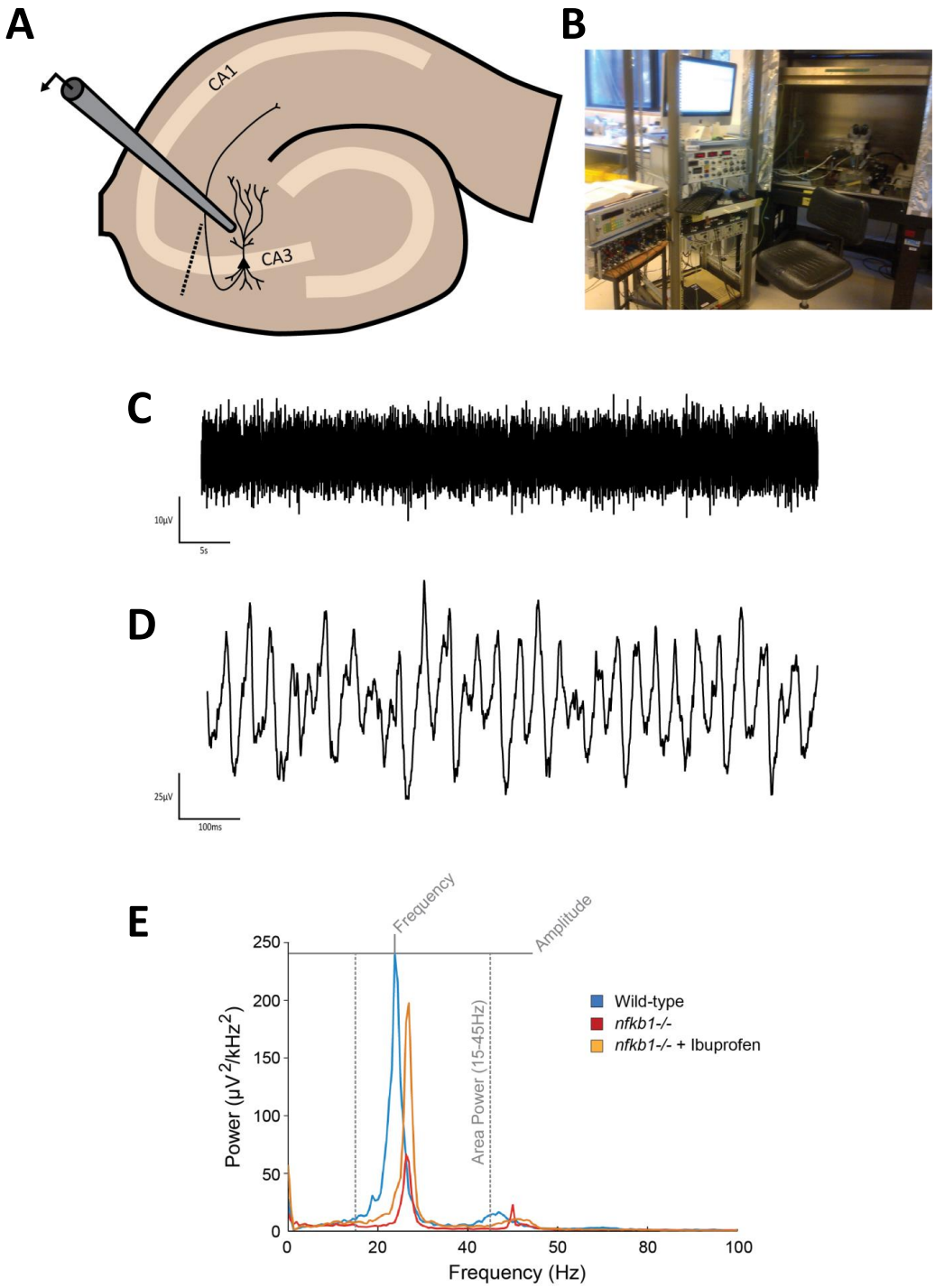

Figure 2.9.2.1: Recording of traces and power spectra from isolated hippocampal slices.

A) Diagram of placement of electrode into stratum radiatum of CA3 in an isolated slice. **B)** Image of set-up electrophysiology rig **C)** Example 60 second epoch from stable-time point. **D)** Example extract of 1 second epoch from trace shown in **C)**. **E)** Representative power spectra following fast-fourier transformation of 60 second epoch trace recordings extracted from stable time-points in CA3 *stratum radiatum* wild-type, *nfkb1* knockout and *nfkb1* knockout treated with Ibuprofen. Area power is measured as the area under curve between 15-45Hz and provides a measure of the strength of the gamma-frequency oscillation. Amplitude in the power of the maximum point of the power-spectra. Frequency is the frequency of the maximum amplitude.

3.0 – Neuro-inflammation, cognitive deficits and senescent-like neurons in a model of chronic inflammation

3.1 - Introduction

Neuro-inflammation is linked to the onset of cognitive impairments and neurodegenerative diseases. Senescence is known to have an important role in inflammation through the release of SASP factors and IL-6 production has been observed in senescent-like neurons. However, the association between senescence-like neurons, inflammation and cognitive deficits has not yet been assessed.

3.1.1- NF-κB in the brain and inflammation

NF-κB is made up from a family of sub-units, as discussed in the introduction. Inducible and active NF-κB family complexes are expressed in the cytoplasm of nearly all cells [365]. NF-κB transcription factors control the expression of over 500 genes, with both physiological and pathogenic roles [366]. Constitutively active NF-κB activity can be seen in glutamatergic neurons, such as granule and pyramidal cells of the hippocampus, and in the cortex [365, 367]. Inducible complexes are also found localised at synapses [368], and respond to synaptic transmission to alter gene expression through retrograde transport to the nucleus after glutamatergic stimuli, leading to activation [369]. It also has a neuro-protective role; blocking NF-κB using recombinant adenovirus induces cell-death [370], and it can be activated by insults such as cerebral ischæmia and excitotoxicity, altering the expression of apoptotic proteins and reducing the amount of neurons that die [371, 372]. However, NF-κB activity is also strongly associated with inflammation and age-dependent changes in gene expression [373, 374].

Chronic activation of NF-κB can drive ageing through increased inflammation, and increased levels of senescent cells [127]. Activity of the NF-κB transcription cassette is induced by a wide-range of insults, these can be immune challenges, such as viruses, LPS and cytokines, as well as from oxidative stress and DNA damage [375, 376]. NF-κB itself regulates a broad-range of genes, inducing the expression of pro-inflammatory cyto- and chemokines, and enzymes such as COX-2 [366, 377]. Many of these factors are key parts of the SASP, and NF-κB activation has a central role in senescence [232, 234]. Evidence of constitutive activation of NF-κB can be seen in a number of chronic inflammatory and immune diseases, including in the CNS in conditions such as AD [378-381].

There is evidence of increased NF-κB activity in the brains of aging mice, where it is associated with

increased release of cytokines such as IL-6 from glial cells [382]. Increased translocation to the nucleus and activity of NF-κB is seen in vulnerable neurons in neurodegenerative diseases, such as dopaminergic neurons in PD [383]. Increased NF-κB activation has been seen to increase alongside COX-2 in the brain of ageing humans and in sporadic AD [380]. NF-κB has low basal activity in glia, and remains largely in an inducible state in unchallenged glia cells [384]; however, it is activated in disease conditions such as AD and ischemia, where it regulates inflammation [384]. NF-κB activity in astrocytes following injury induces CCL2 expression and the infiltration of circulating leukocytes [385]. In microglia, NF-κB regulates the release of pro-inflammatory and pro-oxidative bio-reactive molecules, with over-activation causing and exacerbating degeneration [386].

3.1.2 - *Nfkb1*$^{-/-}$ knockout mice

Nfkb1$^{-/-}$ mice have constituently active NF-κB through the loss of the p50 subunit [387]. The subunits in the *nfkb1* gene (p50/p105) lack transactivation domains and can act as active repressors of NF-κB's pro-inflammatory action [388]. p50:p50 homo-dimers actively repress the transcription of many pro-inflammatory genes [389]. p50 mediates the recruitment of the transcriptional repressor histone deacetylase 1 (HDAC1) to various inflammatory genes containing κB binding motifs, and its loss promotes dysregulation of inflammatory gene transcription [376, 390]. Knockout of this subunit leads to the wide-spread constitutive activation of the pro-inflammatory NF-κB gene cassette, and sterile peripheral inflammation in ageing [127].

The mice appear to develop properly, but show accelerated ageing after development and a significantly shortened lifespan [127, 387]. *Nfkb1*$^{-/-}$ mice show accelerated accumulation of senescent cells in mitotic tissues, which is understood to further contribute to the chronic sterile inflammation and promote the premature ageing seen in the model [127]. The *nfkb1*$^{-/-}$ mouse model shows increased oxidative stress, mitochondrial H_2O_2 production, DNA damage associated telomere dysfunction and increased numbers of senescent cells in mitotic tissues at 9 months of age compared to age-match wild-type controls. In fact, the changes appear indicative of an accelerated ageing phenotype, with the 9 month *nfkb1*$^{-/-}$ mice presenting a similar phenotype to 24 months old wild-types [127]. This results in a much reduced life- and health-span compared to C57Bl/6 wild-type mice.

It has also been reported that these animals show less neuronal apoptosis following ischæmia than wild-type mice [391]. However, after exposure to the neurotoxin Trimethlytin they show increased neuronal degeneration and mortality [392]. *Nfkb1*$^{-/-}$ mice appear more vulnerable to excitotoxic damage from kainite, and in culture show increased oxidative stress after glutamate exposure [393].

Degeneration has also been reported in the optic nerve following axonal injury in the retina [394]. There is some evidence that *nfkb1*$^{-/-}$ mice undergo age-related neurodegeneration [395]. At 6-10 months of age there is a trend towards reduced brain-volume and weight in *nfkb1*$^{-/-}$ mice, a slight reduction in NeuN positive cells in the hippocampus and cortex [395]. Increased lipofuscin was reported in electron microscopy images, as well as increased TUNEL positive cells, caspase-3 immuno-staining and 'dark neurons', in the hippocampus.

There are several papers describing cognitive function in *nfkb1*$^{-/-}$ mice, however, they have been performed on young animals at ages between 1.5-4 months. Reduced anxiety related behaviours such as defecation and increased exploratory activity has been reported at 2 months (B6,129 background) in novel environment tests [396]. However, in 2-3 month old mice on a C57Bl/6 background increased anxiety in open-field and light/dark tests has been reported, mediated by corticosterone [397]. Further, *nfkb1*$^{-/-}$ mice showed improved acquisition and memory in the Morris Water Maze; however, this is a stressful experiment and *nfkb1*$^{-/-}$ showed significantly higher corticosterone levels after the test which may lead to an increased drive to find the platform [397]. The use of the lower-stress Barnes maze in the same paper showed no difference in acquisition or memory at 2-3 months in *nfkb1*$^{-/-}$ mice compared to wild-type controls [397]. Other experiments using the Morris Water Maze have shown a slight trend for improved acquisition at 2 months, but reduced memory of the platform location in subsequent trials [398], and no differences at 3-4 months [399]. So far these experiments have focused on the innate roles of p50 in areas such as neurogenesis [399] or showed links to altered LTP in the hippocampus [398], and have not looked in relation to the sterile inflammation and progeria phenotype of the mice.

3.2 - Overview of Study Plan

To evaluate the effect of *nfkb1* knockout and chronic sterile inflammation on cognitive function and the senescence-like phenotype, I used several cohorts of C57Bl/6 wild-type and *nfkb1*$^{-/-}$ mice at different time points, with short- and long-term Ibuprofen intervention (Figure 3.2.1A). Wild-type and *nfkb1*$^{-/-}$ (on a C57Bl/6 genetic background) mice were housed in a pathogen-free environment.

Some wild-type and *nfkb1*$^{-/-}$ mice were harvested at 3 months of age for tissue analysis (Figure 3.2.1A I). At 6 months of age, wild-type and *nfkb1*$^{-/-}$ mice had mini-pumps surgically implanted that supplied constantly either a vehicle or ibuprofen, replaced every 4 weeks, for 2 months. These mice were then harvested at 8 months of age (Figure 3.2.1A II). As mice that were treated with ibuprofen via minipumps showed difficulties in wound-closing after implantation and future treatments were instead administered by mixing ibuprofen in soaked food placed in the cage (Figure 3.2.1A III-IV). Mice were treated with this soaked diet (± ibuprofen) starting at 3 months of age, and used for electrophysiological characterisation at 8 months (Figure 3.2.1A III). Long-term ibuprofen in soaked food treatment begun at 9 months until the end of the experiment when they were harvested for tissues. At 17 months of age spatial memory was tested using the Barnes Maze and mice were then harvested after, at 18 months of age (Figure 3.2.1A IV).

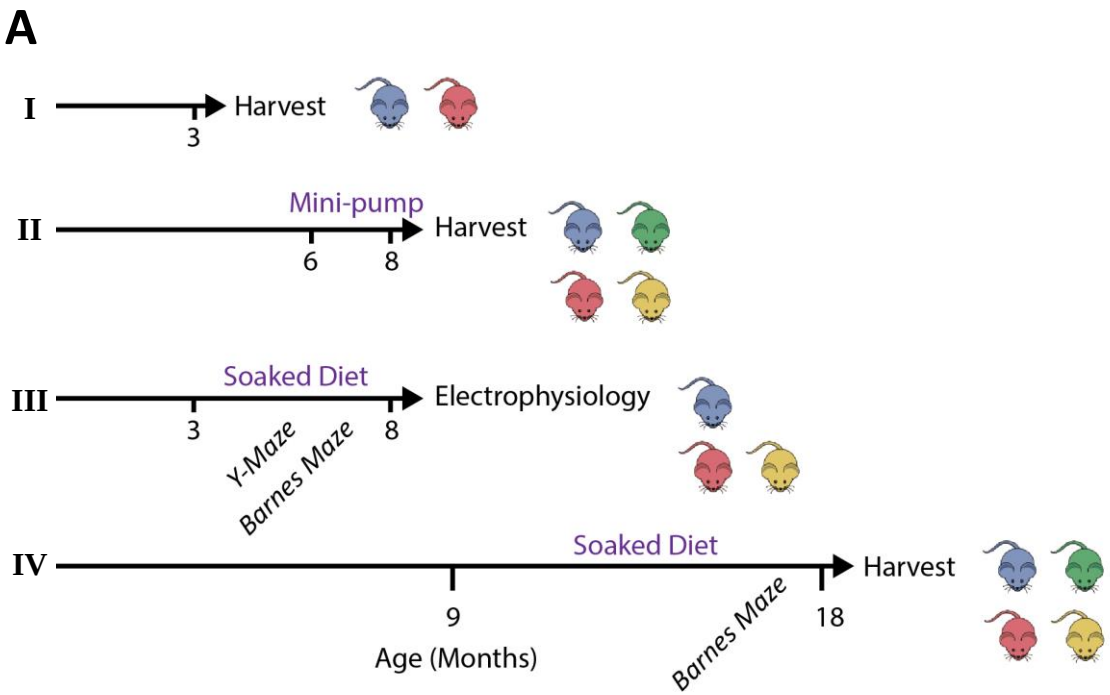

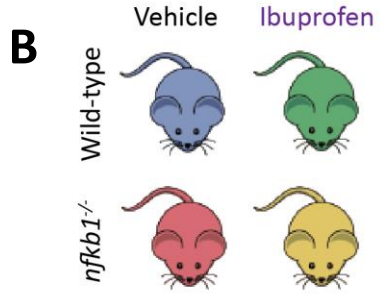

Figure 3.2.1: Study plan

A) Shows overview of timelines for treatments and harvest points. **A_I)** Wild-type and *nfkb1*$^{-/-}$ mice were harvested for post-mortem analysis at 3 of age. **A_{II})** Wild-type and *nfkb1*$^{-/-}$ mice were surgically implanted with a mini-pump that administered ±ibuprofen at 6 months of age. This delivered either vehicle, or Ibuprofen, at a constant rate into the mouse for 2 months before the mice were harvested. **A_{III})** Wild-type and *nfkb1*$^{-/-}$ mice, and *nfkb1*$^{-/-}$ mice fed with ±ibuprofen for 5 months, were used for electrophysiology at the age of 8 months. **A_{IV})** Wild-type and *nfkb1*$^{-/-}$ were treated with soaked diet for 9 months starting at 9 months of age containing ±ibuprofen. **B)** Mice are colour coded (for easy tracking in the following Figures) by genotype and treatment, with blue used for untreated wild-type mice and red for *nfkb1*$^{-/-}$ mice, and green for ibuprofen treated wild-types and yellow for ibuprofen treated *nfkb1*$^{-/-}$ mice.

3.3 - Ageing *nfkb1*$^{-/-}$ mice have increased neuro-inflammation

3.3.1 - Increased inflammatory cytokines in *nfkb1*$^{-/-}$ brains at 18 months of age, and rescue with Ibuprofen

Neuro-inflammation can be observed in neurodegenerative conditions and has been associated with cognitive impairment [400]. However, there appears to be a requirement for 'priming' or vulnerability and an additional inflammatory insult. In humans aged people experience greater cognitive declines than the young following inflammatory insults [94-96]. Systemic and ventricular administration of LPS in aged mice leads to deficits in working memory [401][94] and increased expression of pro-inflammatory genes, such as IL-1B and IL-6 [93]. However, these effects are reduced, or absent, in animals that are not already 'primed' by either ageing [93] or prion disease [401]. Chronic NF-κB activation is known to drive systemic sterile inflammation and ageing [127], but the effects on the brain and, if there is a link between this inflammation and cognitive performance, is not entirely understood.

To test whether inflammation also affected the brain of *nfkb1*$^{-/-}$ mice a cytokine array was performed on whole brain homogenate for 5 mice per group at the ages of 8 and 18 months (Figure 3.3.1.1A). At 8 months of age, *nfkb1*$^{-/-}$ mice did not show significantly elevated levels of cytokines in the brain compared to young wild-type mice. Ageing *nfkb1*$^{-/-}$ mice showed up-regulation across a broad-spectrum of inflammatory factors in the brain (Figure 3.3.1.1A).

IL-6 was significantly upregulated in aged *nfkb1*$^{-/-}$ mice, compared to wild-type controls (Figure 3.3.1.1B). Ageing *nfkb1*$^{-/-}$ mice also showed a significant up-regulation of IL-6 between 8 and 18 months of age, while wild-type mice only showed a trend. Ibuprofen treatment at 18, but not 8 months, showed a trend for reduced levels, but was still significantly higher than age matched wild-type controls (Figure 3.3.1.1B).

RANTES (also known as chemokine C-C motif ligand (CCL) 5, CCL5) was significantly up-regulated in ageing *nfkb1*$^{-/-}$ mice compared to wild-type mice. Again, this also showed a significant up-regulation with age in *nfkb1*$^{-/-}$ mice, but not wild-type mice (Figure 3.3.1.1C). Here there was a significant reduction with Ibuprofen treatment in aged *nfkb1*$^{-/-}$ mice, but not at 8 months. However, the levels were still significantly higher than age matched wild-types controls.

Eotaxin (also known as CCL11) was also significantly higher in ageing *nfkb1*$^{-/-}$ mice than wild-type controls (Figure 3.3.1.1D). Here there was a significant reduction with Ibuprofen treatment in aged

nfkb1$^{-/-}$ mice, but only a trend for an increase at 8 months. No change with age was observed in wild-type mice.

Monocyte chemoattractant protein-1 (MCP-1), also called CCL2, was significantly higher in ageing *nfkb1*$^{-/-}$ mice than wild-type controls (Figure 3.3.1.1E). Ageing *nfkb1*$^{-/-}$ mice also showed a significant up-regulation of IL-6 between 8 and 18 months of age, while wild-type mice only showed a trend. There was a significant increase in 8 month *nfkb1* knockout mice treated with ibuprofen compared to their untreated litter mates, but a significant reduction at 18 months.

Macrophage colony-stimulating factor (M-CSF) was significantly upregulated in ageing *nfkb1*$^{-/-}$ mice, compared to age matched wild-type controls and 8 month *nfkb1*$^{-/-}$ mice (Figure 3.3.1.1F). Ibuprofen significantly reduced the levels of M-CSF at 18 months in *nfkb1* knockout mice, but had no effect at 8 months.

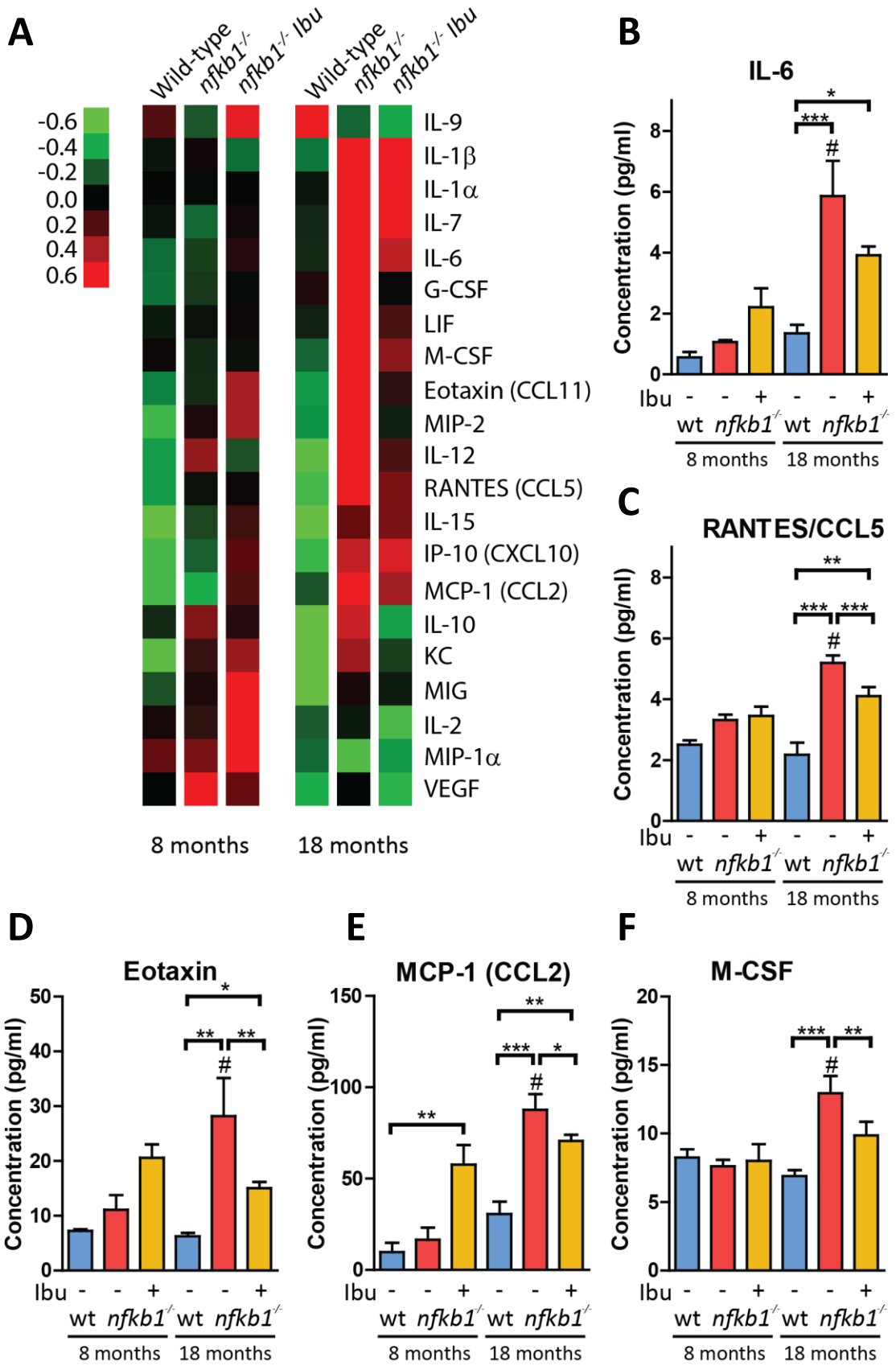
A
Wild-type
nfkb1-/-
nfkb1-/- Ibu
Wild-type
nfkb1-/-
nfkb1-/- Ibu
-0.6
-0.4
-0.2
0.0
0.2
0.4
0.6
IL-9
IL-1β
IL-1α
IL-7
IL-6
G-CSF
LIF
M-CSF
Eotaxin (CCL11)
MIP-2
IL-12
RANTES (CCL5)
IL-15
IP-10 (CXCL10)
MCP-1 (CCL2)
IL-10
KC
MIG
IL-2
MIP-1α
VEGF
8 months
18 months
B
IL-6
Concentration (pg/ml)
Ibu - - + - - +
wt nfkb1-/- wt nfkb1-/-
8 months
18 months
C
RANTES/CCL5
Concentration (pg/ml)
Ibu - - + - - +
wt nfkb1-/- wt nfkb1-/-
8 months
18 months
D
Eotaxin
Concentration (pg/ml)
Ibu - - + - - +
wt nfkb1-/- wt nfkb1-/-
8 months
18 months
E
MCP-1 (CCL2)
Concentration (pg/ml)
Ibu - - + - - +
wt nfkb1-/- wt nfkb1-/-
8 months
18 months
F
M-CSF
Concentration (pg/ml)
Ibu - - + - - +
wt nfkb1-/- wt nfkb1-/-
8 months
18 months

Figure 3.3.1.1: *Nfkb1*$^{-/-}$ mice show increased neuro-inflammation with age, ameliorated by long-term dietary Ibuprofen treatment

A) Secreted protein array of inflammatory and SASP related factors obtained from brain homogenates at 8 and 18 months of age in wild-type, *nfkb1*$^{-/-}$ and *nfkb1*$^{-/-}$ treated with Ibuprofen for 2 and 9 months. Extract of data for **B)** IL-6; **C)** RANTES; **D)** Eotaxin; **E)** MCP-1; **F)** M-CSF. Data are mean of 5 animals per group. Significant differences from One Way Analysis of Variance (Holm-Sidak Post-hoc) shown by * <0.05, ** <0.005, *** <0.001. Difference between ages within genotypes <0.05 shown by #.

3.3.2 - Nfkb1$^{-/-}$ mice show increased density of microglia as well, as activation, with age in the hippocampus.

Given the central role of the hippocampus in spatial learning and memory, and the results of the cytokine array, characterisation of microglia was performed in the hippocampus of wild-type and *nfkb1*$^{-/-}$ at 3, 8 and 18 months of age. Microglia were marked using Iba1, a membrane bound calcium binding protein that is expressed specifically in microglia in the CNS [402].

Microglial are extremely motile and adaptable cells, switching not only their expression of secreted factors, but also their morphology and role in response to differing stimuli [103]. Microglia continuously monitor their environment, extending and retracting their processes, and physically sensing surrounding neurons, glial and vascular cells [403, 404]. Microglia in this state are termed 'ramified' or 'resting' microglia and possess a small, oval-shaped, soma and long, branching processes. Ramified microglia have direct effects on the cells they contact, such as pruning synapses to aid in synaptic plasticity and learning [405]. However, when challenged they shift towards primed and activated states. When activated microglia undergo morphological changes, with a swelling of the soma and retraction of cellular processes. Microglial processes quickly converge on injured lesions [404], and this is accompanied by proliferation towards the site [406]. Normally this should shield the injured site and microglia will phagocytose debris, while secreting factors to promote repair of damaged cells. However, chronic, or excessive, activation can be harmful, leading to secretion of pro-inflammatory factors and neuronal damage [406]. Proliferation of microglia can be seen in models of neurodegeneration, and when blocked slows disease progression [407]. With age microglia become increasingly primed, or 'reactive', and shift towards a more inflammatory phenotype [109]. Microglia isolated from ageing brains express higher levels of pro-inflammatory cytokines such as IL-6 and IL-1β, leading to an amplified response when activated [104].

Microglia were assessed using Ionised calcium binding adapter molecule, Iba1 (Figure 3.3.2.1A). Microglial density differs across the brain, and even in specific sub-structures of the hippocampus, with differences in density between areas suggested as a contributor to differential dysfunction between areas [408]. As such, the hippocampus was subdivided into 3 areas, with the area and number of microglia recorded and used to calculate density. These areas were CA3+CA2 (referred henceforth in this chapter as CA3), CA1 and DG, as all have unique roles in memory function and spatial processing [409]. For CA3 and CA1, the pyramidal layer and associated *stratum* were included, and for DG, granular, molecular and polymorph layers were included.

An age dependent increase in microglial density could be observed in *nfkb1*$^{-/-}$ mice (Figure 3.3.2.1B-D). At 8 and 18 months the density of microglia in CA3 (Figure 3.3.2.1B) and CA1 (Figure 3.3.2.1D)

areas in *nfkb1*$^{-/-}$ mice was significantly higher than in wild-type mice. In the DG there was again an effect with age, but *nfkb1*$^{-/-}$ mice did not show significantly higher levels until 18 months (Figure 3.3.2.1D). Long term treatment until 18 months did have a significant effect on microglial density in the CA3 and DG, but not CA1, in *nfkb1*$^{-/-}$ mice, but not wild-type mice.

Whether this increased density of microglia is accompanied by increased activation of microglia was assessed next (Figure 3.3.2.1D). The size of microglial soma can be used as a measure of microglial activation, and increases significantly during microglial activation [410]. Due to the high density of Iba1 positive cells within the CA3+CA2 in *nfkb1*$^{-/-}$ animals, and its role in encoding spatial memory and pattern recognition [52, 55], analysis of soma size was performed here. While significantly increased density of microglia had been observed in the CA3 at 8 months of age onwards, there was no significant change in microglial activation until 18 months of age (Figure 3.3.2.1D). Untreated *nfkb1*$^{-/-}$ mice showed a significant increase in soma-size, which was ameliorated by treatment with Ibuprofen. This suggests that by 18 months, there is activation of microglia that might, at least in part, contribute to the observed increased release of inflammatory factors. However, that there is no shift towards activation until 18 months in the *nfkb1*$^{-/-}$ mouse does suggest that there may be another factor that accumulates prior to this, and activates microglia.

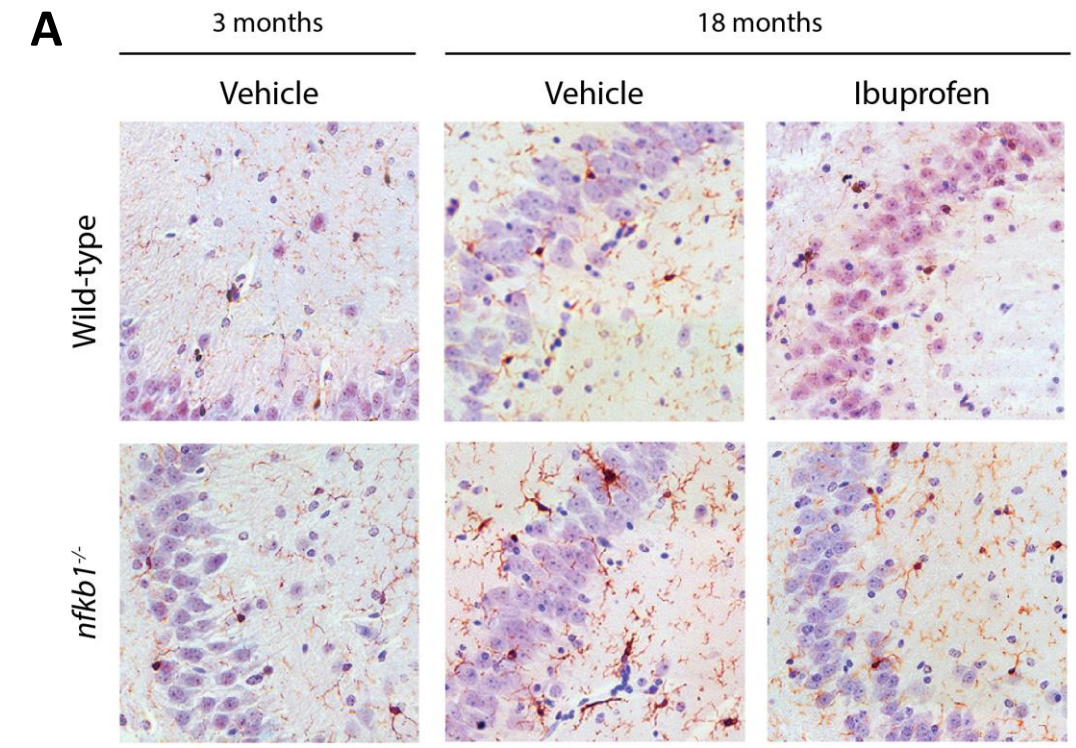
A
3 months
18 months
Vehicle
Vehicle
Ibuprofen
Wild-type
nfkb1-/-

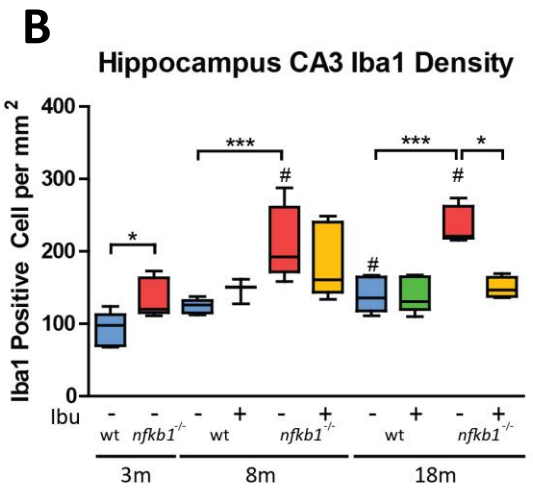
B
Hippocampus CA3 Iba1 Density
Iba1 Positive Cell per mm 2
400
300
200
100
0
***
*
***
*
#
#
#
lbu
- - - + - + - + - +
wt nfkb1-/- wt nfkb1-/- wt nfkb1-/-
3m
8m
18m

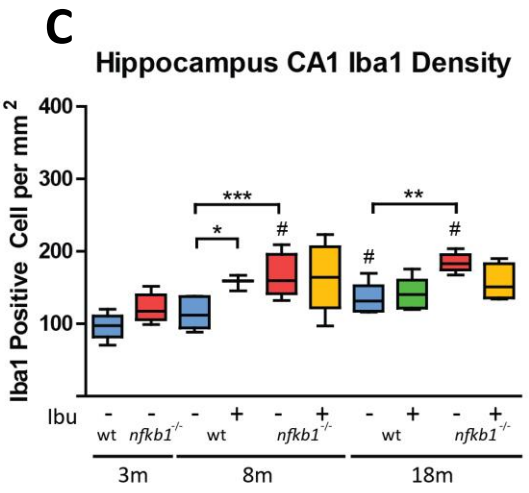
C
Hippocampus CA1 Iba1 Density
Iba1 Positive Cell per mm 2
400
300
200
100
***
*
**
#
#
#
lbu
- - - + - + - + - +
wt nfkb1-/- wt nfkb1-/- wt nfkb1-/-
3m
8m
18m

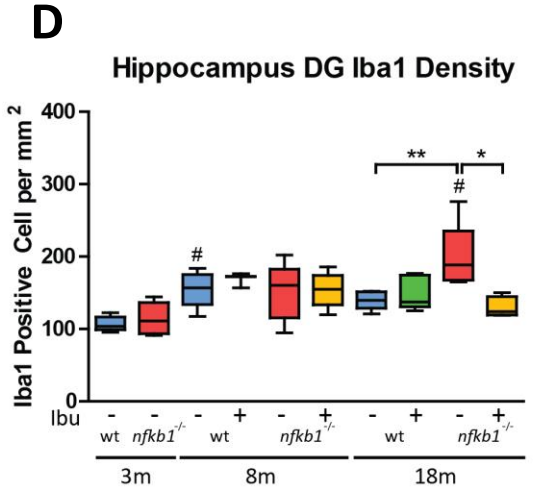
D
Hippocampus DG Iba1 Density
Iba1 Positive Cell per mm 2
400
300
200
100
0
**
*
#
#
lbu
- - - + - + - + - +
wt nfkb1-/- wt nfkb1-/- wt nfkb1-/-
3m
8m
18m

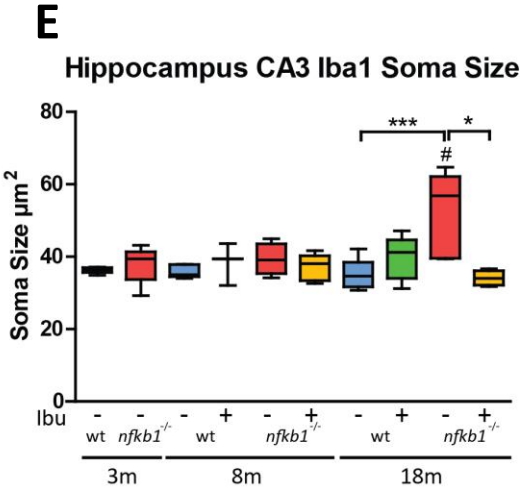
E
Hippocampus CA3 Iba1 Soma Size
Soma Size µm 2
80
60
40
20
0
***
*
#
lbu
- - - + - + - + - +
wt nfkb1-/- wt nfkb1-/- wt nfkb1-/-
3m
8m
18m

Figure 3.3.2.1: *Nfkb1*$^{-/-}$ mice show increased density of microglia with age and microglial activation in the hippocampus.

A) Representative images of Iba1 staining using NovaRed (Brown) and Haematoxylin (blue) to counterstain in wild-type and *nfkb1*$^{-/-}$ mice at 3, 8 and 18 months, with and without ibuprofen. Quantification of iba1 positive cells in wild-type and *nfkb1*$^{-/-}$ mice at 3, 8 and 18 months, with and without Ibuprofen, in the **B)** CA3m **C)** CA1 and **D)** DG. **E)** Quantification of mean soma size of Iba1 positive cells in the CA3. 2-way ANOVA (Holm-Sidak) for age and genotype. Treatments are compared by two-tailed Mann-Whintey U. Significant differences between genotype, as well as treatments, at each age point are displayed by (* $p<0.05$, ** $p<0.005$, *** $p<0.001$), significant difference with age by (# $p<0.05$).

3.3.3 - *Nfkb1*$^{-/-}$ mice show reduced neurogenesis, but no significant differences after Ibuprofen treatment

It has been suggested that adult neurogenesis reinforces the *Dentate Gyrus*'s role in spatial pattern separation between similar stimuli, as required in the Barnes Maze, to effectively differentiate and recall the correct information [411]. Additionally, there has been an observed link between neurogenesis and factors seen up regulated here, e.g. Eotaxin and MCP-1 (Figure 3.3.1.1), as well as in parabiosis experiments between young and old mice [412]. In those experiments the increases in cytokines, including Eotaxin and MCP-1, was associated with declining neurogenesis and impairments in cognitive function [412]. Injections of Eotaxin were sufficient inhibit neurogenesis and radial arm maze performance [412].

Doublecortin was used as a marker for neurogenesis, and its modulation by experimental procedure [413]. Doublecortin is a microtubule associated protein that marks precursor and immature neurons in the dentate gyrus (Figure 3.3.3.1A). It is expressed by dividing neuronal precursors and in neurons early in their maturation, with levels declining 7-30 days after neurogenesis, while mature neuronal markers such as NeuN become increasing expressed in the same period [414].

An age dependent decline was found in both wild-type and *nfkb1*$^{-/-}$ mice (Figure 3.3.3.1B). However, *nfkb1*$^{-/-}$ mice showed decreased levels of neurogenesis compared to wild-type mice. Ibuprofen treatment by mini-pump for 2 months had no significant effect at 8 months of age in either wild-type or *nfkb1*$^{-/-}$ mice. At 18 months, 9 months of treatment with Ibuprofen showed a trend for improvement, but this was not significant. A negative correlation between density of microglia in the dentate gyrus and DCX positive cells was observed (Figure 3.3.3.1C).

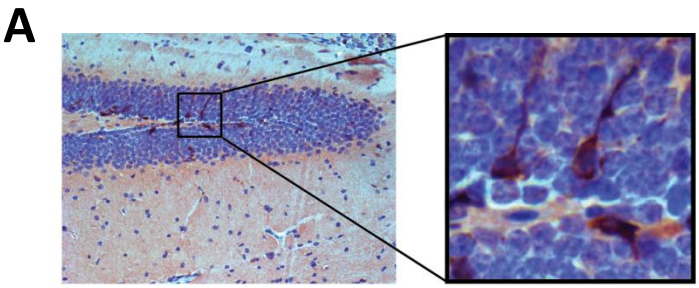
A

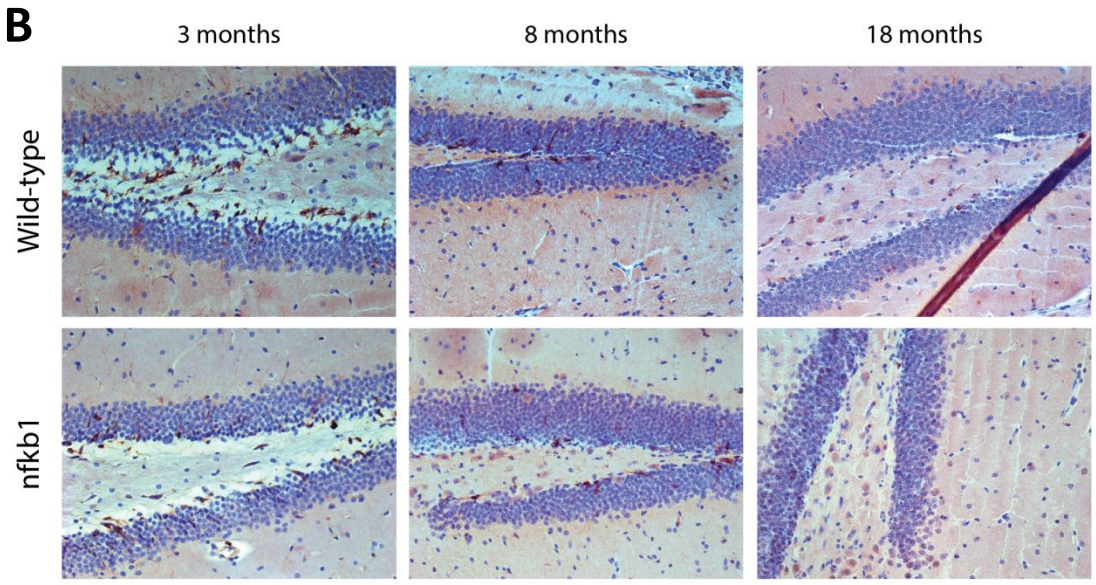
B
3 months
8 months
18 months
Wild-type
nfkb1

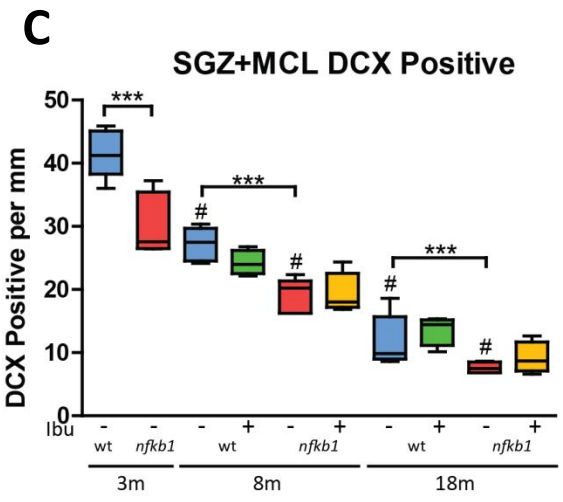
C
SGZ+MCL DCX Positive
DCX Positive per mm
50
40
30
20
10
0
***
***
***
#
#
#
#
Ibu
-
-
-
+
-
+
-
+
-
+
wt
nfkb1
wt
nfkb1
wt
nfkb1
3m
8m
18m

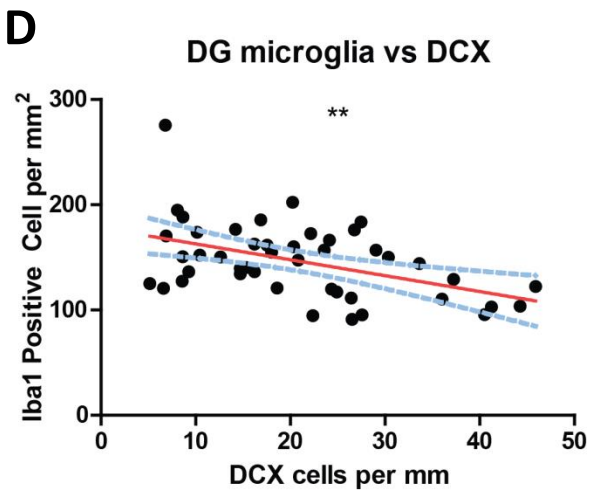
D
DG microglia vs DCX
Iba1 Positive Cell per mm2
300
200
100
0
**
0
10
20
30
40
50
DCX cells per mm

Figure 3.3.3.1: Assessment of neurogenesis in the brains of wild-type and *nfkb1*$^{-/-}$ mice at 3, 8 and 18m, with and without NSAID Ibuprofen treatment

A) DCX marks immature and precursor neuronal cells, here shown in the Dentate Gyrus stained by NovaRed (brown) and counterstained by Haematoxylin in blue. **B)** Representative images of DCX staining in the Dentate Gyrus of wild-type and *nfkb1*$^{-/-}$ mice at 3, 8 and 18 months, with and without ibuprofen. **C)** Quantification of DCX positive cells per mm of DG blade of wild-type and *nfkb1*$^{-/-}$ mice at 3, 8 and 18 months, with and without Ibuprofen. 2-way ANOVA (Holm-Sidak) for age and genotype. Treatments are compared by two-tailed Mann-Whintey U. Significant differences between genotype, as well as treatments, at each age point are displayed by (* $p<0.05$, ** $p<0.005$, *** $p<0.001$), significant difference with age by (# $p<0.05$). **D)** Correlation between microglial density in the DG and DCX positive cells. Significance tested by two-tailed Spearman correlation coefficient (** $p<0.005$, by Gaussian approximation).

3.3.4 - Discussion

Previous work by the lab has shown increased chronic sterile inflammation in the periphery of *nfkb1*$^{-/-}$ knockout mice, and that this drives tissue ageing and the onset of age-associated pathologies [127]. However, how well this inflammation extends to the CNS with age is not well characterised. We hypothesised that increasing neuroinflammation may occur with age in *nfkb1*$^{-/-}$ mice, and this could drive dysfunction in the brain.

As discussed previously, the loss of the p50 subunit in these mice leads to low-level elevation of inflammation from lack of p50:p50 homodimers and loss of the ability to recruit HDAC1 to genes containing the κB motif, reducing competition for activating p65 containing dimers [376]. This leads to dysregulation of multiple pro-inflammatory genes, including CCL2/MCP-1 and GM-CSF [376]. Significant up-regulation of IL-6 can be seen with age in blood plasma in *nfkb1*$^{-/-}$ mice, compared to wild-type mice [127]. While this initially matches wild-type mice at 4.5 months, by 9 months of age levels are significantly increased. In the liver at 9 months of age, this is accompanied by increased infiltration of immune cells and significant upregulation of mRNA, as well as proteins, in a range of inflammatory cytokines, including IL-6, MCP-1, Eotaxin (CCL11) and RANTES (CCL5). In contrast, in the whole-brain homogenate at this age-point, only a trend for a mild increase in pro-inflammatory cytokines was observed in untreated *nfkb1*$^{-/-}$ mice. This could be due to protection of the brain from passive diffusion of circulating cytokines by the blood-brain barrier (BBB). However, peripheral cytokines can stimulate BBB vascular endothelial cells, leading to expression of prostaglandin E synthase and COX-2 and promoting pro-inflammatory cytokine release [415]. Many cytokines, including IL-1α and IL-1β, IL-6, can be actively transported across the blood brain barrier by a variety of transporters [416]. It may be that while circulating plasma levels increase, local production of cytokines in these brains is not significantly up-regulated at this time-point. Yet by 18 months, upregulation of in a wide-range of pro-inflammatory factors could be seen in the brains of *nfkb1*$^{-/-}$ mice. Many of these cytokines point towards the involvement of microglia.

Microglia are the resident immune cells in the brain, and they respond to challenge from both the periphery and CNS in a variety of ways, releasing bioactive molecules, and promoting both repair and degeneration [105]. MCP-1, for example, mediates microglial activation, and a decline in neurogenesis, following cranial irradiation [417]. Microglial proliferation and activation was assessed primarily in the hippocampus, with differentiation between different sub-fields. The counts in the dorsal hippocampus are comparable to those previously published on Iba1 positive cells in young mice, once differences in sectioning and counting techniques are considered [408]. Here I found a small, but significant increase in the CA3 and CA1 sub-regions of the hippocampus in normally ageing

wild-type mice. I found mixed results when searching for existing literature on microglial density in C57Bl/6 mice with ageing. Previous reports in C57Bl/6 mice showed a slight trend for increase by 13-14 months in the CA1, which is similar to what I observed [106]. The trend in the DG here was also not significant, which does match their results, and those reported by Mouton *et al.* in male C57Bl/6 mice [107]. It should be noted that both of these studies stained for complement receptor 3, while I used Iba1, and different stereological methods were used.

Nfkb1$^{-/-}$ mice showed an increased density in microglia number compared to wild-type mice, first in the CA3 at 3 months, followed by the CA1 at 8 months, and in the DG by 18 months. This could be explained by increased proliferation of microglia. Progressive increases in Iba1 positive microglial density in the CA1 can be seen in C57Bl/6 mice injected with brain homogenate from two models of prion disease (ME7 and 22L) [407]. This increased density likely comes from increased proliferation of microglia, as treatment with the cell-cycle inhibitor cytosine arabinoside reduced the number of proliferating cells and prevented an increase in the number of microglia. Interestingly, this promoted activation of these microglia and increased neuro-degeneration in the CA1 of ME7 treated mice [407]. This could reflect the changes seen in *nfkb1*$^{-/-}$ mice, with microglia proliferating in response to damage and inflammatory signals at earlier ages, but not becoming activated at this stage. The increased density in the prion model mice above was regulated by colony-stimulating factor-1 receptor, activating the transcription factors PU.1 and C/EBPa [407]. This receptor is activated by M-CSF/CSF1, which contains an NF-κB consensus element in its promotor. M-CSF was significantly upregulated in *nfkb1*$^{-/-}$ mice, and like microglia levels, downregulated with ibuprofen treatment. Altered *nfkb1*$^{-/-}$ signalling could promote the transcription of this and promote the microglial proliferation.

However, this was also not upregulated till 18 months and increased density was seen prior to this. In line with the inflammatory cytokine arrays, microglia in CA3 of *nfkb1*$^{-/-}$ mice showed a significant increase in activation or priming, as measured by soma hypertrophy, at 18 months of age, but not before. While in normal ageing, as discussed above, the total number of microglia does not appear to increase, priming and inflammatory cytokine release does [109]. This is accompanied by expression of major histocompatibility complex class II molecules and receptors such as complement receptor 3 and retraction of dentritic processes as measured by Iba1 [109]; with ~25% of microglia from ageing BALB/c mice (18-20 months) being MHC II positive, compared to <3% in young adult BALB/c mice as measured by flow-cytometry (3-4 months) [418]. The increased priming or activation seen in *nfkb1*$^{-/-}$ mice could represent an acceleration of age-associated changes, and may explain the increased release of cytokines seen at this point; as microglia from aged mice brains exhibit greater basal levels of cytokine release, and while the fold change in expression in response to stimuli such as LPS remains

the same, this leads to a sum increase in pro-inflammatory cytokine release, together with difficulty switching to a less inflammatory state [104, 109].

nfkb1$^{-/-}$ microglia also appear to have an altered response to inflammatory insult to *nfkb1*$^{+/+}$ microglia, but this regulation is complex. Work from *Rolova et al.* suggests that *in vitro* microglia cultured from *nfkb1*$^{-/-}$ knockout mice show an altered response to LPS, with reduced levels of IL-6, MCP-1 and IL-10 [419]. This is surprising, given that loss of p50 can be thought of in relation to the loss of NF-κB inhibition by the p50:p50 homo-dimer, and since p50 mediates the binding of transcriptional repressor histone deacetylase-1 to MCP-1 [376]. Instead, the loss of the ability to form the p65:p50 dimer appears to result in a loss in the capacity to respond directly to LPS via canonical NF-κB signalling, and decreased production of IL-6 and MCP-1 is seen compared to *nfkb1*$^{+/+}$ microglia [419]. Yet, *in vivo*, injection of LPS in the periphery induces a pro-inflammatory microglial phenotype in *nkfb1*$^{-/-}$ mice, with an increase in inflammatory cytokine production [419].

Rolova *et al.* suggest that while loss of p50 in microglia naturally shifts their phenotype from M1 to M2 in response to LPS due to alterations of canonical NF-κB signalling, a secondary pro-oxidative or pro-inflammatory stimuli from another source triggers an increased pro-inflammatory response *in vivo*. This can be seen in the case of LPS injection, where it was attributed to the increased infiltration of neutrophils, and their production of ROS, triggering the release of TNFα and IL-6 via the JNK pathway and preventing the shift to an M2 state [419]. However, the same increase in pro-inflammatory response was reported when *nfkb1*$^{-/-}$ mice were crossed with APP-transgenic AD mice, but no increased neutrophil infiltration was reported, leaving the interacting cell that promotes pro-inflammatory activation of microglia in *nfkb1*$^{-/-}$ unknown [419].

Work from Taetzsch *et al.*provides additional evidence [420]. They also reported an increased and longer lasting pro-inflammatory cytokine response following (this time peripheral, not central) LPS injection, together with increased M1 microglial morphology. This was reduced with treatment with the radical scavenger 5,5-Dimethyl-1-Pyrroline-N-Oxide, supporting the role of ROS in mediating microglial activation in *nfkb1*$^{-/-}$ mice. In contrast to Rolova *et al.*, using cultured microglia from *nfkb1*$^{-/-}$ mice, they reported an increased and longer lasting pro-inflammatory cytokine release compared to *nfkb1*$^{+/+}$ microglia. The main difference that I can find here is that when harvested, these are actually mixed astrocyte/microglia cultures, and while Rolova *et al.* separated microglia from this culture, Taetzsch *et al.* does not. Increased astrocytosis has been observed in *nfkb1*$^{-/-}$ mice by 11 months of age [421], and this additionally implicates astrocytes as a potential source of ROS that trigger prolonged M1 activation in *nfkb1*$^{-/-}$ microglia.

Given that the increases in microglial density in *nfkb1*$^{-/-}$ mice occurred first in the CA3, and were then followed by other areas of the hippocampus at later time-points, it is possible that there is localised cytokine signalling that cannot be detected at the whole brain level. Neurons in the CA3 are vulnerable to age-related changes such as hyper-excitability [39, 68], and this could trigger, possibly initially protective, localised microglial proliferation. Neurons can provide an activating stimuli to microglia through factors such as M-CSF and MCP-1, following focal brain injury [422] and impaired oxidative metabolism [423], these are initially produced by neurons and trigger the initial microglial activation and proliferation. Additionally, localised increased microglial proliferation and priming can be seen due to DNA damage accumulation from DNA damage repair deficiencies in specific populations of neurons [424]. As such, there are multiple potential initial triggers that might lead to sustained *in vivo* activation of microglia in *nfkb1*$^{-/-}$ mice.

I observed a decrease in both pro-inflammatory cytokines, microglia proliferation and hypertrophy, with long-term dietary ibuprofen (a COX inhibitor) treatment at 18 months in *nfkb1*$^{-/-}$ mice. Which could suggest that these increases in *nfkb1*$^{-/-}$ mice occur, at least partially, through COX mediated pathways. There are a number of potential explanations for how COX-2 activity and inhibition could mediate the observed changes. The decreased microglia activation could be accounted for by reduced systemic inflammation, infiltration of immune cells and inflammatory cytokines, as decreased infiltration of CD3+ cells has been observed in the liver of 8 month *nfkb1*$^{-/-}$ mice with 2 months Ibuprofen treatment [127]. Additionally, inhibition of COX (1 and/or 2) by ibuprofen in BBB vascular endothelial cells, may reduce the generation of prostaglandins stimulated by systemic inflammation, that stimulates inflammatory signalling in the brain [415].

Ibuprofen also appears to be blood brain barrier permeable [425], and could have a direct effect on microglia, as well as cells that may trigger their activation, such as astrocytes and neurons. Activated microglia show increased COX-2 expression through NF-κB signalling [426]. However, Taetzsch *et al.* reported (although did not show the data) no effect on COX-2 expression in *nfkb1*$^{-/-}$ mixed glia culture compared to *nfkb1*$^{+/+}$ mixed glia culture, or in BV2 microglia treated with *nfkb1* siRNA [420]. This could suggest that the effects are not mediated by an intrinsic effect of altered NF-κB signalling on COX-2 levels in microglia in *nfkb1*$^{-/-}$ mice. However, ibuprofen could still directly target microglia, as ibuprofen can induce S-phase cell-cycle arrest and apoptosis of microglia *in vitro* in BV2 microglia [427]. Which would explain the reduced cytokine release, and proliferation and activation of microglia in 18 month ibuprofen treated *nfkb1*$^{-/-}$ mice.

Increased COX-2 activity has also been reported in astrocytic gliosis [428]. Ibuprofen treatment has shown reduced astrocyte activation in Dementia with Lewy-bodies transgenic mice [428]. Reduced

astrocyte activation could reduce the triggering of microglial activation, given that their presence, and the production of ROS, was required for activation of *nfkb1*$^{-/-}$ microglia in culture [419, 420].

Additionally, there may be changes in COX-2 expression in neurons as a result of altered NF-κB signalling. While COX-2 has a physiological role in neurons [429], increased COX-2 activity has neurotoxic effects and can be seen early in neurodegenerative diseases, such as Alzheimer's [333, 380] and in normal ageing [380], and is associated with NF-κB DNA binding to the COX-2 promotor [380]. Neuronal COX-2 is an NF-κB target gene, and p65 and COX-2 can be seen *in vivo* in neurons, with suppression of both by aspirin [377]. COX-2 promotor activity in *in vitro* neuroblastoma cell lines is dependent on NF-κB, and COX-2 is strongly upregulated by NF-κB inducing stimuli [377]. Loss of p50 could potentially lead to persistent upregulation of COX-2 activity in neurons, which ibuprofen may reduce. However, it should be noted that p50 was also active together with p65, and it is uncertain how the loss of this sub-unit would affect COX-2 activity in neurons. In mitotic cells *nfkb1*$^{-/-}$ knockdown appears to promote NF-κB activation of COX-2 and the production of ROS [127]. The same could be happening in neuronal and astrocyte cells here with COX-2 activity promoting ROS generation and triggering microglial activation in untreated *nfkb1*$^{-/-}$ mice, and with a reduction in ibuprofen treated *nfkb1*$^{-/-}$ mice.

However, in the brains of 8 month mice, *nfkb1*$^{-/-}$ treated with Ibuprofen for 2 months by mini-pump there was an trend for increase in levels of IL-6, Eotaxin, IL-2, IL-9, and a significant increase in MCP-1, with but no significant effect on microglial parameters. The exact cause for this is unclear; however, Ibuprofen treatment in the mini-pump treated animals (both wild-type and *nfkb1*$^{-/-}$) did lead to problems with surgical wound healing, and re-opening of the wounds. In mice infected with Vibrio vulnificus, ibuprofen treatment has been reported to lead to increased levels of IL-6, IL1β, TNF-α and MIP-2 [430]. While the mice are in low pathogen conditions, it was not quarantine level, and an open wound around the pump may have contributed to infection or increased sterile inflammation.

Analysis of neurogenesis was also performed in these mice. Upregulation of Eotaxin and MCP-1 has been reported by Wyss-Coray's research group in their parabiosis studies of young and old mice [412]. They identified a number of factors, including Eotaxin and MCP-1, that were elevated in normal old mice, and young mice that had been joined to an old-mouse via parabiosis surgery. Eotaxin was the most strongly upregulated of these factors and was also found to increase with age in the cerebrospinal fluid of humans. Young mice show impairments in learning during radial arm water maze testing after injection with eotaxin [412]. This was linked to altered neurogenesis and as such I measured the numbers of DCX positive cells in the DG.

In *nfkb1*$^{-/-}$ mice I found a down-regulation of DCX positive cells compared to wild-type mice. There was also an association between DCX and microglia numbers in the DG, when all groups were pooled, as has previously been observed in ageing wild-type mice [431]. However, although there were trends, the number of DCX positive cells in the DG was not significantly ameliorated by long-term ibuprofen treatment in *nfkb1*$^{-/-}$ mice, despite reduced levels of MCP-1 and Eotaxin. This may be explained by intrinsic effects of *nfkb1*$^{-/-}$ on neurogenesis that are not related to inflammation [399]; it has previously been observed in young *nfkb1*$^{-/-}$ mice that while there is no change in the net rate of neural precursor cell proliferation in the hippocampus sub-granular zone, there is a reduction in the number of immature neurons that survive to maturity [399]. Further, experiments on IkB/tTA NF-κB repressor mice (a neuron-specific ablation of all NF-κB subunits through increased IκB-α attached to a neuronal promotor), showed a decrease in successful integration of the immature neurons [432]. As DCX marks both immature neurons and precursor cells; the numbers may come primarily from reduced survival of immature cells, due to an intrinsic increase in vulnerability.

Together this suggests that *nfkb1*$^{-/-}$ do show an increasing neuro-inflammatory profile with ageing. Increased proliferation of microglia can be seen in the hippocampus, but it is worth bearing in mind that microglia can also be protective and this may reflect a response to damage. However, by 18 months microglial hypertrophy and a significant upregulation of numerous pro-inflammatory cytokines can be seen. This was ameliorated by long-term dietary treatment with ibuprofen. This may not come directly from the effects of *nfkb1*$^{-/-}$ and altered NF-κB signalling on microglia, as these appear to show a decreased basal response, but through a secondary ROS or inflammation mediated insult and a defect in microglia switching from M1 to M2 activation states. Neurogenesis was significantly lower than in wild-type mice. These alterations may be due to microglia and inflammation, but since this was not significantly ameliorated by ibuprofen, may also reflect an intrinsic vulnerability of newly generate neurons in *nfkb1*$^{-/-}$ mice. Both neuroinflammation, and neurogenesis have been linked to the onset of age-associated cognitive deficits, and as such, these were assessed in the next sub-chapter.

3.4 - *Nfkb1*$^{-/-}$ mice show deficits in spatial discrimination and memory

3.4.1 - *Nfkb1*$^{-/-}$ mice show significant deficits in novel arm discrimination in Y-maze, rescued by Ibuprofen at 6 months of age

Alternation tasks, such as the Y-maze, use the propensity of rodents to explore novel environments, and allow the testing of their working memory [433]. Here a forced-alternation testing paradigm was used, with the mouse placed in the home arm of the Y-maze, with one arm blocked and one arm open (Figure 3.4.1.1A). The mouse was allowed to explore for 10 minutes and then returned to the home cage. One hour later, the mouse was placed into the home arm of the Y-maze again for 2 minutes (Figure 3.4.1.1A). If mice remember the maze properly, they should choose the novel arm to enter, and show a preference for exploration of this arm.

Wild-type mice at 6 and 10 months of age showed a strong preference for the novel arm (forced alternation), with 89% and 80% of mice entering it as they're first choice, respectively (Figure 3.4.1.1B). *Nfkb1*$^{-/-}$ mice showed no clear preference for the novel arm during the trial, with mice entering the novel arm first only 50% of the time (Figure 3.4.1.1B). *Nfkb1*$^{-/-}$ mice treated with ibuprofen in soaked food for 2 months entered the novel arm more, at 80% of choices. *Nfkb1*$^{-/-}$ mice also showed significantly increased latency to enter the novel arm compared to wild-type controls, with no change seen between 6 and 10 months in wild-type mice (Figure 3.4.1.1C). Ibuprofen treated *nfkb1*$^{-/-}$ mice showed a trend for reduced primary latency, being closer to wild-type values (Figure 3.4.1.1C).

The arm discrimination index is the time spent in the novel arm, divided by time spent in both novel and familiar arms (Figure 3.4.1.1D). *Nfkb1*$^{-/-}$ mice scored a significantly lower discrimination index score than age-matched wild-type control mice. *Nfkb1*$^{-/-}$ mice treated with Ibuprofen had a significantly higher arm discrimination index score than their untreated litter-mates.

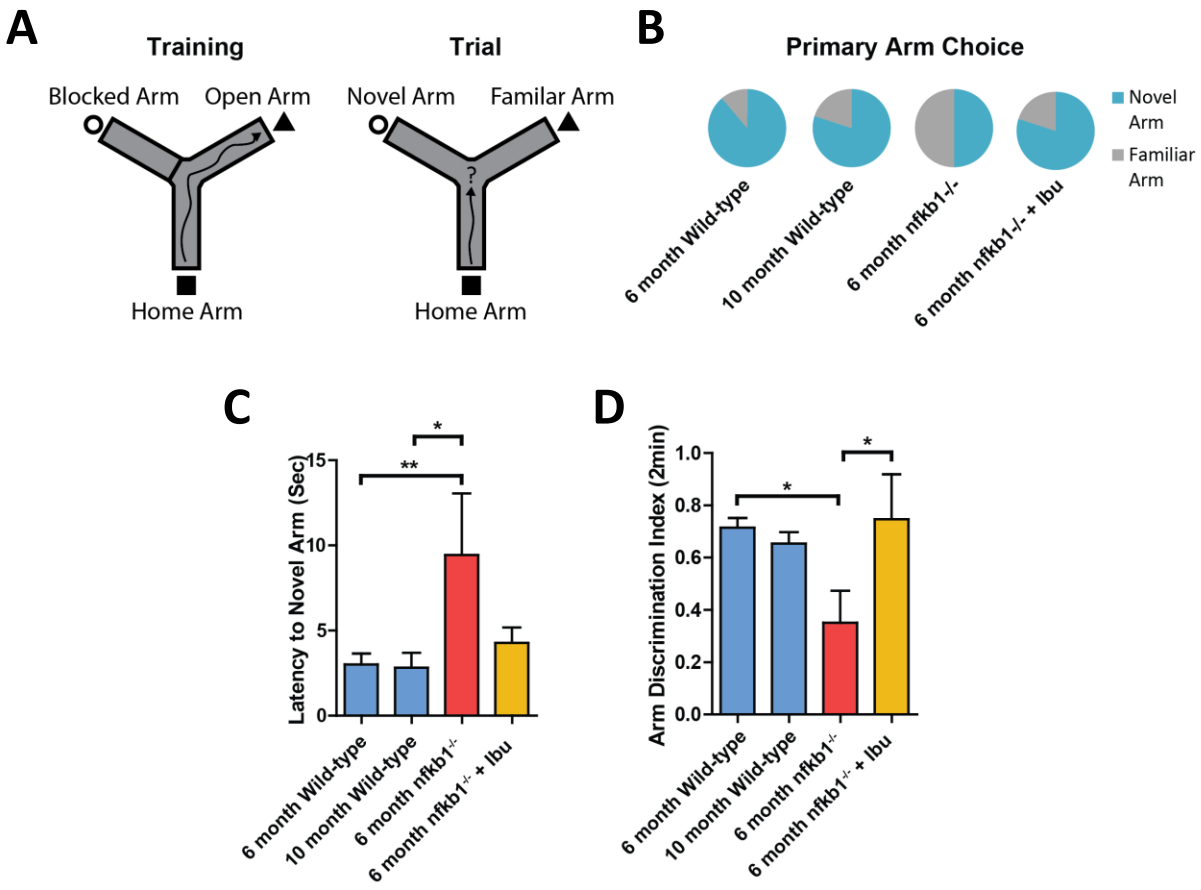

Figure 3.4.1.1: *Nfkb1*$^{-/-}$ mice show reduced spatial discrimination and memory in forced alternation Y-maze

A) Mice were given a training session in Y-maze with one arm-closed, and one- open. 60 minutes later, a retrieval trial was conducted and multiple parameters recorded: **B)** Pie chart showing the choice of arm first entered by each genotype. **C)** Time taken to reach novel arm. **D)** Arm Discrimination Index for the first 2 minutes. **E)** Arm Discrimination index after 5 minutes. Graphs are mean+/-SEM (n = 4-18 mice). Significant differences from One Way Analysis of Variance (Holm-Sidak Post-hoc) shown by *<0.05; ** <0.005; *** <0.001.

3.4.2 – *Nfkb1*$^{-/-}$ mice show deficits in long-term spatial memory in the Barnes Maze at 7 months

3.4.2.1 - At 7 months Nfkb1$^{-/-}$ *mice show no significant deficits in spatial learning in the Barnes Maze*

The Barnes maze [36] is a dry-land test for the assessment of spatial learning and memory. While initially designed for use in rat models, the small size of mice and their ability to fit through smaller holes make the test well suited for the use in mice [361, 434-436]. Spatial memory in the Barnes Maze is dependent on hippocampal functioning and mice with damage to this region perform worse [434, 437]. As a dry-land test, and unlike water-based mazes, it does not involve the strong aversive stimuli to water and constant exertion from paddling. It instead relies on an aversion to bright light and open spaces, and is considered to be a lower stress alternative to the Morris water maze [438, 439]. While mice may be more inclined to further exploration or passive behaviour, here the Barnes Maze was considered a better choice due to the potential confounding effects of differing stress and anxiety response of *nfkb1*$^{-/-}$ mice compared to wild-types that has been observed in the MWM [397]. Additionally, given the age and frailty of the mice tested, with *nfbk1*$^{-/-}$ mice near the end of their typical life-span, the use of a dry-land test should minimise stress and suffering to the animals while reducing confounding factors from muscle-strength.

The method mice use to locate the target hole can be categorised into 3 different groups. The mouse can move directly to the target hole or adjacent hole and this is termed a 'Direct' search pattern. When mice reach the holes or edge of the maze, they will frequently check a hole, then the next, and repeat this search until they reach the target hole. This is termed a 'Serial' search. Additionally the mouse may employ a random search pattern, employing a mix of serial searches and crossing the centre of the board and this is termed a 'Mixed' search pattern (Figure 3.4.2.1A).

Wild-type and *nfkb1*$^{-/-}$ mice showed a decline in the use of mixed search strategies across training, in favour of direct or serial search patterns (Figure 3.4.2.1B). *Nfkb1*$^{-/-}$ mice employed less mixed search strategies on the first day, but after this there was little difference. Wild-type and *nfkb1*$^{-/-}$ mice both showed a corresponding increase in the use of direct searches across training. Treatment of *nfkb1*$^{-/-}$ mice with ibuprofen showed a similar use of strategies to un-treated mice on days 1, 2 and 4, but large use of direct searches on day 3.

By day 4, there was no significant difference between wild-type and *nfkb1*$^{-/-}$ mice in the number of incorrect searches prior to finding the target hole (Figure 3.4.2.1C), or in the time taken to find the

target hole (Figure 3.4.2.1D). *nfkb1*$^{-/-}$ mice showed a trend for finding the target hole quicker during the first day than wild-types. *nfkb1*$^{-/-}$ mice treated with ibuprofen did not show a significantly altered primary latency on days 2-4 compared to untreated littermates, but showed a trend for reduced errors on day one, and increased errors on day 4.

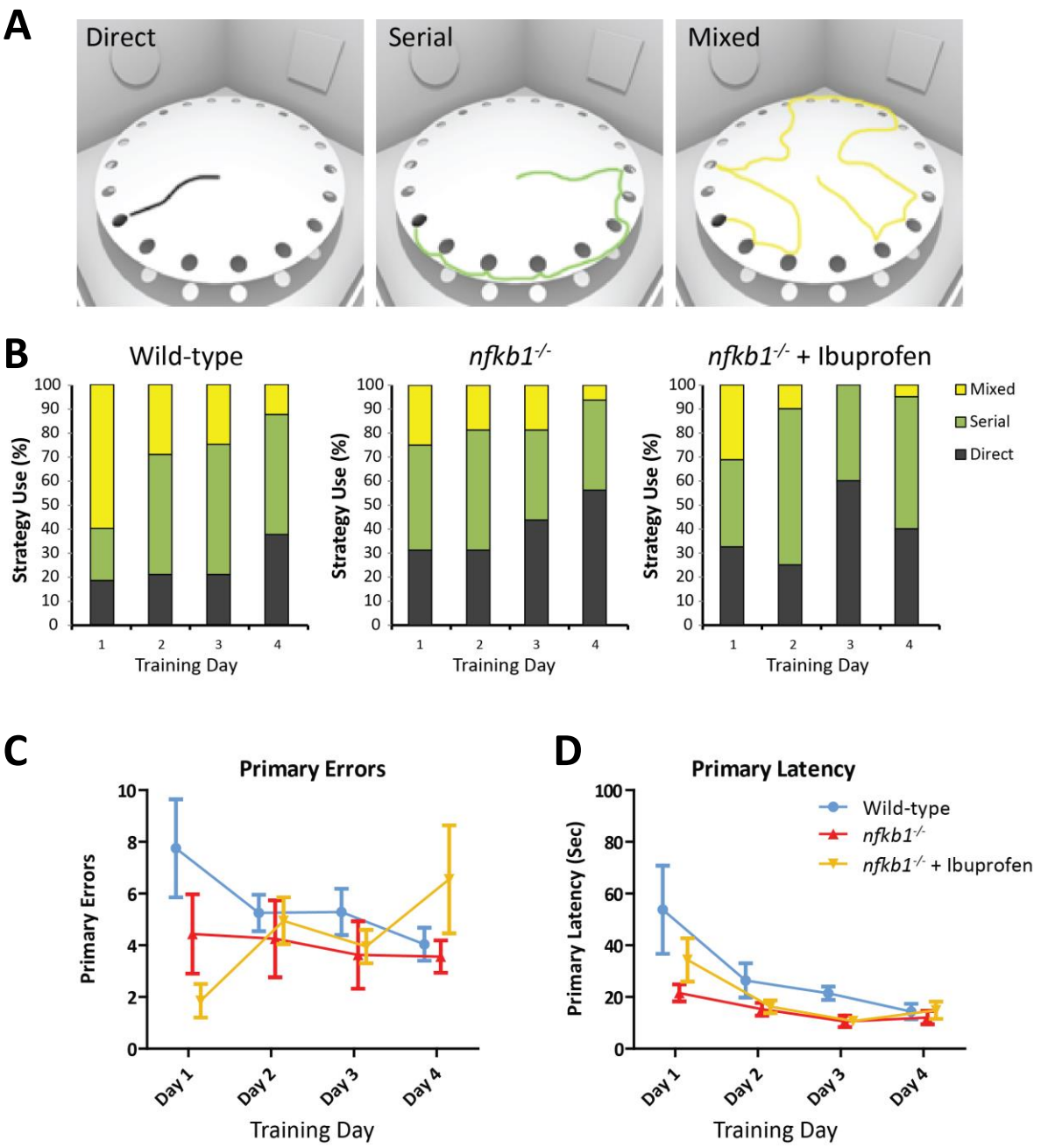

Figure 3.4.2.1: Performance during training days in 7 month old wild-type and *nfkb1*$^{-/-}$ mice

A) Visual depictions of search strategies, showing an example mouse's path for each search strategy. Direct (Black) search pattern is classified as the mouse having moved either directly to the target hole, or an adjacent hole. Serial (Green) is classified as having searched two or more holes in a serial pattern before finding the target hole. Mixed (Yellow) employs seemingly random searching, with serial and direct searches and having crossed the centre of the maze one or more times. **B)** Shows the average percentage of each strategy used across the training batteries (4 tests per day) on the 4 training days for *nfkb1*$^{-/-}$ (± ibuprofen) and wild-type C57Bl/6. The average number of incorrect holes searched **(C)** and time taken **(D)** before finding the target (escape) hole.

3.4.2.2 - At 7 months nfkb1$^{-/-}$ mice show deficits in long-term memory in the Barnes Maze

After 4 days of training had been completed with the escape box in place, two further 90 second trials were conducted without the escape box, one on day 5, and another a week later on day 12. More detailed analysis of the search was performed on these trials. Errors, time taken and search strategy to initially find the target hole are still recorded (Figure 3.4.2.2.1). No significant difference was found in the number of primary errors, or latency (Figure 3.4.2.2.1A-B). A decreased frequency of direct searches was used by untreated *nfkb1*$^{-/-}$ mice during the long-term memory trial, this was rescued with Ibuprofen treatment (Figure 3.4.2.2.1C).

During the short-term memory test (Figure 3.4.2.2.2A), wild-type mice directed their search primarily at the target hole and the adjacent holes, with some further exploration of the board. *nfkb1*$^{-/-}$ mice's search was not significantly lower at the target and adjacent hole compared to wild-type mice, but did show more searches at off-target markers (present at -5, +5 and ±10 positions) (Figure 3.4.2.2.2A). *nfkb1*$^{-/-}$ mice treated with Ibuprofen showed no significant differences to untreated *nfkb1*$^{-/-}$ mice (Figure 3.4.2.2.2A).

Only wild-type mice showed no significant decrease in preference for the target and adjacent hole in the long-term memory tests (Figure 3.4.2.2.2A); however, *nfkb1*$^{-/-}$ mice performed significantly worse than wild-types, although the decrease compared to the short-term test was not significant. Ibuprofen treated *nfkb1*$^{-/-}$ mice did not perform significantly better than untreated mice.

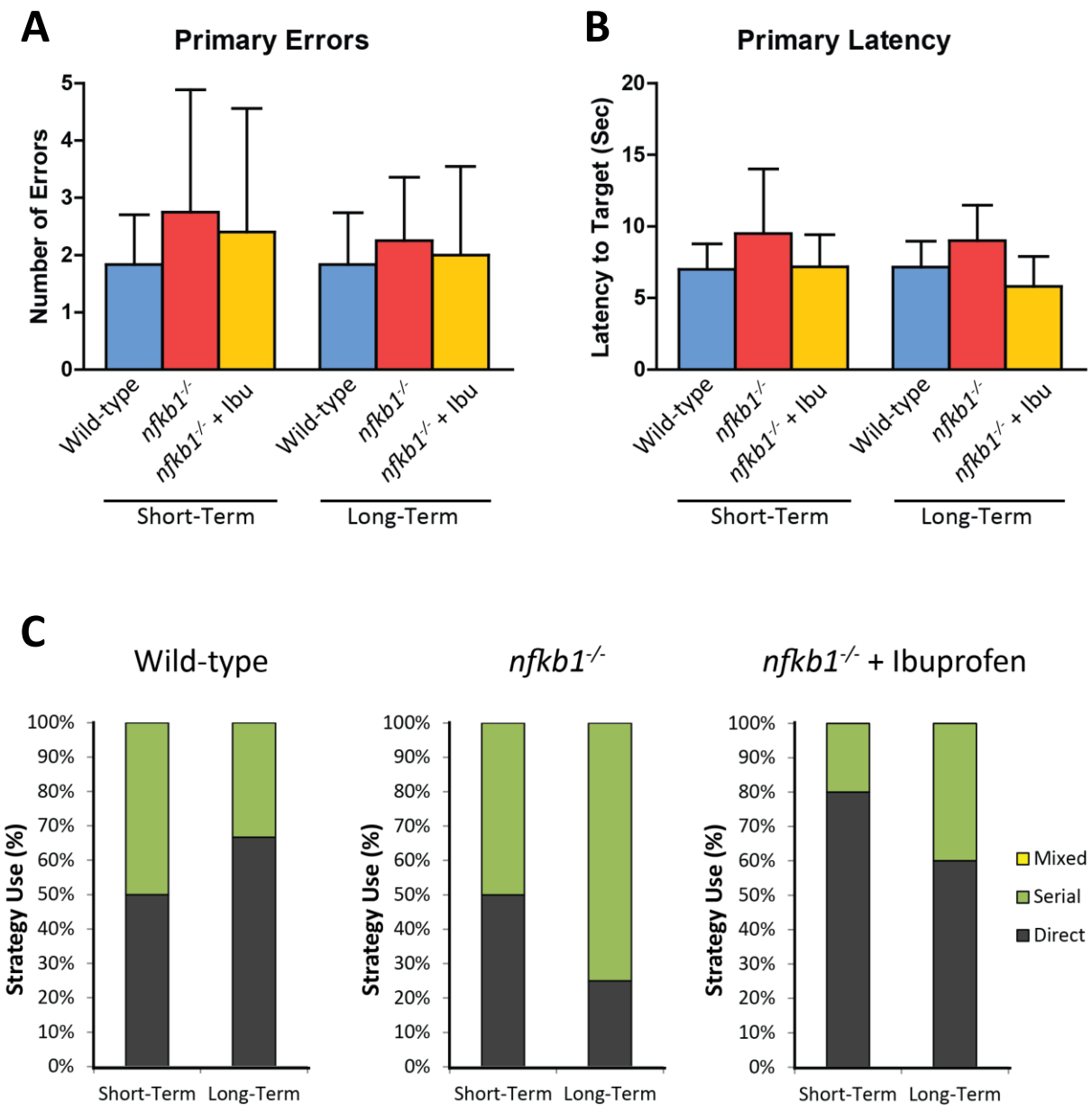

Figure 3.4.2.2.1: Performance during of short- and long-term memory tests in 7 month old wild-type and *nfkb1*$^{-/-}$ mice

Graphs are showing **A)** the average number of errors prior to finding the target hole, **B)** the average time taken to find the target hole and **C)** the choice of search strategy employed by each group. Graphs are mean+/-SEM (n = 4-6 mice). No significant differences found by 2-way RM ANOVA for primary errors or latency.

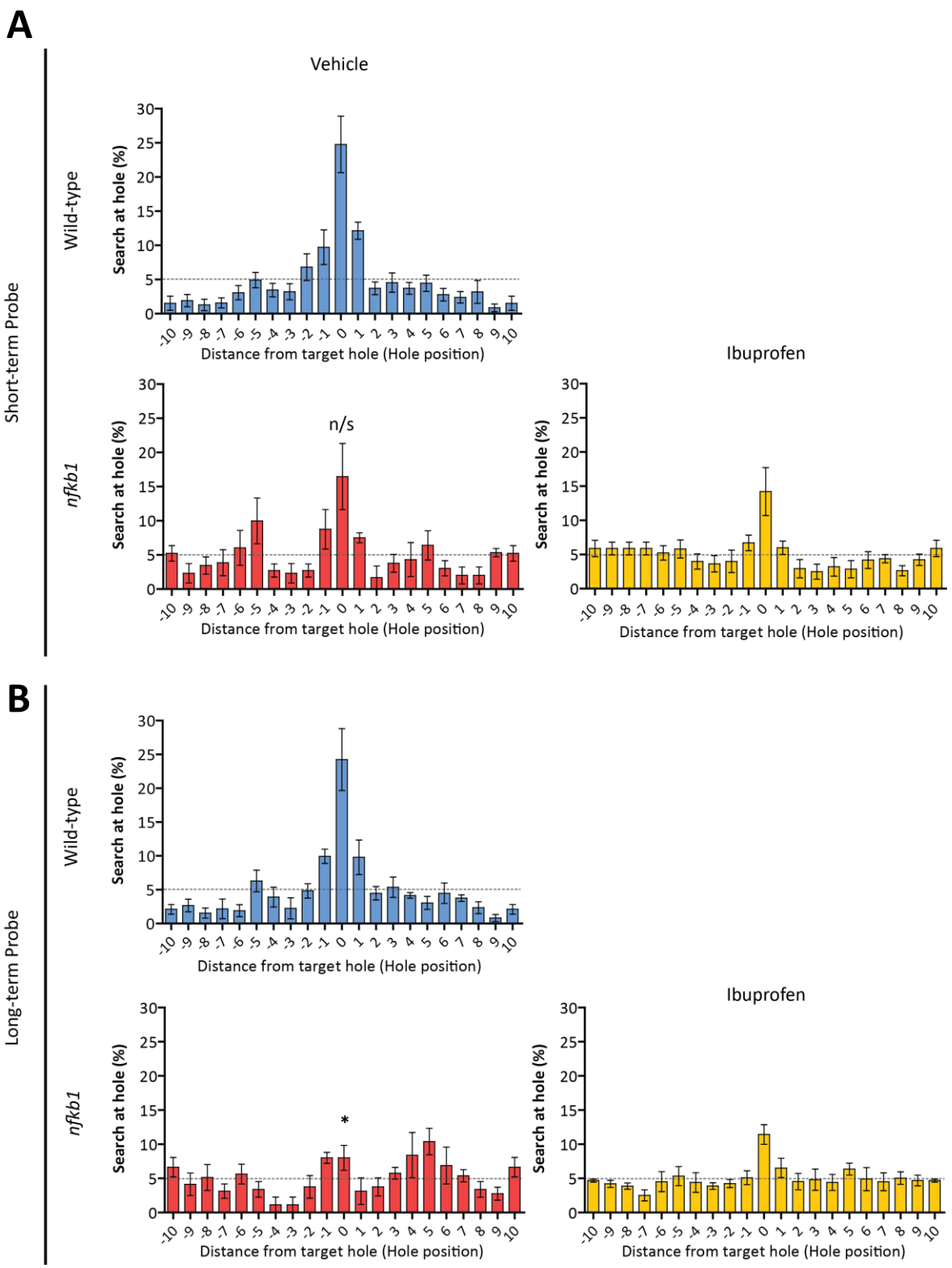
A
Short-term Probe
Wild-type
nfkb1
Vehicle
Ibuprofen
n/s
Search at hole (%)
Distance from target hole (Hole position)
B
Long-term Probe
Wild-type
nfkb1
Vehicle
Ibuprofen
*
Search at hole (%)
Distance from target hole (Hole position)

Figure 3.4.2.2.2: Search distribution during short and long-term memory tests in the Barnes Maze at 7 months in wild-type and *nfkb1*$^{-/-}$ mice

The head-pokes into each hole of the Barnes maze were recorded during the short- and long-term memory retention tests for each mouse. From this the percentage of the total head-pokes in each hole was determined to give the search distribution (Bars and whiskers show average mean + SEM). **A-B)** The graphs show number of searches per hole for wild-type and *nfkb1*$^{-/-}$ mice, un-treated and treated with Ibuprofen. The target hole is located at position 0, with each of the additional 19 holes around the board marked numerically relative to the target hole. As such positions -10 and +10 are the same hole, being opposite to position 0. Dotted line shows the expected 5% for each hole if the search was random. **A)** Shows search distribution during short-term memory and **B)** shows the search distribution during long-term memory testing. Graphs are mean+/-SEM (n = 8-24 mice) 2-way RM ANOVA. * $p<0.05$ between genotype in vehicle treated, or treatment within genotype.

3.4.3 – *Nfkb1*$^{-/-}$ mice show deficits in short- and long-term spatial memory in the Barnes Maze at 18 months

3.4.3.1 - Chronic inflammation alters use of spatial search strategy, but had no effect on errors made in 18 month old *nfkb1*$^{-/-}$ mice during training days

Wild-type and *nfkb1*$^{-/-}$ mice showed a decline in the use of mixed search strategies across training, in favour of direct or serial search patterns (Figure 3.4.3.1.1A). This decrease was more pronounced in the wild-type mice, and mixed searching remained more common in the *nfkb1*$^{-/-}$mice, still at approximately 30% of searches by the end of the training period. Wild-type mice showed a corresponding increase in the use of direct searches across training, while *nfkb1*$^{-/-}$ mice showed no improvement in this regard, with the change instead being due to increased use of serial searches. Treatment of *nfkb1*$^{-/-}$ mice with the NSAID Ibuprofen lead to a closer phenocopying of the wild-type mice in the use of mixed searches, and a greater incidence of direct search patterns. In this cohort, an additional wild-type treated with Ibuprofen was used. In wild-type mice, treatment with Ibuprofen did not effect the decline in mixed searches, but lead to a seeming decline in the use of direct searches, with none observed at all on day 3.

However, while trends in the search pattern could be observed, there was little difference in the number of incorrect searches prior to finding the target hole (Figure 3.4.3.1.1B), or in the time taken to find the target hole (Figure 3.4.3.1.1C). *nfkb1*$^{-/-}$ mice were significantly faster in finding the target hole during the first day than wild-types, while those that were treated with Ibuprofen were not significantly different to untreated wild-type mice.

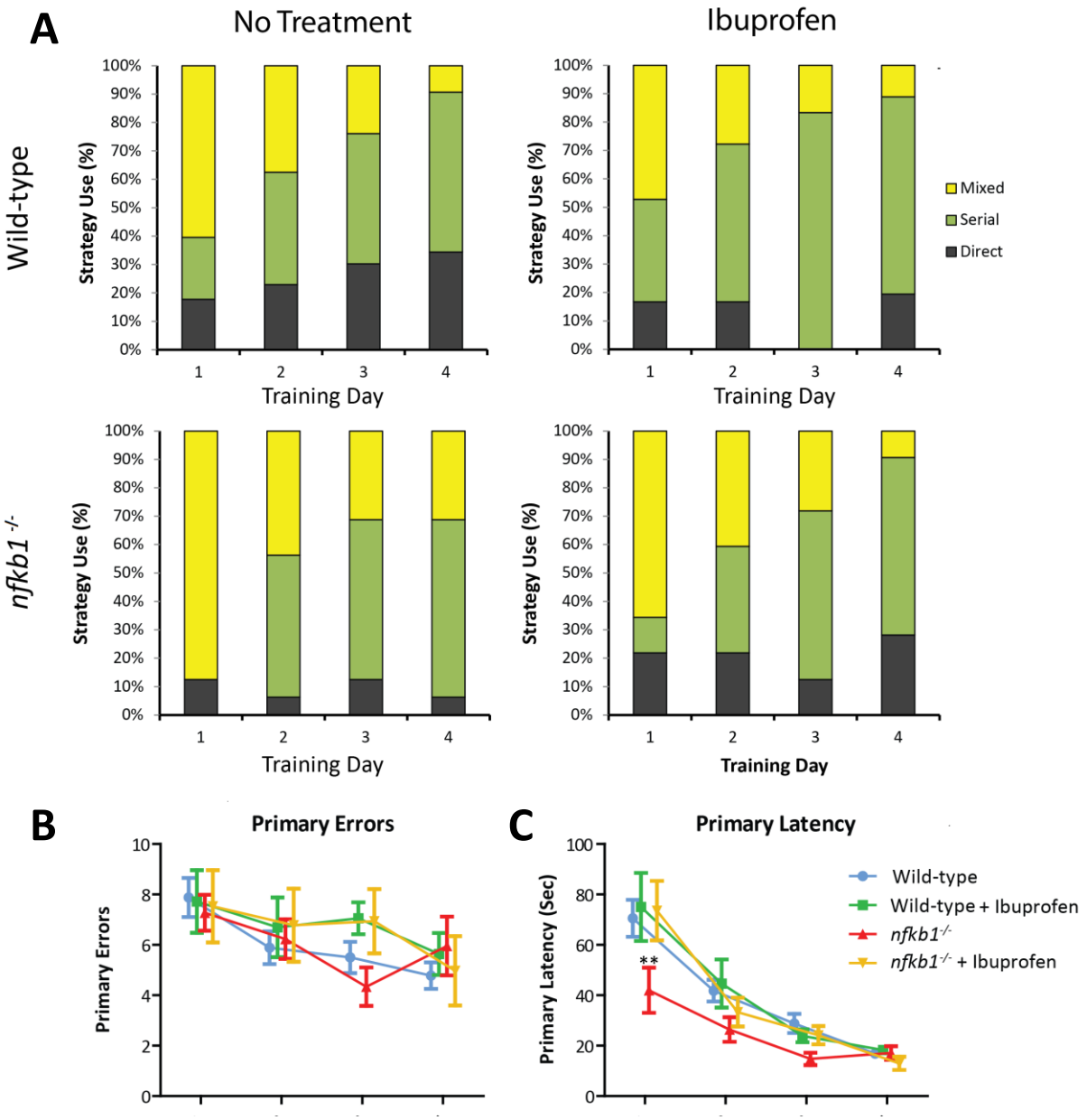

Figure 3.4.3.1.1: Performance during training days in 18 months old wild-type and *nfkb1*$^{-/-}$ mice, with and without ibuprofen

A) Visual depictions of search strategies, showing an example mouse's path for each search strategy. Direct (Black) search pattern is classified as the mouse having moved either directly to the target hole, or an adjacent hole. Serial (Green) is classified as having searched two or more holes in a serial pattern before finding the target hole. Mixed (Yellow) employs seemingly random searching, with serial and direct searches and having crossed the centre of the maze one or more times. **B)** Average percentage of each strategy used across the training batteries (4 tests per day) on the 4 training days for *nfkb1*$^{-/-}$ and wild-type C57Bl/6, with and without Ibuprofen treatment. The average number of incorrect holes searched **(C)** and time taken **(D)** before finding the target (escape) hole. Graphs are mean+/-SEM (n = 8-24 mice) 2-way RM ANOVA. p-values shown by # ($p<0.05$) between short- and long-term memory, (** $p<0.01$) between genotype in vehicle treated, or treatment within genotype.

3.4.3.2 - Chronic inflammation impacts short- and long-term spatial memory in 18 month nfkb1$^{-/-}$ mice

During the short-term memory test on day 5 *nfkb1*$^{-/-}$ mice made significantly more errors prior (Figure 3.4.3.2.1A) and took significantly longer to find the target hole compared to wild-type mice (Figure 3.4.3.2.1B). Ibuprofen treatment appeared to worsen the performance of the wild-type mice making more errors and taking significantly longer to find the target. Ibuprofen treated *nfkb1*$^{-/-}$ mice were not significantly different in the short-term test in these parameters to un-treated mice. During the long-term memory test untreated wild-type mice made significantly more errors and took longer to find the target hole than they did in the short-term memory test (Figure 3.4.3.2.1A-B). Ibuprofen treated *nfkb1*$^{-/-}$ mice made fewer errors than untreated *nfkb1*$^{-/-}$ mice during the long-term search.

In choice of strategy, 50% of wild-type mice employed a direct search strategy, with only 12.5% using mixed search strategies (Figure 3.4.3.2.1C). *nfkb1*$^{-/-}$ employed less direct spatial searches and an increased use of mixed searches. Ibuprofen treatment seemed to have opposite effects depending on genotype, with treated wild-type mice making fewer direct, and more mixed searches. Treated *nfkb1*$^{-/-}$ mice employed more direct searches and less mixed searches than their untreated littermates. During the long-term test, use of search strategy was similar amongst untreated *nfkb1*$^{-/-}$ and treated and untreated wild-types. In the long-term test, ibuprofen treated *nfkb1*$^{-/-}$ used predominantly direct searches, and no mixed searches.

Since the escape box is removed after the initial training days, mice cannot exit the maze, they continue to search, frequently coming back to the target hole. One can track the distribution of this search around the maze to give further indication of how well the mice remember the position of the target hole (Figure 3.4.3.2.2). This is performed by recording how many times the mouse poked its head into, or deflected its head over, each hole. To account for the seemingly altered locomotive speed, anxiety of the *nfkb1*$^{-/-}$ mice, the percentage of total searches around the board is displayed, rather than the raw number. If the search pattern was random, each hole would be expected to be visited 5% of the time.

During the short-term memory test (Figure 3.4.3.2.2A), wild-type mice directed their search primarily at the target hole and the adjacent holes, with some further exploration of the board. *nfkb1*$^{-/-}$ mice's search pattern was more evenly distributed, with less head pokes at the target hole or adjacent holes than wild-type mice, indicating a decreased recall of the location of the target hole. *nfkb1*$^{-/-}$ mice treated with Ibuprofen showed significant improvement in recall for the target hole, with a search pattern close to wild-type mice. Ibuprofen treatment in wild-type mice, however, decreased the

number of head-pokes in the target hole and they showed a search pattern resembling those of *nfkb1*$^{-/-}$ mice.

Only wild-type mice showed a significant decrease in percentage of search at the target hole during the long-term memory tests (Figure 3.4.3.2.2B), but still performed significantly better than *nfkb1*$^{-/-}$ mice. Wild-type mice treated with Ibuprofen, interestingly, were not significantly different to the un-treated wild-type mice. Additionally, Ibuprofen treated *nfkb1*$^{-/-}$ mice again performed better than untreated males, with a profile closer to wild-type mice.

A visual comparison, showing the results in Figure 3.4.2.2.2 and Figure 3.4.3.2.2 super-imposed onto the Barnes maze, is shown in Figure 3.4.3.2.3. Wild-type mice showed no change in short-term memory (Figure 3.4.3.2.3A) between these ages, but a reduction in preference for the target and adjacent hole in long-term memory trial by 18 months (Figure 3.4.3.2.3B). *Nfkb1*$^{-/-}$ had reduced, but still somewhat intact short-term memory at this age, but this was reduced by 18 months (Figure 3.4.3.2.3A). Long-term memory preference was close to random (5% of search at each hole) in both ages in untreated *nfkb1*$^{-/-}$ mice (Figure 3.4.3.2.3B).

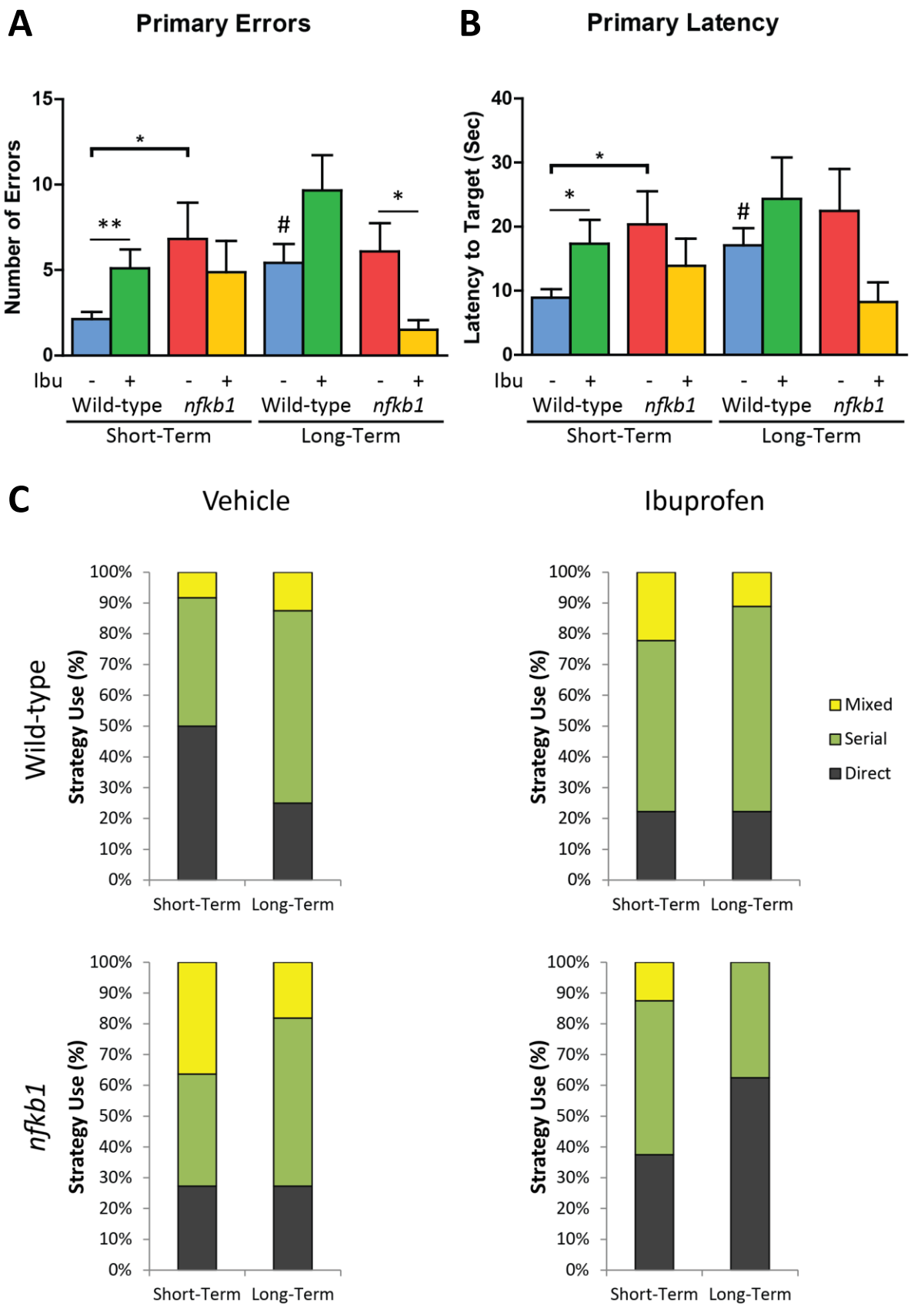
A
Primary Errors
Number of Errors
15
10
5
0
*
**
#
*
Ibu - + - + - + - +
Wild-type nfkb1 Wild-type nfkb1
Short-Term Long-Term
B
Primary Latency
Latency to Target (Sec)
40
30
20
10
0
*
*
#
Ibu - + - + - + - +
Wild-type nfkb1 Wild-type nfkb1
Short-Term Long-Term
C
Vehicle
Ibuprofen
Wild-type
nfkb1
Strategy Use (%)
100%
90%
80%
70%
60%
50%
40%
30%
20%
10%
0%
Short-Term Long-Term
Mixed
Serial
Direct

Figure 3.4.3.2.1: Performance during of short- and long-term memory tests in 18 months old wild-type and *nfkb1*$^{-/-}$ mice, with and without ibuprofen

Graphs are showing **A)** the average number of errors prior to finding the target hole, **B)** the average time taken to find the target hole and **C)** the choice of search strategy employed by each group. Graphs are mean+/-SEM (n = 8-24 mice) 2-way RM ANOVA. p-values shown by # ($p<0.05$) between short- and long-term memory, (* $p<0.05$, ** $p<0.01$, ***<0.001) between genotype in vehicle treated, or treatment within genotype.

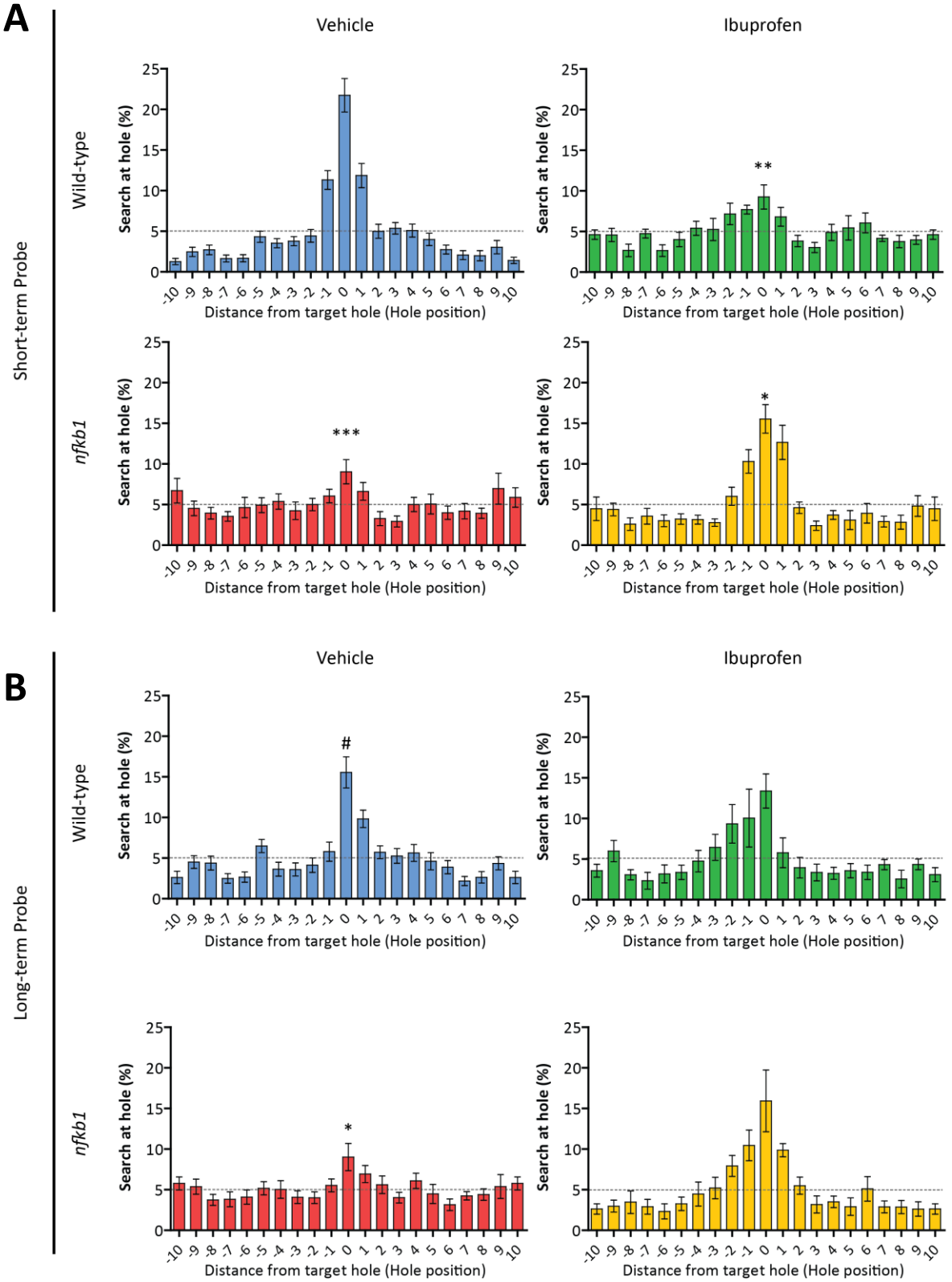
A
Short-term Probe
Vehicle
Ibuprofen
Wild-type
nfkb1
Search at hole (%)
Distance from target hole (Hole position)
**
***
*
B
Long-term Probe
#
*

Figure 3.4.3.2.2: Search distribution during short and long-term memory tests in the Barnes maze in 18 month old wild-type and *nfkb1*$^{-/-}$ mice, with and without ibuprofen

The head-pokes into each hole were recorded during the short- and long-term memory retention tests for each mouse. From this the percentage of the total head-pokes in each hole was determined to give the search distribution (Bars and whiskers show average mean + SEM). **A-B)** The graphs show number of searches per hole for wild-type and *nfkb1*$^{-/-}$ mice, un-treated and treated with Ibuprofen. The target hole is located at position 0, with each of the additional 19 holes around the board marked numerically relative to this. As such positions -10 and +10 are the same hole, being opposite to position 0. Dotted line shows the expected 5% for each hole if the search was random. **A)** The graph shows the search distribution during short-term memory and **B)** the search distribution during long-term memory. Graphs are mean+/-SEM (n = 8-24 mice) 2-way RM ANOVA. p-values shown by # ($p<0.05$) between short- and long-term memory, (* $p<0.05$, ** $p<0.01$) between genotype in vehicle treated, or treatment within genotype.

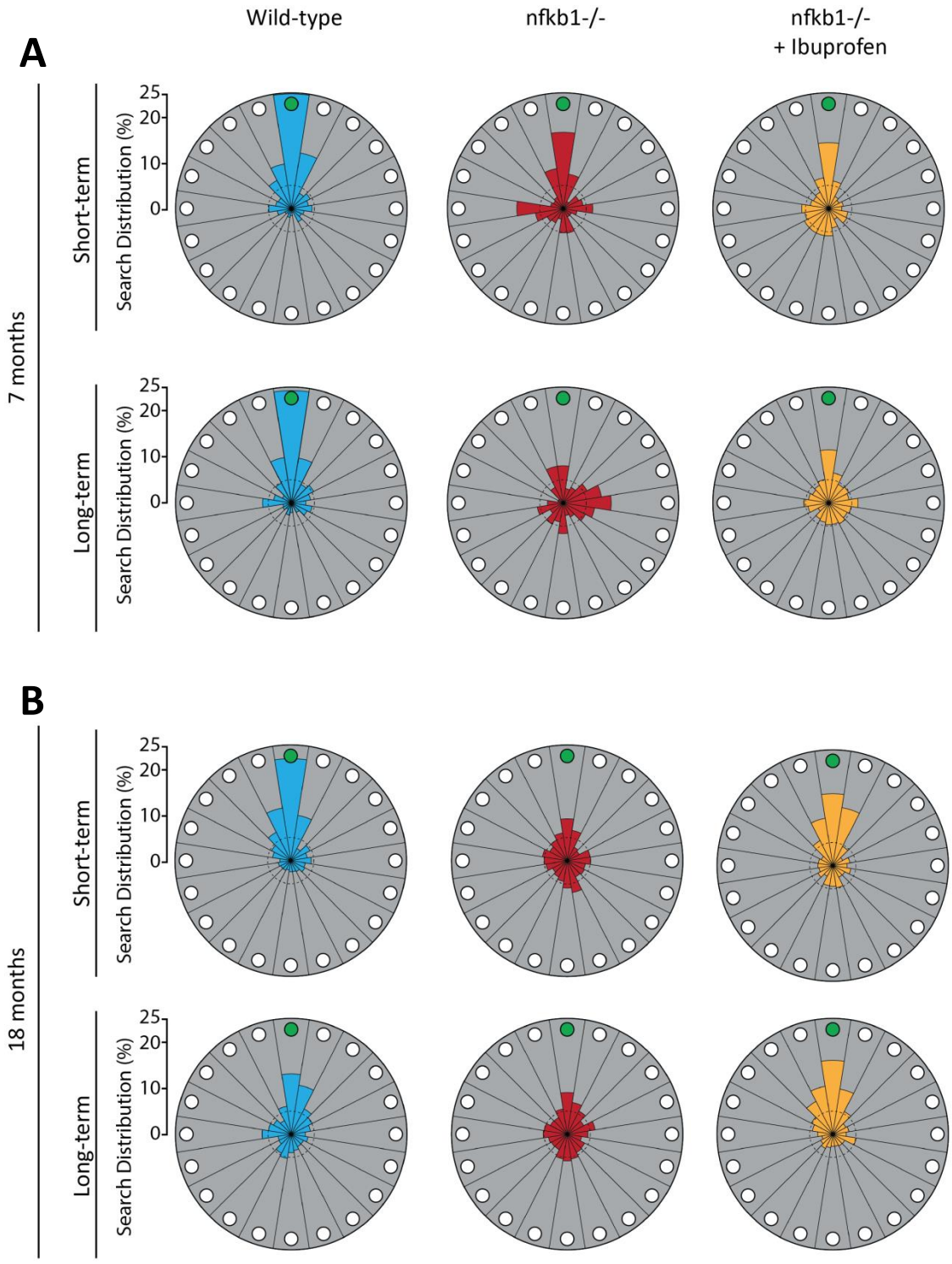

Figure 3.4.3.2.3: Visual comparison of Barnes Maze search distribution at 7 and 18 months of age in wild-type and *nfkb1*$^{-/-}$ mice

Visual representation of distribution of search around Barnes Maze in short- and long-term memory proves in 7 and 18 month mice (A and B, respectively). Target hole is displayed at top of each distribution graph and coloured green. Dotted line around centre represents 5% demarcation, which would be expected for a completely random search. Since there is a visual marker at 0, 90, 180 and 270° positions, mis-targeted searches can be seen, especially in *nfkb1*$^{-/-}$ mice. Significance or error bars are omitted for clarity, but available in previous representations.

3.4.4 - Discussion

We hypothesized that increased neuro-inflammation with age would lead to cognitive deficits in the *nfkb1*$^{-/-}$ mouse. To test spatial memory, I used two different tests of spatial memory, the Y-maze and the Barnes Maze. The Y-maze was used at 6 months, and the Barnes maze at 7 and 18 months. Previous research on *nfkb1*$^{-/-}$ mice has been performed at young ages, between 1.5 and 4 months of age, with contradicting results for *in vivo* cognitive function and memory [392, 396-399]. These studies have so far focused on the intrinsic roles of the loss of p50 in NF-κB activity, but and have not focused on the potential role of inflammation and ageing.

I found reduced memory function in the Y-maze in *nfkb1*$^{-/-}$ mice at 6 months of age compared to wild-type mice. The Y-maze (Forced alternation) has been previously used by Denis-Donini *et al.* to assess cognitive function in younger 3-4 month *nfkb1*$^{-/-}$ mice [399]. However, they used multiple memory tests, at 20, 30 and 40 minutes after acquisition. In Denis-Donini *et al.'s* study, *nfkb1*$^{-/-}$ mice initially showed no difference to wild-type mice when tested 20 minutes after the acquisition phase, with both showing increased entry into the novel arm compared to the other two arms. At 30 minutes, wild-type mice still showed a preference for the novel arm, but *nfkb1*$^{-/-}$ did not. Neither group showed a preference at the 40 minute time point. I tested 6 month *nfkb1*$^{-/-}$ mice 1 hour after acquisition, and found a reduced discrimination index scoring for the novel arm and increased primary latency in *nfkb1*$^{-/-}$ mice compared to wild-type mice. This suggests that *nfkb1*$^{-/-}$ mice show a significant deficit in retention of spatial memory compared to wild-type mice at an early age.

However, it appears that Denis-Donini *et al.* tested the same mice at 20, 30 and 40 minutes [399]. This is perhaps closer to a re-training paradigm, given that wild-type mice also showed no preference in the 40 minute trial, while I found a distinct preference when tested 1 hour after. This could be affected by alterations in exploratory activity and learning rather than purely memory. Increased exploratory behaviour has been reported in 2 month old *nfkb1*$^{-/-}$ mice compared to wild-types by Kassed et al. [396]. Additionally, *nfkb1*$^{-/-}$ mice have shown some indication of improvements in the acquisition phase of the Morris water maze at 2-3 months [397, 398] that might lead to earlier switch to an alternating search pattern. Due to the different protocols, additional testing would be required to determine from what age *nfkb1*$^{-/-}$ start to show a deficit.

I found improvements during training in untreated *nfkb1*$^{-/-}$ mice during the Barnes Maze at 7 months of age. *Nfkb1*$^{-/-}$ mice showed increased use of direct searches and took less time to find the target hole compared to wild-type mice. At 18 months, *nfkb1*$^{-/-}$ mice still showed reduced latency on the first day

of training compared not only to wild-type mice, but also ibuprofen treated *nfkb1*$^{-/-}$ mice. A possible explanation could be increased anxiety leading to the mouse to want to exit the maze faster. While Lehmann *et al*. showed increased anxiety in open field and light/dark tests in in 2-3 month *nfkb1*$^{-/-}$ mice, they found no difference during the acquisition phase of the Barnes Maze, in contrast to my results here [397]. Additionally, work by Kassed *et al.* showed decreased defecation and freezing during novel environment tests, and increased exploratory behaviour, which would suggest reduced anxiety [396]. Yet, during the Y- and Barnes maze, I noted a trend for increased solid defecation in *nfkb1*$^{-/-}$ mice compared to wild-type mice and urination, which was rarely seen with wild-type mice. This could represent an age-related change in anxiety, but may also be due to different genetic backgrounds, housing conditions and experimental conditions such as light intensity.

Despite decreases in primary latency in untreated *nfkb1*$^{-/-}$ mice at 18 months, I found a decreased use of direct searches. This suggests that they do have difficulty in remembering the exact location of the target hole. A possible explanation for the decreased latency would be that they move faster. This could be a product of their mass. By 18 months *nfkb1*$^{-/-}$ mice had significantly lower body weights compared to wild-type mice (data not shown). *nfkb1*$^{-/-}$ mice treated with ibuprofen showed a trend for increased body weight and did not show the same decreased primary latency. Velocity has previously been reported in the Morris water maze in *nfkb1*$^{-/-}$ mice, but with contradictory results, with 2 month mice showing a generally slower speed [398], but 11 month mice showing an increased swim speed [421]. However, this is in water, which may counter obesity driven changes.

Retention of spatial memory in the Barnes maze was tested 24 hours after acquisition (short-term) and 7 days after acquisition (long-term). Lehmann *et al*. have previously reported no differences between wild-type and *nfkb1*$^{-/-}$ mice in short-term memory at 2-3 months of age [397]. At 7 months, I observed a trend for reduced short-term memory and observed a significant deficit in long-term memory (which had not been tested in the protocol used by Lehmann *et al*.). By 18 months, *nfkb1*$^{-/-}$ mice showed a significant deficit in both short- and long-term spatial memory. In contrast, wild-type mice showed no age-related deterioration in short-term memory performance with age, but did show a decline in long-term memory. Together, this suggests that *nfkb1*$^{-/-}$ mice undergo an age-dependent decline in short-term spatial memory.

It should be noted that there were differences in the maze used here and by Lehmann *et al.* (100cm diameter compared to 92cm here; 21 holes, compared to 20 here; 5 minute trial and 2 minutes in the target box, compared to 3 minutes and 1 minute here) [397]. Training protocol in their experiments was 4 trials per day for 5 days, compared to 4 trials per day for 4 days here. Additionally, their short-

term probe was conducted 3 hours after the final training trial, while I conducted it 24 hours after the final training trial. As such, the protocol I used may be somewhat more sensitive to detecting changes in spatial memory as it provided less training, with a longer delay.

Spatial memory 24 hours after acquisition has also been reported in *nfkb1*$^{-/-}$ mice using the Morris water maze, by Denis-Donini *et al.* [399] and Oikawa *et al.* [398] (although this was termed 'long-term' in the papers). Denis-Donini *et al.*'s protocol used 1 training task per day, across 10 days, in 3-4 month *nfkb1*$^{-/-}$ mice [399]. This is a less vigorous training pattern than employed in the Barnes Maze, but the target platform can be located visually and no difference was seen between wild-type and *nfkb1*$^{-/-}$ mice. This suggests that both visual acuity and target-cued memory was not affected at this age. When the platform was removed and mice were tested, both *nfkb1*$^{-/-}$ and wild-type mice showed a preference for previous platform location and there was no difference between genotypes. This would lend support for this type of spatial memory being unaltered at this age, as observed in the Barnes Maze at 2-3 months by Lehmann *et al.* [397].

Oikawa *et al.* used younger 2 month old *nfkb1*$^{-/-}$ mice and in contrast showed decreased retention of spatial memory [398]. In Oikawa *et al.*'s Morris water maze protocol, mice were tested for 4 trials a day, for 7 days, the retention of this spatial memory was again tested by removing the platform and recording the search. However, this was not a single memory trial 24 hours after, but instead a block of 3 days (24, 48 and 72 hours after acquisition), with 4 no-platform trials per day. In this block trial approach, *nfkb1*$^{-/-}$ mice performed significantly worse than wild-type mice on the first day of testing without the platform. Yet, they showed no difference on the next two days. This could represent that both strains are capable of recognising that the platform is no longer there, and an attempt to find a new position, as searches at the target location on the last two days were below the time that would be expected by chance.

Long-term spatial memory (tested 7 days after acquisition) has not, to my knowledge, been previously assessed using the Barnes maze in *nfkb1*$^{-/-}$ mice. Interestingly, preference for the target hole was significantly impaired in *nfkb1*$^{-/-}$ mice at both 7 and 18 months of age. Two possible explanations would be; that there is an age-dependent change affecting spatial memory before 7 months of age; or, that there is an intrinsic deficit in *nfkb1*$^{-/-}$ mice. Testing wild-type and *nfkb1*$^{-/-}$ mice at an earlier age would be required to determine if the deficit observed in the Barnes maze long-term memory test was age-dependent effect, or an intrinsic feature of the model.

One possible explanation for the observed deficits in spatial memory would be a deficit in LTP. Oikawa et al. investigated LTP in isolated hippocampal slices from young 2 month *nfkb1*$^{-/-}$ mice [398]. They found that while LTP can be reliably induced in both *nfkb1*$^{-/-}$ and wild-type mice by high frequency stimulation; 3 hours post-stimulation there is significantly reduced late-LTP in *nfkb1*$^{-/-}$ slices. This could explain the decreased performance in the long-term memory test I performed in the Barnes Maze, with *nfkb1*$^{-/-}$ mice having difficulty properly reinforcing or retrieving spatial memory over long periods. This defect may be due to an intrinsic effect of the loss of p50 and p65:p50 dimers. Inhibition of NF-κ B's DNA binding capacity, with kB decoy DNA, has previously been shown to reduce LTP magnitude [440]. Additionally, blockade of IKK/NF-κB signalling reduces levels of post-synaptic proteins and mature spine numbers and appears to rely on p65 [441]. p65 is densely located at dendritic spines [442] and the loss of p50 could reduce the ability of neurons to respond appropriately to stimulation via p65:p50 signalling, reducing the ability to alter gene expression and protein synthesis required to reinforce late-LTP [368]

The reductions in neurogenesis reported in the last chapter may have an effect, as these were reduced already by 3 months of age. A relationship between decreased neurogenesis, and reduced spatial memory and pattern separation has previously been suggested [411]. However, at 18 months while performance in the Barnes Maze was improved with ibuprofen in *nfkb1*$^{-/-}$, there was not a significant change in DCX positive cell numbers. Clelland *et al.* found a significant deficit in spatial discrimination with complete ablation of neurogenesis [411]. However, here the reduction in neurogenesis measured by DCX is less severe, at a 24-33% reduction in median values in *nfkb1*$^{-/-}$ mice compared to wild-type mice, depending on age. Additionally, there is still disagreement over the exact contribution of adult neurogenesis in rodent brains [411, 412, 443], and how much adult neurogenesis contributes towards spatial pattern separation has been brought into doubt in recent years [443]. Groves et al. prevented neurogenesis through Ganciclovir treatment, but found that this did not lead to any significant differences in pattern separation, or fear conditioning [443]. Meta-analysis by the same group failed to find a significant relation between adult neurogenesis, and spatial memory, or anxiety [443]. As such, the reductions in DCX positive cells in the DG observed in *nfkb1*$^{-/-}$ mice do not appear to fully explain the observed deficits in spatial memory.

The increasing neuroinflammation observed earlier in the chapter may account for the observed decreases in spatial memory with age. Neuroinflammation can have a significant effect on memory function [92, 93], and even transient inflammatory events can induce long-term defects in spatial memory performance, with even more pronounced effects in AD transgenic mouse models [444]. Arm discrimination was restored to wild-type levels by a 3 month dietary ibuprofen treatment at 6 months

of age in *nfkb1*$^{-/-}$ mice. While there was no significant effect in Barnes maze performance at this age, long term dietary treatment with ibuprofen at 18 months did show an improvement compared to untreated *nfkb1*$^{-/-}$ mice. This treatment also ameliorated the levels of inflammatory cytokines, and microglial proliferation and activation. IL-6 was one of the cytokines that showed upregulation by 18 months in untreated *nfkb1*$^{-/-}$ mice, and was reduced in ibuprofen treated *nfkb1*$^{-/-}$ mice. IL-6 appears important in mediating changes within spatial memory and LTP, even in basal conditions [445]. IL-6 also appears to be required to trigger the increased production of cytokines in the hippocampus and deficits in spatial memory induced by peripheral inflammation [446]. Chronic activation of microglia may also damage neurons and could contribute to hippocampal damage [447].

One point of interest was a decrease in short-term memory in 18 month wild-type mice treated with Ibuprofen. While NSAID use has been associated with a reduced risk of developing neurodegenerative conditions, untreated wild-type mice showed little age-associated change in spatial memory by this point. COX-2 has additional and direct roles in normal cognitive function that may explain the observed deficit in wild-type mice treated with Ibuprofen. COX-2 is expressed in the cell-bodies and dendrites of neuronal populations (both typically post-synaptic areas), including pyramidal and dentate gyrus cells in the hippocampus and Purkinje cells in the cerebellum [448, 449]. This activity is dependent on excitatory activity and has been linked to a role in the modulation of synaptic plasticity and spatial learning, through the release of brain-derived neurotrophic factor [331, 450]. In rats, treatment with Ibuprofen does not appear to affect non-hippocampal learning tasks, such as the visible target tests, or properties of baseline synaptic transmission, but does have an effect on hippocampus dependent tasks and the induction of LTP [450]. This appears to be specific to COX-2, as specific inhibitors, such as NS-398 and celecoxib, increase latency to target and impair the consolidation and retention of spatial memory in the Morris Water Maze [429, 451]. This is consistent with the deficits in performance in the Barnes maze observed in ibuprofen treated wild-type mice.

Together, this data suggests that *nfkb1*$^{-/-}$ mice show deficits in spatial memory that can be rescued by ibuprofen treatment, as tested by the Y-maze at 7 months and Barnes maze at 18 months. Untreated *nfkb1*$^{-/-}$ mice show increasing deficits in spatial memory with age, compared to wild-type mice, as assessed by Barnes maze. The observed differences in spatial memory following ibuprofen treatment in *nfkb1*$^{-/-}$ mice would imply that inflammation, or a NF-κB-COX-2 mediated pathway, is contributing to the observed cognitive deficits.

3.5 - *Nfkb1*$^{-/-}$ mice show deficits in the power and synchronicity of gamma frequency neuronal oscillations in isolated hippocampus.

3.5.1 - Gamma frequency oscillations in the hippocampus

Neuronal oscillations are rhythmic changes in neuronal activity and occur at the level of individual neurons and in the synchronous firing of arrays of neurons [452]. Neuronal network oscillations are seen throughout the entire mammalian brain and can bind the activity of arrays of neurons, often between multiple brain areas and hemispheres [453, 454]. This allows the coordination of activity in a manner dependent on network connectivity, rather than physical proximity, and enables proper cognitive function [453, 454].

Oscillations can be divided into broad categories by frequency, varying substantially from the slower delta (<4Hz), theta (4-12Hz) ranges into the higher gamma frequencies (20-80Hz). While these are found across much of the brain, including the hippocampus, their exact frequencies, mechanism and behavioural correlates vary [455]. Due to their differing frequencies, oscillations can be nested within each other, allowing for the handling of multiple neuronal arrays and the control of input from different brain areas [456].

In the hippocampus there are multiple oscillations present, with theta frequency (5-12Hz) and gamma frequency oscillations (20-80Hz) being particularly prominent [457, 458]. Multiple aspects of spatial information can be represented by a specific code of gamma-frequency sub-cycles, created by the firing of different neurons depending on the phase of the overall theta cycle [457]. These gamma-frequency oscillations contribute to memory formation, with an increase seen dependent on memory load [454, 459].

Gamma oscillations can be generated in the DG, and CA1-3 regions of the hippocampus. The CA3 can act internally as a slow gamma (~40Hz in vivo) oscillation generator [460]. Oscillations in CA3 can be generated through the interaction of the two main populations of neurons in the hippocampus [460]. Principal neurons are slow-firing (1-3Hz) excitatory glutamatergic pyramidal cells and form the majority of cells in the hippocampus. In the CA3 region, pyramidal cells receive input from the mossy-fibres of the DG and project into CA1 and sub-cortical regions. Faster-firing (~40Hz) inhibitory GABAergic interneurons form another population of neurons. These have a widespread axonal plexus and can inhibit multiple neurons in synchrony. These neurons are heavily interconnected through synapses and gap junctions, which allows for synchronous excitatory and inhibitory bursts throughout the local circuit [364, 461]. A cycle of excitation and inhibition between these pyramidal cells and the interneurons helps to generate gamma-frequency oscillations [462]. The gamma-cycle begins with the

pyramidal cells firing, exciting GABAergic interneurons which act by feed-forward inhibition to inhibit the pyramidal cells. No longer stimulated by the pyramidal cells, the inhibitory input from the interneurons declines and a fresh cycle can begin, this leads to a phase-locked firing pattern in the gamma frequency [463].

Gamma frequency firing of CA3 pyramidal neurons projecting to the CA1 can excite inhibitory interneurons in this region [460, 464]. These interneurons then control the firing of CA1 pyramidal neurons through feed-forward inhibition [464]. This entrains the firing of the CA1 subfield to the CA3, propagating a synchronous gamma-frequency oscillation to the CA1 [464]. The firing of the CA3 assists in the rapid acquisition of novel spatial information, pattern separation of similar spatial information, and the retrieval of information from place cells [54] [55] [52]. In 'normal' ageing the CA3, unlike the CA1, undergoes a number of changes in excitatory properties and their ability to adjust firing to novel environments [39, 68]. Similarly, in ageing C57Bl/6 mice reductions in gamma oscillations can be observed in the *in vitro* hippocampus by 16 months of age [465, 466]. Further, alterations to gamma oscillations can be seen in multiple neurological disorders, reductions in neurodegenerative conditions such as Alzheimer's disease, and is believed to play a significant role in the characteristics of these diseases [465, 467].

3.5.2 - *Nfkb1*$^{-/-}$ mice show significant deficits in the generation of Carbachol-induced gamma frequency oscillations in CA3 of the hippocampus

Neuronal oscillations can be measured by monitoring changes in the electrical field potential in the brain. When neuro-transmitters, such as glutamate, are released at a synapse, positive ions can move into the dendrite leaving a negative extracellular space (Sink). These currents can move along the dendrite, and the ions exit again creating a positive extra-cellular space (Source), creating an electrical field between the sink and source. These were originally recorded via electroencephalogram, with electrodes attached to a subject's head that can detect this electrical potential through the scalp. However, this will only be seen if enough neurons are firing in together in phase as individual impulses would otherwise cancel each other out when summed together. More direct and sensitive measurements can be performed by inserting electrodes directly into brain tissue and measuring the local field-potential in specific areas.

During the first hour after bath administration of Carbachol to the slices, a gradual increase in the power of the oscillations can be observed and after 75 minutes, the slices begin to approach their eventual stable values (Figure 3.5.2.1A). *Nfkb1*$^{-/-}$ slices do not show the same degree of increase compared to slices from wild-type animals, and the area power of these oscillations diverged

significantly by 75 minutes and remained significantly different until the stable time-point. There was a large degree of variability in power between slices, which increased with the oscillation power after Carbachol administration. *nfkb1*$^{-/-}$ mice treated with Ibuprofen showed a trend for stronger gamma oscillations, with gamma power typically falling between the values for wild-type and untreated *nfkb1*$^{-/-}$ slices, and were not significantly different to wild-type slices until 120 minutes after Carbachol administration, where variability decreased as oscillations stabilised. Once slices had stabilised, wild-type slices had significantly higher median area powers than slices from untreated *nfkb1*$^{-/-}$ (Figure 3.5.2.1B). Slices from wild-type mice showed higher variability, with some area powers up to 8μV^2. The area power of slices from ibuprofen treated *nfkb1*$^{-/-}$ mice fell between wild-type and untreated *nfkb1*$^{-/-}$ slices, but was still significantly lower than wild-type values.

The maximum amplitude of the oscillations followed the same pattern as area power, but with more variability. A significant deficit became apparent after 120 minutes in *nfkb1*$^{-/-}$ mice (Figure 3.5.2.2A). *nfkb1*$^{-/-}$ mice treated with Ibuprofen showed a trend for a rescue in oscillation amplitude and area-power, with values falling between wild-type and untreated *nfkb1*$^{-/-}$ mice, although it was not significantly different to either during the 180 minutes after Carbachol administration. However, given the number of animals and range of potential values (between untreated *nfkb1*$^{-/-}$ mice and the wild-type level they might be restored to) this is not surprising. At the stable time-point, slices from untreated *nfkb1*$^{-/-}$ mice had significantly lower amplitude values than wild-type mice (Figure 3.5.2.2B). Slices from ibuprofen treated *nfkb1*$^{-/-}$ mice showed a trend for increased oscillation amplitude, but was still significantly lower than slices from wild-type mice.

However, in contrast, the frequency of oscillations (once they could be observed) started in the gamma frequency range (15-45Hz), and remained stable across 180 minutes post-Carbachol administration, with most values falling between 20 to 30 Hz (Figure 3.5.2.3A). There was no significant differences between genotype or in Ibuprofen treated animals during the 180 minutes post-Carbachol administration, or at the stable time-point (Figure 3.5.2.3B).

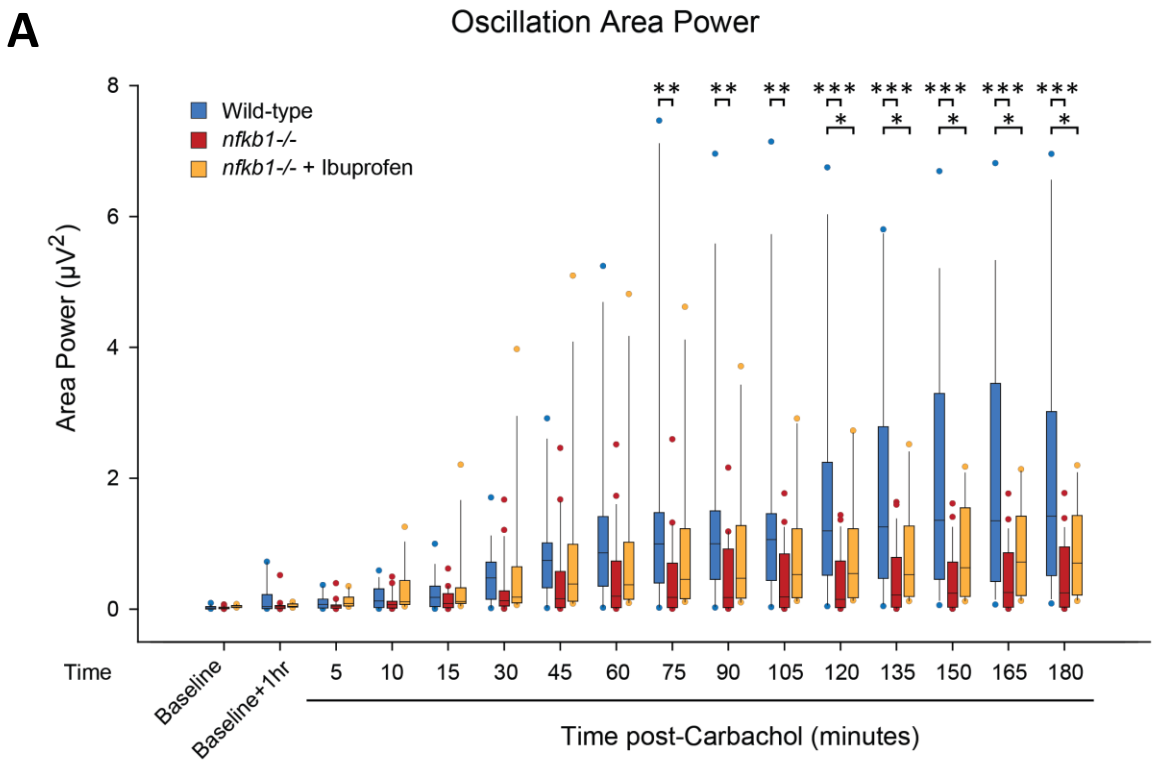
A
Oscillation Area Power
Wild-type
nfkb1-/-
nfkb1-/- + Ibuprofen
Area Power (μV2)
Time
Baseline
Baseline+1hr
5
10
15
30
45
60
75
90
105
120
135
150
165
180
Time post-Carbachol (minutes)

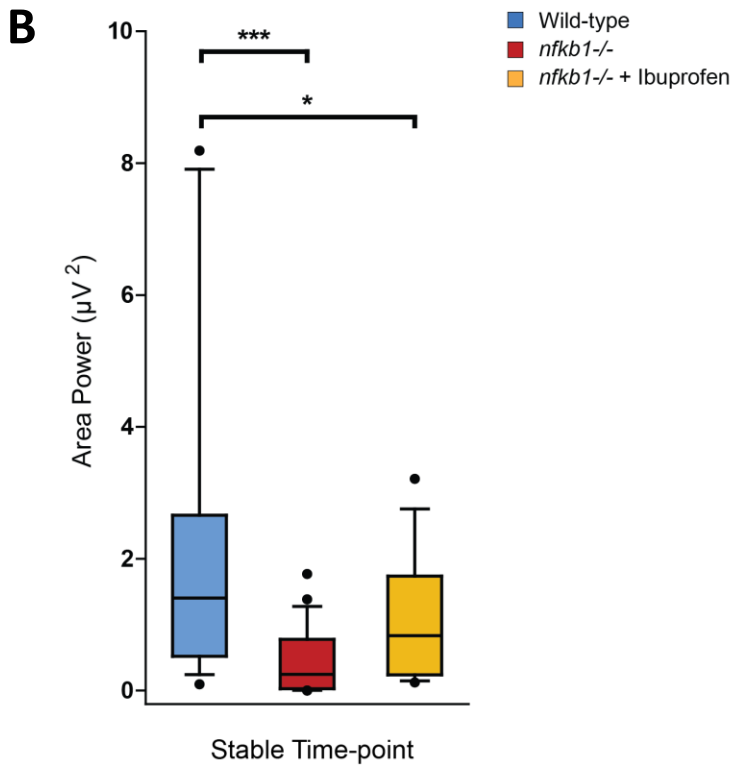
B
Wild-type
nfkb1-/-
nfkb1-/- + Ibuprofen
Area Power (μV 2)
Stable Time-point

Figure 3.5.2.1: ***Nfkb1*$^{-/-}$ mice show significantly reduced gamma-frequency oscillation area power in extracellular field recordings from CA3 *stratum radiatum* in isolated hippocampal slices**

A) Oscillation area power at baseline, after rest for 1 hour, then for 3 hours post-Carbachol bath administration for wild-type, *nfkb1*$^{-/-}$ mice, and *nfkb1*$^{-/-}$ mice with Ibuprofen. **B)** Oscillation area power at stable time-point in wild-type, *nfkb1*$^{-/-}$ mice, and *nfkb1*$^{-/-}$ mice with Ibuprofen. n is hippocampal slices, with 4-5 animals per group and 3-6 slices per animal. Outliers are shown. 2-way Repeated Measures ANOVA without interactions was performed on the build-up, p-values shown by * <0.05, ** <0.005, *** <0.001. Performed with Clare Tweedy, performing brain removal and electrode placement, and advice from Fiona LeBeau.

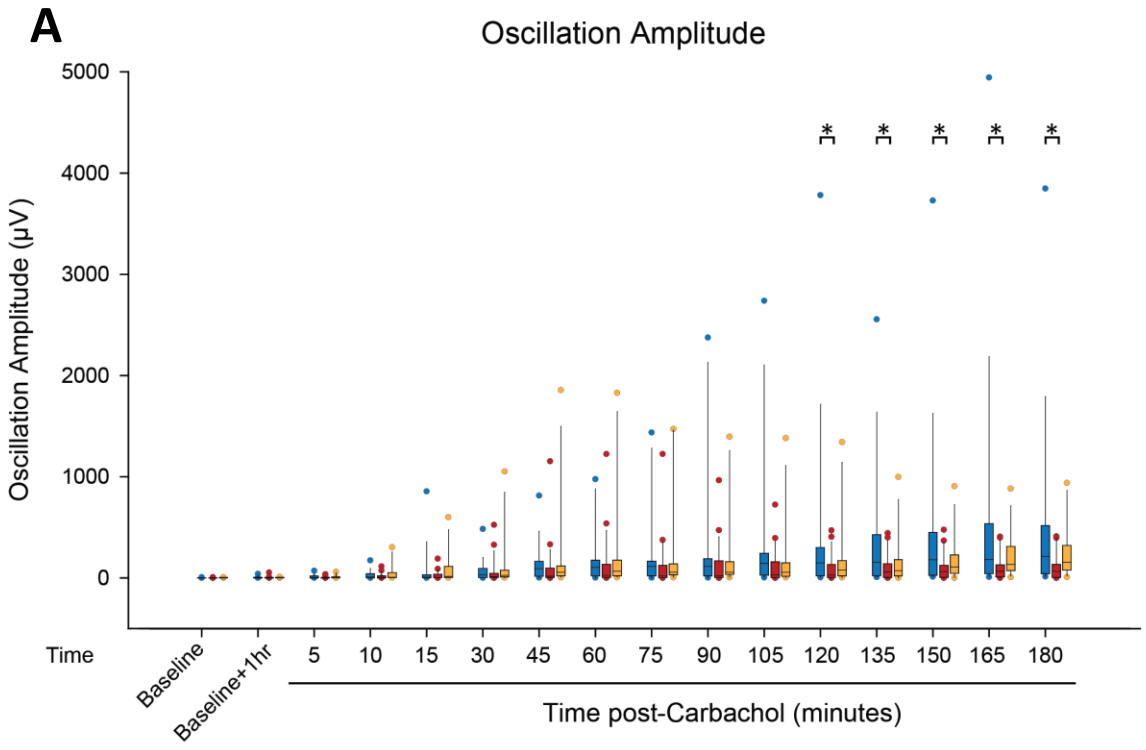
A
Oscillation Amplitude
Oscillation Amplitude (µV)
5000
4000
3000
2000
1000
0
*
Time
Baseline
Baseline+1hr
5
10
15
30
45
60
75
90
105
120
135
150
165
180
Time post-Carbachol (minutes)

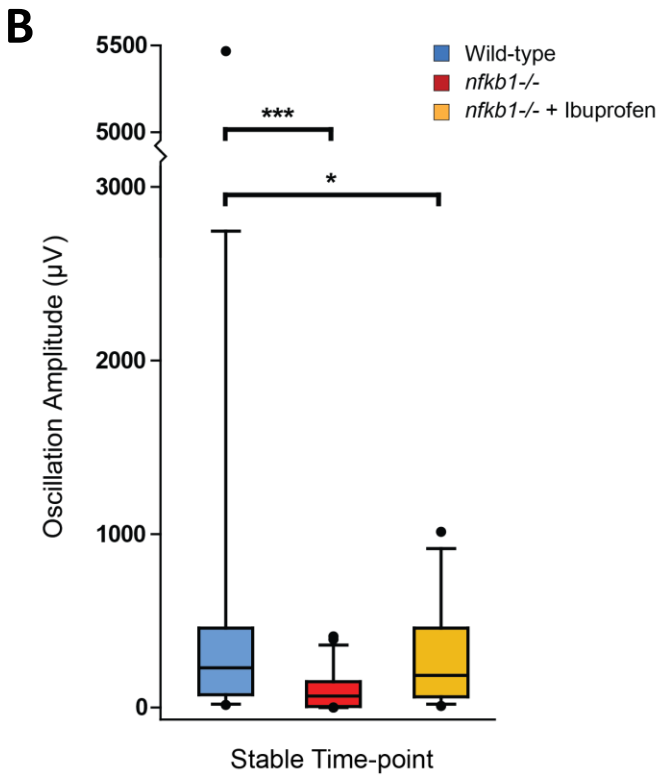
B
Wild-type
nfkb1-/-
nfkb1-/- + Ibuprofen
5500
5000
3000
2000
1000
0
***
*
Oscillation Amplitude (µV)
Stable Time-point

Figure 3.5.2.2: ***Nfkb1*$^{-/-}$ mice show significantly reduced gamma-frequency oscillation maximum amplitude from extracellular field recordings from CA3 *stratum radiatum* in isolated hippocampal slices**

A) Oscillation area power at baseline, after rest for 1 hour, then for 3 hours post-Carbachol bath administration for wild-type, *nfkb1*$^{-/-}$ mice, and *nfkb1*$^{-/-}$ mice with Ibuprofen. **B)** Oscillation area power at stable time-point in wild-type, *nfkb1*$^{-/-}$ mice, and *nfkb1*$^{-/-}$ mice with Ibuprofen. n is hippocampal slices, with 4-5 animals per group and 3-6 slices per animal. Outliers are shown. 2-way Repeated Measures ANOVA without interactions was performed on the build-up, p-values shown by * <0.05, ** <0.005, *** <0.001.

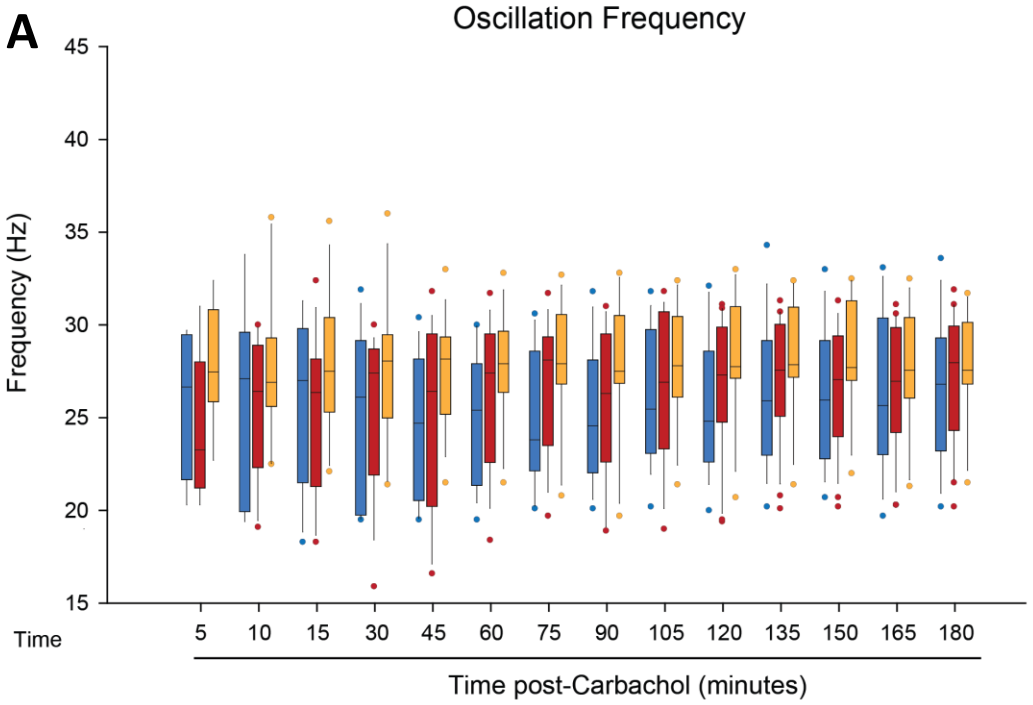
A
Oscillation Frequency
Frequency (Hz)
45
40
35
30
25
20
15
Time
5
10
15
30
45
60
75
90
105
120
135
150
165
180
Time post-Carbachol (minutes)

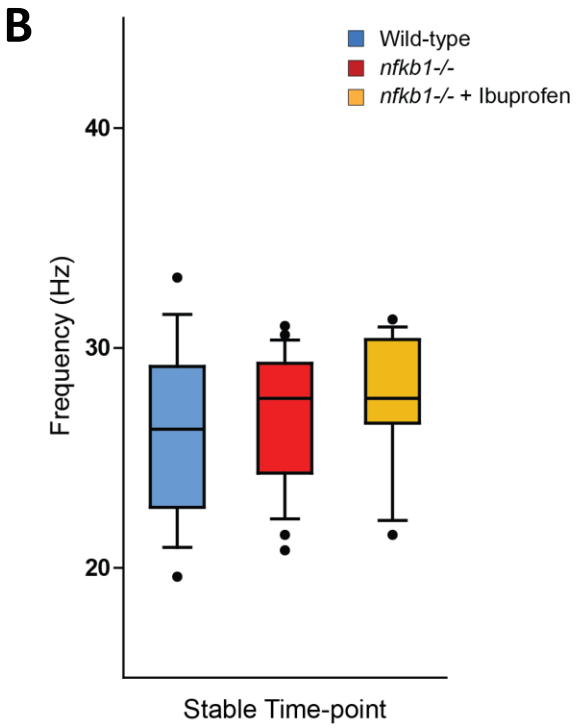
B
Wild-type
nfkb1-/-
nfkb1-/- + Ibuprofen
40
30
20
Frequency (Hz)
Stable Time-point

Figure 3.5.2.3: No significant differences between wild-type and *nfkb1*$^{-/-}$ mice in gamma-frequency oscillation frequency from extracellular field recordings from CA3 *stratum radiatum* in isolated hippocampal slices

A) Oscillation frequency at baseline, after rest for 1 hour, then for 3 hours post-Carbachol bath administration. **B)** Oscillation frequency at stable time-point. n is hippocampal slices, with 4-5 animals per group and 3-6 slices per animal. Outliers are shown. 2-way Repeated Measures ANOVA without interactions was performed on the build-up, no significant differences found.

3.5.3 - *Nfkb1*$^{-/-}$ show significant deficits in the rhythmicity of Carbachol-induced gamma frequency oscillations in the hippocampus

The generation of gamma frequency oscillations relies on a delicate circuit between pyramidal and interneurons and requires the precise timing of firing to generate a cohesive and stable oscillation. As the data suggests that there are impairments in the generation of gamma frequency oscillations in the CA3 stratum radiatum of *nfkb1*$^{-/-}$ mice, the rhythmicity of these oscillations was also recorded. This should provide a measure of how stable the gamma frequency oscillation generated by the circuit is, and how well it communicates these oscillations to the CA1.

Auto-correlations of recordings from stable-time point recordings in CA3 *stratum radiatum* were taken in wild-type, *nfkb1*$^{-/-}$ mice and ibuprofen treated *nfkb1*$^{-/-}$ mice (Figure 3.5.3.1A). A visual representation of representative normalised auto-correlations from wild-type, untreated *nfkb1*$^{-/-}$ and ibuprofen treated *nfkb1*$^{-/-}$ slices can be seen in (Figure 3.5.3.1A), with a greater degree of correlation in wild-type slices than *nfkb1*$^{-/-}$ slices, shown by the size of the peaks. These were recorded and analysed from traces taken from both the *stratum radiatum* (Figure 3.5.3.1B) and *stratum pyramidale* (Figure 3.5.3.1C).

Gamma frequency oscillations in the *stratum radiatum* of wild-type slices showed high rhythmicity index scores, indicating a stable gamma frequency oscillation is being generated (Figure 3.5.3.1D). *Nfkb1*$^{-/-}$ slices show a significant reduction in the rhythmicity of gamma frequency oscillations compared to wild-type slices, while there was a trend for improvement in ibuprofen treated *nfkb1*$^{-/-}$ slices, with the median rhythmicity index falling between the median of wild-type and *nfkb1*$^{-/-}$ slice values.

In contrast, the rhythmicity of recordings taken from the pyramidal layer showed no differences in the median rhythmicity index between wild-type or *nfkb1*$^{-/-}$ slices, and no significant effect with ibuprofen treatment, although an increase in variability can be observed in *nfkb1*$^{-/-}$ slices (Figure 3.5.3.1E).

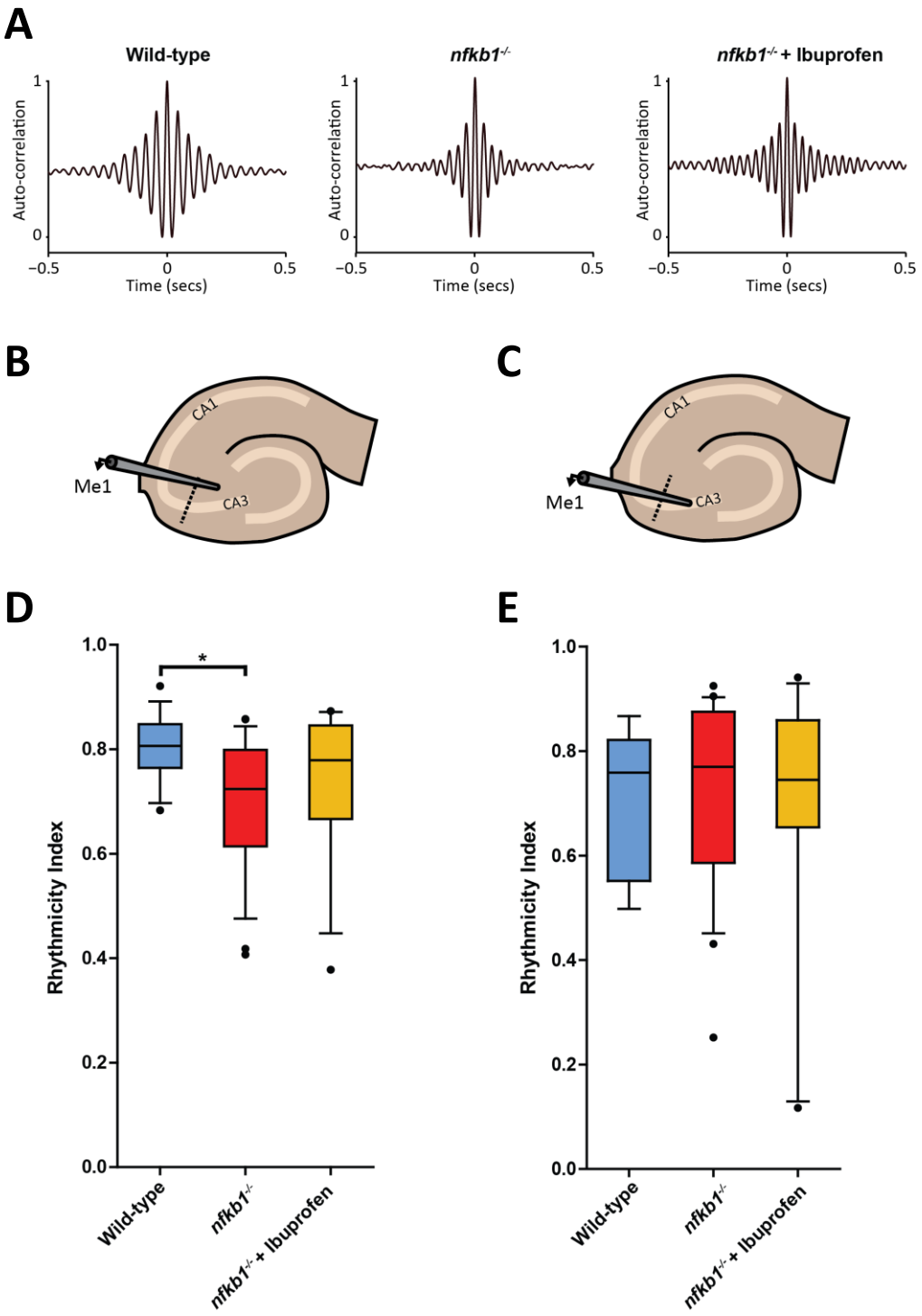

Figure 3.5.2.1: *Nfkb1*$^{-/-}$ show reduced gamma oscillation synchronicity in CA3 *stratum radiatum*

A) Representative auto-correlations of gamma oscillations recorded CA3 *stratum radiatum* of wild-type, *nfkb1*$^{-/-}$ and *nfkb1*$^{-/-}$ mice treated with Ibuprofen. Schematic diagrams of electrode placement in slices for the recording of LFPs in **B)** the stratum radiatum and **C)** the statum pyramidale. Normalised rhythmicity of gamma frequency oscillations in D**)** CA3 *stratum radiatum* and E**)** CA3 *stratum pyramidale* of wild-type, *nfkb1*$^{-/-}$ and *nfkb1*$^{-/-}$ mice treated with Ibuprofen. n is hippocampal slices, 13-24 slices per group. Outliers are shown. 2-way ANOVA without interactions. Significant differences between genotype, as well as treatments, are displayed by (* $p<0.05$).

3.5.4 - *Nfkb1*$^{-/-}$ mice show significant deficits in the propagation of synchronous signal between CA3 and CA1

As previously described, gamma oscillations generated in the CA3 propagate the oscillation to the CA1 *stratum radiatum* via the schaffer collateral [460, 464]. This entrains the firing of the CA1 subfield to the CA3; this communication is important for the rapid formation of spatial memories and especially the retrieval of previously stored spatial information based on spatial cues [52, 54, 55, 409].

To measure the propagation of gamma oscillations from CA3 to CA1, a second electrode was placed in the CA1 *stratum radiatum* distal to the CA3 once the slices had stabilised. If a gamma oscillation could be detected in this region, then slice was deemed to be propagating properly, if not the CA1 electrode was moved to a medial position. If an oscillations was still not evident then the electrode was moved again to a more proximal position.

In wild-type mice 92% of slices showed gamma frequency oscillations in the distal portion of the CA1 *stratum radiatum*, with the remaining 8% showing an oscillation once the electrode was moved to the medial portion, demonstrating normal projection of gamma activity from the CA3 to the CA1 (Figure 3.5.4.1A). However, only 75% of untreated n*fkb1*$^{-/-}$ slices showed oscillations in the distal region of CA1, a further 17% showed a gamma frequency oscillation in the medial proportion, and 8% showed no oscillations in any position of the CA1; demonstrating an impaired ability to project gamma activity from CA3 to CA1. In ibuprofen treated n*fkb1*$^{-/-}$ slices, 79% of slices showed an oscillation in the distal CA1, and 14% when moved to the medial position, and the remaining 7% only when moved to the proximal position. However, all slices propagated to at least one position in the CA1, showing an improvement in the propagation of gamma activity from CA3 to CA1.

Cross-correlations compare two simultaneous recordings, one in CA3 against one in CA1, in the same way that at auto-correlation compares the rhythmicity of a recording against itself. This provides a measure of the synchronicity of the oscillations between CA3 and CA1 and provide insight into how well the CA3 entrains the firing of CA1. Wild-type slices showed a strong level of synchronicity between CA3 and CA1 in the *stratum radiatum*, signifying that the oscillation in CA1 is well entrained to CA3 (Figure 3.5.4.1B). However, *nfkb1*$^{-/-}$ slices showed a significant reduction in rhythmicity between the oscillations in CA3 and in CA1 *stratum radiatum* compared to wild-type controls. Ibuprofen treated *nfkb1*$^{-/-}$ slices showed a significant improvement compared to untreated *nfkb1*$^{-/-}$ slices, and were not significantly different to wild-type controls. However, when the electrodes were moved to *stratum pyramidale* of these respective areas, no significant differences were between the groups could be observed (Figure 3.5.4.1C). Seven of the *nfkb1*$^{-/-}$ mice used in the Y-maze were used in the

electrophysiology experiments, a correlation could be observed between their arm discrimination index in the first two minutes of the trial and the average CA3-CA1 cross correlation rhythmicity index from slices taken from that animal (Figure 3.5.4.1D). A trend for decreased latency to the primary arm with increasing CA3-CA1 cross-correlation , and a higher values in animals that made the correct primary arm choice could also be observed, but were not significant (Figure 3.5.4.1E-F, respectively).

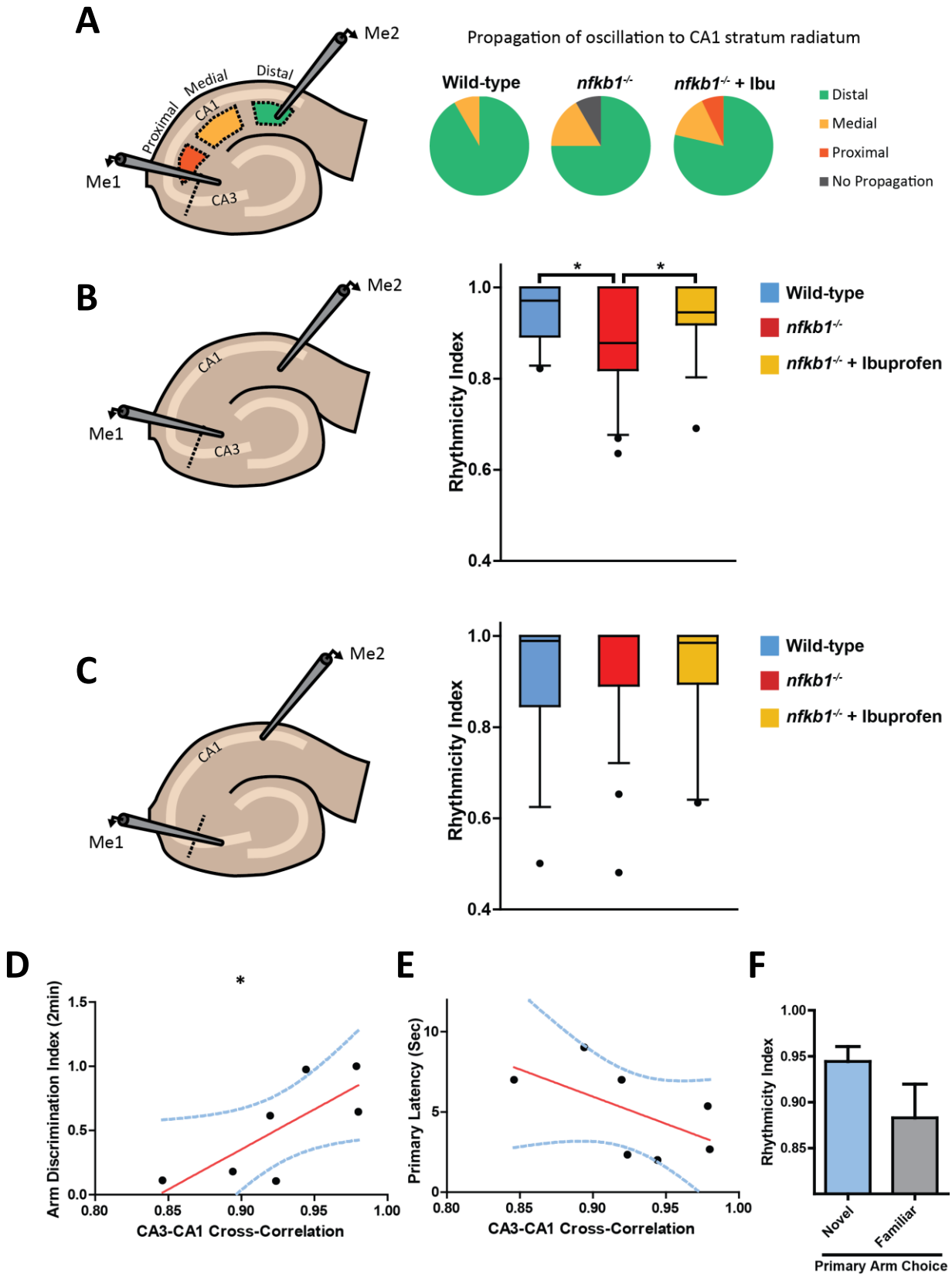
A
Me2
Me1
Proximal
Medial
Distal
CA1
CA3
Propagation of oscillation to CA1 stratum radiatum
Wild-type
nfkb1-/-
nfkb1-/- + Ibu
Distal
Medial
Proximal
No Propagation
B
Me2
Me1
CA1
CA3
Rhythmicity Index
1.0
0.8
0.6
0.4
*
*
Wild-type
nfkb1-/-
nfkb1-/- + Ibuprofen
C
Me2
Me1
CA1
Rhythmicity Index
1.0
0.8
0.6
0.4
Wild-type
nfkb1-/-
nfkb1-/- + Ibuprofen
D
*
Arm Discrimination Index (2min)
1.5
1.0
0.5
0.0
0.80
0.85
0.90
0.95
1.00
CA3-CA1 Cross-Correlation
E
Primary Latency (Sec)
10
5
0
0.80
0.85
0.90
0.95
1.00
CA3-CA1 Cross-Correlation
F
Rhythmicity Index
1.00
0.95
0.90
0.85
Novel
Familiar
Primary Arm Choice

Figure 3.5.4.1: *Nfkb1*$^{-/-}$ mice show reduced propagation of gamma oscillations to CA1 *stratum radiatum*

A) Placement of electrodes to measure presence of gamma oscillations in distal, medial and proximal portions of CA1 *stratum radiatum* of wild-type, *nfkb1*$^{-/-}$, and *nfkb1*$^{-/-}$ mice treated with ibuprofen. Pie charts show proportion of slices propagating into CA1, with distal recorded, then if there is no oscillation, medial and then for proximal if still no oscillation. A lower proportion of *nfkb1*$^{-/-}$ mice had oscillations present in the distal portion, with some showing no oscillation in CA1. **B)** Cross-correlations of oscillations recorded in CA3, and distal CA1 *stratum radiatum*, if the slice is oscillating at this point. **C)** Measurements of cross-correlations in CA3 and distal CA1 *stratum pyramidale*. 2-way ANOVA without interactions, p-values shown by * <0.05. **D-F)** Mice were tracked and their performance in the Y-maze correlated with the average cross-correlation of slices taken from the animal between CA3 and CA1. Spearman correlation, significance is shown by *<0.05.

3.5.5 - *Nfkb1*$^{-/-}$ mice show spontaneous hyper-excitable bursting in CA3 of the hippocampus

Network hyper-excitablity can be observed in seizure and neurodegenerative disease such as AD. These are bursts of activity from sharp-wave ripples and burst discharges that cause a sudden depolarisation in the LFP. Sharp wave and burst discharges (henceforth termed 'Hyper-excitable events') were recorded from 60s epochs as events which exceeded 5x the Standard Deviation of the entire 60s epoch (Figure 3.5.3.1A-B). They were recorded at Baseline+1 hour time point, where the slices had been allowed to rest in the rigs, 15 minutes post-Carbachol administration when gamma oscillations were beginning to occur in some slices and once oscillations had stabilised (Figure 3.5.3.1C).

Spontaneous hyper-excitable events could be observed in slices from both wild-type and n*fkb1*$^{-/-}$ mice prior to Carbachol administration (Figure 3.5.5.1C). *Nfkb1*$^{-/-}$ mice showed significantly more hyper-excitable events prior to Carbachol administration compared to wild-type controls. In slices from ibuprofen treated n*fkb1*$^{-/-}$ mice, there was a trend for a decrease in the median number of events per slice, with the value closer to wild-type slices and this was not significantly different to either group. Carbachol administration should reduce the number of hyper-excitable events was reduced following Carbachol administration in all groups as gamma oscillations formed, but showed a trend for increased number of events in slices from untreated *nfkb1*$^{-/-}$ mice.

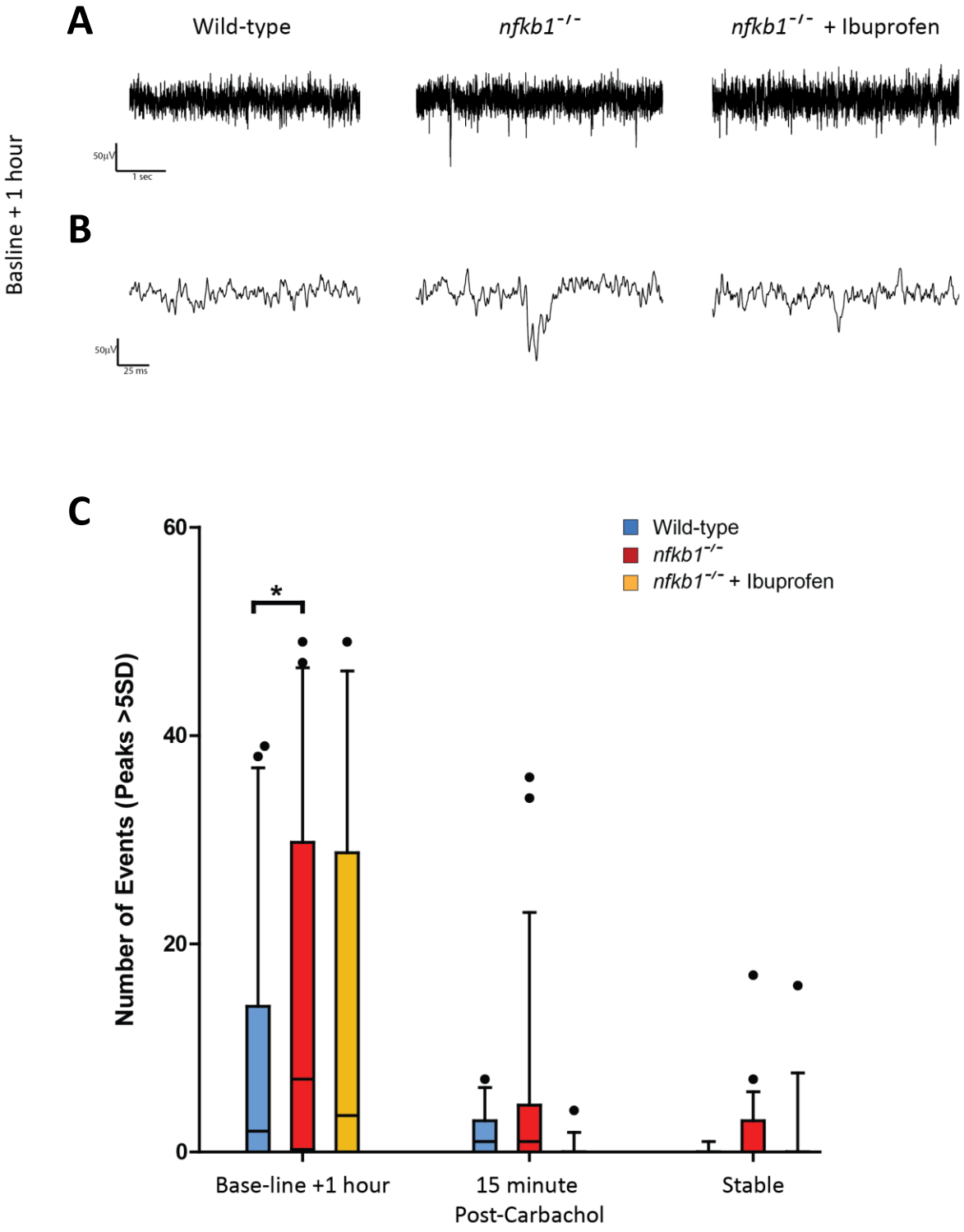

Figure 3.5.3.1: *Nfkb1*$^{-/-}$ slices show increased number of hyperexcitable events

Example **A)** 5 seconds and **B)** 200ms extracts taken from representative 60s epochs at Base-line + 1 hour time-point. **C)** show number of spontaneous discharges at baseline+1 hour recording (pre-Carbacohol administration), 15 minutes after Carbachol and at stable timepoint. Box-plots showing number of hyper-exictable discharges from 16-24 slices per group, pooled from 4-5 animals. Outliers are shown. 2-way Repeated Measures ANOVA without interactions was performed on base-line +1, 15 min post-Carbachol and stable time-point, p-values shown by * <0.05.

3.5.6 – Discussion

I had previously observed increased microglial presence and activation in the hippocampus region, reduced neurogenesis, as well as alterations in the neuro-inflammatory profile of cytokines associated with hippocampal dysfunction. Additionally, I observed deficits in performance in the Y-maze and Barnes Maze of *nfkb1*$^{-/-}$ mice, measures of spatial learning and memory [433]. To investigate if there was an alteration in hippocampal function in *nfkb1*$^{-/-}$ mice that would explain the observed deficits in spatial memory, I tested gamma frequency oscillations in isolated hippocampal slices**.** Deficits in gamma-frequency oscillations can be observed with normal ageing, as well as multiple neurological disorders, such as Alzheimer's disease, where it is believed to underlie some of the cognitive deficits observed [465-467].

The data here show that there is an impairment in the build-up, power and amplitude of Carbachol-induced gamma-frequency oscillations generated in the CA3 of *nfkb1*$^{-/-}$ mice, compared to age-matched wild-type controls. In ageing C57Bl/6 mice reductions in the power of gamma oscillations can be observed in the *in vitro* hippocampus by 16 months of age, compared to younger wild-type animals [465, 466]. The defects in the build-up of the oscillation after Carbachol are similar to what is observed in older wild-type mice, as well as neurodegenerative models [465]. I also observed a small, but significant decrease in the rhythmicity of gamma-frequency oscillations within the *stratum radiatum* of CA3 in *nfkb1*$^{-/-}$ mice, with a trend for a partial rescue of activity in ibuprofen treated mice. Decreases in neuronal synchrony, especially in the gamma frequency range, can be observed in brain disorders and diseases such as Alzheimer's [468]. In normal ageing, only slight reductions in the cross-correlation within CA3 can be observed [466], and, while significant, the decrease in auto-correlation in CA3 observed here was not large in *nfkb1*$^{-/-}$ mice.

The gamma oscillation deficits in *nfkb1*$^{-/-}$ mice may reflect the premature ageing phenotype observed in the mouse as a whole occurring in the neuronal circuit, or neurodegenerative changes. Since the generation of gamma oscillations requires the precise timing of synchronous firing from arrays of pyramidal neurons and interneurons, it is vulnerable to disruptions within this circuit. The percentage decrease observed in Carbachol-induced gamma frequency power, in *nfkb1*$^{-/-}$ mice compared to wild-type control mice, is similar to that previously observed between 5 month and 22 month wild-type mice [466]. Which suggests that if this is acceleration of an age-related decline, then *nfkb1*$^{-/-}$ mice are match wild-type mice at this age-range [466]. Additionally, this is backed up by the lack of a significant change in the peak frequency of the gamma oscillations was observed, which is in line with results from normally ageing mice [466].

However, since these readings were taken at a single time-point it cannot be totally ruled out that these are deficits specific to the model and not an accelerated age-dependent change. Slices from *nfk1b*$^{-/-}$ mice treated with ibuprofen showed a trend for improved oscillation build up, with no significant difference to slices from wild-type control mice in the build-up of gamma oscillations until later in the build-up. However, these trends were not significant compared to their untreated *nfkb1*$^{-/-}$ littermates. The lack of significance may be explained by the large variability in results, and a comparatively narrow window between *nfkb1*$^{-/-}$ and wild-type mice, as it would likely not be a complete rescue of the phenotype.

Nfkb1$^{-/-}$ mice showed a significant deficit in propagation of gamma activity from CA3 to CA1 compared to wild-type mice, which was ameliorated with ibuprofen treatment. This may reflect an impairment in the Schaffer collaterals, which run from CA3 to CA1. Computational models and hippocampal lesions have shown that CA3-CA1 communication is important for the retrieval of memory in hippocampal-dependent tasks [469]([470]. These studies propose CA3 pyramidal neurons act as an auto-associative network to store new memories, and retrieve memories from CA1, when presented with limited cue information [469]([54, 470]. Increased CA3-CA1 gamma synchrony in local field potentials can be seen at the point of arm-choice in delayed alternation continuous T-maze [52], which suggests that CA3-CA1 gamma synchrony is involved in the retrieval of information about the previous trial. Gamma synchrony between areas appears to also be necessary across the circuit, high synchrony can be observed in the CA3, CA3 to CA1 and a burst of high CA1-entorhinal cortex synchrony can be observed in various T-maze setups, just prior to the correct choice of arm, but not before an incorrect arm choice [52, 471, 472].

The defects observed here, especially in CA3-CA1 gamma synchrony, in *nfkb1*$^{-/-}$ mice would explain their reduced preference for the novel-arm in the Y-maze, and might represent CA3 dysfunction and a failure to entrain CA1 firing to recall the correct arm. Furthermore, ibuprofen treatment improved both of these parameters in *nfkb1*$^{-/-}$ mice, more closely matching wild-type mice. When compared to the performance of *nfkb1*$^{-/-}$ mice in the Y-maze, there was a degree of correlation between average CA3-CA1 stratum radiatum cross-correlation and arm discrimination index, additionally the mice who made failed to enter the Y-maze arm correctly the first time showed a trend for lower average cross-correlation, which observation is in line with the existing evidence and models. There was no observable correlation with auto-correlative capacity. This would suggest that, at least in this model, chronic inflammation is linked to decreased CA3-CA1 communication. This could be due to deficits in the Schaffer collateral and its ability to entrain CA1 firing, such as reduced synapse or collateral density, which may explain deficits in the retrieval of previous learnt spatial information.

The deficits in oscillation power, and reduced rhythmicity of oscillations in *nfkb1*$^{-/-}$ slices suggests that there are abnormalities within the circuit that generates slow-gamma oscillations. There are number of possible explanations for the observed defects in gamma oscillations. Phenotypic changes to constituent cells within the circuit, as well as loss of cells, could explain the observed deficits. As gamma frequency oscillations require the precise firing of excitatory pyramidal cells and inhibitory interneurons, disruptions to this balance can result in deficits in gamma oscillations.

Gamma oscillations are driven by the firing of parvalbumin positive GABAergic interneurons, which inhibit the soma of excitatory pyramidal cells [473]. Parvalbumin is a calcium binding protein expressed on a sub-population of GABAergic interneuron [474]; these calcium proteins are vital for calcium buffering, the correct firing of these neurons [475] and the generation of gamma oscillations [473]. There are reductions in the number of cells positive for these interneuron markers, including parvalbumin, in the hippocampus with age and disease (although the relative decreases vary between region and the CA3 sees only mild decreases in positive cells) [476-478]. However, normally ageing wild-type mice show well preserved neuron numbers in the hippocampus, even in mice with cognitive impairment, and little change in pyramidal cell number [31, 58, 59]. Instead the decline in parvalbumin positive neurons appears to be driven by phenotypic change rather than cell loss, with reductions in the expression of parvalbumin, leading to a reduction in pre-synaptic calcium buffering capacity and reduced GABA release, which may directly contribute to the observed changes in gamma oscillations [479-481].

The death of neurons in the circuit could also contribute to the decreased area power. Loss of neurons in the CA3 can be seen in neurodegenerative diseases such as AD [482], although deficits in gamma oscillations appear to occur earlier in disease pathology [465]. Within the *nfkb1*$^{-/-}$ mouse some alterations in hippocampal number have been previously reported. Lu *et al.* reported with no differences at 6 months, and an approximately 10% reduction hippocampal NeuN positive cells at 10 months, and activated caspase-3 at both ages [395] However, these numbers were reported from the whole hippocampus, with randomly selected fields within the hippocampus, so it is not clear if this is region specific degeneration or not. Additionally, a 20% reduction in CA2 neurons has been reported in male *nfkb1*$^{-/-}$ mice at 11 months [421]. A reduced number of neurons contributing to the gamma oscillation could explain the reduced area power of the oscillations. Future experiments on the number of parvalbumin positive cells and expression, along with other neuronal markers, would help ascertain if there is a specific vulnerabilities that would disrupt the gamma generating circuit.

Interestingly, I observed network hyper-excitability in 8 month *nfkb1*$^{-/-}$ mice, which could be due to reduced inhibitory input from interneurons. CA3 neurons show increased basal rates of firing with normal ageing [39, 68], and deficits in their capacity to respond to novel environments [39]. Hyper-excitability has also been linked to a decrease in pattern separation [69], and treatment with anti-epileptic drugs (which reduce hyper-excitability) help improve cognition [71]. This could also contribute to the observed deficits in spatial memory. Hippocampal neurons from *nfkb1*$^{-/-}$ mice show increased vulnerability to excitotoxic injury following glutamate exposure, and show increased oxidative stress, which could promote loss of neurons [393]. However, the 'hyper-excitable events' I recorded here were in the local field potential, and can be generated by defects in both interneurons and pyramidal cells. Intracellular recordings of inhibitory and excitatory post-synaptic potentials would be required to ascertain the relative contributions of these cell types.

The firing of neurons and the generation of a network gamma frequency oscillations is also a highly energy intensive task [483]. It is associated with high rates oxygen consumption and alterations in redox state, and oscillations are vulnerable to disruption if there is a loss of energy supply or mitochondrial dysfunction [483]. Deficits in gamma oscillations can be seen with mitochondrial dysfunction, redox dysregulation and oxidative stress [484-486]. In mice with decreased glutathione expression, increased oxidative stress can be seen selectively in the CA3 and DG of the hippocampus, accompanied by impairment of Parvalbumin interneurons and deficits in gamma oscillations [485]. However, work I performed in my Master's thesis on whole brain homogenate from *nfkb1*$^{-/-}$ mice aged 9 to 10 months did not show a significant change in mitochondrial metabolism, however, although there was a slight trend for superoxide production from complex I. However, this was from whole brain homogenate and does not rule out the possibility that there could be changes in mitochondrial function at an individual cell level, or in specific areas, that would contribute towards the observed deficits in gamma oscillation.

The observed deficits in gamma oscillations in *nfkb1*$^{-/-}$mice outlined above could be due to the increased neuro-inflammation. *Nfkb1*$^{-/-}$ treated with ibuprofen showed a trend for improved performance in gamma oscillation generation and significant improvements in CA3-CA1 synchrony. Chronic inflammation has been shown to impair long-term potentiation in CA1 pyramidal neurons induced by input to the schaffer collaterals [102], which could explain the deficits in propagation of the gamma frequency oscillation in *nfkb1*$^{-/-}$ mice. As discussed previously, increased IL-6 levels are associated with cognitive dysfunction in a number of conditions. A trend for increased IL-6 at 8 months could be seen in whole brain homogenate from *nfkb1*$^{-/-}$ mice, and a significant increase can be seen in aged *nfkb1*$^{-/-}$mice; additionally, significantly increased circulating levels of IL-6 have been reported in

nfkb1$^{-/-}$ mice at this age [127]. IL-6 can modulate glutamatergic neuro-transmission [487] and appears to mediate age-related loss of parvalbumin GABAergic interneurons in the hippocampus, through increased NADPH oxidase super-oxide production [484]. Studies have shown that reductions in parvalbumin positive cells were especially pronounced in the CA3 region in 22-26 month wild-type mice, but attenuated in IL-6 knockout and mice treated with anti-oxidants, which showed improved spatial memory in the Morris Water Maze [484]. Increased p65 binding could be seen in aged mice extracts and was decreased in IL-6 knockout mice; *in vivo*, application of IL-6 induced oxidative stress and a reduction in the expression of parvalbumin – these were both blocked through the inhibition of NF-κB activity [484]. This could underlie the early defects in gamma oscillations seen in the *nfkb1*$^{-/-}$ model. Although, whether p65 nuclear localisation would be disrupted by the loss of p50, or mediated by additional NF-κB dimer types is not clear.

Together, these data suggest *nfkb1*$^{-/-}$ mice show a significant deficit in the generation of Carbachol induced gamma frequency oscillations in CA3 of the hippocampus. Further, there is a loss of propagation of the oscillation to the CA1. These may explain the deficits seen in hippocampal dependent spatial memory observed earlier in the chapter. The trends for improvement in oscillation build up, and significant rescue of CA3-CA1 oscillation synchrony with ibuprofen treatment suggests that this may be mediated through a COX-2 dependent pathway. A previously unexplored contributor to the observed deficits in spatial memory and gamma oscillations - and the phenotypic changes which can contribute to these deficits - could be the senescent-like neuronal phenotype. Senescence-associated markers have been observed with ageing in the hippocampus, and other neuronal populations [112], but little is currently known about the phenotype; Dysregulation and shifts in gene expression can be seen in senescent cells, and could contribute to changes in factors such as Parvalbumin, neurotransmission and altered receptor densities [121]. Alterations in morphology are also observed, that could affect axonal, dendritic and synapse formation, and projection to other areas [86]. Alterations in calcium handling and signalling have now been observed in cellular senescence, and there is an emerging link between increased intracellular free calcium levels, mitochondrial dysfunction and the cell-cycle arrest, and the secretory phenotype of senescence [488]. Further, mitochondrial dysfunction and the generation of ROS is seen downstream of DNA damage signalling and promotes, then stabilises, the senescent phenotype [177]. As such, in the next sub-chapter, I investigated DDR and senescence-associated markers in neurons in wild-type and *nfkb1*$^{-/-}$ mice.

3.6 - Ageing and chronic inflammation lead to increased DDR signalling and senescence-associated markers in neurons.

3.6.1 - Introduction

Microglial proliferation, cytokine levels increase and cognitive deficits increase with age in *nfkb1*$^{-/-}$ mice and are ameliorated by long-term ibuprofen treatment. Microglia in *nfkb1*$^{-/-}$ mice show prolonged and elevated pro-inflammatory release once activated, but appear to require a secondary ROS driven stimuli. Work by the team has previously established the role of cellular senescence in mitotic cells in the premature ageing phenotype of *nfkb1*$^{-/-}$ mice [127]. In mitotic tissues, increased sterile inflammation in *nfkb1*$^{-/-}$ mice accelerates the accumulation of senescent cells, which further exacerbates inflammation and leads to the accumulation of further senescent cells, through the release of pro-inflammatory and pro-oxidative molecules [127]. Further, the team has shown the presence, and increasing frequency, of senescence-like neurons in multiple brain areas of normally ageing wild-type mice [112]. Whether these neurons are associated with inflammation in the brain and the activation of glial cells has not been previously shown, nor has if these cells are associated with cognitive deficits. Senescent-like neurons have previously been established as being positive for inflammatory cytokines such as IL-6 and markers of oxidative damage, which may increase tissue levels of the cytokine and prime microglia.

Increased inflammation can trigger the accumulation of senescent cells through activation of the DDR [127, 489]. Circulating and resident immune cells can release ROS and RNS species [490]. In chronic inflammation, these radical species can react with DNA, either directly or indirectly, to form oxidative adducts and breaks [490]. This has been linked to the propagation of inflammation, through activation of the DDR and the release of SASP factors through downstream pathways such as NF-κB [119, 232]. The release of these factors can further induce cellular senescence in bystander cells [122]. The direct transfer of ROS is mediated through cell to cell transfer through gap junctions [122], and inflammatory chemo- and cytokines through secretion [86].

Two main neuronal cell types were chosen for analysis in these brains. Purkinje cells in the cerebellum were chosen due to the previously observed increase of senescent-like neurons in mice with telomere dysfunction [112] and the deficits in neuro-muscular coordination in *nfkb1*$^{-/-}$ mice [127]. Pyramidal layer neurons of the hippocampus were chosen for their roles in spatial learning and memory, and the observed deficits in gamma frequency oscillation generation. Multiple senescence markers were used, as a single marker is insufficient to approximate the rate of senescent cells [121]. Markers of the DDR,

such as DNA damage and the activation of downstream pathways were assessed through measurement of γH2A.X foci and activation of p21. Exclusion of High Mobility Group Box 1 from the nucleus was used as an additional marker [121, 491]; together with the accumulation of auto-fluorescent lipofuscin aggregates [492].

3.6.2 - Telomere-associated foci (TAF) increase in purkinje and pyramidal neurons with age and chronic inflammation.

Both total number of γH2A.X foci, and number of foci co-localising with telomeres were counted per neuron, and then mean number of γH2A.X foci, TAF and frequency of neurons with multiple TAFs were recorded (Figure 3.6.2.1A). Telomere associated γH2A.X foci were distinguished from regular foci by their co-localisation with PNA telomere probe (Figure 3.6.2.1B).

In Purkinje neurons no significant difference in the total number of foci between untreated wild-type and *nfkb1*$^{-/-}$ mice, or treated animals, was observed (Figure 3.6.2.1C). By 18 months significantly higher rates of γH2A.X foci in CA1 neurons could be observed in *nfkb1*$^{-/-}$ compared to wild-type animals (Figure 3.6.2.1D). Ibuprofen treated wild-type animals also exhibited higher number of foci (Figure 3.6.2.1D). Increasing heterogeneity between animals in each group could be observed with age.

A significant increase in the number of TAFs could be observed with age in both purkinje neurons (Figure 3.6.2.1E) and pyramidal neurons (Figure 3.6.2.1F). This occurred first in Purkinje neurons of *nfkb1*$^{-/-}$ mice, which showed significantly elevated levels by 8 months of age (Figure 3.6.2.1E), and in both purkinje and CA1 pyramidal neurons in both genotypes by 18 months of age (Figure 3.6.2.1F). *Nfkb1*$^{-/-}$ mice showed significantly higher levels of TAFs, and cells positive for multiple TAFs, at all ages and in both Purkinje and pyramidal cells compared to wild-type mice (Figure 3.6.2.1G-H). Long-term Ibuprofen treatment reduced these levels towards wild-type levels, and there was a slight trend for reduction with the short-term mini-pump Ibuprofen treatment at 8 months of age (Figure 3.6.2.1E-H). The mean number of TAFs, and the frequency of neurons with multiple TAFs, remained comparatively stable between 3 and 8 months of age in wild-type mice, while *nfkb1*$^{-/-}$ showed an earlier age-related increase.

In the pyramidal neurons of wild-type mice, the number of non-TAF γH2A.X foci (n.b. this is not total γH2A.X foci, which includes all foci types) did not increase linearly with age, with no change between 3 and 8 months, and a small increase at 18 months in (Figure 3.6.2.2A). However, the ratio of TAFs did increase linearly with age (Figure 3.6.2.2B). The same was true in *nfkb1*$^{-/-}$ mice, but with higher rates of foci (Figure 3.6.2.2C-D).

To test whether these TAF were Telomere-induced foci (TIF) in ageing mice, the telomere intensity of each telomere associated with yH2A.X was measured in CA3 hippocampal neurons from 18month old wild-type mice (Figure 3.6.2.3). TIFs are yH2A.X foci induced by the loss of T- and D-loop conformation due to telomere shortening, leading to the unfolding of the telomere complex and exposure of the chromosome end, which is recognised as a double-stranded break. I found longer telomeres were significantly enriched for yH2A.X foci, compared to short-telomeres in 3 different animals (Figure 3.6.2.3A-C). This suggests that it is not the un-capping of shorter telomeres that is responsible for the presence of TAFs, but rather the increased likelihood of a longer telomere being damaged.

One factor that became apparent during the analysis of pyramidal neurons in the hippocampus was a difference in damage levels between different sub-regions (Figure 3.6.2.4A). Initially images were taken at intervals along the pyramidal structure, starting in CA1, but with some images taken in CA2 to CA3. During quantification it appeared that neurons in CA2 and CA3 displayed higher levels of DNA damage. Following this observation I removed the counts of data from CA3 regions, leaving the pyramidal counts as solely as CA1 pyramidal neurons. There was a trend for higher numbers of yH2AX foci in n*fkb1*$^{-/-}$ mice (Figure 3.6.2.4B). *Nfkb1*$^{-/-}$ mice showed a significant increase in the mean number of TAFs in CA3 neurons (Figure 3.6.2.4C), as well as the number of cells bearing multiple TAFs (Figure 3.6.2.4D). Further, a large proportion of neurons was found to have much higher numbers of TAFs than previously observed, with 10-15% of CA3 neurons in *nfkb1*$^{-/-}$ mice having 5 or more TAFs (Figure 3.6.2.4E) – where as in CA1 pyramidal neurons it was unusual to see more than 3 . A comparison between levels of DNA damage and TAFs in neurons from CA1 and CA3 found that *nfkb1*$^{-/-}$ mice had increased levels of TAFs in CA3, compared to CA1, while wild-type mice showed no significant difference (Figure 3.6.2.4F-J). There was significantly higher frequency of the cell-cycle inhibitor p21 in CA3 neurons (Figure 3.6.2.4I).

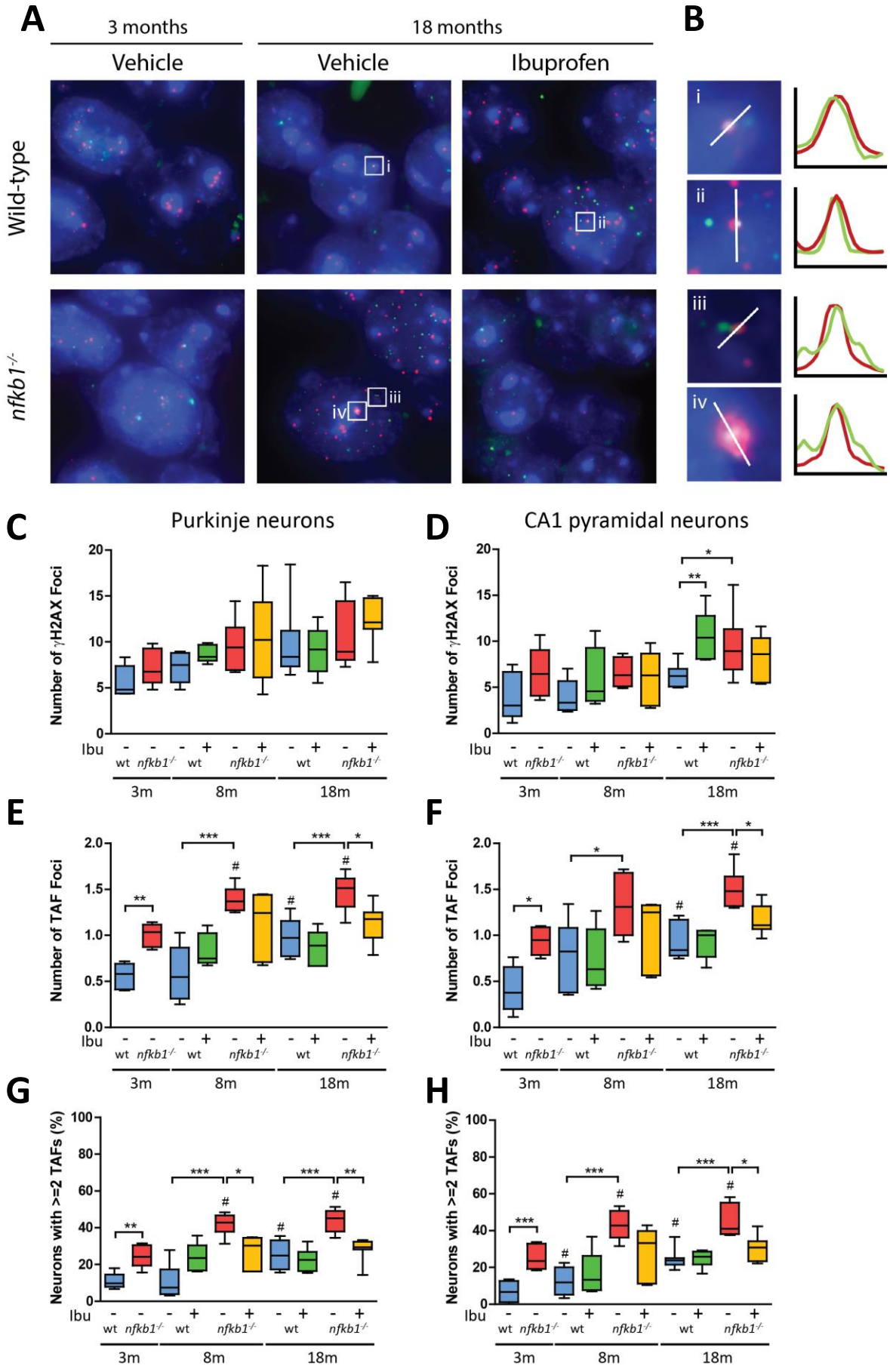
A
3 months
18 months
Vehicle
Vehicle
Ibuprofen
Wild-type
nfkb1-/-
i
ii
iii
iv
B
C
Purkinje neurons
Number of γH2AX Foci
D
CA1 pyramidal neurons
Number of γH2AX Foci
E
Number of TAF Foci
F
Number of TAF Foci
G
Neurons with >=2 TAFs (%)
H
Neurons with >=2 TAFs (%)
Ibu
wt
nfkb1-/-
3m
8m
18m

Figure 3.4.2.1: Telomere associated DNA damage increases with age in Purkinje neurons and CA1 hippocampal cells, and is elevated in *nfkb1*$^{-/-}$ mice

A) Representative image of yH2A.X (green), Telomere probe (Red) and nuclear stained using DAPI (blue) in CA1 neurons from wild-type and *nfkb1*$^{-/-}$ mice, treated and untreated at 3 and 18 months. **B)** Several TAFs in A) are highlighted and co-localisation between yH2A.X and telomere probe shown by normalised intensity plot. **C)** Quantification of mean yH2A.X foci in Purkinje neurons and **D)** CA1 pyramidal neurons. **E)** Quantification of mean TAF foci in Purkinje neurons and **F)** CA1 pyramidal neurons. **G)** Quantification of percentage of neurons with 2 or more TAF foci in Purkinje neurons and **H)** CA1 pyramidal neurons. 2-way ANOVA (Holm-Sidak) for age and genotype. Treatments are compared by two-tailed Mann-Whintey U. Significant differences between genotype, as well as treatments, at each age point are displayed by (* $p<0.05$, ** $p<0.005$, *** $p<0.001$), significant difference with age by (# $p<0.05$).

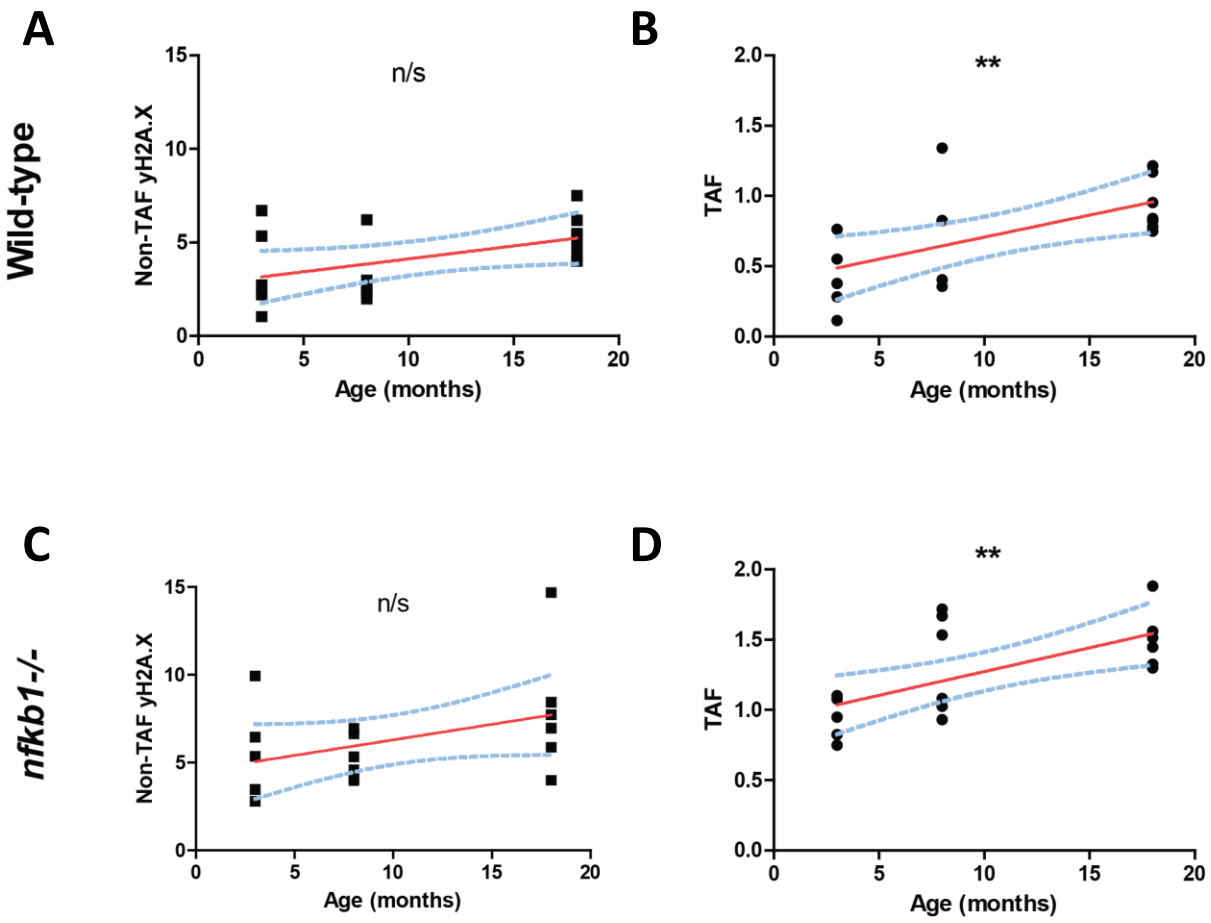

Figure 3.6.2.2: TAF accumulate linearly with age in pyramidal neurons, with no significant linear increase in non-telomere associated foci

A) Linear regression of mean yH2A.X foci in untreated wild-type mice at 3, 8 and 18 months. **B)** Linear regression of mean yH2A.X foci in untreated wild-type mice at 3, 8 and 18 months. **C)** Linear regression of mean yH2A.X foci in untreated *nfkb1*$^{-/-}$ mice at 3, 8 and 18 months. **B)** Linear regression of mean yH2A.X foci in untreated *nfkb1*$^{-/-}$ animals at 3, 8 and 18 months. Significance tested by two-tailed Spearman correlation coefficient (* $p<0.05$, ** $p<0.005$, *** $p<0.001$ by Gaussian approximation).

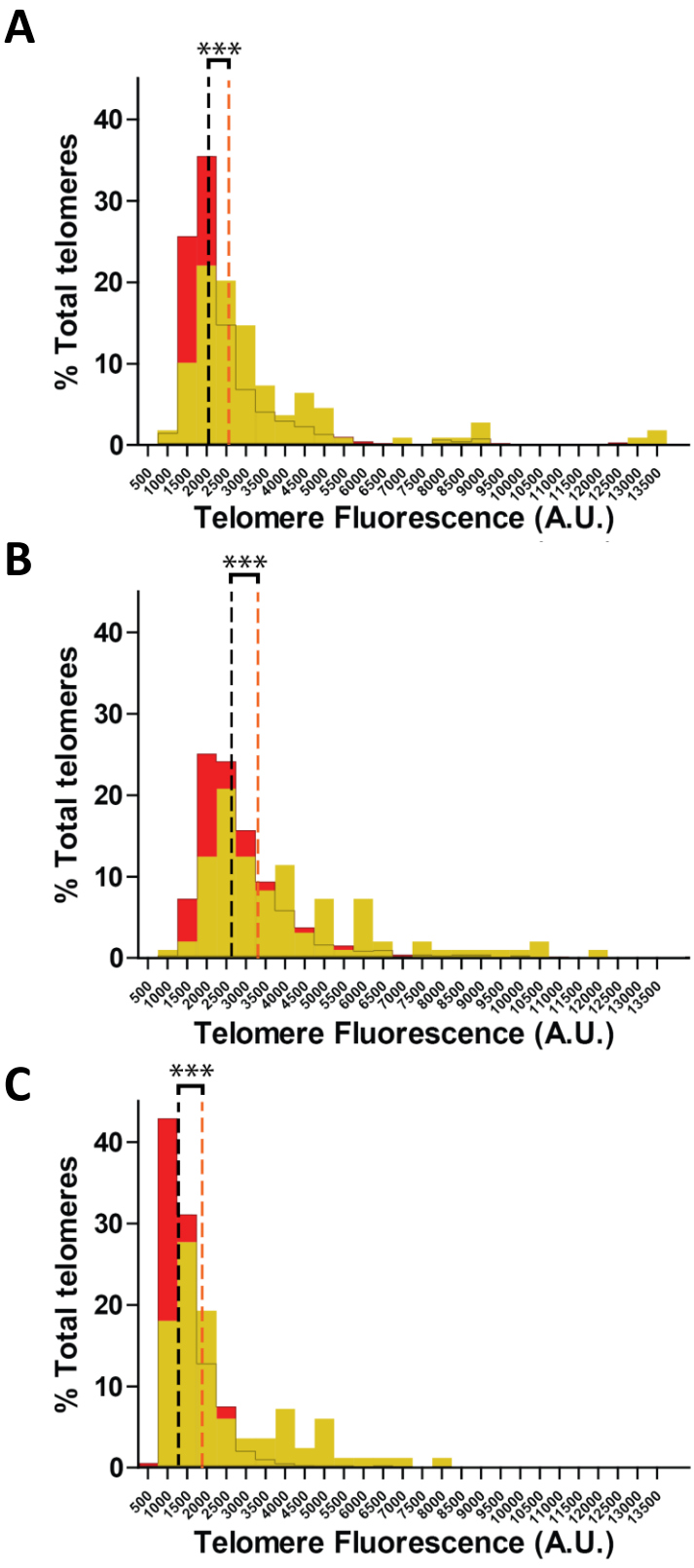
A
***
% Total telomeres
0
10
20
30
40
500
1000
1500
2000
2500
3000
3500
4000
4500
5000
5500
6000
6500
7000
7500
8000
8500
9000
9500
10000
10500
11000
11500
12000
12500
13000
13500
Telomere Fluorescence (A.U.)
B
***
% Total telomeres
Telomere Fluorescence (A.U.)
C
***
% Total telomeres
Telomere Fluorescence (A.U.)

Figure 3.6.2.3: Telomere-Associated Foci accumulate preferentially in longer telomeres in neurons

Histograms showing telomere-intensities of telomeres co-localising (yellow) and not co-localising (red) with γH2A.X foci in hippocampal neurons of 3 wild-type mice (**A-C**). Black dotted-line shows median intensity for telomeres not associated with γH2A.X foci with each histogram. Orange dotted-line shows median intensity for telomeres that are associated with γH2A.X foci with each histogram. An average of 1058 telomeres were analysed per animal. Tested by Mann-Whitney U for each animal, significance shown by *** = $p<0.0001$.

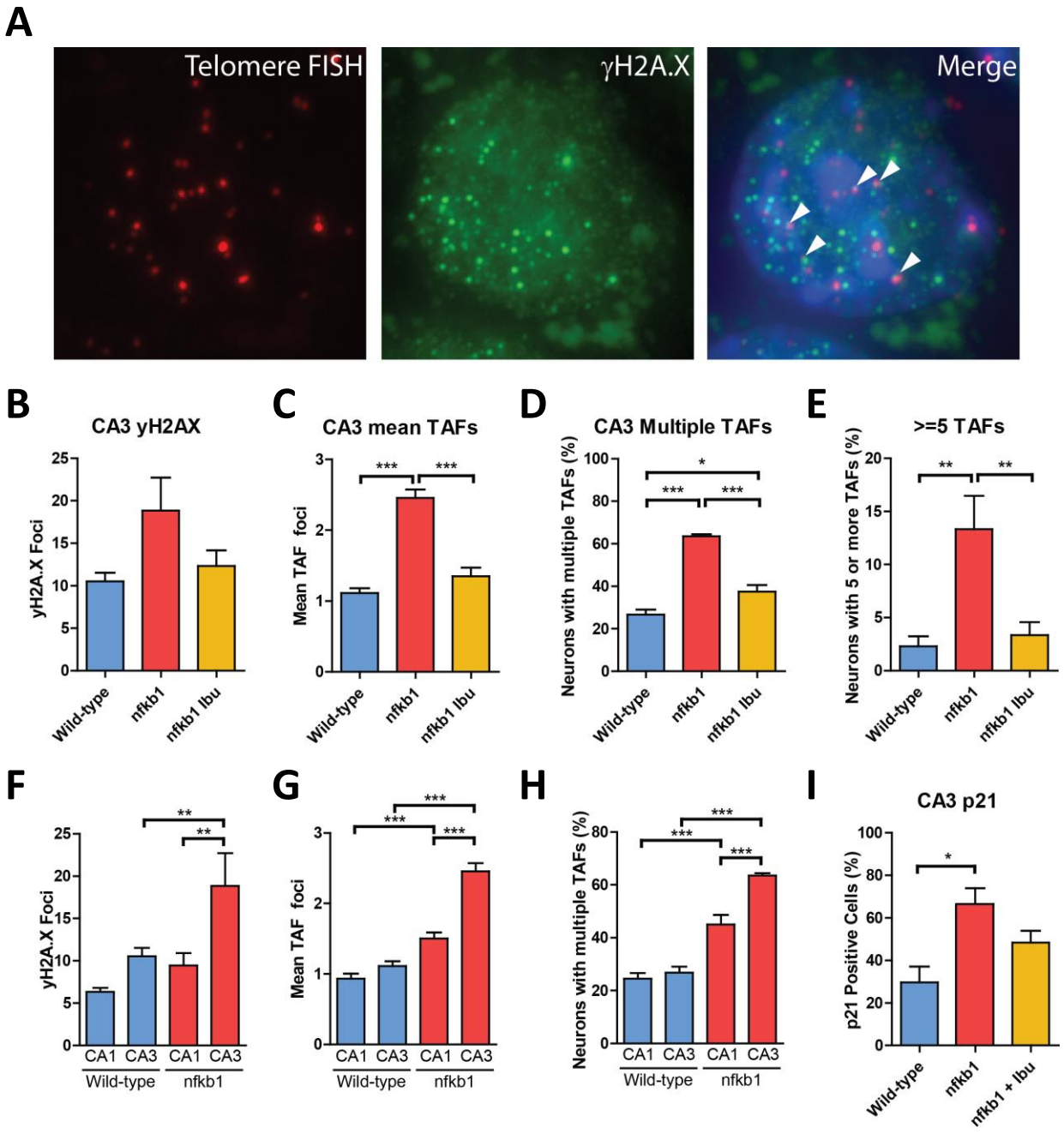

Figure 3.6.2.4: Increased telomere associated DNA Damage in CA3 pyramidal neurons in *nfkb1*$^{-/-}$ mice

A) Representative image of γH2A.X Immuno-FISH in CA3 Hippocampus Neuron 18 month old animals γH2A.X in Green, PNA probe (Telomeres) in Red, DAPI in Blue. **B)** Mean γH2A.X foci and **C)** mean TAF in CA3 neurons of wild-type, *nfkb1*$^{-/-}$ and *nfkb1*$^{-/-}$ treated with Ibuprofen **D)** Percentage of CA3 neurons positive for multiple telomere-associated DNA damage foci TAF). **E)** Percentage of CA3 neurons positive for 5 or more telomere-associated DNA damage foci (TAF). Comparison between CA1 and CA3 in wild-type and *nfkb1*$^{-/-}$ mice for **F)** γH2A.X foci **G)** mean TAF and **H)** percentage of neurons with 2 or more TAFs. One Way ANOVA, Bonferoni Post-hoc, n=5-6 animals for DNA Damage markers, n=3-4 for p21.I) Comparison of DNA damage in CA1 and CA3. Two Way ANOVA, Holm-Šidák Post-hoc. Significance marked as (* = p<0.05, ** = p<0.05, *** p<0.001). All bars are mean +SEM.

3.6.3 - p21 expression increases in parallel with DDR foci in neurons with ageing and chronic inflammation.

The activation of cyclin kinase inhibitor p21, a downstream factor in the DDR pathway, is associated with arrest of the cell-cycle and is elevated in senescence in mitotic cells [177, 222]. It appears to be a requirement for the development of the senescence-like phenotype, as mice with short-telomeres and p21 knockout show greatly reduced rates of senescence-associated markers such as Senescence-associated Beta Galactosidase activity, phospho-p38 MAPK, IL-6 and markers of oxidative and DNA damage [112]. It is likely that this is either due to p21 signalling being required for the development of senescence-associated features, or due to a lack of cell-cycle inhibition leading to increased re-entry and cell-death in damaged neurons.

The levels of nuclear p21 in Purkinje neurons of ageing wild-type and *nfkb1*$^{-/-}$ mice were investigated (Figure 3.6.3.1A). *Nfkb1*$^{-/-}$ mice showed increased p21 levels with age at 8 and 18 months, and significantly higher levels than wild-type mice at these ages (Figure 3.6.3.1B). Long-term Ibuprofen treatment was able to reduce these levels in *nfkb1*$^{-/-}$ mice, but did not have a significant effect in wild-type mice. Considering all animals and ages there was a significant correlation between γH2AX foci and TAFs (Figure 3.6.3.1C-E). Both *nfkb1*$^{-/-}$ and wild-type mice showed a linear increase in p21 positive neurons with age (Figure 3.6.3.2A-B); moreover, there was a significantly increased rate of accumulation in *nfkb1*$^{-/-}$ compared to wild-type mice (Figure 3.6.3.2C).

p21 can be activated by the DDR, and forms a positive feedback loop through ROS creating further DNA damage [177]. As such, I tested for an association with DNA damage levels and p21. A significant correlation between p21 levels and DNA damage could be observed when looking at individual animals between 3 and 18 months. I was concerned that age might be the driving factor in these associations, so I additionally tested only animals at 18 months (Figure 3.6.3.3). At 18 months I found no association between total γH2A.X foci and p21 activity (Figure 3.6.3.3A), but found an association with mean number of TAFs and frequency of cells with 2 or more TAFs (Figure 3.6.3.3B-C). Additionally p21 correlated with additional senescence markers such as autofluorescent aggregates and loss of nuclear HMGB1 (Figure 3.6.3.3D-E).

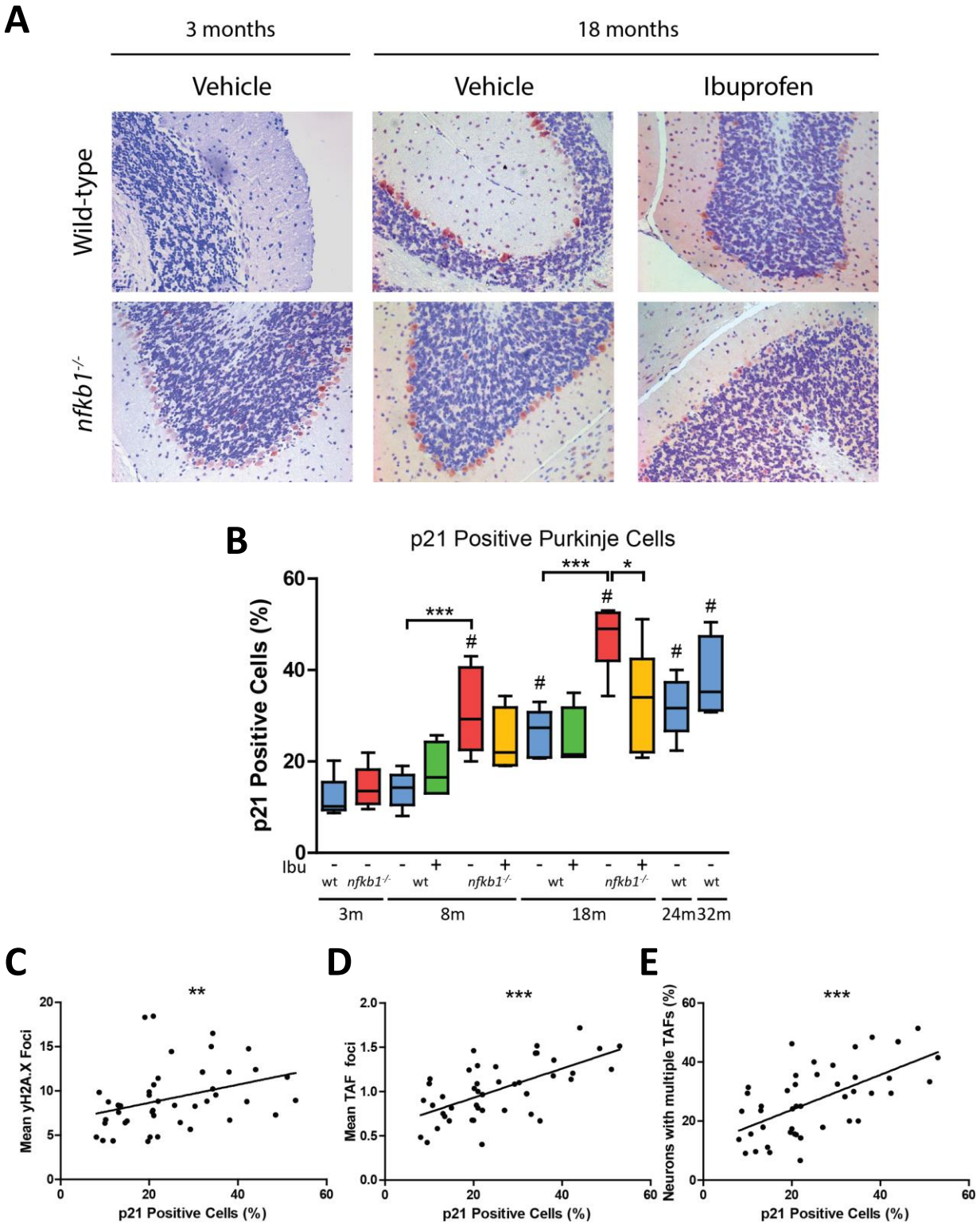
A
3 months
18 months
Vehicle
Vehicle
Ibuprofen
Wild-type
nfkb1-/-
B
p21 Positive Purkinje Cells
p21 Positive Cells (%)
Ibu
wt
nfkb1-/-
3m
8m
18m
24m
32m
C
Mean γH2A.X Foci
p21 Positive Cells (%)
D
Mean TAF foci
p21 Positive Cells (%)
E
Neurons with multiple TAFs (%)
p21 Positive Cells (%)

Figure 3.6.3.1: Increasing p21 positive Purkinje neurons in the Cerebellum with age, and in *nfkb1*$^{-/-}$ mice

A) Representative images of p21 staining in the cerebellum of 3, 8 and 18 month old mice. p21 stained with NovaRed (Brown), counterstained with Haematoxylin (Blue) **B)** Graph showing percentage of neurons positive for p21 staining at each age group. Samples were available for wild-type mice aged 24 and 32 months, and were included for reference. Box and whiskers show the median of the means. 2-way ANOVA (Holm-Sidak) for age and genotype. Treatments are compared by two-tailed Mann-Whintey U, as are 24 and 36 month wild-type mice to retain interactions in 2-way ANOVA. Significant differences between genotype, as well as treatments, at each age point are displayed by (* $p<0.05$, ** $p<0.005$, *** $p<0.001$), significant difference with age by (# $p<0.05$). **C-E)** Correlation between numbers of neurons positive for nuclear p21 staining and mean yH2A.X foci, mean TAF and percentage of cells positive for multiple TAFs, respectively, per animal in 3 to 18 months old wild-type and *nfkb1*$^{-/-}$ mice. Significance tested by two-tailed Spearman correlation coefficient (** $p<0.005$, *** $p<0.001$ by Gaussian approximation).

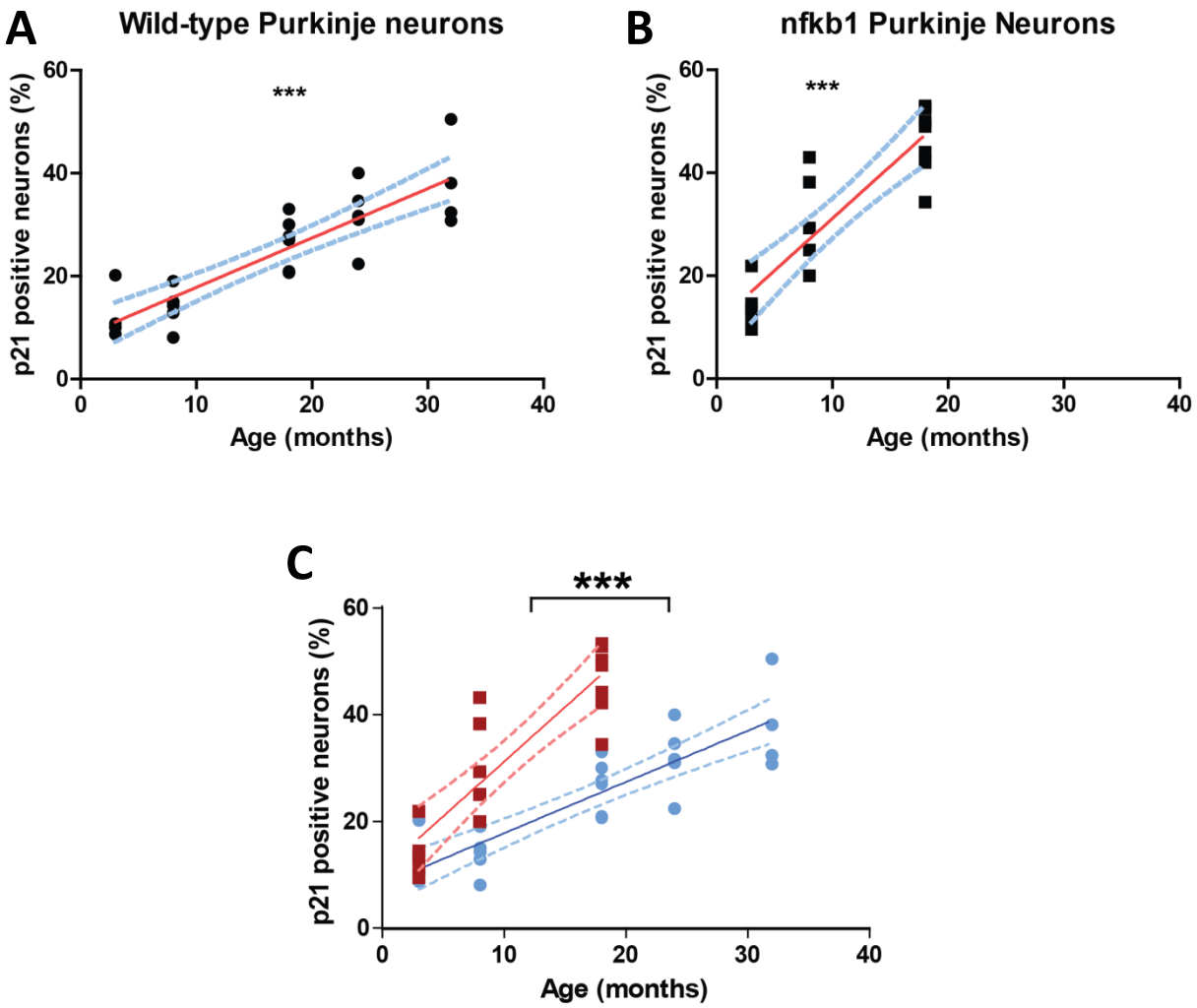

Figure 3.6.3.2: Correlations between p21 and age in Purkinje cells of wild-type and *nfkb1*$^{-/-}$ mice

A-B) Correlation between numbers of neurons positive for nuclear p21 staining and age in wild-type and *nfkb1*$^{-/-}$ purkinje neurons. Red line shows linear regression, dotted blue lines show 95% confidence intervals. **C)** Comparison of rate of increase in *nfkb1*$^{-/-}$ and wild-type mice with ageing. Significance tested by two-tailed Spearman correlation coefficient (* $p<0.05$, ** $p<0.005$, *** $p<0.001$ by Gaussian approximation).

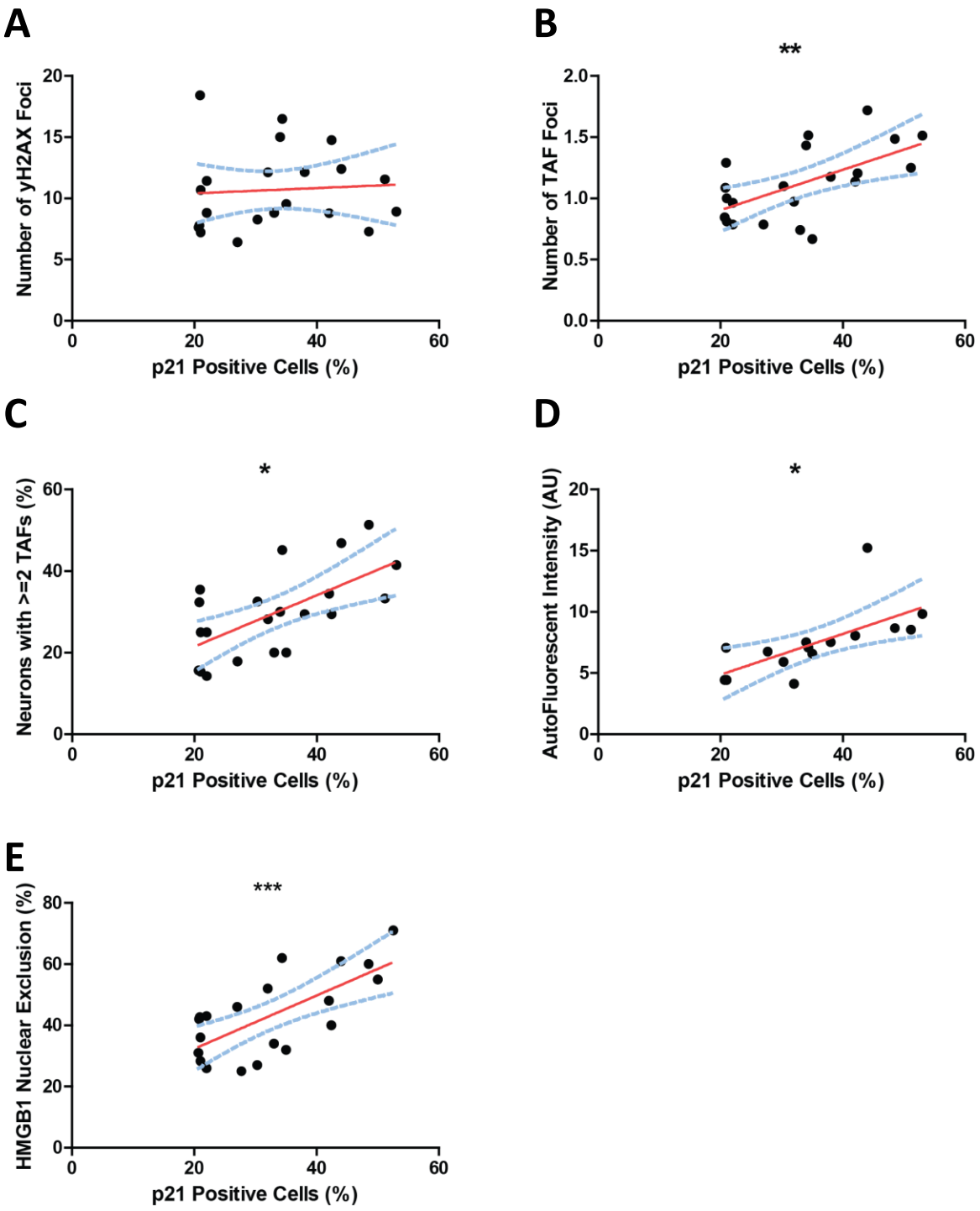

Figure 3.6.3.3: Correlations between p21 and other senescence-associated markers in Purkinje cells in 18 month animals

A-E) Correlation between numbers of neurons positive for nuclear p21 staining and markers of senescence **A)** gH2AX, **B)** mean TAF, **C)** 2≥ TAF, **D)** autofluorescence and **E)** HMGB1, per animal, in 18 month old wild-type and *nfkb1*$^{-/-}$ mice, with and without ibuprofen. Red line shows linear regression, dotted blue lines show 95% confidence intervals. Significance tested by two-tailed Spearman correlation coefficient (* $p<0.05$, ** $p<0.005$, *** $p<0.001$ by Gaussian approximation).

3.6.4 - High Mobility Group Box 1 translocates from the nucleus in *nfkb1*$^{-/-}$ neurons

High Mobility Group Box 1 (HMGB1) is a highly conserved non-histone chromatin binding protein that, when localised to the nucleus, regulates chromatin architecture [493]. It can bend DNA to allow access for other proteins, such as transcription factors [493]. However, the protein leads a double life and is also a pro-inflammatory cytokine and Alarmin [494]. In undamaged cells HMGB1 is primarily located in the nucleus; however, following hyper-acetylation on lysine groups HMGB1 is transported from the nucleus to the cytoplasm [494]. From here it can be secreted into the extra-cellular milieu where it takes the role of a pro-inflammatory cytokine, activating receptor for advanced glycation end products and Toll-like receptors, leading to activation of NF-κB and COX-2 [494]. In tissues it mediates inflammation related tissue damage, for example in brain ischæmia [494, 495]. It is released passively by necrotic cells and actively secreted by immune cells [496]. HMGB1 is also a key regulator of senescence and is actively exported from the nuclei of senescent cells into the extra-cellular milieu through p53-mediated pathway [491]. Relocation of HMGB1 in senescent cells is required for stimulation of NF-κB activity and secretion of IL-6 [491]. This was assessed by immunohistochemical staining for HMGB1 for positive and negative nuclei (Figure 3.6.4.1A)

Nfkb1$^{-/-}$ mice showed a significant increase in HMGB1 translocation in Purkinje neurons with age (Figure 3.6.4.1B). While wild-type mice showed a trend, this was not significant. *Nfkb1*$^{-/-}$ mice had significantly higher frequencies of neurons with no nuclear HMGB1 than wild-type mice at 8 and 18 months, while long-term Ibuprofen treatment ameliorated this. Whether HMGB1 has been excluded from the nucleus was also measured in granule cells immediately adjacent to HMGB1 nuclear positive, and negative, Purkinje neurons (Figure 3.6.4.1C). Granule cells surrounding HMGB1 negative neurons were significantly more likely have also have no HMGB1 in their nucleus, suggesting a manner of bystander effect or localised damage.

CA3 pyramidal layer cells in *nfkb1*$^{-/-}$ mice showed an age-dependent increase in HMGB1 translocation, and were significantly elevated compared to wild-type controls (Figure 3.6.4.1D). There was a trend for reduced HMGB1 translocation at 18 months with Ibuprofen treatment, and it was significantly rescued by long-term ibuprofen treatment at 18 months.

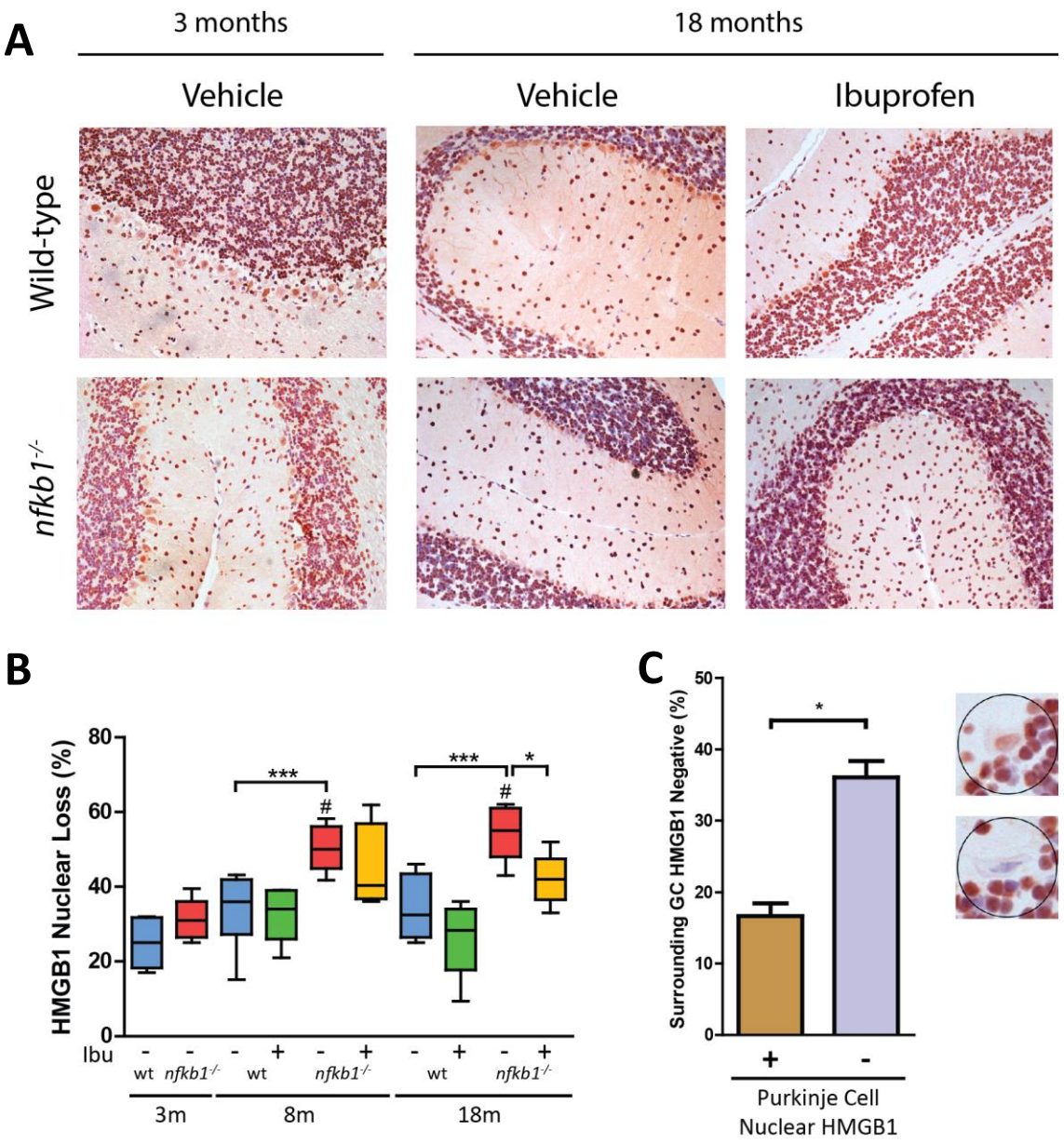
A
3 months
18 months
Vehicle
Vehicle
Ibuprofen
Wild-type
nfkb1-/-
B
HMGB1 Nuclear Loss (%)
lbu
wt
nfkb1-/-
3m
8m
18m
C
Surrounding GC HMGB1 Negative (%)
Purkinje Cell
Nuclear HMGB1
D
HMGB1 Nuclear Loss (%)

Figure 3.6.4.1: *Nfkb1*$^{-/-}$ show age dependent loss of nuclear HMGB1 in neurons

A) Representative images of HMGB1 staining in the cerebellum of 3 and 18 month old mice. HMGB1 stained with NovaRed (Brown) counterstained with Haematoxylin (Blue) **B)** Quantification of purkinje neurons with no nuclear HMGB1 at 3, 8 and 18 months in wild-type and *nfkb1*$^{-/-}$ mice, with and without ibuprofen treatment. **C)** Increased frequency of HMGB1 nuclear negative granule cells surrounding HMGB1 nuclear negative Purkinje neurons. Graph shows mean of 100 purkinje neurons in each group, in 3 18 month wild-type animals. **D)** Quantification of CA3 pyramidal layer cells with no nuclear HMGB1 at 3, 8 and 18 months in wild-type and *nfkb1*$^{-/-}$ mice, with and without ibuprofen treatment. 2-way ANOVA (Holm-Sidak) for age and genotype. Treatments are compared by two-tailed Mann-Whintey U. Significant differences between genotype, as well as treatments, at each age point are displayed by (* $p<0.05$, ** $p<0.005$, *** $p<0.001$), significant difference with age by (# $p<0.05$). HMGB1 bystander assessed by paired two-tailed t-test, significance shown by * $p<0.05$

3.6.5 – *Nfkb1*$^{-/-}$ mice show increased autofluorescent lipofuscin accumulation in neurons

Lipofuscin is an electron-rich lysosomally accumulated aggregate that increases with age in many cell types [497] and accumulates in senescent cells [492, 498]. The aggregates are complex and multifaceted, including oxidatively damaged lipids and proteins. As such, Lipofuscin is often used as a marker of oxidative damage, and increases in parallel with markers of oxidative damage, such as 8-oxo-dG [177]. Many trapped proteins contain metal ions, and aggregates can account for up to 16% of metals within a cell [499]. The presence of these ions contribute significantly to the electron-rich nature of the aggregate and leads to a bright autofluorescence excitement across a broad spectrum during fluorescence microscopy [500, 501]. While this autofluorescence is often problematic for fluorescent image analysis, it can be analysed in its own-right to assess lipofuscin accumulation. Due to the size of the Purkinje cell, this can be performed easily on un-processed paraffin-fixed sections (Figure 3.6.5.1); however, for cells with a smaller soma such as pyramidal neurons it is necessary to process the slide and instead count individual foci (Figure 3.6.5.2).

Purkinje neurons in both wild-type and *nfkb1*$^{-/-}$ mice showed increased auto-fluorescence with age (Figure 3.6.5.1A). *Nfkb1*$^{-/-}$ mice had significantly higher levels at all 3 ages (Figure 3.6.5.1B). Ibuprofen treatment reduced the levels of autofluorescence at both 8 and 18 months of age in *nfkb1*$^{-/-}$ mice, but did not significantly effect wild-type mice. Pyramidal neurons also showed an increase with age. Pyramidal neurons from 18 month *nfkb1*$^{-/-}$ mice had significantly higher levels than wild-type mice. While there was a slight trend for decreased autofluorescent granules with long-term Ibuprofen treatment, it was not significant.

Due to the small soma-size of hippocampal neurons, de-paraffinated slides were used instead, and the number of average number of autofluorescent granules per cell counted in pyramidal neurons (Figure 3.6.5.2A). Both wild-type and *nfkb1*$^{-/-}$ neurons showed a significant increase in the number of autofluorescent granules with age (Figure 3.6.5.2B). Ibuprofen treatment lead to a significantly increased average number of granules in wild-type mice at 18 months, and in *nfkb1*$^{-/-}$ mice at 18 months showed a trend for decreased average number of granules (Figure 3.6.5.2B).

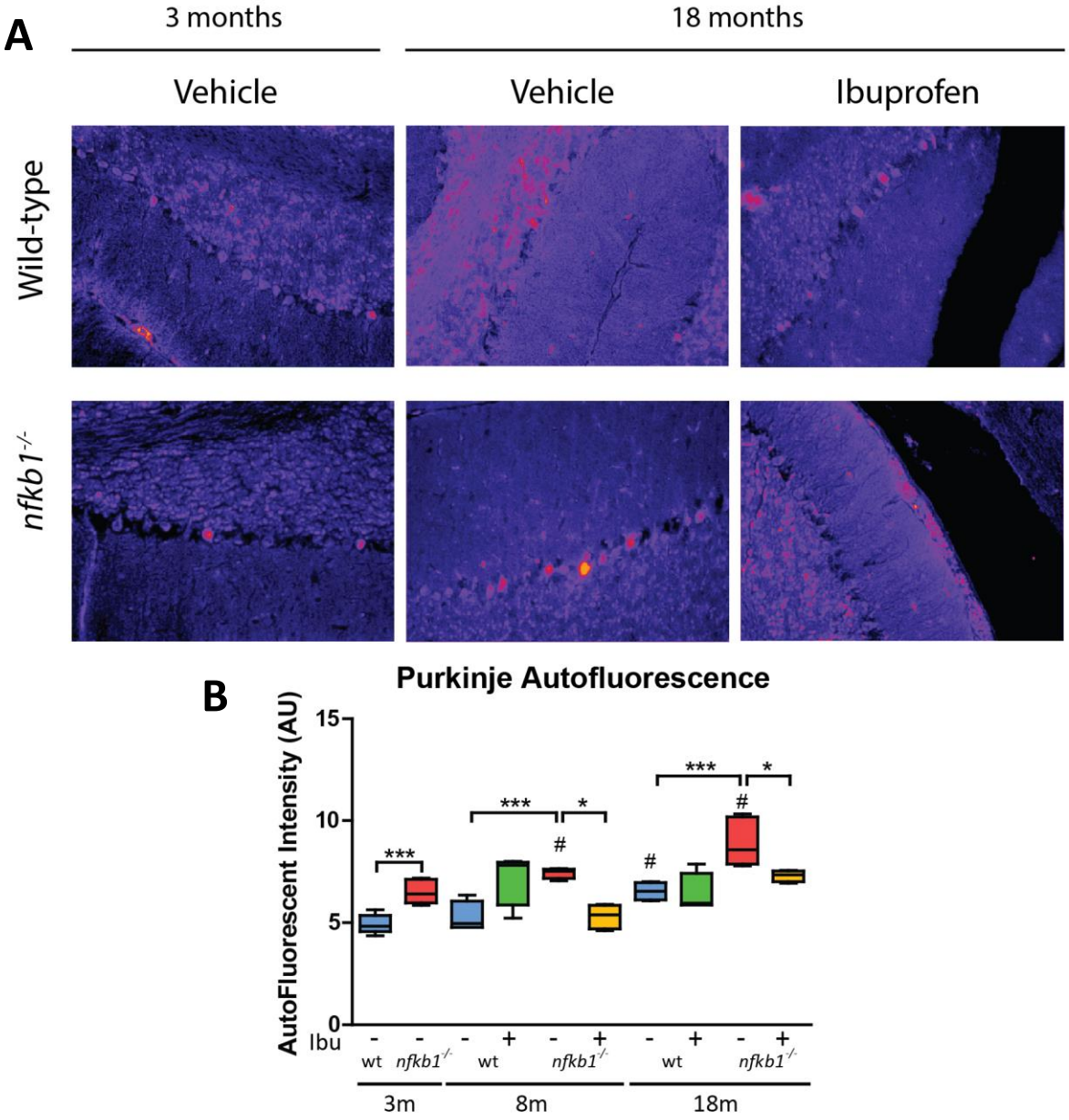

Figure 3.6.5.1: *Nfkb1*$^{-/-}$ mice show increased Purkinje cell autofluorescence

A) Representative images of autofluorescence in the cerebellum of 3 and 18 month old wild-type and *nfkb1*$^{-/-}$ mice, with and without iburprofen **B)** Graph showing mean number of autofluorescent intensity per neuron, per mouse, in each age group. Box and whiskers show the median of the means. 2-way ANOVA (Holm-Sidak) for age and genotype. Treatments are compared by two-tailed Mann-Whintey U. Significant differences between genotype, as well as treatments, at each age point are displayed by (* $p<0.05$, ** $p<0.005$, *** $p<0.001$), significant difference with age by (# $p<0.05$).

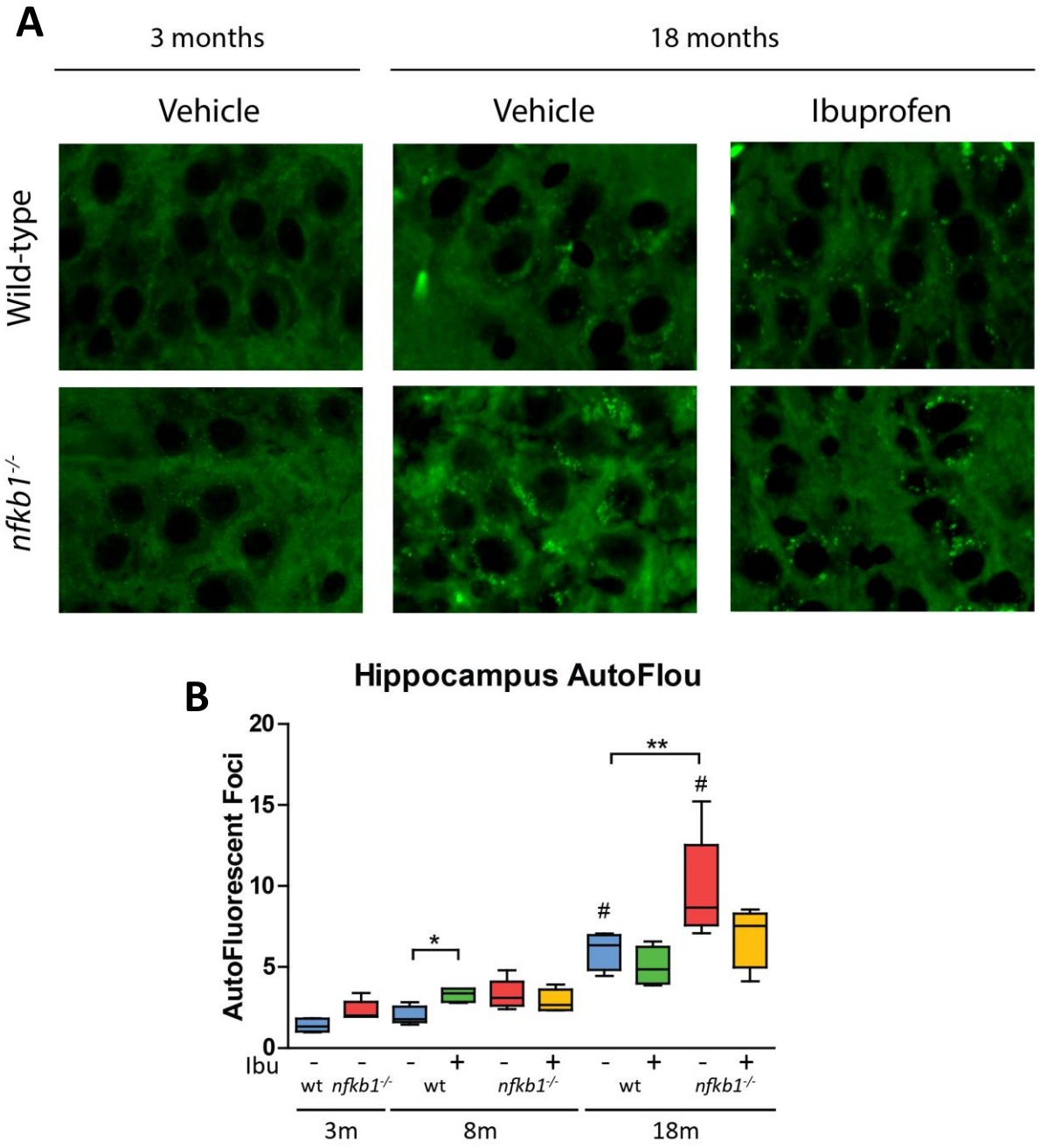

Figure 3.6.5.2: Pyramidal neurons show increased autofluorescent granules with age, and in *nfkb1*$^{-/-}$ mice

A) Representative images of autofluorescence in the CA3 hippocampus of 3 and 18 month old wild-type and *nfkb1*$^{-/-}$ mice, with and without ibuprofen **D)** Graph showing mean number of autofluorescent granules per neuron, per mouse, in each age group. Box and whiskers show the median of the means. 2-way ANOVA (Holm-Sidak) for age and genotype. Treatments are compared by two-tailed Mann-Whintey U. Significant differences between genotype, as well as treatments, at each age point and correlations are displayed by (* $p<0.05$, ** $p<0.005$, *** $p<0.001$). Significant difference with age by (# $p<0.05$).

3.6.6 - Discussion

The presence of senescent cells is known to drive ageing and age-associated diseases in mice [124]. The frequency of senescent-like neurons has been observed to increase in ageing mice brain [112], but it is not yet known if it plays a role in age and disease associated cognitive decline. As discussed previously in the chapter, *nfkb1*$^{-/-}$ mice show increased glial activation, neuro-inflammation, deficits in gamma frequency oscillations and deficits in spatial memory compared to wild-type mice. These showed partial rescue with long-term dietary ibuprofen, suggesting that inflammation at least partially drives this dysfunction. We hypothesised that the presence of senescent-like neurons is involved with these chronic-inflammatory associated cognitive deficits. In neurons from *nfkb1*$^{-/-}$ mice I observed an increase in the frequency of senescence associated markers, such as DDR activation, p21 activation and HMGB1 release. There was a partial rescue in a number of these factors and cognitive function with long-term ibuprofen treatment, suggesting that the inflammation seen in *nfkb1*$^{-/-}$ mice is playing a role in senescence induction.

Senescence can be initiated through activation of the DDR [174] and increasing ROS production and generating new damage [177]. In order to test this I investigated the presence of yH2A.X foci to assess double-stranded breaks in neurons. While there were trends, no significant changes could be seen in the total number of yH2A.X foci in Purkinje neurons with age, or genotype. This matches existing data on DNA damage markers in these neurons in terms of single-stranded damage, Purkinje cells have the highest level of DNA strand breaks, as measured by in situ nick translation, but do not show an age-related increase between 11 and 28 months [502]. yH2A.X in neurons has been previously reported to increase with age in Purkinje neurons [112]. However, this was measured in terms of cell positive or negative by IHC, rather than the foci number by IF reported here and is likely less sensitive. Further, no increase was reported until 32 months of age, with no visible difference between 4 and 8 months of age. The oldest age tested here was 18 months in wild-types, and an increase may not be seen until later, or could be related to the loss of pyramidal neurons observed in late age [502]. No such age associated loss of neurons occurs in pyramidal cells despite an age-dependent increase in single-strand damage [502] and double-strand breaks in old baboon hippocampal neurons [211] previously observed. Increased levels here could be observed in pyramidal neurons in *nfkb1*$^{-/-}$ mice at 18 months, but not before, which may indicate an acceleration of age-accumulated damage.

The variability in total yH2A.X could be related to its physiological roles within neurons, which could mask the number of damage associated breaks. Increases in the number of yH2A.X foci in hippocampal neurons can be seen after 2 hours of exposure to novel environments [208]. However, if returned to their home cage for 24 hours, the number of yH2A.X foci returns to the same level as

mice who never left the home cage. This could be linked to the increased neuronal activity, which could lead to increased ROS production and Ca2+ influx as a by-product. It would also indicate either a rapid repair of this transient damage. It is not yet known if these breaks contribute to DDR signalling. However, the location of these breaks appears more targeted, specifically to promotor regions of neuronal early-response genes. The rapid expression of these genes is important for synaptic plasticity, learning and memory. The yH2A.X positive foci in the promotor regions of these genes are physiologically generated by topoisomerase IIβ and allow physical access to the DNA for transcription factors [207]. Since post-mortem represents a single snap shot, factors such as rehousing prior to autopsy, or other exposure to novel environments may contribute to variation.

yH2A.X and DDR induction by X-ray irradiation in neurons does not appear significantly related to apoptosis, but rather signals G_0 to G_1 cell-cycle transition through ATM-p53-p21 signalling [309]. This was tested in sensory ganglion neurons, but appears consistent with experiments involving irradiation of mouse brains, which showed an increase in damage in vivo in surviving hippocampal neurons even 3 months after damage [211]. In both cases, DNA damage could be defined as being in one of two categories, transient repairable DDR foci, and persistent DDR foci [211, 309]. After X-ray irradiation induced double-stranded damage in ganglion neurons, yH2A.X foci can be observed, however, these are repaired within a day, while persistent yH2A.X foci can still be observed 15 days after [309]. These were both positive for DDR factors, such as pATM and 53BP1, that indicate downstream DDR signalling, but also epigenetic changes in chromatin condensation [309]. In irradiated mouse brains, hippocampal neurons, breaks can be seen immediately after IR, but a significant number were still present after 3 months [211]. However, this damage was preferentially located at telomeres, which comprise a mere 0.02% of the genome [211].

Telomere dysfunction appears to be an important driver in the generation of senescent-like neurons [112]. Late generation *terc*$^{-/-}$ mice, lack the catalytic subunit of telomerase, leading to generation dependent telomere shortening and an accelerated ageing phenotype. Telomeres in these mice, can become uncapped as they are unable to properly form a protective T-loop, which otherwise shelters the chromosome end, and its recognition as a double-strand break [197, 198, 202, 203]. In these mice, a substantial increase in the number of Purkinje and cortical neurons with an active DDR and senescent-like features can be observed [112]. This would be consistent with critically short telomeres within neurons resulting in telomere uncapping, triggering of the DDR signalling and the induction of the senescent-like phenotype.

To assess telomere dysfunction in *nfkb1*$^{-/-}$ mice neurons, I measured the number of yH2A.X foci co-localising with telomeres (TAFs). Unlike yH2A.X located outside of the telomere region, the number of TAFs could be seen to increase with age in neurons in wild-type and *nfkb1*$^{-/-}$ mice. This is consistent with a study which showed an age-dependent increase in 53BP-1 foci co-localising with telomeres in baboon neurons [211], and increasing TAF numbers with age in other tissues such as the liver [127] and lung [503]. These levels were significantly higher in untreated *nfkb1*$^{-/-}$ mice; however, long-term dietary ibuprofen treatment reduced the average number of TAFs in *nfkb1*$^{-/-}$ mice, but had no effect on wild-type mice. This could suggest that chronic inflammation may be driving telomere dysfunction in these neurons, which is consistent with results previously observed in the livers of *nfkb1*$^{-/-}$ mice.

Yet, in mitotic cells telomere shortening and uncapping is typically a function of DNA replication and the loss of the telomeric end-repeat sequence. Furthermore, unless genetically altered (as in the *terc*$^{-/-}$ mice mentioned previously), mice constitutively express telomerase and maintain long-telomeres throughout life. However, DNA damage can occur at telomeres even in the absence of uncapping, and is sheltered from repair factors by the shelterin complex [209, 211]. 3 months after irradiation of mouse hippocampal neurons, 40% of DNA damage found was located at the telomeres and was not located preferentially at shortened telomeres [211]. With the data from Hewitt *et al.,* this indicates that DNA damage can be located within telomeres independent of length, where it is sheltered from DNA repair by the shelterin complex [504] leading to persistent DDR foci [209, 211]. I confirmed this in ageing in wild-type mice CA3 neurons at 18 months, and found that not only TAF were not found preferentially in short telomeres, but were significantly weighted towards longer telomeres. This data, together with how common telomere damage was compared to non-telomeric damage (despite only being 0.02% of the genome), suggests that telomere regions are highly susceptible to damage and that longer telomeres may be more vulnerable to damage as they provide more space for the damage to occur.

The increasing levels of damage located at the telomeres could provide a consistent level of DDR signalling that stabilises the expression of non-apoptotic ATM-p53-p21 signalling. Activation of this pathway can be seen increasing in the 3 days following X-ray irradiation induced DNA damage in neurons [309]. This persistent signalling of the DDR in mitotic cells leads to the induction of stress-induced senescence [209, 211]. This occurs partially through the stabilisation of p21-p38 MAPK expression and the stimulation of ROS production [177] and leads to the production of inflammatory cytokines known as the SASP [210]. p21 activation appears to be important in driving the senescent-like phenotype in ageing mice, as evidenced by the reduction in neurons bearing senescence-associated markers in late generation *terc*$^{-/-}$ mice lacking p21 [112]. Increased levels of p21 positive

neurons could be observed with age in both wild-type and *nfkb1*$^{-/-}$ mice. By 8 months this was significantly higher than in wild-type mice and followed an accelerated trajectory with age compared to wild-types. This was significantly correlated with the numbers of TAFs and neurons positive for 2 or more TAFs in purkinje neurons when all groups were considered. However, as this could be a factor of age, I also looked at these parameters purely in 18 month mice. This showed no significant correlation with the number of yH2A.X foci, but was again correlated with TAF and cells positive for 2 or more TAFs. Additionally, the frequency of p21 positive neurons was associated with other senescent-markers, including increases in oxidative damage associated autofluorescent intensity and nuclear release of HMGB1.

One possible mechanism behind this DNA damage and telomere dysfunction in *nfkb1*$^{-/-}$ mice neurons could be the presence of inflammation, as the number of TAFs was reduced with long-term anti-inflammatory treatment. Inflammation is capable of driving of cell-senescence through paracrine signalling pathways [323]. This can be induced by factors such as IL-1a, TGFB and MCP-1, through p15 and p21 signalling [323]. Inflammatory signals are associated with the pathways that promote oxidative stress and telomere dysfunction [119, 127, 177, 213]. For example, CXCR2 binding pro-inflammatory cytokines, such as IL-8, can promote the intracellular accumulation of ROS via CXCR2 mediated signalling [213]. This can promote DDR signalling through the generation of DNA damage, and in turn promote further ROS generation [177] and inflammatory cytokine secretion [119]. Previous work in our lab found elevated oxidative stress in *nfkb1*$^{-/-}$ mice, with treatment with the anti-oxidant BHA reducing the frequency of telomere associated damage in the liver [127]. This generation of ROS, and subsequent telomere damage appears to be mediated through COX-2 activation, although the specific mechanism is not yet know. *In vitro,* work on mouse adult fibroblasts isolated from *nfkb1*$^{-/-}$ mice suggested that the associated COX-2 expression, increased ROS production and secretion of cytokines was a consequence of the induction of senescence [127]. This may act to drive the accumulation of persistent DNA damage and the presence of senescence markers in neurons, as long-term treatment with the COX-2 inhibitor ibuprofen reduced the levels of telomere associated damage.

Inflammation in *nfkb1*$^{-/-}$ mice may come from either the periphery, or directly from cells in the brain. *nfkb1*$^{-/-}$ mice show an elevated response to peripheral pro-inflammatory insults, such as systemic LPS injection, in the midbrain [420]. Indeed, peripheral inflammation can cross the blood brain barrier, and is linked to the priming and activation of microglia and inflammatory responses in the brain, which can lead to delayed and progressive degeneration [505]. *Nfkb1*$^{-/-}$ mice show increased expression of numerous inflammatory factors in the periphery by 9 months of age [127], which could induce priming in microglia. Increased priming of microglia can be seen in normally ageing, with an increased and

exaggerated pro-inflammatory response, and decreased activation threshold of this response [87] and appears accelerated in *nfkb1*$^{-/-}$ mice. Additionally, *nfkb1*$^{-/-}$ microglia have previously been shown to have a deficit in in resolving the inflammatory M1 response, which can lead to prolonged inflammatory activation [420].

However, microglia in *nfkb1*$^{-/-}$ require a secondary, ROS mediated stimuli, in order to trigger their pro-inflammatory activation [419, 420]. The observed increase in DDR signalling in *nfkb1*$^{-/-}$ neurons could itself drive glial activation. This would match what has been observed in another accelerated ageing model, *ercc1*$^{\Delta/-}$ mice [424, 506]. These mice show reduced DNA repair, glial activation and a similar loss of cognitive function to that observed here [424, 506]. A neuron specific *ercc1* knockout was also generated, these are *Ercc1*$^{f/-}$*CaMKII-Cre*$^{+}$ mice [506]. These and have heterozygous *ercc1* expression in the whole body (which is largely phenotype free), but homozygous *ercc1* knockout in αCaMKII expressing cells (primarily excitatory pyramidal neurons in the forebrain). In the brains of these animals show increased in astrogliosis with age that was restricted to brain areas with αCaMKII expressing neurons, particularly the hippocampus and cortex [506]. Suggesting that DNA damage in neurons is capable of activating glial cells; this was accompanied by activation of p53 in neurons, suggesting DDR activation by the unrepaired damage. Further work from Raj *et al.* [424] shows increased microglial priming (marked by hypertrophy and Mac2 expression) specifically in the areas where *Ercc1*$^{f/-}$*CaMKII-Cre*$^{+}$ neurons are present [424]. This is similar to the observed increase in microglial density and soma hypertrophy, accompanied by persistent DDR signalling and elevated senescence-markers, which I observed in the hippocampus of *nfkb1*$^{-/-}$ mice. Interestingly, no such increase was observed in GFAP-Cre targeted *Ercc1*$^{\Delta/-}$ mice [424], suggesting that DNA damage accumulation in astrocytes was not capable of inducing microglial priming or hypertrophy. This would be in line with the lack of a DDR, due to transcriptional repression of DDR factors, in mature astrocytes [507].

Progressive age-associated deficits in LTP could be observed in isolated hippocampal slices from *Ercc1*$^{f/-}$*CaMKII-Cre*$^{+}$ mice, together with decreased performance in the Morris Water Maze [506], which is similar to the deficits in spatial memory I observed. While a mild loss of neurons could be observed in these mice, as previously suggested by type-II TUNEL staining in *nfkb1*$^{-/-}$ mice [395], the observed decrease in LTP could be better explained by altered or disrupted gene transcription from DNA damage, or DDR signalling. Unrepaired DNA damage in neurons is accumulated in transcriptionally silent chromatin domains, but still signals the DDR [508] and dysregulation of gene expression has been observed in senescence of mitotic cells [121]. These could contribute to defects in LTP and altered protein expression observed with age in neurons.

Thus, in *nfkb1*$^{-/-}$ mice increased inflammation and microglial activation could promote DDR activation through pro-inflammatory and pro-oxidative molecules; while a DDR driven senescence-like phenotype in neurons may further promote this, leading to a positive feedback loop. Although, it is difficult to establish causality in a whole body *nfkb1*$^{-/-}$ knockout, further testing in cell-specific *nfkb1*$^{-/-}$ could contribute evidence towards this.

There are a number of mechanisms that may trigger the activation of microglia by neurons. Senescent cells release elevated levels of pro-oxidative and pro-inflammatory molecules, known as the SASP, which not only reinforce senescence [323], but also induce DDR activation and senescence in surrounding cells via gap junctions [122]. This senescence bystander effect is driven through the release of ROS from dysfunctional mitochondria and the activation NF-κB, triggering DNA damage in surrounding cells [509]. Persistent DDR signalling can then trigger the production of ROS [177], and SASP factors, such as IL-6, from senescent cells [119]. That this occurs in neurons is supported by the increased staining for IL-6 previously observed in senescent-like neurons, which was elevated in mice with telomere dysfunction [112].

Additionally, here I observed an increase in the loss of nuclear HMGB1 from *nfkb1*$^{-/-}$ mice compared to wild-type mice. Here I found that the frequency of neurons without nuclear HMGB1 was associated with increased DDR signalling by p21 and TAFs. HMGB1 is actively transported from the nuclei of cells by p53 signalling, and stimulates the activation of NF-κB and IL-6 secretion through Toll-like Receptor 4 [491]. However, it also acts as a pro-inflammatory cytokine, and oxidised HMGB1 is secreted from senescent fibroblasts, inducing secretion of cytokines in an auto- and para-crine fashion through Toll-like Receptor 4 [491]. Here, I observed a possibly bystander effect between purkinje cells and surrounding granule cells, with HMGB1 negative purkinje cells being surrounded by relatively more HMGB1 negative granule cells, compared to positively stained Purkinje cells.

HMGB1 can mediate microglial priming and potentiates the neuro-inflammatory response to inflammation, with increased NF-κB pathway activity, and production of cytokines such as IL-6 in response to inflammatory challenge [510]. Its release has previously been observed from neurons and activated microglial cells in the brain upon stress [495] and excitotoxic damage [511]. It appears to play an important role in mediating delayed neuro-inflammation following ischæmic damage, as suppression of expression with short-hairpin RNA substantially reduces microglial activation, the induction of pro-inflammatory markers and a reduced infarct size [511]. HMGB1 binds to macrophage antigen complex 1 on microglia, which leads to activation of NF-κB and localising cytosolic sub-units of NADPH oxidase to the cell-membrane [496]. This leads to the secretion of pro-inflammatory

cytokines and super-oxide [496]. As such its release from senescent-like neurons could indicate potential mechanism by microglia become primed with age. Recent research has shown that circulating levels of HMGB1, in the CSF, and total mRNA and protein levels, in the hippocampus, are known to increase in normally ageing rodents [512]. This could contribute to age-related priming of microglia and the subsequently increased inflammatory response and effects on cognition seen in the aged after inflammatory insult [94, 97, 98].

It should be noted that HMGB1 is also released passively from necrotic neurons [513], and the release of HMGB1 by damaged neurons has been implicated in forming a positive inflammatory and degenerative feed-back loop in Parkinson's models [496]. Although, I attempted to exclude necrotic cells here by not counting cells with a necrotic or shrunken morphology. It is possible that this partially underlies the changes in *nfkb1*$^{-/-}$ mice as cell death has been reported in the *nfkb1*$^{-/-}$ mouse brain [395]. Additionally, I was also aware that these may well be 'dark neurons', a fixation artefact that complicates post-mortem analysis in the brain, and mimics a necrotic appearance closely but does not lead to cell death [514]. These are comparatively common in brains from animals not perfused with paraformaldehyde at dissection, as was the case in these mice, and if the brain is physically compressed in removal [514]. In this study the mice were not perfused to allow for the collection of frozen tissues, and the hearts were also needed, which would have been damaged by injection perfusion.

In this chapter, I hypothesised that a DDR induced senescence-like phenotype is involved in the age-associated increases in neuro-inflammation and associated cognitive deficits. My data show an increase in persistent DNA damage, DDR activation and senescence associated markers in purkinje and hippocampal pyramidal neurons in *nfkb1*$^{-/-}$ mice. Both of which are associated with aged-related changes in phenotype and cognitive function. This may be mediated through intrinsic effects of nfkb1/p50 knockdown, or through an associated increase in inflammation. It appears to partially mediated through a COX-2 dependent mechanism, although if this is inflammation or ROS generation is not clear. It is not currently clear if changes within neurons, systemic circulating factors, microglial activation, or a combination of all of these factors drives the observed dysfunction.

4.0 - Senolytic treatment reduces the number of senescent-like neurons in ageing wild-type mice

4.1 - Introduction

Senescent-like neurons have been observed to increase in the brain, with age (here and [112]). This occurs in areas associated with age-related changes, such as the cerebellum and hippocampus. In the previous chapter I demonstrated that the numbers of senescent-like neurons in these areas increases in a model of chronic inflammation, together with a decreased performance in hippocampal-dependent memory tasks and a deficit in the generation of gamma-oscillations.

From the existing body of literature, the existence of senescence-like neurons is likely linked to the reactivation, or prevention of reactivation, of the cell-cycle. The frequency of neurons with signs of partial G1 and S-phase cell-cycle reactivation increases in the brains of patients with cognitive impairment and Alzheimer's disease, especially in the CA3-4 to CA1 of the hippocampus [292, 293]. This reactivation eventually leads to apoptosis of the cell [297, 298], while preventing this cell-cycle re-entry lowers the rates of neuronal apoptosis [289, 306, 307, 309]. Given the observed frequency of neurons *in vivo* and known rate of cell death, it is likely that these cells are persistent for long periods [293].

It is unclear if senescence and senescent-like neurons actually contribute towards neuro-inflammation and cognitive impairment through the 'bystander' effect, or are simply innocent bystanders. Senescent cells can induce tissue dysfunction though the release of pro-inflammatory and pro-oxidative factors that can promote further senescence in surrounding cells [86, 122, 509, 515]. Their presence in other tissues are associated with a number of, typically age-related, pathologies such as liver disease [139, 516], pulmonary disease, [355, 503], atherosclerosis [358], cardiac and kidney dysfunction [124]. Yet, senescence is beneficial in other circumstances, such as wound healing [517], tissue repair [518] tumour suppression [519] or embryonic development [118]. So far, it is still unknown whether a senescent-like phenotype in neurons serves a specific function and has evolved as such and if it is beneficial or detrimental to the organism.

Polyploid neurons from young mice maintain distal connections, and show some signs of activity, such as early intermediate gene expression [311]. This suggests that there is still at least a degree of

functional integration. As such, there exists the possibility that this simply is a protective mechanism against cell death *in vitro* and *in vivo* [289, 306, 307, 309], and that these cells do not negatively contribute to overall network connectivity. Therefore, elimination of senescent cells in the whole body may counter ageing, but the killing of senescent-like neurons carries the risk of damaging brain function.

4.1.2 - Treatment of chronologically aged mice with senolytic compounds

To assess if clearance of senescent cells was linked to either an improvement in cognition, or a decline, our laboratory, in collaboration with the laboratory of James Kirkland at the Mayo Clinic, Rochester, Minnesota, assessed cognitive function in an aged cohort of mice using two different senolytic approaches. A cohort of aged INK-ATTAC mice (25-30 months at start of treatment) was used. Baseline measurements of cognition were taken prior to the administration of the 2 different senolytic approaches, pharmacological clearance by Dasatinib and Quercetin (DQ), and pharmacogenetic clearance by AP20187. Cognitive and behavioural analyses were performed in Mayo Clinic, by Mikołaj Ogrodnik, *post-mortem* the brain tissues were shipped to the UK where I performed the characterisation of senescent-like neurons in the brain.

The pharmacogenetic INK-ATTAC approach [123, 124] involves replacing the promotor of dimerising caspase-8 with part of the promotor region of p16, which is activated in many senescent cells (Termed INK-ATTAC). When the drug AP20187 is added, it promotes the dimerization of caspase-8. This then promotes apoptosis in cells where this is expressed, namely p16 expressing cells. This approach has been shown to result in a reduction in the number of p16 positive senescent cells and in improvements in median lifespan and age-associated pathology in aged mice [124, 351]. Dasatinib and Quercetin (DQ) is a combination therapy of two drugs that have proven effective in killing senescent cells *in vitro* and *in vivo*. Recently, it has demonstrated that a single dose of DQ was sufficient to effectively clear a high percentage of p16 positive cells in the liver [346]. Pharmacogenetic clearance through AP20187 has shown improvements in healthspan and median lifespan in wild-type mice at 18 months [124]. Both AP20187 and DQ show improvements in several parameters of healthspan in progeroid models, AP20187 in BubR1 mice [123], and DQ in *ercc1*$^{-/-}$ mice [356].

There was high mortality in this study, likely due to the advanced age of the mice (27-32 months by end of treatment). During the study the total mortality for male mice was 27%. The use of AP20187 has previously been demonstrated to improve median life-span in INK-ATTAC C57Bl/6 and mixed background mice [124]. This was administered twice per week from 12 months till end of life, in

contrast to the intermittent treatment used her for 2 months. Mortality was highest in Vehicle treated mice at 40%, 30% in DQ treated mice, and 8% in AP20187 treated mice.

4.1.3 - Intermittent treatment with the senolytic compounds Dasatinib and Quercetin, and AP20187, prevent age-associated memory decline in aged wild-type mice.

Treatments with the senolytic compounds DQ and AP20187 have been shown by Mikołaj Ogrodnik to improve cognitive function in aged INK-ATTAC mice (Figure 4.1.3.1). Learning and memory impairment was assessed using a shallow-water motivated Stone T-Maze paradigm [520]. As a T-maze variant, it is a series of left-right turns, which the mouse must memorise, in order to navigate from the start point to a dry escape box [520]. Impaired learning in the Stone T-Maze can be seen with lesions to the striatum and septo-hippocampal system [521]. Performance in the maze decreases with age, with deficits in learning and retention [520].

The water-motivated T-maze [520] used here has the maze partially filled with water, which allows the mouse to maintain contact with the ground, while keeping their head above the water and motivating their escape. They were acclimatised and trained on the first day with a 'straight run' that presented no choices, but showed that advance means escape. Mice were defined as successful if they reached the goal box in under 10 seconds, in 6 of 9 training trials. If they failed they were excluded from further analysis. The next day the maze version was introduced, with mice having 9 trials within the day, with 5 to 12 minutes between trials in a heated holding box with a drying towel. Primary latency and wrong turns (errors) to the escape box were recorded. Mice were allowed a total of 5 minutes in the maze before failure, and trial termination, 3 failures lead to exclusion from further analysis.

In the cognitive data from the Stone T-Maze, aged 27-32 month INK-ATTAC male mice, compared to 5 month control mice, make significantly more errors (Figure 4.1.3.1a,c), and take longer to complete the maze than young control mice (Figure 4.1.3.1b,d). In young mice, two months of intermittent treatment with the senolytics DQ and AP20187 did not significantly affect the number of errors, or time taken to complete the maze (Figure 4.1.3.1a,b). In contrast, in aged INK-ATTAC mice, treatment with DQ and AP20187 significantly improved performance in the maze, with fewer errors made and a significant decrease in latency (Figure 4.1.3.1c,d).

To account for the possibility of survivor bias and to track if there are changes in cognition, the data was also normalised to percentage change compared to base-line testing, which was performed prior to the start of treatment (Figure 4.1.3.2a-d). Vehicle treated aged INK-ATTAC mice showed a deterioration in Stone T-Maze performance, performing at 150% of baseline (1.5x worse), while

AP20187 treated mice remained comparatively constant (90-100% of baseline), and DQ treated mice showed an improvement (60% of baseline) (Figure 4.1.3.2c,d).

The improvements in performance do not seem to be linked to a greater ability to memorise the maze, as the rate of improvement seen across training are comparable. Instead senolytic treated aged INK-ATTAC mice performed better from the first trials, indicating better overall memory function (Figure 4.1.3.2c,d). Together this implies that the clearing senescent cells protects aged male INK-ATTAC mice from age-dependent declines in memory, and possibly even an improvement with DQ treated mice. This was observed at both a group, and individual level, so does not appear attributable to survivorship bias from the improved survival of senolytic treated groups.

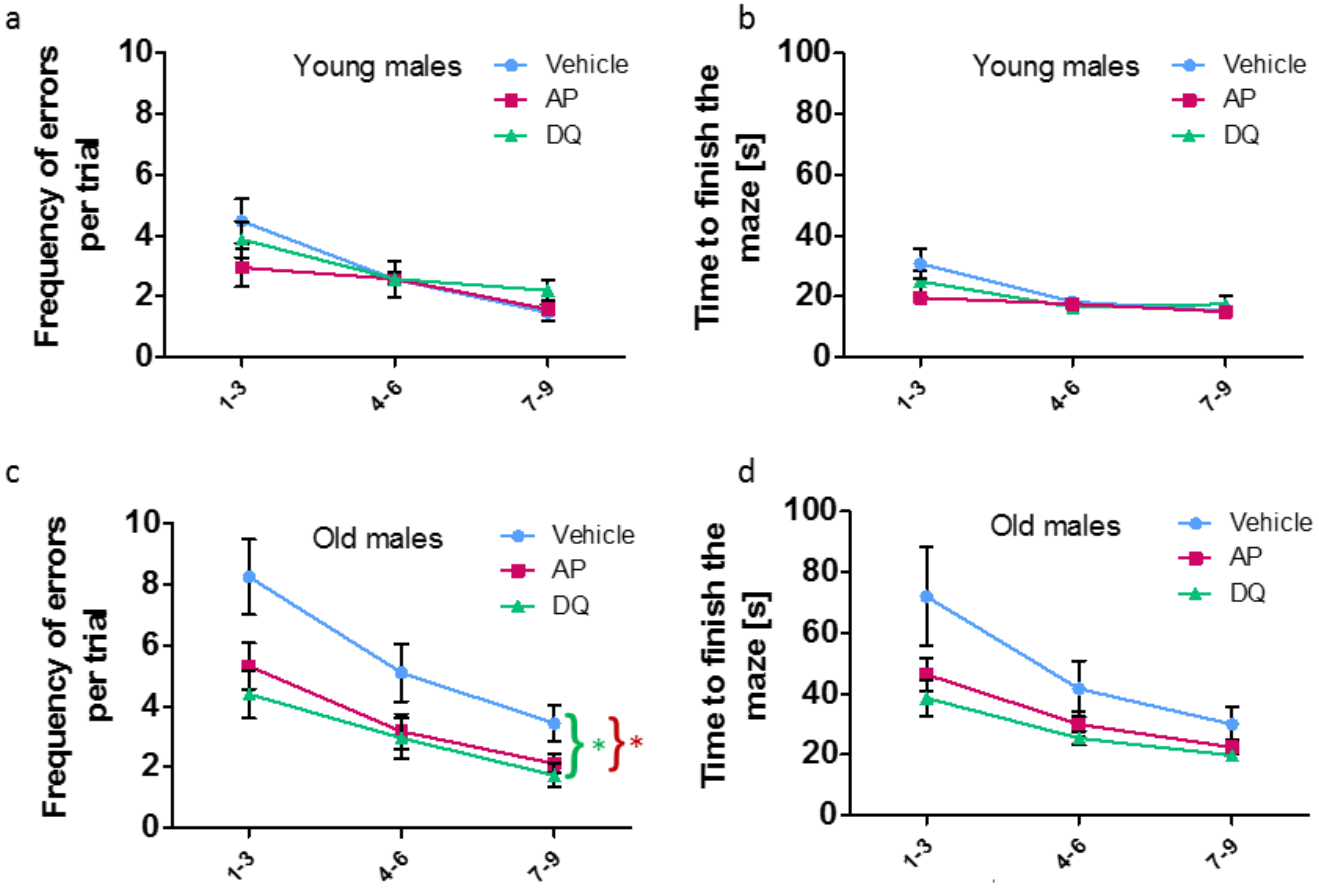

Figure 4.1.3.1: Memory function in young and old INK-ATTAC mice after AP20187 and Dasatinib & Quercetin treatment

(a-b) young (5 month) and **(c-d)** aged (27-32 month) male INK-ATTAC mice were tested in the Stone T Maze, after two months of intermittent treatment with AP20187 and DQ. Memory function in the Stone's maze is defined by **(a, c)** the frequency of errors they make during the test session and **(b, d)** the escape time from the maze. All data are mean ± s.e.m. with n=7-8 for young males, n=9-11 for old males. Significance between groups shown by * P<0.05 (two-way ANOVA). Reproduced with permission form Mikołaj Ogrodnik.

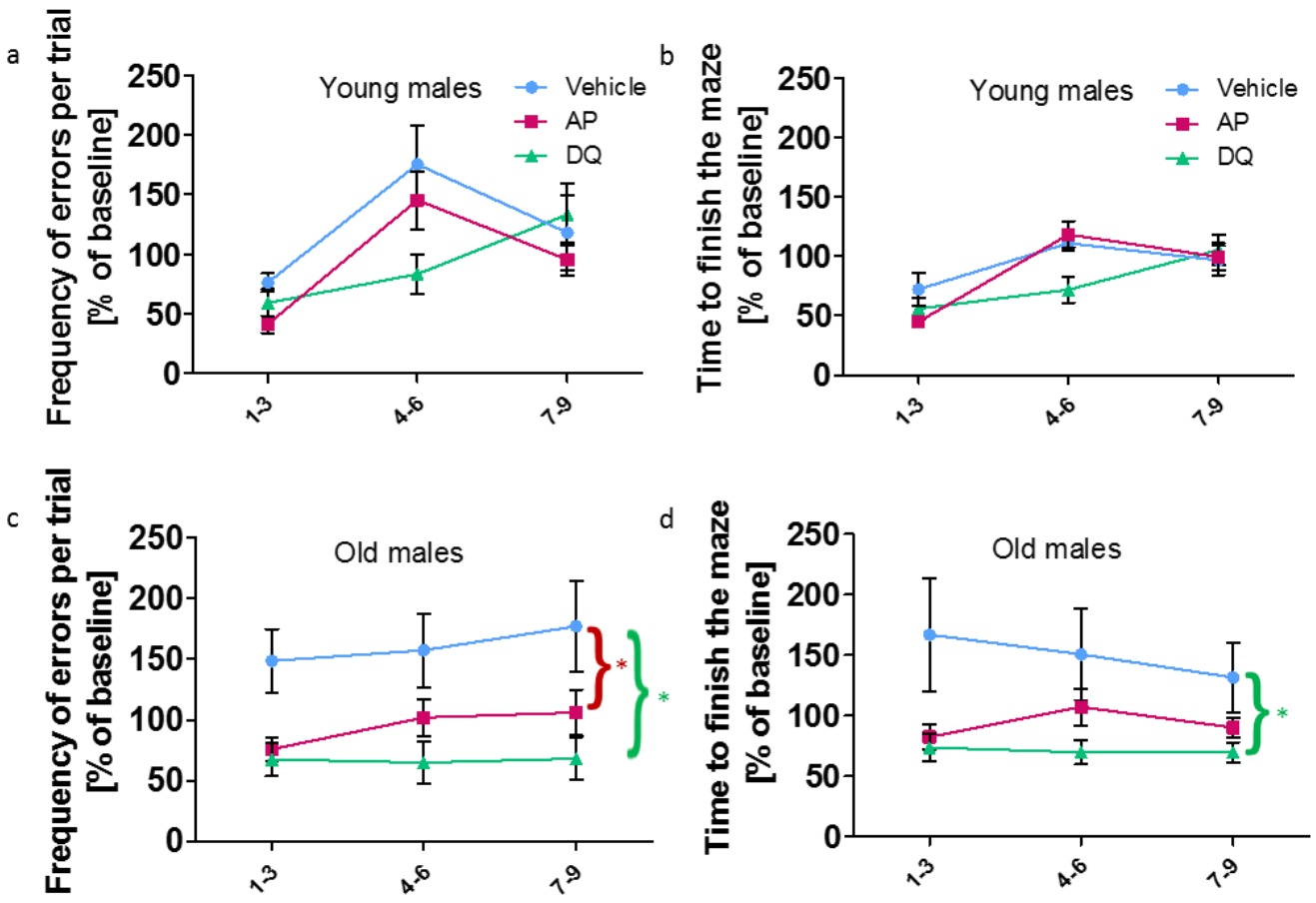

Figure 4.1.3.2: Performance of INK-ATTAC mice in the Stone's Maze normalized to the baseline

As the outcome of the AP20187, D&Q or vehicle treatment on memory function parameters **(a, c)** frequencies of errors and **(b, d)** the time to finish the maze were normalized to the baseline tests taken prior to the start of treatment and analysed. All data are mean ± s.e.m. with n=7-8 for young males, n=9-11 for old males. Significance between groups shown by *P<0.05 (two-way ANOVA). Reproduced with permission from Mikołaj Ogrodnik.

4.2 - Dasatinib and Quercetin reduces senescence-associated markers in hippocampal neurons

To assess if there was clearance of senescent-like neurons with senolytic treatment, a number of senescence- associated markers were assessed. The hippocampus was selected as the primary target of investigation in aged INK-ATTAC mice following treatment with AP20187 (which induces apoptosis of p16 expressing cells through dimerization of FKBP-fused Casp8 in INKATTAC mice) and DQ. These mice showed an improvement, and a prevention of age-associated decline, in the Stone T-Maze following treatment with DQ and AP20187. The Stones T-Maze is dependent on the septo-hippocampal system [521]. In the last chapter, I observed deficits in hippocampal gamma oscillations and hippocampus-dependent spatial memory tasks in mice, with increased levels of senescence-like neurons in this region.

To assess the rates of senescent cells requires the use of multiple markers, as even the most accurate only show 90% accuracy [121]. The expression of p16 and p21 were assessed, as was the loss of HMGB1 from the nuclear compartment. Measurement of the DNA damage, and telomere associated damage as a persistent DNA damage, were also assessed, as these have proved to be good markers of cellular senescence and clearance of p16 senescent cells has decreased telomere-associated foci in liver [516]; aorta [354]; Cardiomyocytes (Anderson *et al.* unpublished) and predict mouse lifespan [127].

4.2.1 - Dasatanib and Quercetin, but not AP20187, significantly reduces p16 positive cells in the CA3 of the Hippocampus

p16 is a cyclin-dependent kinase inhibitor that binds to Cdk4/6 to inhibit the formation of the Cyclin D-Cdk4/6 and progression from G1 to S-phase. It is activated in response to various mitotic and senescence inducing stressors [118, 216]. p16 is expressed in many senescent cell-types and increases can be seen in multiple mouse tissues, including the heart and cortex [349]. It provides a secondary 'lock' to p53 signalling in establishing a permanent exit from the cell-cycle [216, 522] and blocks cytokinesis (even in the event of cell-cycle slippage and DNA synthesis by p53 and pRb inactivation) via suppression of mitotic exit network kinase by a ROS-PKCd positive feedback loop [216]. An increase in p16, amongst other cell-cycle markers, has previously been observed in Alzheimer's disease [276, 277, 279, 291, 359], but their exact contribution to the disease and cognitive deficits is not yet known.

It is widely accepted in the senescence scientific community that most commercially available antibodies against p16 do not work in mice tissues. For that reason, I had to use an alternative method

to detect p16 positive cells and performed RNA *in situ hybridization* (RNA*ISH)*. Cells positive for p16 mRNA foci, detected by RNA*ISH*, were analysed in the pyramidal layer of CA3 (including CA2) and CA1, and the granule layer of the DG (Figure 4.2.1.1A).

In this experiment, I analysed brain tissues from aged INK-ATTAC mice (age 27-32) treated either with AP20187 to mediate pharmacogenetic clearance of p16 expressing cells, or pharmacological treatment with the senolytic cocktail DQ. I found that with DQ treatment there was a significant reduction in the number of p16 mRNA foci positive cells in the pyramidal layer of CA3 compared to vehicle treated mice (Figure 4.2.1.1A). However, while AP-treated mice had a lower median number of positive cells when compared to vehicle treated mice, the reduction was less than that seen with DQ, and was not statistically significantly. In the CA1 layer, a lower median number of p16 mRNA foci positive cells could be seen with DQ and AP20187 compared to vehicle treated animals, but this was not statistically significant (Figure 4.2.1.1B). No changes could be seen with DQ treatment compared to vehicle treated animals in the granule layer of the DG, and interestingly, AP treated animals showed a trend for increased number of positive cells (Figure 4.2.1.1D). When correlated with average number of errors in the final 3 trials of the Stone T-Maze, while there was a slight trend with the CA3, no significant differences could be observed with number of p16 mRNA positive cells in any of the 3 areas (Figure4.2.1.1E-G).

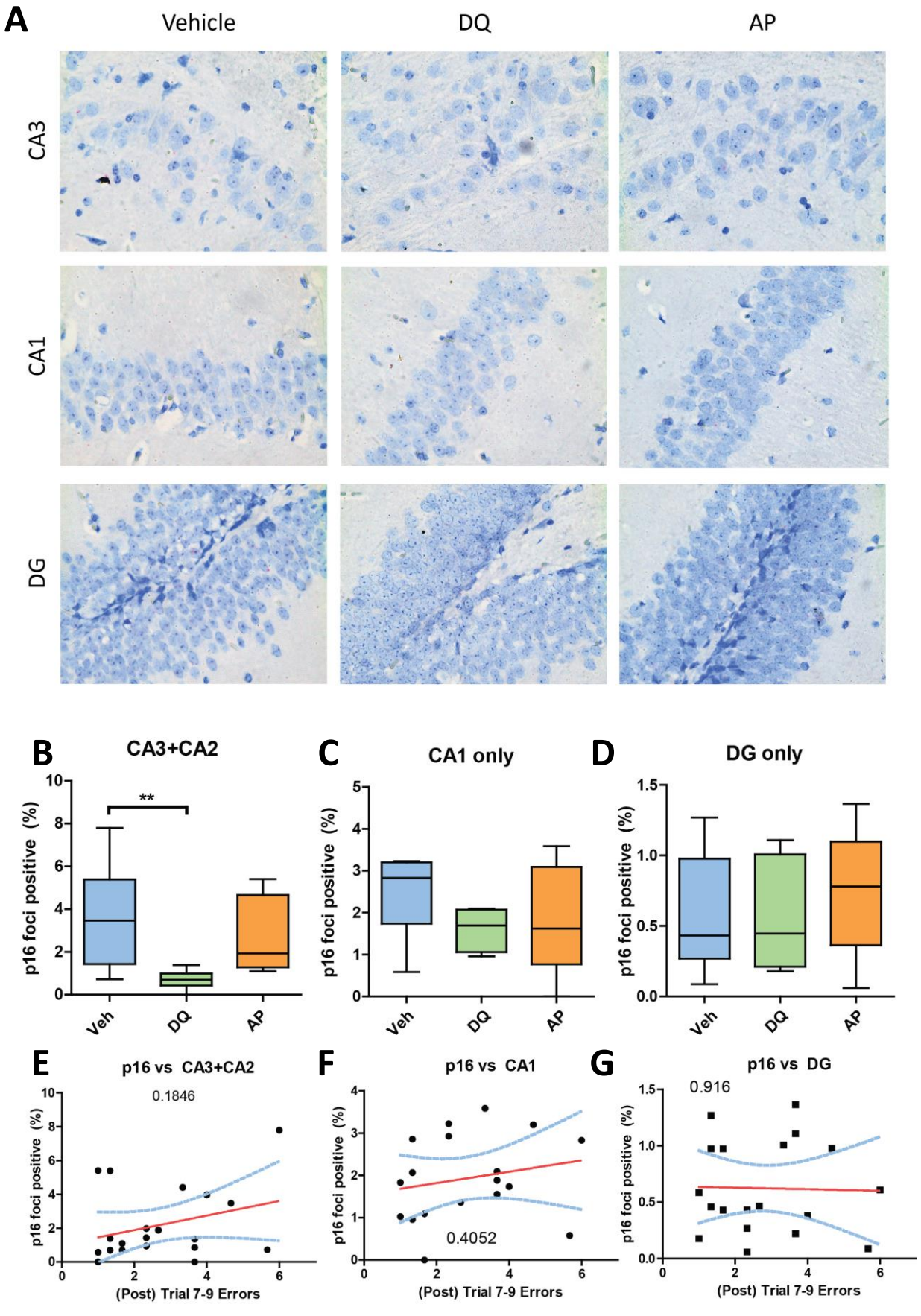
A
Vehicle
DQ
AP
CA3
CA1
DG
B
CA3+CA2
p16 foci positive (%)
**
Veh
DQ
AP
C
CA1 only
p16 foci positive (%)
Veh
DQ
AP
D
DG only
p16 foci positive (%)
Veh
DQ
AP
E
p16 vs CA3+CA2
0.1846
p16 foci positive (%)
(Post) Trial 7-9 Errors
F
p16 vs CA1
0.4052
p16 foci positive (%)
(Post) Trial 7-9 Errors
G
p16 vs DG
0.916
p16 foci positive (%)
(Post) Trial 7-9 Errors

Figure 4.2.1.5: Treatment with Dasatinib and Quercetin, but not AP20187, reduces p16 mRNA positive cells in the CA3 layer in aged INK-ATTAC mice

A) Representative images of p16 RNAISH staining in the hippocampus **B)** Quantification of p16 mRNA positive cells in the pyramidal layer of the CA3+CA2 region hippocampus **C)** Quantification of p16 mRNA positive cells in the pyramidal layer of the CA1. **D)** Quantification of p16 mRNA positive cells in the granule layer of the DG. **E)** Comparison of p16 mRNA positive cells in the CA3 and CA2. Kruskal-Wallis, Dunns Post-Hoc (Vehicle control), n=6-7 animals per group. Significant differences between treatment groups displayed by by (* $p<0.05$, ** $p<0.005$).

4.2.2 - Dasatinib and Quercetin treatment significantly reduces the number of Telomere-associated yH2A.X foci (TAF) in the CA3 layer

A DNA damage response located at telomeres regions appears to be persistent during senescence, with data suggesting that telomere regions (particularly components of shelterin complex) inhibit non homologous end joining repair[209, 211]. A persistent DDR signalling has been shown to be important for the maintenance of the cell-cycle arrest during senescence and also contributes to the induction of the SASP (since the central initiator of the DNA damage response –ATM has been shown to be a SASP regulator (Rodier et al.)[86, 177, 209, 211]. I previously observed increased in telomere associated DNA damage foci with age in neurons from wild-type and *nfkb1*$^{-/-}$ mice in neurons, which was associated with the presence of p21, the loss of HMGB1 from the nucleus and increased lipofuscin levels. For these reasons, I investigated whether pharmacogenetics clearance of p16 positive cells or treatment with senolytic drugs impacted on telomere dysfunction in aged mice. The total number of yH2A.X foci, the number of foci co-localising with telomeres, and the number of cells with 2 or more TAFs were analysed in the CA3 and CA1 of mice treated with Vehicle, DQ or AP20187 (Figure 4.2.2.1A).

In CA3 neurons DQ treated mice showed a trend for a lower median value of mean yH2A.X foci per cell compared to vehicle treated mice, but this was not significant (Figure 4.2.2.1B). The median value forAP20187 treated animals fell between these two values; this was not significantly different to vehicle treated control mice and a higher degree of variation could be observed. However, I observed a significant reduction in the mean number of TAFs per neuron in DQ, but not AP, treated mice (Figure 4.2.2.1C).

In the CA1, there was a similar pattern to the CA3, with a trend for reduced mean yH2A.X foci per cell in DQ animals, with AP treated animals falling in between (Figure 4.2.2.1D). Neither of these trends was significant. A trend for a reduced mean number of TAFs per cell was observed with DQ treatment, but not with AP20187 treatment (Figure 4.2.2.1E).

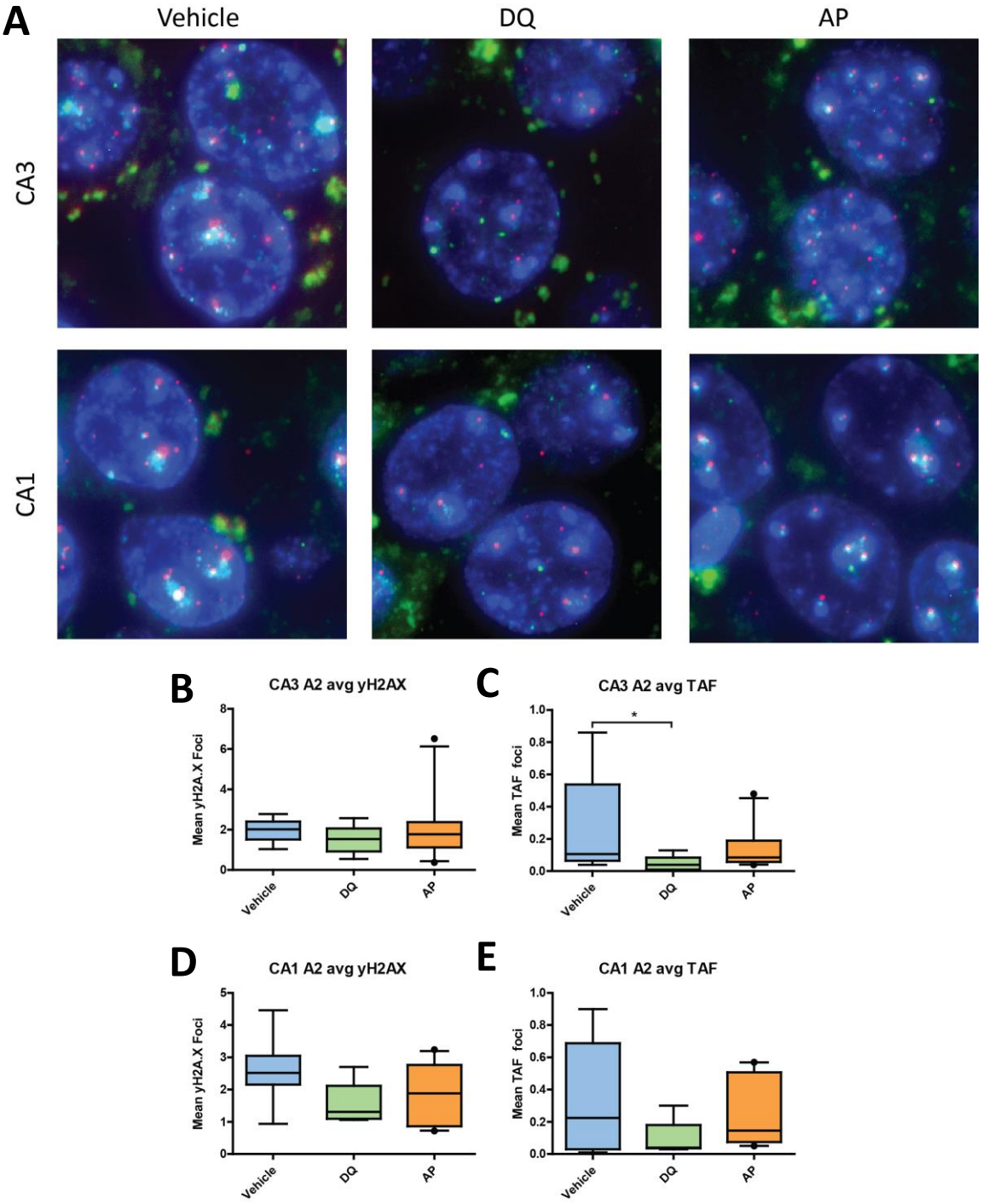

Figure 4.2.2.1: Dasatinib and Quercetin reduces Telomere associated DNA damage in CA3 pyramidal neurons in aged INK-ATTAC mice

A) Representative images of TAF stainings in the CA3 and CA1 of the hippocampus, yH2A.X in green, telomere probe in red and nuclear stained with DAPI in blue. Quantification in NeuN positive CA3 cells of **B)** total yH2A.X foci per neuron, **C)** Average TAF. Quantification in NeuN positive CA1 cells of **D)** total yH2A.X foci per neuron, **E)** Average TAF. Box and whiskers show the median of the means -Min to +Max. Kruskal-Wallis, Dunns Post-Hoc (Vehicle control), n=5-10 animals per group, significant differences between genotype, as well as treatments, at each age point are displayed by (* $p<0.05$). Imaged and quantified by Patrick Krüger.

4.2.3 – p21 positive cells positively correlate with cognition, but are not modified significantly by senolytic treatment.

In the last chapter I observed an upregulation of p21 protein in neurons, with ageing in wild-type mice and in *nfkb1*$^{-/-}$ mice. p21 is activated downstream of the DDR through p53 [178, 181]. It silences the expression of Cdk2, and inhibits both Cyclin E-Cdk2 and Cyclin A-Cdk2, preventing transition into S-phase and ensuring that Rb remains hypo-phosphorylated and inactive [88, 89]. In S-phase, it can displace polymerase from PCNA and prevent DNA-synthesis [179, 180]. In senescent cells, in addition to its roles in inhibition of the cell-cycle, it has a role in the initial stabilisation of the senescent-phenotype [177, 222]. It was hypothesised that ROS generated downstream of p21 contributed to a positive feedback loop which stabilised the DDR thereby stabilising the cell-cycle arrest during senescence [177].

The number of cells positive for p21 by RNA*ISH* was also analysed in the pyramidal layer of CA3 (including CA2) and CA1, and the granule layer of the DG (Figure 4.2.3.1A). In contrast to p16 mRNA foci, far more cells were positive for p21 mRNA foci in all 3 areas analysed (Figure 4.2.3.1B-D). With DQ treatment, there was a trend for a reduced number of cell positive for p21 mRNA in the CA3 of the hippocampus compared to vehicle treated controls, with the median value for AP20187 treated animals falling in between these values (Figure 4.2.3.1B). No significant differences were observed in the CA1 (Figure 4.2.3.1C) or DG (Figure 4.2.3.1D) between either DQ, or AP20187, treated mice and vehicle treated controls. In contrast to p16 mRNA, while there was no significant difference between groups in the percentage of cells positive for p21 mRNA foci in the 3 areas. However, there was a significant correlation between number of errors made in the final 3 trials of the Stone T-Maze and the number of p21 positive cells in the CA3 (Figure 4.2.3.1E), and CA1 (Figure 4.2.3.1G) when comparing all groups. This was not significant in the DG (Figure 4.2.3.1G).

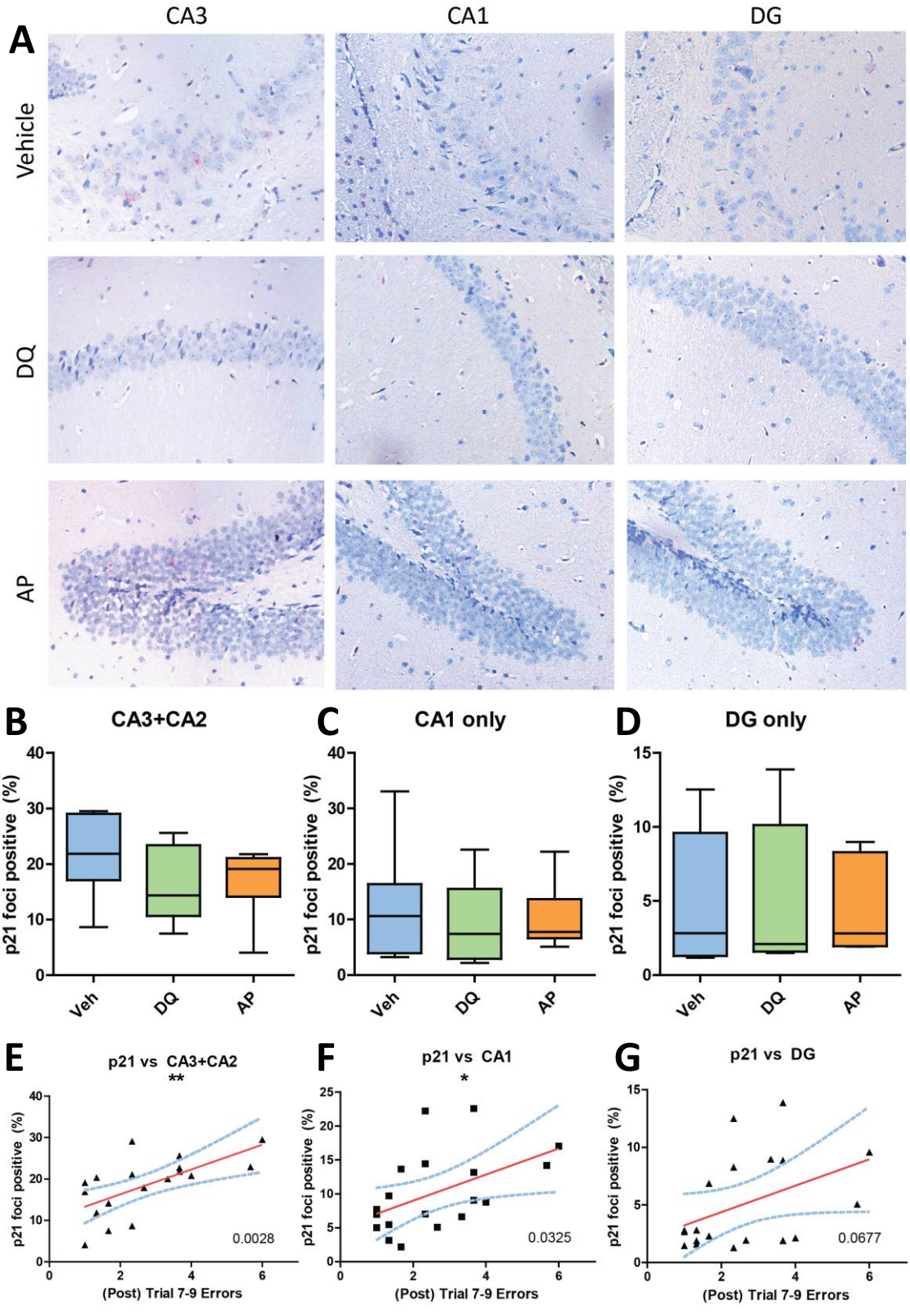
A
CA3
CA1
DG
Vehicle
DQ
AP
B
CA3+CA2
C
CA1 only
D
DG only
p21 foci positive (%)
Veh
DQ
AP
E
p21 vs CA3+CA2
**
0.0028
F
p21 vs CA1
*
0.0325
G
p21 vs DG
0.0677
(Post) Trial 7-9 Errors

Figure 4.6.3.1: No significant effects with Dasatinib and Quercetin, or AP20187, on p21 RNA*ISH* positive cells in the hippocampus

A) Representative images of p21 RNA*ISH* staining in the hippocampus **B B)** Quantification of p21 mRNA positive cells in the pyramidal layer of the CA3+CA2 region hippocampus **C)** Quantification of p21 mRNA positive cells in the pyramidal layer of the CA1. **D)** Quantification of p21 mRNA positive cells in the granule layer of the DG. E**)** Comparison of p21 positive cells in the CA3 and CA2. Kruskal-Wallis, Dunns Post-Hoc (Vehicle control). n=6-8 animals per group. Significant differences between treatment groups displayed by by (* $p<0.05$, ** $p<0.005$).

4.2.4 - Dasatinib and Quercetin, and AP20187, reduce percentage of HMGB1 negative cells in the pyramidal layer of the CA3

As previously discussed, HMGB1 is a chromatin binding protein that can be relocated from the nucleus, to the cytosol and extra-cellular space, where it can act as a pro-inflammatory cytokine [493, 494]. Its release from neurons and glial cells can mediate inflammation related tissue damage [494-496], and it is a key regulator of senescence and the SASP following nuclear export [491]. Previously I observed increased release of HMGB1 from neurons in *nfkb1*$^{-/-}$ mice compared to wild-type mice, and with age, in pyramidal neurons of the hippocampus.

The presence of nuclear HMGB1 was analysed in the pyramidal layers of CA3 to CA1 and granule layer of the DG in mice treated with Vehicle, DQ and AP (Figure 4.2.4.1A). 3 sections were counted per animal, and the average taken for each area. Dark neurons were not counted, as we could not exclude the possibility that these were a fixation artefact [514].

In CA3 neurons, aged mice treated with both DQ and AP20187 showed a significant reduction in the percentage of HMGB1 negative neurons compared to vehicle treated controls (Figure 4.2.4.1B). The change in median percentage of cells was slightly greater in DQ treated animals, and with less variation. In the CA1, a trend for reduced percentage of HMGB1 negative neurons could be seen with DQ, but not with AP20187 (Figure 4.2.4.1C); however, neither was significantly different to vehicle treated animals. There was a lesser trend in the *Dentate Gyrus,* although both DQ and AP treated animals showed a trend for reduced median percentage of HMGB1 negative neurons.

When correlated with the average number of errors in the final 3 trials of the Stone T-Maze, a significant correlation could be seen with percentage of HMGB1 nuclear negative neurons in the CA3 (Figure 4.2.4.1E), and a slight, but non-significant trend with HMGB1 negative neurons in in the CA1 (Figure 4.2.4.1F) and DG (Figure 4.2.4.1G).

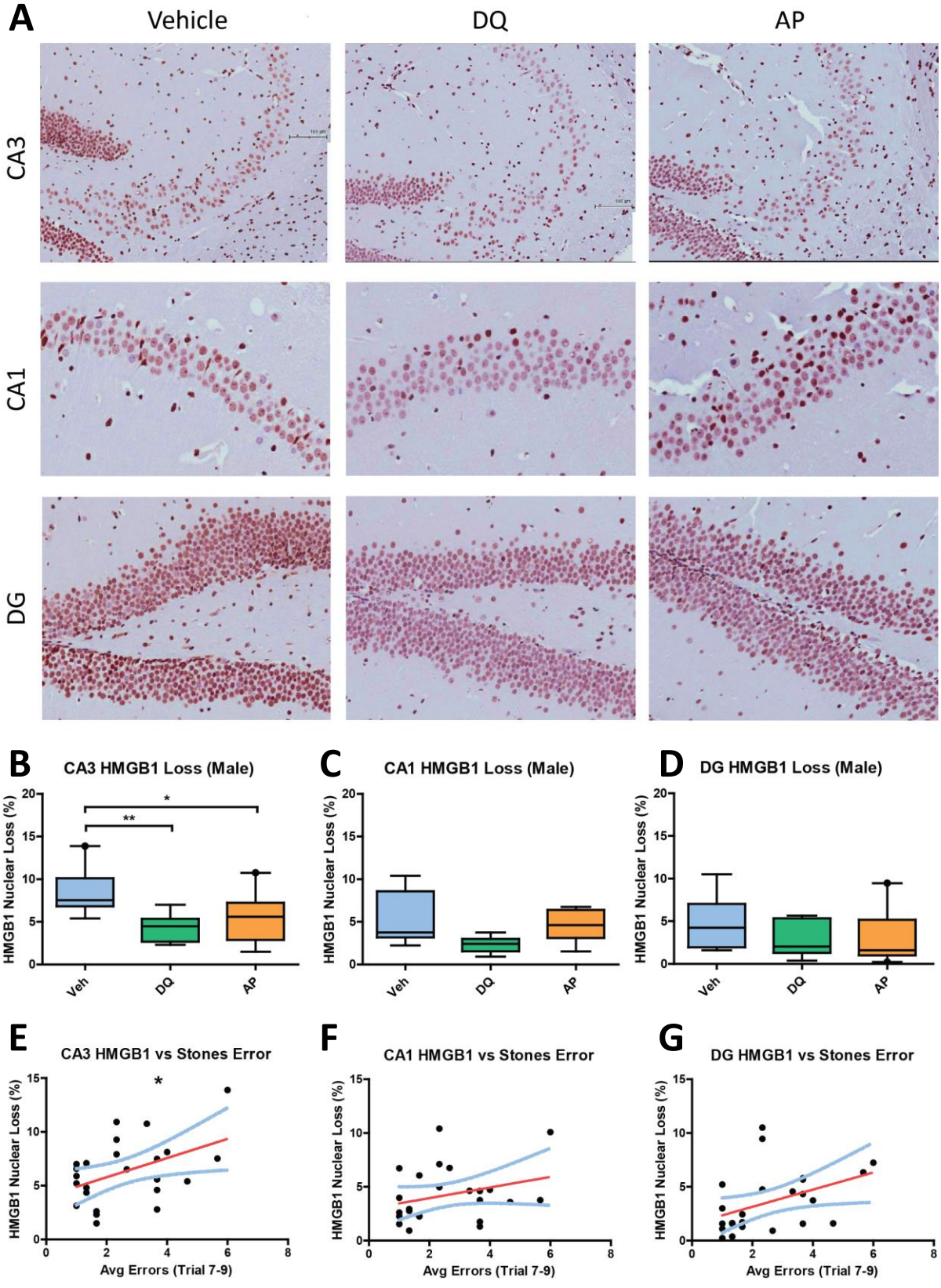
A
Vehicle
DQ
AP
CA3
CA1
DG
B
CA3 HMGB1 Loss (Male)
HMGB1 Nuclear Loss (%)
Veh
DQ
AP
C
CA1 HMGB1 Loss (Male)
D
DG HMGB1 Loss (Male)
E
CA3 HMGB1 vs Stones Error
Avg Errors (Trial 7-9)
F
CA1 HMGB1 vs Stones Error
G
DG HMGB1 vs Stones Error

Figure 4.2.4.1: Dasatinib and Quercetin, and AP20187, reduce the percentage of HMGB1 negative neurons in the CA3

A) Representative images of HMGB1 staining in the hippocampus, HMGB1 stained by NovaRed (Brown) and counterstained with Haematoxylin (Blue). **B-D)** Quantification of neurons with no HMGB1 in the nucleus in the pyramidal layer of the **B)** CA3+CA2, **C)** CA1 and **D)** DG regions of the hippocampus. Kruskal-Wallis, Dunns Post-Hoc (Vehicle control). n=6-9 animals per group. Significant differences between treatment groups displayed by (* $p<0.05$, ** $p<0.005$). **E-G)** Correlation between number of average number of errors in trials 7-9 of the Stones Maze and percentage of neurons with no HMGB1 in the nucleus in the pyramidal layer of the **E)** CA3+CA2, F**)** CA1 and **G)** DG regions hippocampus. Red line shows linear regression, dotted blue lines show 95% confidence intervals. Significance tested by two-tailed Pearson correlation coefficient (* $p<0.05$).

4.3 - Discussion

In this work we hypothesised that senescent cells may contribute to loss of function in the brain. To assess this, we aged INK-ATTAC mice and induced clearance of p16 positive cells by pharmacogenetics means (through the administration of AP20187) and through use of a drug combination (Dasatinib and Quercetin) has previously been shown to eliminate senescent cells *in vitro* and *in vivo*.

Prior to the experiments we predicted three possible outcomes: one was that clearance of senescent neurons may be detrimental for ageing mice, since senescence is characterised by resistance to apoptosis [250-252, 523] and its existence in neurons may be a mechanism to avoid neuronal cell death with age [196]. Another, would be that senescent neurons are detrimental during ageing due to loss of function and by induction of paracrine damage. Consistent with this hypothesis, previous data has indicated that whole body clearance of senescent cells lead to marked improvements in healthspan in aged mice [124] and in several models of age-related diseases (such as osteoarthritis, liver disease, bone loss, atherosclerosis and pulmonary fibrosis). The third possibility is that any effects of clearance of senescent cells is due to non-cell autonomous mechanisms and that elimination of senescent cells in others parts of the body, besides the brain, contributes to any observed phenotype.

Initial reports of cognitive testing in 18 month INK-ATTAC mice (C57Bl/6 and mixed background) treated with AP20187 by Baker et al. suggested no significant effect in memory function using novel-object recognition (NOR) [124]. These data suggested that there was no outright damaging effect, but NOR is a form of non-spatial memory testing and sensitive to changes in visual and olfactory function. While there are defects in mice with hippocampal lesions, the contribution of hippocampal memory to novel object recognition is still unclear [524]. Furthermore, the mice used in Baker et al. were at comparatively young age, at 18 months (compared to the mice we used which were 25 to 30 months of age at the start of the 2 month treatment). While defects can be seen by this age in parameters of spatial memory such as the Barnes Maze, the NOR appears more resistant [525]. In NOR, using same-day testing parameters, there is no significant change in ageing C57Bl/6 mice compared to 4 month control mice, even by 28 months when using short rest periods (1 minute, compared to 5 minutes in Baker et al.) [525]. Differences are observed when using a 24 hour delay though. As such, the method used by Baker et al. may not have been sensitive enough to adequately detect any changes. In contrast the Stone T-Maze is understood not to be affected by changes in visual and olfactory function, and has been used successfully to assess age-related changes in cognition [520].

Our data on performance in the Stone T-Maze in aged INK-ATTAC mice following treatments with DQ or pharmacogenetic clearance of p16 positive cells through AP20187 suggests that senescent cells

may contribute to declines in cognitive performance. In young mice, we observed no significant changes in cognitive function, suggesting that neither pharmacogenetic clearance with AP20187 or DQ had any outright damaging effects on cognition. In aged INK-ATTAC mice, AP20187 treatment held performance comparatively stable compared to baseline testing prior to testing, suggesting that clearance of senescent cells in the body prevents further deterioration. Intriguingly, DQ treated mice actually showed improvements in performance compared to baseline testing, suggesting that this compound may not simply delay further deficits.

My data suggests that treatment with DQ is capable of reducing the numbers of senescent-like neurons in the pyramidal layer of the hippocampus. There was a significant reduction in the percentage of p16 positive cells detected by RNA*ISH* in the CA3 of DQ treated INK-ATTAC mice compared to vehicle treated animals. There was a similar trend in CA1, but no observable difference in DG.

In contrast, AP20187 was less effective, and did not show significant differences to vehicle treated INK-ATTAC mice in many factors. There was no significant rescue in the CA3-CA1 in numbers of p16 mRNA foci positive cells, and median values typically fell between those of vehicle treated and DQ treated mice. This is a similar pattern to the results found in the Stone T-Maze. This was surprising since AP20187 should be a more specific intervention in promoting the killing cells expressing p16 through the activation of caspase-8 [123, 124]. This may be explained by reduced BBB penetrance of AP20187, which will be discussed later in this section.

The role of p16 in neurons is still not understood. In proliferation competent cells, p16 is expressed in late senescence and is associated with the maintenance of stable cell-cycle arrest after p21 levels subside [526]. Increases in p16 positive cells have been observed in vulnerable areas of the brain, such as the hippocampus in Alzheimer's disease [277, 279, 291, 527, 528]. pRb and p16 expression has been shown to be protective against apoptosis in neurons [360], which may explain the persistence of these cells in the disease. In 5XFAD Alzheimer's model mice, increases could be seen in p16 expression in pyramidal neurons (some in astrocytes, none in microglia), with an association with cognitive deficits in spatial memory in [527].

Activation of the DDR, and the presence of persistent DNA damage has been shown to trigger and maintain senescence in mitotic tissues [177, 209, 210]. Double-stranded breaks can be marked by DDR proteins such as yH2A.X and are potent inducers of the DDR [112, 129]. This can lead to downstream activation of either pro-apoptotic and pro-survival pathways [136, 137]. The data here did not show a significant decrease in the number of yH2A.X with senolytic treatment. There was a slight trend for

reduction with DQ, but no change with AP20187 in pyramidal neurons from CA3. In CA1 neurons there was a trend for reduction with DQ and AP20187. This is consistent with my previous data in ageing wild-type mice - while we observe a significant increase in TAF with age, we did not observe any age-dependent changes in total γH2A.X. This may be due to the fact that double-stranded breaks located in non telomeric regions are quickly repaired; where as previously shown, telomere regions inhibit NHEJ [211]. It is possible that these non-telomeric foci are constantly being induced and rapidly repaired as shown in senescent fibroblasts grown in vitro [177, 209], therefore not accumulating with age. It should however be noted that studies indicate that the efficiency of NHEJ repair does decrease with age [147-149]. As mentioned previously, double stranded breaks have been shown to be physiologically generated by topoisomerase II in order to regulate the expression of neuronal early response genes required for synaptic plasticity and learning in hippocampal pyramidal neurons [207, 208]. This factor may introduce an additional degree of variability into this measure, especially if the mice are exposed to novel environments prior to harvest, that may mask age and senescence-associated differences [208]. Prior research, and my work in the previous chapter, suggests that damage located at telomeres is persistent in neurons. Data from the d'adda di Fagagna lab, has shown that 3 months after whole body irradiation, 40% of remaining DDR foci are located at telomeres [211]. I observed that TAF increase with chronological age, and in prematurely ageing *nfkb1*$^{-/-}$ mice. This was associated with activation of downstream DDR factors such as p21, and the accumulation of senescence associated markers in neurons. A significant reduction in the average number of TAFs in the CA3 could be seen with DQ, along with a similar trend in the CA1. If these breaks are persistent, then this would be consistent with the removal of cells, which is given partial support by a corresponding decrease in the number of cells positive for multiple TAFs. Furthermore, the same decrease was not observed with AP20187 treatment, which may be explained by poor blood-brain barrier penetrance.

It should be noted that number of TAF was considerably lower in this cohort of mice than previously reported in the previous chapter. I believe this could be due to technical reasons related with difference in microscope parameters used during quantification by Patrick Krüger, and for that reason I am in the process of independently repeating these experiments.

The presence of neurons positive for p21 detected by RNA*ISH* could be seen in a large number of cells in the CA3-CA1 pyramidal layer, where there was a trend for decrease in DQ treated animals. However, there was substantial variability and this was not significant. Yet, I did find a significant association with the increased number of p21 mRNA positive cells in the pyramidal layer in CA3-CA1 and decreased performance in the Stone's maze in aged mice. In this analysis I quantified the number of

cells containing at least 1 p21 focus. Future work should be conducted to analyse the number of p21 foci (detected by RNA*ISH*) per cell. This may allow a more sensitive detection of differences between experimental groups. p21 has additional roles, apart from its role in senescence, in suppressing apoptosis [181, 260], single-strand break repair [181] and limited G_0-G_1 re-entry for NHEJ [281]. These may operate at a 'sub-senescence' level and would explain basal levels in neurons. It may take prolonged DDR, such as that from TAFs, or pro-mitotic signalling to induce the senescence-associated aspects of p21 activation.

Decreases in the number of CA3 pyramidal layer cells without HMGB1 in their nucleus were also seen with DQ and AP20187 treatment. HMGB1 translocates out of the nucleus in senescent cells and is considered a senescent marker [121]. It can be released from the cytoplasm into the extra-cellular space where it acts as a pro-inflammatory cytokine [493, 494]. Release of such factors by neurons may promote microglial activation by disrupting the balance 'on' and 'off' signals that control microglial function and activation [529]. Indeed, several of the known 'on' signals are associated with the SASP, including CXCL10/IP-10 and MMP-2 [529], and if senescence-like neurons are secreting these factors it may contribute to microglial priming and activation.

Increased microglial priming and activation with age is an important mediator of cognitive dysfunction [108, 109], and is associated with age-related reductions in long-term potentiation [110]. HMGB1 has a significant role in activating microglia and driving chronic inflammation and degeneration [496, 511] and appears to mediate age-related neuro-inflammatory priming [510, 512]. Lowered HMGB1 release in the brain could desensitise microglia to further activation, and possibly counter any inflammatory positive feedback loops that drive degeneration [510]. It is not yet known if HMGB1 is consistently released from these neurons. While nuclear exclusion appears permanent in senescent cells, it may also that if removing the source of stress in neurons would allow relocation to the nucleus. This would make it difficult to assess if neurons are directly cleared.

It is still possible that these neurons were not cleared directly, and that instead the reduced amount represents a reduced rate of generation from an improved tissue micro-environment. The reductions in p16 mRNA and average TAF suggest that it might be related to clearance. Although the exact kinetics of telomere associated damage repair in neurons damage are still unknown, but Fumagalli et al. observed a significantly elevated level 3 months after whole-body irradiation, suggesting that they are persistent for at least this time [211], while the treatment here was for 2 months. Additionally, the reduction in median for the average number of TAFs was greater than the decrease in non-TAFs in DQ treated animals compared to vehicle treated animals. In DQ treated animals compared to vehicle treated animals, there was a 62% reduction in the median average number of TAFs, there was only a

21% reduction in the median average number of non-TAF yH2A.X. In AP treated animals, this was only a 33% decrease in TAFs, and the same reduction in the number of non-TAF yH2A.X foci as DQ. Again, this would support the idea that DQ is actually more effective at clearing TAF carrying cells, while both AP20187 and DQ are reducing the generation of yH2A.X, possibly by improving the whole-body environment or removing senescent glial cells. Although the yH2A.X from damage may still be masked by the afore mentioned physiological break generation. This would be consistent with the clearance of senescent-like neurons by senolytic treatment.

If these cells are killed by senolytic treatments, then this will likely lead to an effect on microglia, which as the resident phagocytic cell would help clear the debris. This may present some difficulties in the assessment of microglia in these brains. Careful characterisation of the mode of microglial activation is needed, in addition to counts in density. It is quite likely that increased microglial presence, and activation will be observed to deal with cellular debris.

A possible explanation for the differences between DQ and AP20187 is the penetrance of these drugs through the blood-brain barrier (BBB). AP20187 has been long used to activate fusion proteins with F36V mutant FKBP domains, and there is existing literature on its BBB penetrance. Currently, there is mixed evidence on the BBB penetrance of AP20187. To my knowledge, there is one paper that suggests AP20187 can penetrate the blood-brain barrier [530], and 5 papers that suggest it cannot [531-535]. This could explain the lack of significant effects in INK-ATTAC treated mice on senescent-like neuron number. In contrast, both compounds in DQ appear to have effective penetration in the brain. Dasatinib effectively crosses the blood brain barrier and has been used clinically for the treatment of CNS leukæmia [536]. Orally administered Quercetin also appears to be effective in penetrating the blood-brain barrier [537].

However, other factors may affect our interpretation of the results- particularly when using aged mice. C57Bl/6 mice show increasing BBB dysfunction with age [538, 539]. By 24 months chronologically aged mice show increased capillary permeability and a decline in BBB tight junction protein expression [538, 539] and increased junction breaks compared to young control mice [539]. Furthermore, cellular senescence in vascular appears to contribute to this loss of integrity in progeroid mice [540]. It is not clear if AP20187 would have increased penetrance in the event of a compromised BBB, but if it does, then differing rates of BBB integrity would affect clearance and increase heterogeneity of the results. The effect of senolytic treatment on BBB senescence and integrity are not yet known, but warrants further investigation.

Interestingly, imatinib (a close relative of Dasatinib) treatment has shown effectiveness in preserving BBB integrity following subarachnoid hæmorrhage, with a decreased permeability and decreased production of metalloproteinases [541]. Quercetin has also been linked to protection of endothelial cells in the microvasculature of the brain from AB fibrils, increasing cell viability, decreasing ROS production and improving BBB integrity [542]. This suggests that DQ therapy may improve BBB health, potentially through senolytic effects, which could improve the brain microenvironment. However, this requires further work. Staining for markers of neurovasculature, such as the scaffold protein zonula occludens-1, and looking for breaks [539] would provide some post-mortem evidence. Additionally, tracking blood and oxygen flow with neuroimaging before and following senolytic treatment could provide evidence of changes in neurovasculature and blood flow that would aid cognitive function.

Indeed, it is difficult to say if the improvements in cognitive function are directly related to the clearance of senescence-like neurons, or through the elimination of senescence in other brain cells, and the whole body. In the previous chapter I showed that they can be seen to increase in areas vulnerable to age-associated declines, and a change in cognitive function could be observed with spatial memory and in the generation of gamma oscillations. However, the brain is incredibly complex and there are no doubt a large number of contributing processes. Investigating if there are alterations in gamma oscillations in ageing mice and in models with known deficits, after senolytic treatment, would provide additional evidence of improvements in hippocampal function.

It should also be noted that neurons are not the only population of cells within the brain that undergo senescence [347]. Despite the lack of a DNA damage response in terminally differentiated astrocytes [507], cultured astrocytes display a number of senescence associated features *in vitro* after H_2O_2, including p16 and p21 expression, altered morphology, Sen-β-Gal expression, and release of SASP factors after both H_2O_2 and irradiation [543, 544].

Senescence in microglia may also play a role in the process [347]. With age, there appear to be reductions in microglia's ability to respond appropriately and a resistance to regulation [109]. Dystrophic microglia morphology has been observed, with deramification and fragmentation of processes, and has been suggested as a sign of microglial cell senescence [545]. Both X-ray irradiation (a known inducer of senescence) and ageing have been shown to induce similar changes in the transcriptome of murine microglia [546]. When microglia are isolated from mouse brains 1 month after 10Gy cranial irradiation, they showed the upregulation of M1 macrophage-associated genes, as might be expected from activated inflammatory microglia. However, the expression of extra-cellular matrix factors, such as matrix metallo-proteinases, and fibrosis associated pathways was also observed [546]. These were not previously associated with M1 or M2 activation, and re-analysis of

transcriptomes of microglia from aged mice showed that these genes were highly enriched [546]. These are factors associated with cellular senescence and the SASP [86, 121], and this suggests the possibility of DNA damage and ageing induced microglial senescence contributing towards inflammation.

However, these changes may also reflect increased microglial priming with age [109]. Both aged, and accelerated ageing, models of mice show increased priming of microglia with age [109, 424] and many of age-associated changes in microglia gene expression overlap with those for primed microglia [547]. Additionally, in 5XFAD Alzheimer model mice, while some p16 expression can be seen in astrocytes, there was none in observed in microglia, with the strongest changes in neurons [527]. We have not yet characterised changes in senescence markers in astrocytes, or microglia in ageing mice, and with senolytic treatment.

AP20187 treated mice, also showed improvements in the number of errors, despite the weaker evidence of senescent-like neuron clearance, and issues with blood brain barrier penetrance of the compound. Senolytic treatment should counter ageing, and partially rejuvenate the whole body [124]. A reduction in age-associated systemic factors in the blood and choroid plexus (together with any changes in BBB integrity with senolytic treatment) could lead to improvements in the brain, through modulation of factors such as neurogenesis and decreased systemic inflammation. Work done by Tony Wyss-Corey's lab suggest that circulating factors in aged mice can have a significant effect on brain function in ageing [412, 548, 549]. The addition of plasma from young mice into aged mice improved synaptic plasticity, neurogenesis and performance in the radial arm water maze [412, 548]. Senolytic drugs may also improve neurogenesis, as p16 knockout mice show increased signs of neurogenesis in the olfactory bulb and subventricular zone, and proliferation of isolated progenitor cells [550]. While no differences were seen in p21 or p16 mRNA positive cells in the granule layer of the DG, neurogenesis in the DG, olfactory bulb, and subventricular zone, has not yet been investigated yet in these mice.

However, the improvements observed with young blood appear to be primarily mediated through the improvements in synaptic plasticity via activation of cyclic AMP response element binding protein, rather than neurogenesis [548, 549], with the addition of TIMP2 from human umbilical cord giving similar results for synaptic plasticity and spatial memory, without modulation of neurogenesis [549]. Further work could focus on testing plasma concentrations of such factors, and seeing if similar changes in gene expression are observed.

Plasma inflammatory cytokine array data by Mikołaj Ogrodnik from our lab (not shown here), however, has suggested only a mild improvement in the circulating environment, at least in terms of inflammatory factors, following clearance of senescent cells by AP20187 and DQ. Further, the improvements in AP20187 treated mice were mild, and when normalised to baseline appear to show that they come from prevention of further age-related decline, rather than an improvement in cognition. In contrast, DQ treated mice show an approximate 40% improvement in their performance after treatment compared to base-line. Which could suggest that clearance of senescent cells in the brain has an additional positive effect on cognition.

Together, these data suggest that senescent-like neurons can be cleared by pharmacological treatment. This treatment and the clearance of senescent-like neurons does not appear to be detrimental for cognitive function at this age point. Indeed, there was prevention of further age-related decline and even improved performance in cognitive function. This provides evidence against the hypothesis that clearance of senescent neurons would be detrimental for ageing mice due to the loss of neurons. The data provides evidence that the prevention of further decline, and improvements in cognition, may be the result of elimination of senescent cells in both the brain and in other regions of the body.

5.0 – Conclusions

Work in this thesis addresses important questions regarding senescent-like neurons in ageing, and their impact on cognition, in prematurely and naturally aged mice. The definition of senescence was originally limited to proliferation competent cell types. However, recent data indicates that phenotypes characteristic of senescent cells, such as telomere dysfunction and expression of cyclin dependent kinase inhibitors can also be present in post-mitotic cells. The relevance of this phenotype for the ageing process is still not understood. The introduction of this thesis highlights existing literature which may be applied to the understanding of a senescent-like phenotype in neurons; including the role of DNA damage, cell-cycle re-activation and progression in neurons, as well as the use of therapies specifically targeting senescent cells and its by-products.

In neurons, re-entry into the cell-cycle from G_0 to G_1 has been implicated in activating DNA repair machinery; however, unless restrained, further progression can lead to the apoptotic death of the neuron. Despite the 'post-mitotic' name, neurons require a functional and active cell-cycle control network. There is evidence of this re-activation and arrest through the cell-cycle inhibitors p21 and p16, both key proteins in senescence induction, in ageing and neurodegenerative diseases such as Alzheimer's. These neurons appear to be survive for long-periods following cell-cycle re-entry and arrest, which is consistent with senescence induction. Furthermore, phenotypic changes and inflammatory signalling may represent a neuronal mimic of the changes seen in senescence in mitotic cells, like the associated secretory phenotype.

Yet, little is known directly about the relationship between senescent-like neurons, and neuro-inflammation or cognitive dysfunction. In this thesis, I presented evidence of increasing age-associated neuro-inflammation and microglial proliferation in *nfkb1*$^{-/-}$ mice compared to age-matched wild-types. I showed deficits in spatial memory and discrimination of *nfkb1*$^{-/-}$ mice, compared to the wild-type, as assessed by the Y-maze. In these mice, first long-term spatial memory declined by 7 months, then both short- and long-term memory were affected by 18 months, as assessed by the Barnes Maze. This expands on previously observed alterations in learning in younger *nfkb1*$^{-/-}$ mice; however, these have previously only discussed the model in relation to intrinsic effects of p50 and NF-κB signalling, and not ageing or inflammation.

Partial amelioration of neuro-inflammatory and cognitive deficits with dietary ibuprofen treatment suggest that a NF-κB-COX-2 mediated pathway is important in regulating these effects. Previously, in mitotic tissues of *nfkb1*$^{-/-}$ mice, this pathway was shown by our lab to promote telomere dysfunction

and senescence through the generation of ROS. I found a similar accumulation of telomere associated damage in neurons with age, both in wild-type mice, and with increased levels in *nfkb1*$^{-/-}$ mice. Further, I show that damage is preferentially located in longer telomeres, suggesting that it is not uncapping of short-telomeres that is driving the activation of a DDR, but instead accumulation of damage. Telomere damage was associated with increased p21 and senescence-associated markers. I propose that increased persistent DDR signalling results in the induction of downstream DDR signalling pathways such as p21, mediating the onset of senescence-associated features. This is can be seen in mitotic cells, and in neurons may potentially be a by-product an anti-apoptotic cell-cycle arrest.

Increased levels of telomeric damage could be observed in CA3 of the hippocampus in *nfkb1*$^{-/-}$ mice, compared to CA1 levels and wild-type mice. This is accompanied by increased proliferation and hypertrophy of microglia. A deficit in the generation of Carbachol-induced gamma frequency oscillations in the CA3 was also observed. These oscillations couple the firing of CA1 to CA3 during memory tasks, and a decrease in propagation and coherence between these two areas could be seen in *nfkb1*$^{-/-}$ mice. Dysfunction in this area may explain some of the observed deficits in spatial memory tasks. It is possible that the induction of the DDR and senescence-associated pathways may drive the phenotypic changes that can be seen in this area, such as morphological changes and the loss of parvalbumin expression in interneurons. This could affect their firing and account for the observed deficits. Additionally, release of pro-inflammatory factors, such as HMGB1, may account for the increased proliferation and priming of microglia. However, this data is mostly associative and does not establish a cause-effect relationship.

Targeting and clearing senescent cells is a promising avenue in preventing and treating age-related pathologies, but it is not known if these treatments clear senescent-like neurons. My work provides novel evidence that pharmacological treatment with Dasatinib and Quercetin can clear senescent-like neurons. Reductions in telomere dysfunction, p16 positive cells and HMGB1 translocation have been observed. This is associated with improvements in cognitive function, as assessed by the Stone T-Maze. Using INK-ATTAC mice, clearance of senescent cells was not effective in the brain and this may be due to low efficiency of the drug AP20187 in penetrating the blood-brain barrier.

Together, my data supports the role of senescent-like neurons in neuro-inflammation and age-related cognitive deficits. Additionally it suggests that removal of senescent cells may be an option for countering cognitive decline.

6.0 - References

[1] Grady CL, Craik FI (2000) Changes in memory processing with age. *Curr Opin Neurobiol* **10**, 224-231.

[2] Harada CN, Natelson Love MC, Triebel K (2013) Normal Cognitive Aging. *Clin Geriatr Med* **29**, 737-752.

[3] Hof PR, Morrison JH (2004) The aging brain: morphomolecular senescence of cortical circuits. *Trends Neurosci* **27**, 607-613.

[4] Salthouse TA (2010) Selective review of cognitive aging. *J Int Neuropsychol Soc* **16**, 754-760.

[5] Elobeid A, Libard S, Leino M, Popova SN, Alafuzoff I (2016) Altered Proteins in the Aging Brain. *J Neuropathol Exp Neurol* **75**, 316-325.

[6] Kawas CH, Kim RC, Sonnen JA, Bullain SS, Trieu T, Corrada MM (2015) Multiple pathologies are common and related to dementia in the oldest-old: The 90+ Study. *Neurology* **85**, 535-542.

[7] Raz N, Rodrigue KM, Head D, Kennedy KM, Acker JD (2004) Differential aging of the medial temporal lobe: a study of a five-year change. *Neurology* **62**, 433-438.

[8] Sowell ER, Peterson BS, Thompson PM, Welcome SE, Henkenius AL, Toga AW (2003) Mapping cortical change across the human life span. *Nat Neurosci* **6**, 309-315.

[9] Carroll JB, Lerch JP, Franciosi S, Spreeuw A, Bissada N, Henkelman RM, Hayden MR (2011) Natural history of disease in the YAC128 mouse reveals a discrete signature of pathology in Huntington disease. *Neurobiol Dis* **43**, 257-265.

[10] Kaup AR, Mirzakhanian H, Jeste DV, Eyler LT (2011) A Review of the Brain Structure Correlates of Successful Cognitive Aging. *The Journal of neuropsychiatry and clinical neurosciences* **23**, 6-15.

[11] Taylor AM, Groom A, Byrd PJ (2004) Ataxia-telangiectasia-like disorder (ATLD)-its clinical presentation and molecular basis. *DNA Repair (Amst)* **3**, 1219-1225.

[12] Coleman PD, Flood DG (1987) Neuron numbers and dendritic extent in normal aging and Alzheimer's disease. *Neurobiol Aging* **8**, 521-545.

[13] West MJ, Coleman PD, Flood DG, Troncoso JC (1994) Differences in the pattern of hippocampal neuronal loss in normal ageing and Alzheimer's disease. *Lancet* **344**, 769-772.

[14] Freeman SH, Kandel R, Cruz L, Rozkalne A, Newell K, Frosch MP, Hedley-Whyte ET, Locascio JJ, Lipsitz L, Hyman BT (2008) Preservation of Neuronal Number Despite Age-Related Cortical Brain Atrophy In Elderly Subjects Without Alzheimer Disease. *J Neuropathol Exp Neurol* **67**, 1205-1212.

[15] Curcio CA, Coleman PD (1982) Stability of neuron number in cortical barrels of aging mice. *Journal of Comparative Neurology* **212**, 158-172.

[16] Sturrock RR (1992) Stability of neuron number in the ageing mouse paraventricular nucleus. *Ann Anat* **174**, 337-340.

[17] Lessard-Beaudoin M, Laroche M, Demers MJ, Grenier G, Graham RK (2015) Characterization of age-associated changes in peripheral organ and brain region weights in C57BL/6 mice. *Exp Gerontol* **63**, 27-34.

[18] Morrison JH, Hof PR (1997) Life and death of neurons in the aging brain. *Science* **278**, 412-419.

[19] Burke SN, Barnes CA (2006) Neural plasticity in the ageing brain. *Nat Rev Neurosci* **7**, 30-40.

[20] Pannese E (2011) Morphological changes in nerve cells during normal aging. *Brain Struct Funct* **216**, 85-89.

[21] Dickstein DL, Kabaso D, Rocher AB, Luebke JI, Wearne SL, Hof PR (2007) Changes in the structural complexity of the aged brain. *Aging Cell* **6**, 275-284.

[22] Scheibel AB (1979) The hippocampus: Organizational patterns in health and senescence. *Mech Ageing Dev* **9**, 89-102.

[23] Burke SN, Barnes CA (2006) Neural plasticity in the ageing brain. *Nat Rev Neurosci* **7**.

[24] Flood DG, Buell SJ, Defiore CH, Horwitz GJ, Coleman PD (1985) Age-related dendritic growth in dentate gyrus of human brain is followed by regression in the 'oldest old'. *Brain Res* **345**, 366-368.
[25] Flood DG (1993) Critical issues in the analysis of dendritic extent in aging humans, primates, and rodents. *Neurobiol Aging* **14**, 649-654.
[26] von Bohlen und Halbach O, Zacher C, Gass P, Unsicker K (2006) Age-related alterations in hippocampal spines and deficiencies in spatial memory in mice. *J Neurosci Res* **83**, 525-531.
[27] Gazzaley AH, Thakker MM, Hof PR, Morrison JH (1997) Preserved number of entorhinal cortex layer II neurons in aged macaque monkeys. *Neurobiology of aging* **18**, 549-553.
[28] Hof PR, Duan H, Page TL, Einstein M, Wicinski B, He Y, Erwin JM, Morrison JH (2002) Age-related changes in GluR2 and NMDAR1 glutamate receptor subunit protein immunoreactivity in corticocortically projecting neurons in macaque and patas monkeys. *Brain research* **928**, 175-186.
[29] Terry RD, Katzman R (2001) Life span and synapses: will there be a primary senile dementia? *Neurobiol Aging* **22**, 347-348.
[30] Shimada A, Tsuzuki M, Keino H, Satoh M, Chiba Y, Saitoh Y, Hosokawa M (2006) Apical vulnerability to dendritic retraction in prefrontal neurones of ageing SAMP10 mouse: a model of cerebral degeneration. *Neuropathol Appl Neurobiol* **32**, 1-14.
[31] Calhoun ME, Kurth D, Phinney AL, Long JM, Hengemihle J, Mouton PR, Ingram DK, Jucker M (1998) Hippocampal neuron and synaptophysin-positive bouton number in aging C57BL/6 mice. *Neurobiol Aging* **19**, 599-606.
[32] VanGuilder HD, Farley JA, Yan H, Van Kirk CA, Mitschelen M, Sonntag WE, Freeman WM (2011) Hippocampal dysregulation of synaptic plasticity-associated proteins with age-related cognitive decline. *Neurobiol Dis* **43**, 201-212.
[33] Norris CM, Korol DL, Foster TC (1996) Increased susceptibility to induction of long-term depression and long-term potentiation reversal during aging. *J Neurosci* **16**, 5382-5392.
[34] Tombaugh GC, Rowe WB, Chow AR, Michael TH, Rose GM (2002) Theta-frequency synaptic potentiation in CA1 in vitro distinguishes cognitively impaired from unimpaired aged Fischer 344 rats. *J Neurosci* **22**, 9932-9940.
[35] Barnes CA (1979) Memory deficits associated with senescence: a neurophysiological and behavioral study in the rat. *J Comp Physiol Psychol* **93**.
[36] Barnes CA (1979) Memory deficits associated with senescence: a neurophysiological and behavioral study in the rat. *J Comp Physiol Psychol* **93**, 74-104.
[37] Gant JC, Thibault O (2009) Action potential throughput in aged rat hippocampal neurons: regulation by selective forms of hyperpolarization. *Neurobiol Aging* **30**, 2053-2064.
[38] Lu CB, Hamilton JB, Powell AD, Toescu EC, Vreugdenhil M (2011) Effect of ageing on CA3 interneuron sAHP and gamma oscillations is activity-dependent. *Neurobiol Aging* **32**, 956-965.
[39] Wilson IA, Ikonen S, Gallagher M, Eichenbaum H, Tanila H (2005) Age-Associated Alterations of Hippocampal Place Cells Are Subregion Specific. *J Neurosci* **25**, 6877.
[40] Aranzio JC (1587) *De humano foetu liber*, ex officinâ Felicis de Haro.
[41] Spellman T, Rigotti M, Ahmari SE, Fusi S, Gogos JA, Gordon JA (2015) Hippocampal-prefrontal input supports spatial encoding in working memory. *Nature* **522**, 309-314.
[42] Burgess N, Maguire EA, O'Keefe J (2002) The Human Hippocampus and Spatial and Episodic Memory. *Neuron* **35**, 625-641.
[43] Small SA, Schobel SA, Buxton RB, Witter MP, Barnes CA (2011) A pathophysiological framework of hippocampal dysfunction in ageing and disease. *Nat Rev Neurosci* **12**, 585-601.
[44] Dudek SM, Alexander GM, Farris S (2016) Rediscovering area CA2: unique properties and functions. *Nat Rev Neurosci* **17**, 89-102.
[45] Caruana DA, Alexander GM, Dudek SM (2012) New insights into the regulation of synaptic plasticity from an unexpected place: hippocampal area CA2. *Learn Mem* **19**, 391-400.

[46] Ellen P, Deloache J (1968) Hippocampal lesions and spontaneous alternation behavior in the rat. *Physiol Behav* **3**, 857-860.
[47] Roberts WW, Dember WN, Brodwick M (1962) Alternation and exploration in rats with hippocampal lesions. *J Comp Physiol Psychol* **55**, 695-700.
[48] Eichenbaum H, Cohen Neal J (2014) Can We Reconcile the Declarative Memory and Spatial Navigation Views on Hippocampal Function? *Neuron* **83**, 764-770.
[49] O'Keefe J, Nadel L (1978) *The hippocampus as a cognitive map*, Oxford: Clarendon Press.
[50] Moser EI, Kropff E, Moser MB (2008) Place cells, grid cells, and the brain's spatial representation system. *Annu Rev Neurosci* **31**, 69-89.
[51] Vazdarjanova A, Guzowski JF (2004) Differences in hippocampal neuronal population responses to modifications of an environmental context: evidence for distinct, yet complementary, functions of CA3 and CA1 ensembles. *J Neurosci* **24**, 6489-6496.
[52] Montgomery SM, Buzsáki G (2007) Gamma oscillations dynamically couple hippocampal CA3 and CA1 regions during memory task performance. *Proc Natl Acad Sci U S A* **104**, 14495-14500.
[53] Mann EO, Mody I (2010) Control of hippocampal gamma oscillation frequency by tonic inhibition and excitation of interneurons. *Nat Neurosci* **13**, 205-212.
[54] Nakazawa K, Sun LD, Quirk MC, Rondi-Reig L, Wilson MA, Tonegawa S (2003) Hippocampal CA3 NMDA receptors are crucial for memory acquisition of one-time experience. *Neuron* **38**, 305-315.
[55] Leutgeb JK, Leutgeb S, Moser MB, Moser EI (2007) Pattern separation in the dentate gyrus and CA3 of the hippocampus. *Science* **315**, 961-966.
[56] Cerasti E, Treves A (2013) The spatial representations acquired in CA3 by self-organizing recurrent connections. *Front Cell Neurosci* **7**, 112.
[57] Kesner RP (2013) A process analysis of the CA3 subregion of the hippocampus. *Front Cell Neurosci* **7**, 78.
[58] Rapp PR, Gallagher M (1996) Preserved neuron number in the hippocampus of aged rats with spatial learning deficits. *Proc Natl Acad Sci U S A* **93**, 9926-9930.
[59] Rasmussen T, Schliemann T, Sorensen JC, Zimmer J, West MJ (1996) Memory impaired aged rats: no loss of principal hippocampal and subicular neurons. *Neurobiol Aging* **17**, 143-147.
[60] Bach ME, Barad M, Son H, Zhuo M, Lu YF, Shih R, Mansuy I, Hawkins RD, Kandel ER (1999) Age-related defects in spatial memory are correlated with defects in the late phase of hippocampal long-term potentiation in vitro and are attenuated by drugs that enhance the cAMP signaling pathway. *Proc Natl Acad Sci U S A* **96**, 5280-5285.
[61] Lister JP, Barnes CA (2009) NEurobiological changes in the hippocampus during normative aging. *Archives of Neurology* **66**, 829-833.
[62] Newman MC, Kaszniak AW (2000) Spatial memory and aging: performance on a human analog of the Morris water maze. *Aging, Neuropsychology, and Cognition* **7**, 86-93.
[63] Mueller SG, Schuff N, Yaffe K, Madison C, Miller B, Weiner MW (2010) Hippocampal atrophy patterns in mild cognitive impairment and Alzheimer's disease. *Hum Brain Mapp* **31**, 1339-1347.
[64] Mueller SG, Weiner MW (2009) Selective effect of age, Apo e4, and Alzheimer's disease on hippocampal subfields. *Hippocampus* **19**, 558-564.
[65] Small SA, Chawla MK, Buonocore M, Rapp PR, Barnes CA (2004) Imaging correlates of brain function in monkeys and rats isolates a hippocampal subregion differentially vulnerable to aging. *Proc Natl Acad Sci U S A* **101**, 7181-7186.
[66] Thibault O, Hadley R, Landfield PW (2001) Elevated postsynaptic [Ca2+]i and L-type calcium channel activity in aged hippocampal neurons: relationship to impaired synaptic plasticity. *J Neurosci* **21**, 9744-9756.

[67] Kumar A, Thinschmidt JS, Foster TC, King MA (2007) Aging effects on the limits and stability of long-term synaptic potentiation and depression in rat hippocampal area CA1. *J Neurophysiol* **98**, 594-601.
[68] Simkin D, Hattori S, Ybarra N, Musial TF, Buss EW, Richter H, Oh MM, Nicholson DA, Disterhoft JF (2015) Aging-Related Hyperexcitability in CA3 Pyramidal Neurons Is Mediated by Enhanced A-Type K(+) Channel Function and Expression. *J Neurosci* **35**, 13206-13218.
[69] Yassa MA, Lacy JW, Stark SM, Albert MS, Gallagher M, Stark CE (2011) Pattern separation deficits associated with increased hippocampal CA3 and dentate gyrus activity in nondemented older adults. *Hippocampus* **21**, 968-979.
[70] Dickerson BC, Salat DH, Greve DN, Chua EF, Rand-Giovannetti E, Rentz DM, Bertram L, Mullin K, Tanzi RE, Blacker D, Albert MS, Sperling RA (2005) Increased hippocampal activation in mild cognitive impairment compared to normal aging and AD. *Neurology* **65**, 404-411.
[71] Bakker A, Krauss GL, Albert MS, Speck CL, Jones LR, Stark CE, Yassa MA, Bassett SS, Shelton AL, Gallagher M (2012) Reduction of hippocampal hyperactivity improves cognition in amnestic mild cognitive impairment. *Neuron* **74**, 467-474.
[72] Apps R, Garwicz M (2005) Anatomical and physiological foundations of cerebellar information processing. *Nat Rev Neurosci* **6**, 297-311.
[73] Martin LA, Escher T, Goldowitz D, Mittleman G (2004) A relationship between cerebellar Purkinje cells and spatial working memory demonstrated in a lurcher/chimera mouse model system. *Genes, Brain and Behav* **3**, 158-166.
[74] Hilber P, Caston J (2001) Motor skills and motor learning in Lurcher mutant mice during aging. *Neuroscience* **102**, 615-623.
[75] Yoon CH (1972) Developmental mechanism for changes in cerebellum of "staggerer" mouse, a neurological mutant of genetic origin. *Neurology* **22**, 743-754.
[76] Andersen BB, Gundersen HJ, Pakkenberg B (2003) Aging of the human cerebellum: a stereological study. *J Comp Neurol* **466**, 356-365.
[77] Zhang C, Zhu Q, Hua T (2010) Aging of cerebellar Purkinje cells. *Cell Tissue Res* **341**, 341-347.
[78] Woodruff-Pak DS (2006) Stereological estimation of Purkinje neuron number in C57BL/6 mice and its relation to associative learning. *Neuroscience* **141**, 233-243.
[79] Ogata R, Ikari K, Hayashi M, Tamai K, Tagawa K (1984) Age-related changes in the Purkinje's cells in the rat cerebellar cortex: a quantitative electron microscopic study. *Folia Psychiatr Neurol Jpn* **38**, 159-167.
[80] Glick R, Bondareff W (1979) Loss of synapses in the cerebellar cortex of the senescent rat. *J Gerontol* **34**, 818-822.
[81] Rogers J, Zornetzer SF, Bloom FE (1981) Senescent pathology of cerebellum: Purkinje neurons and their parallel fiber afferents. *Neurobiol Aging* **2**, 15-25.
[82] Woodruff-Pak DS, Foy MR, Akopian GG, Lee KH, Zach J, Nguyen KPT, Comalli DM, Kennard JA, Agelan A, Thompson RF (2010) Differential effects and rates of normal aging in cerebellum and hippocampus. *Proceedings of the National Academy of Sciences of the United States of America* **107**, 1624-1629.
[83] Weiskopf D, Weinberger B, Grubeck-Loebenstein B (2009) The aging of the immune system. *Transpl Int* **22**, 1041-1050.
[84] Franceschi C, Bonafe M, Valensin S, Olivieri F, De Luca M, Ottaviani E, De Benedictis G (2000) Inflamm-aging. An evolutionary perspective on immunosenescence. *Ann N Y Acad Sci* **908**, 244-254.
[85] Lasry A, Ben-Neriah Y (2015) Senescence-associated inflammatory responses: aging and cancer perspectives. *Trends Immunol* **36**, 217-228.
[86] Rodier F, Campisi J (2011) Four faces of cellular senescence. *J Cell Biol* **192**, 547-556.
[87] Barrientos RM, Kitt MM, Watkins LR, Maier SF (2015) Neuroinflammation in the normal aging hippocampus. *Neuroscience* **309**, 84-99.

[88] Weaver JD, Huang MH, Albert M, Harris T, Rowe JW, Seeman TE (2002) Interleukin-6 and risk of cognitive decline: MacArthur studies of successful aging. *Neurology* **59**, 371-378.
[89] Zhang G, Li J, Purkayastha S, Tang Y, Zhang H, Yin Y, Li B, Liu G, Cai D (2013) Hypothalamic programming of systemic ageing involving IKK-β, NF-κB and GnRH. *Nature* **497**, 211-216.
[90] Wrona D (2006) Neural-immune interactions: an integrative view of the bidirectional relationship between the brain and immune systems. *J Neuroimmunol* **172**, 38-58.
[91] Lee CK, Weindruch R, Prolla TA (2000) Gene-expression profile of the ageing brain in mice. *Nat Genet* **25**, 294-297.
[92] Hein AM, Stasko MR, Matousek SB, Scott-McKean JJ, Maier SF, Olschowka JA, Costa ACS, O'Banion MK (2010) Sustained hippocampal IL-1β overexpression impairs contextual and spatial memory in transgenic mice. *Brain, Behav, Immun* **24**, 243.
[93] Chen J, Buchanan JB, Sparkman NL, Godbout JP, Freund GG, Johnson RW (2008) Neuroinflammation and disruption in working memory in aged mice after acute stimulation of the peripheral innate immune system. *Brain, Behav, Immun* **22**, 301-311.
[94] Craft S, Foster TC, Landfield PW, Maier SF, Resnick SM, Yaffe K (2012) Session III: Mechanisms of age-related cognitive change and targets for intervention: inflammatory, oxidative, and metabolic processes. *J Gerontol A Biol Sci Med Sci* **67**, 754-759.
[95] Xie G, Zhang W, Chang Y, Chu Q (2009) Relationship between perioperative inflammatory response and postoperative cognitive dysfunction in the elderly. *Med Hypotheses* **73**, 402-403.
[96] Moller JT, Cluitmans P, Rasmussen LS, Houx P, Rasmussen H, Canet J, Rabbitt P, Jolles J, Larsen K, Hanning CD, Langeron O, Johnson T, Lauven PM, Kristensen PA, Biedler A, van Beem H, Fraidakis O, Silverstein JH, Beneken JEW, Gravenstein JS (1998) Long-term postoperative cognitive dysfunction in the elderly: ISPOCD1 study. *The Lancet* **351**, 857-861.
[97] Barrientos RM, Higgins EA, Biedenkapp JC, Sprunger DB, Wright-Hardesty KJ, Watkins LR, Rudy JW, Maier SF (2006) Peripheral infection and aging interact to impair hippocampal memory consolidation. *Neurobiol Aging* **27**, 723-732.
[98] Cao XZ, Ma H, Wang JK, Liu F, Wu BY, Tian AY, Wang LL, Tan WF (2010) Postoperative cognitive deficits and neuroinflammation in the hippocampus triggered by surgical trauma are exacerbated in aged rats. *Prog Neuropsychopharmacol Biol Psychiatry* **34**, 1426-1432.
[99] Bonow RH, Aid S, Zhang Y, Becker KG, Bosetti F (2009) The brain expression of genes involved in inflammatory response, the ribosome, and learning and memory is altered by centrally injected lipopolysaccharide in mice. *Pharmacogenomics J* **9**, 116-126.
[100] Monje ML, Toda H, Palmer TD (2003) Inflammatory blockade restores adult hippocampal neurogenesis. *Science* **302**, 1760-1765.
[101] Motoki K, Kishi H, Hori E, Tajiri K, Nishijo H, Muraguchi A (2009) The direct excitatory effect of IL-1beta on cerebellar Purkinje cell. *Biochem Biophys Res Commun* **379**, 665-668.
[102] Min SS, Quan HY, Ma J, Han JS, Jeon BH, Seol GH (2009) Chronic brain inflammation impairs two forms of long-term potentiation in the rat hippocampal CA1 area. *Neurosci Lett* **456**, 20-24.
[103] Ransohoff RM, Perry VH (2009) Microglial physiology: unique stimuli, specialized responses. *Annu Rev Immunol* **27**, 119-145.
[104] Sierra A, Gottfried-Blackmore AC, McEwen BS, Bulloch K (2007) Microglia derived from aging mice exhibit an altered inflammatory profile. *Glia* **55**, 412-424.
[105] Boche D, Perry VH, Nicoll JA (2013) Review: activation patterns of microglia and their identification in the human brain. *Neuropathol Appl Neurobiol* **39**, 3-18.
[106] Long JM, Kalehua AN, Muth NJ, Calhoun ME, Jucker M, Hengemihle JM, Ingram DK, Mouton PR (1998) Stereological analysis of astrocyte and microglia in aging mouse hippocampus. *Neurobiol Aging* **19**, 497-503.
[107] Mouton PR, Long JM, Lei D-L, Howard V, Jucker M, Calhoun ME, Ingram DK (2002) Age and gender effects on microglia and astrocyte numbers in brains of mice. *Brain Res* **956**, 30-35.

[108] Ye SM, Johnson RW (1999) Increased interleukin-6 expression by microglia from brain of aged mice. *J Neuroimmunol* **93**, 139-148.
[109] Norden DM, Godbout JP (2013) Review: Microglia of the aged brain: primed to be activated and resistant to regulation. *Neuropathol Appl Neurobiol* **39**, 19-34.
[110] Griffin R, Nally R, Nolan Y, McCartney Y, Linden J, Lynch MA (2006) The age-related attenuation in long-term potentiation is associated with microglial activation. *J Neurochem* **99**, 1263-1272.
[111] Campisi J, di Fagagna FdA (2007) Cellular senescence: when bad things happen to good cells. *Nat Rev Mol Cell Biol* **8**, 729-740.
[112] Jurk D, Wang C, Miwa S, Maddick M, Korolchuk V, Tsolou A, Gonos ES, Thrasivoulou C, Jill Saffrey M, Cameron K (2012) Postmitotic neurons develop a p21-dependent senescence-like phenotype driven by a DNA damage response. *Aging Cell* **11**, 996-1004.
[113] Williams GC (1957) Pleiotropy, natural selection, and the evolution of senescence. *Evolution* **11**, 398-411.
[114] Hayflick L (1965) The limited in vitro lifetime of human diploid cell strains. *Exp Cell Res* **37**, 614-636.
[115] Shelton DN, Chang E, Whittier PS, Choi D, Funk WD (1999) Microarray analysis of replicative senescence. *Curr Biol* **9**, 939-945.
[116] Jackson JG, Pereira-Smith OM (2006) p53 is preferentially recruited to the promoters of growth arrest genes p21 and GADD45 during replicative senescence of normal human fibroblasts. *Cancer Res* **66**, 8356-8360.
[117] Campisi J (2001) Cellular senescence as a tumor-suppressor mechanism. *Trends Cell Biol* **11**, S27-31.
[118] Munoz-Espin D, Serrano M (2014) Cellular senescence: from physiology to pathology. *Nat Rev Mol Cell Biol* **15**, 482-496.
[119] Rodier F, Coppé J-P, Patil CK, Hoeijmakers WAM, Muñoz DP, Raza SR, Freund A, Campeau E, Davalos AR, Campisi J (2009) Persistent DNA damage signalling triggers senescence-associated inflammatory cytokine secretion. *Nat Cell Biol* **11**, 973-979.
[120] Coppé J-P, Patil CK, Rodier F, Sun Y, Muñoz DP, Goldstein J, Nelson PS, Desprez P-Y, Campisi J (2008) Senescence-associated secretory phenotypes reveal cell-nonautonomous functions of oncogenic RAS and the p53 tumor suppressor. *PLoS Biol* **6**, e301.
[121] Wiley CD, Flynn JM, Morrissey C, Lebofsky R, Shuga J, Dong X, Unger MA, Vijg J, Melov S, Campisi J (2017) Analysis of individual cells identifies cell-to-cell variability following induction of cellular senescence. *Aging Cell*.
[122] Nelson G, Wordsworth J, Wang C, Jurk D, Lawless C, Martin-Ruiz C, von Zglinicki T (2012) A senescent cell bystander effect: senescence-induced senescence. *Aging Cell* **11**, 345-349.
[123] Baker DJ, Wijshake T, Tchkonia T, LeBrasseur NK, Childs BG, van de Sluis B, Kirkland JL, van Deursen JM (2011) Clearance of p16Ink4a-positive senescent cells delays ageing-associated disorders. *Nature* **479**, 232-236.
[124] Baker DJ, Childs BG, Durik M, Wijers ME, Sieben CJ, Zhong J, Saltness RA, Jeganathan KB, Verzosa GC, Pezeshki A (2016) Naturally occurring p16Ink4a-positive cells shorten healthy lifespan. *Nature* **530**, 184-189.
[125] Campisi J (2005) Senescent cells, tumor suppression, and organismal aging: good citizens, bad neighbors. *Cell* **120**, 513-522.
[126] Dimri GP, Lee X, Basile G, Acosta M, Scott G, Roskelley C, Medrano EE, Linskens M, Rubelj I, Pereira-Smith O (1995) A biomarker that identifies senescent human cells in culture and in aging skin in vivo. *Proc Natl Acad Sci U S A* **92**, 9363-9367.
[127] Jurk D, Wilson C, Passos JF, Oakley F, Correia-Melo C, Greaves L, Saretzki G, Fox C, Lawless C, Anderson R (2014) Chronic inflammation induces telomere dysfunction and accelerates ageing in mice. *Nat Commun* **2**, 4172.

[128] Magistretti P, Allaman I (2013) Brain Energy Metabolism In *Neuroscience in the 21st Century*, Pfaff D, ed. Springer New York, pp. 1591-1620.
[129] Katyal S, McKinnon PJ (2008) DNA strand breaks, neurodegeneration and aging in the brain. *Mech Ageing Dev* **129**, 483-491.
[130] Parihar VK, Limoli CL (2013) Cranial irradiation compromises neuronal architecture in the hippocampus. *Proc Natl Acad Sci U S A* **110**, 12822-12827.
[131] Dropcho EJ (2004) Neurotoxicity of cancer chemotherapy. *Semin Neurol* **24**, 419-426.
[132] Langston JW, Forno LS, Tetrud J, Reeves AG, Kaplan JA, Karluk D (1999) Evidence of active nerve cell degeneration in the substantia nigra of humans years after 1-methyl-4-phenyl-1, 2, 3, 6-tetrahydropyridine exposure. *Ann Neurol* **46**, 598-605.
[133] Lu T, Pan Y, Kao S-Y, Li C, Kohane I, Chan J, Yankner BA (2004) Gene regulation and DNA damage in the ageing human brain. *Nature* **429**, 883-891.
[134] Trushina E, McMurray CT (2007) Oxidative stress and mitochondrial dysfunction in neurodegenerative diseases. *Neuroscience* **145**, 1233-1248.
[135] Coppedè F, Migliore L (2009) DNA damage and repair in Alzheimer's disease. *Curr Alzheimer Res* **6**, 36-47.
[136] Kaina B (2003) DNA damage-triggered apoptosis: critical role of DNA repair, double-strand breaks, cell proliferation and signaling. *Biochem Pharmacol* **66**, 1547-1554.
[137] di Fagagna FdA (2008) Living on a break: cellular senescence as a DNA-damage response. *Nat Rev Cancer* **8**, 512-522.
[138] Sedelnikova OA, Horikawa I, Zimonjic DB, Popescu NC, Bonner WM, Barrett JC (2004) Senescing human cells and ageing mice accumulate DNA lesions with unrepairable double-strand breaks. *Nat Cell Biol* **6**, 168-170.
[139] Wang C, Jurk D, Maddick M, Nelson G, Martin-Ruiz C, Von Zglinicki T (2009) DNA damage response and cellular senescence in tissues of aging mice. *Aging Cell* **8**, 311-323.
[140] Ward JF (1988) DNA damage produced by ionizing radiation in mammalian cells: identities, mechanisms of formation, and reparability. *Prog Nucleic Acid Res Mol Biol* **35**, 95-125.
[141] Van Der Schans GP (1978) Gamma-ray induced double-strand breaks in DNA resulting from randomly-inflicted single-strand breaks: temporal local denaturation, a new radiation phenomenon? *Int J Radiat Biol Relat Stud Phys Chem Med* **33**, 105-120.
[142] Woodbine L, Brunton H, Goodarzi AA, Shibata A, Jeggo PA (2011) Endogenously induced DNA double strand breaks arise in heterochromatic DNA regions and require ataxia telangiectasia mutated and Artemis for their repair. *Nucleic Acids Res* **39**, 6986-6997.
[143] Henner WD, Grunberg SM, Haseltine WA (1982) Sites and structure of gamma radiation-induced DNA strand breaks. *J Biol Chem* **257**, 11750-11754.
[144] Rothkamm K, Lobrich M (2003) Evidence for a lack of DNA double-strand break repair in human cells exposed to very low x-ray doses. *Proc Natl Acad Sci U S A* **100**, 5057-5062.
[145] Lieber MR (2010) The mechanism of double-strand DNA break repair by the nonhomologous DNA end-joining pathway. *Annu Rev Biochem* **79**, 181-211.
[146] Lieber MR, Ma Y, Pannicke U, Schwarz K (2003) Mechanism and regulation of human non-homologous DNA end-joining. *Nat Rev Mol Cell Biol* **4**, 712-720.
[147] Rao KS (2007) DNA repair in aging rat neurons. *Neuroscience* **145**, 1330-1340.
[148] Ren K, Ortiz D, Peña S (2002) Non-homologous DNA end joining in the mature rat brain. *J Neurochem* **80**, 949-959.
[149] Goukassian D, Gad F, Yaar M, Eller MS, Nehal US, Gilchrest BA (2000) Mechanisms and implications of the age-associated decrease in DNA repair capacity. *FASEB J* **14**, 1325-1334.
[150] Polo SE, Jackson SP (2011) Dynamics of DNA damage response proteins at DNA breaks: a focus on protein modifications. *Genes Dev* **25**, 409-433.
[151] Mimori T, Hardin JA (1986) Mechanism of interaction between Ku protein and DNA. *J Biol Chem* **261**, 10375-10379.

[152] de Jager M, van Noort J, van Gent DC, Dekker C, Kanaar R, Wyman C (2001) Human Rad50/Mre11 is a flexible complex that can tether DNA ends. *Mol Cell* **8**, 1129-1135.
[153] Mirzoeva OK, Petrini JH (2001) DNA damage-dependent nuclear dynamics of the Mre11 complex. *Mol Cell Biol* **21**, 281-288.
[154] Dupre A, Boyer-Chatenet L, Gautier J (2006) Two-step activation of ATM by DNA and the Mre11-Rad50-Nbs1 complex. *Nat Struct Mol Biol* **13**, 451-457.
[155] Walker JR, Corpina RA, Goldberg J (2001) Structure of the Ku heterodimer bound to DNA and its implications for double-strand break repair. *Nature* **412**, 607-614.
[156] Gottlieb TM, Jackson SP (1993) The DNA-dependent protein kinase: requirement for DNA ends and association with Ku antigen. *Cell* **72**, 131-142.
[157] Jiang W, Crowe JL, Liu X, Nakajima S, Wang Y, Li C, Lee BJ, Dubois RL, Liu C, Yu X (2015) Differential phosphorylation of DNA-PKcs regulates the interplay between end-processing and end-ligation during nonhomologous end-joining. *Mol Cell* **58**, 172-185.
[158] Uziel T, Lerenthal Y, Moyal L, Andegeko Y, Mittelman L, Shiloh Y (2003) Requirement of the MRN complex for ATM activation by DNA damage. *EMBO J* **22**, 5612-5621.
[159] Bakkenist CJ, Kastan MB (2003) DNA damage activates ATM through intermolecular autophosphorylation and dimer dissociation. *Nature* **421**, 499-506.
[160] Girard P-M, Riballo E, Begg AC, Waugh A, Jeggo PA (2002) Nbs1 promotes ATM dependent phosphorylation events including those required for G1/S arrest. *Oncogene* **21**, 4191-4199.
[161] Lavin MF, Kozlov S, Gatei M, Kijas AW (2015) ATM-Dependent Phosphorylation of All Three Members of the MRN Complex: From Sensor to Adaptor. *Biomolecules* **5**, 2877-2902.
[162] Savitsky K, Bar-Shira A, Gilad S, Rotman G, Ziv Y, Vanagaite L, Tagle DA, Smith S, Uziel T, Sfez S, Ashkenazi M, Pecker I, Frydman M, Harnik R, Patanjali SR, Simmons A, Clines GA, Sartiel A, Gatti RA, Chessa L, Sanal O, Lavin MF, Jaspers NG, Taylor AM, Arlett CF, Miki T, Weissman SM, Lovett M, Collins FS, Shiloh Y (1995) A single ataxia telangiectasia gene with a product similar to PI-3 kinase. *Science* **268**, 1749-1753.
[163] Taylor AMR, Byrd PJ (2005) Molecular pathology of ataxia telangiectasia. *J Clin Pathol* **58**, 1009-1015.
[164] Stewart GS, Maser RS, Stankovic T, Bressan DA, Kaplan MI, Jaspers NGJ, Raams A, Byrd PJ, Petrini JHJ, Taylor AMR (1999) The DNA double-strand break repair gene hMRE11 is mutated in individuals with an ataxia-telangiectasia-like disorder. *Cell* **99**, 577-587.
[165] Carney JP, Maser RS, Olivares H, Davis EM, Le Beau M, Yates JR, Hays L, Morgan WF, Petrini JHJ (1998) The hMre11/hRad50 protein complex and Nijmegen breakage syndrome: linkage of double-strand break repair to the cellular DNA damage response. *Cell* **93**, 477-486.
[166] Stiff T, O'Driscoll M, Rief N, Iwabuchi K, Löbrich M, Jeggo PA (2004) ATM and DNA-PK function redundantly to phosphorylate H2AX after exposure to ionizing radiation. *Cancer Res* **64**, 2390-2396.
[167] Burma S, Chen BP, Murphy M, Kurimasa A, Chen DJ (2001) ATM phosphorylates histone H2AX in response to DNA double-strand breaks. *J Biol Chem* **276**, 42462-42467.
[168] Rogakou EP, Pilch DR, Orr AH, Ivanova VS, Bonner WM (1998) DNA double-stranded breaks induce histone H2AX phosphorylation on serine 139. *J Biol Chem* **273**, 5858-5868.
[169] Pina B, Suau P (1987) Changes in histones H2A and H3 variant composition in differentiating and mature rat brain cortical neurons. *Dev Biol* **123**, 51-58.
[170] Xu Y, Sun Y, Jiang X, Ayrapetov MK, Moskwa P, Yang S, Weinstock DM, Price BD (2010) The p400 ATPase regulates nucleosome stability and chromatin ubiquitination during DNA repair. *J Cell Biol* **191**, 31-43.
[171] Kusch T, Florens L, MacDonald WH, Swanson SK, Glaser RL, Yates JR, Abmayr SM, Washburn MP, Workman JL (2004) Acetylation by Tip60 is required for selective histone variant exchange at DNA lesions. *Science* **306**, 2084-2087.
[172] Savic V, Yin B, Maas NL, Bredemeyer AL, Carpenter AC, Helmink BA, Yang-Iott KS, Sleckman BP, Bassing CH (2009) Formation of dynamic γ-H2AX domains along broken DNA strands is

distinctly regulated by ATM and MDC1 and dependent upon H2AX densities in chromatin. *Mol Cell* **34**, 298-310.
[173] Giglia-Mari G, Zotter A, Vermeulen W (2011) DNA damage response. *Cold Spring Harb Perspect Biol* **3**, a000745.
[174] D'Adda Di Fagagna F, Reaper PM, Clay-Farrace L, Fiegler H, Carr P, Von Zglinicki T, Saretzki G, Carter NP, Jackson SP (2003) A DNA damage checkpoint response in telomere-initiated senescence. *Nature* **426**, 194-198.
[175] Falck J, Coates J, Jackson SP (2005) Conserved modes of recruitment of ATM, ATR and DNA-PKcs to sites of DNA damage. *Nature* **434**, 605-611.
[176] Shiloh Y (2003) ATM and related protein kinases: safeguarding genome integrity. *Nat Rev Cancer* **3**, 155-168.
[177] Passos JF, Nelson G, Wang C, Richter T, Simillion C, Proctor CJ, Miwa S, Olijslagers S, Hallinan J, Wipat A, Saretzki G, Rudolph KL, Kirkwood TBL, von Zglinicki T (2010) Feedback between p21 and reactive oxygen production is necessary for cell senescence. *Mol Syst Biol* **6**, 347.
[178] Meek DW, Anderson CW (2009) Posttranslational modification of p53: cooperative integrators of function. *Cold Spring Harb Perspect Biol* **1**, a000950.
[179] Chen J, Peters R, Saha P, Lee P, Theodoras A, Pagano M, Wagner G, Dutta A (1996) A 39 amino acid fragment of the cell cycle regulator p21 is sufficient to bind PCNA and partially inhibit DNA replication in vivo. *Nucleic Acids Res* **24**, 1727-1733.
[180] Oku T, Ikeda S, Sasaki H, Fukuda K, Morioka H, Ohtsuka E, Yoshikawa H, Tsurimoto T (1998) Functional sites of human PCNA which interact with p21 (Cip1/Waf1), DNA polymerase δ and replication factor C. *Genes Cells* **3**, 357-369.
[181] Dutto I, Tillhon M, Cazzalini O, Stivala LA, Prosperi E (2015) Biology of the cell cycle inhibitor p21(CDKN1A): molecular mechanisms and relevance in chemical toxicology. *Arch Toxicol* **89**, 155-178.
[182] Wang W, Furneaux H, Cheng H, Caldwell MC, Hutter D, Liu Y, Holbrook N, Gorospe M (2000) HuR regulates p21 mRNA stabilization by UV light. *Mol Cell Biol* **20**, 760-769.
[183] Gervais JL, Seth P, Zhang H (1998) Cleavage of CDK inhibitor p21(Cip1/Waf1) by caspases is an early event during DNA damage-induced apoptosis. *J Biol Chem* **273**, 19207-19212.
[184] Saito Si, Goodarzi AA, Higashimoto Y, Noda Y, Lees-Miller SP, Appella E, Anderson CW (2002) ATM mediates phosphorylation at multiple p53 sites, including Ser46, in response to ionizing radiation. *J Biol Chem* **277**, 12491-12494.
[185] Yang Y, Li C-CH, Weissman AM (2004) Regulating the p53 system through ubiquitination. *Oncogene* **23**, 2096-2106.
[186] Kerr JFR, Wyllie AH, Currie AR (1972) Apoptosis: a basic biological phenomenon with wide-ranging implications in tissue kinetics. *Br J Cancer* **26**, 239-257.
[187] Kristiansen M, Ham J (2014) Programmed cell death during neuronal development: the sympathetic neuron model. *Cell Death Differ* **21**, 1025-1035.
[188] Mattson MP (2000) Apoptosis in neurodegenerative disorders. *Nat Rev Mol Cell Biol* **1**, 120-130.
[189] Kumazawa T, Nishimura K, Katagiri N, Hashimoto S, Hayashi Y, Kimura K (2015) Gradual reduction in rRNA transcription triggers p53 acetylation and apoptosis via MYBBP1A. *Sci Rep* **5**, 10854.
[190] Roos WP, Kaina B (2013) DNA damage-induced cell death: from specific DNA lesions to the DNA damage response and apoptosis. *Cancer Lett* **332**, 237-248.
[191] Knights CD, Catania J, Di Giovanni S, Muratoglu S, Perez R, Swartzbeck A, Quong AA, Zhang X, Beerman T, Pestell RG (2006) Distinct p53 acetylation cassettes differentially influence gene-expression patterns and cell fate. *J Cell Biol* **173**, 533-544.
[192] Timofeev O, Schlereth K, Wanzel M, Braun A, Nieswandt B, Pagenstecher A, Rosenwald A, Elsässer H-P, Stiewe T (2013) p53 DNA binding cooperativity is essential for apoptosis and tumor suppression in vivo. *Cell Rep* **3**, 1512-1525.

[193] Schlereth K, Charles JP, Bretz AC, Stiewe T (2010) Life or death: p53-induced apoptosis requires DNA binding cooperativity. *Cell Cycle* **9**, 4068-4076.
[194] Hill R, Madureira PA, Waisman DM, Lee PWK (2011) DNA-PKCS binding to p53 on the p21WAF1/CIP1 promoter blocks transcription resulting in cell death. *Oncotarget* **2**, 1094-1108.
[195] Kracikova M, Akiri G, George A, Sachidanandam R, Aaronson SA (2013) A threshold mechanism mediates p53 cell fate decision between growth arrest and apoptosis. *Cell Death Differ* **20**, 576-588.
[196] Fielder E, von Zglinicki T, Jurk D (2017) The DNA Damage Response in Neurons: Die by Apoptosis or Survive in a Senescence-Like State? *J Alzheimers Dis*.
[197] Takai H, Smogorzewska A, de Lange T (2003) DNA damage foci at dysfunctional telomeres. *Curr Biol* **13**, 1549-1556.
[198] Karlseder J, Broccoli D, Dai Y, Hardy S, de Lange T (1999) p53- and ATM-dependent apoptosis induced by telomeres lacking TRF2. *Science* **283**, 1321-1325.
[199] van Steensel B, Smogorzewska A, de Lange T (1998) TRF2 Protects Human Telomeres from End-to-End Fusions. *Cell* **92**, 401-413.
[200] van Gent DC, Hoeijmakers JH, Kanaar R (2001) Chromosomal stability and the DNA double-stranded break connection. *Nat Rev Genet* **2**, 196-206.
[201] Griffith JD, Comeau L, Rosenfield S, Stansel RM, Bianchi A, Moss H, de Lange T (1999) Mammalian Telomeres End in a Large Duplex Loop. *Cell* **97**, 503-514.
[202] Blackburn Eh , Chan S , Chang J F, T. B., Krauskopf A, McEachern M, P, J., ' Roy J, Smith C, Smith C W, H. (2000) Molecular manifestations and molecular determinants of telomere capping. *Cold Spring Habour symposia on quantitative biology* **2000**, 253-263.
[203] Stewart SA, Ben-Porath I, Carey VJ, O'Connor BF, Hahn WC, Weinberg RA (2003) Erosion of the telomeric single-strand overhang at replicative senescence. *Nat Genet* **33**, 492-496.
[204] Wang C, Jurk D, Nelson G, Martin-Ruiz C, von Zglinicki T (2009) DNA damage response and cellular senescence in aging mice. *Aging Cell* **8**, 311-323.
[205] Parrinello S, Samper E, Krtolica A, Goldstein J, Melov S, Campisi J (2003) Oxygen sensitivity severely limits the replicative lifespan of murine fibroblasts. *Nat Cell Biol* **5**, 741-747.
[206] Sancar A, Lindsey-Boltz LA, Kang TH, Reardon JT, Lee JH, Ozturk N (2010) Circadian clock control of the cellular response to DNA damage. *FEBS Lett* **584**, 2618-2625.
[207] Madabhushi R, Gao F, Pfenning AR, Pan L, Yamakawa S, Seo J, Rueda R, Phan TX, Yamakawa H, Pao P-C (2015) Activity-induced DNA breaks govern the expression of neuronal early-response genes. *Cell* **161**, 1592-1605.
[208] Suberbielle E, Sanchez PE, Kravitz AV, Wang X, Ho K, Eilertson K, Devidze N, Kreitzer AC, Mucke L (2013) Physiologic brain activity causes DNA double-strand breaks in neurons, with exacerbation by amyloid-[beta]. *Nat Neurosci* **16**, 613-621.
[209] Hewitt G, Jurk D, Marques FDM, Correia-Melo C, Hardy T, Gackowska A, Anderson R, Taschuk M, Mann J, Passos JF (2012) Telomeres are favoured targets of a persistent DNA damage response in ageing and stress-induced senescence. *Nat Commun* **3**, 708.
[210] Fumagalli M, Rossiello F, Mondello C, di Fagagna FdA (2014) Stable cellular senescence is associated with persistent DDR activation. *PLoS One* **9**, e110969.
[211] Fumagalli M, Rossiello F, Clerici M, Barozzi S, Cittaro D, Kaplunov JM, Bucci G, Dobreva M, Matti V, Beausejour CM (2012) Telomeric DNA damage is irreparable and causes persistent DNA-damage-response activation. *Nat Cell Biol* **14**, 355-365.
[212] Kuilman T, Michaloglou C, Vredeveld LCW, Douma S, van Doorn R, Desmet CJ, Aarden LA, Mooi WJ, Peeper DS (2008) Oncogene-Induced Senescence Relayed by an Interleukin-Dependent Inflammatory Network. *Cell* **133**, 1019-1031.
[213] Acosta JC, O'Loghlen A, Banito A, Guijarro MV, Augert A, Raguz S, Fumagalli M, Da Costa M, Brown C, Popov N (2008) Chemokine signaling via the CXCR2 receptor reinforces senescence. *Cell* **133**, 1006-1018.

[214] Saretzki G, Murphy MP, Von Zglinicki T (2003) MitoQ counteracts telomere shortening and elongates lifespan of fibroblasts under mild oxidative stress. *Aging Cell* **2**, 141-143.
[215] Passos JF, Saretzki G, Ahmed S, Nelson G, Richter T, Peters H, Wappler I, Birket MJ, Harold G, Schaeuble K (2007) Mitochondrial dysfunction accounts for the stochastic heterogeneity in telomere-dependent senescence. *PLoS Biol* **5**, e110.
[216] Takahashi A, Ohtani N, Yamakoshi K, Iida S-i, Tahara H, Nakayama K, Nakayama KI, Ide T, Saya H, Hara E (2006) Mitogenic signalling and the p16INK4a–Rb pathway cooperate to enforce irreversible cellular senescence. *Nat Cell Biol* **8**, 1291-1297.
[217] Correia-Melo C, Marques FDM, Anderson R, Hewitt G, Hewitt R, Cole J, Carroll BM, Miwa S, Birch J, Merz A (2016) Mitochondria are required for pro-ageing features of the senescent phenotype. *EMBO J*, e201592862.
[218] Jazwinski SM (2013) The retrograde response: when mitochondrial quality control is not enough. *Biochim Biophys Acta* **1833**, 400-409.
[219] Liu Z, Butow RA (2006) Mitochondrial retrograde signaling. *Annu Rev Genet* **40**, 159-185.
[220] Owusu-Ansah E, Yavari A, Mandal S, Banerjee U (2008) Distinct mitochondrial retrograde signals control the G1-S cell cycle checkpoint. *Nat Genet* **40**, 356-361.
[221] Moiseeva O, Bourdeau V, Roux A, Deschênes-Simard X, Ferbeyre G (2009) Mitochondrial dysfunction contributes to oncogene-induced senescence. *Mol Cell Biol* **29**, 4495-4507.
[222] Kim YY, Jee HJ, Um JH, Kim YM, Bae SS, Yun J (2017) Cooperation between p21 and Akt is required for p53-dependent cellular senescence. *Aging Cell*.
[223] Konishi H, Yamauchi E, Taniguchi H, Yamamoto T, Matsuzaki H, Takemura Y, Ohmae K, Kikkawa U, Nishizuka Y (2001) Phosphorylation sites of protein kinase C δ in H2O2-treated cells and its activation by tyrosine kinase in vitro. *Proc Natl Acad Sci U S A* **98**, 6587-6592.
[224] Cosentino-Gomes D, Rocco-Machado N, Meyer-Fernandes JR (2012) Cell signaling through protein kinase C oxidation and activation. *Int J Mol Sci* **13**, 10697-10721.
[225] Korolchuk VI, Miwa S, Carroll B, von Zglinicki T (2017) Mitochondria in Cell Senescence: Is Mitophagy the Weakest Link? *EBioMedicine* **21**, 7-13.
[226] Kojima H, Inoue T, Kunimoto H, Nakajima K (2013) IL-6-STAT3 signaling and premature senescence. *JAK-STAT* **2**, e25763.
[227] Eggert T, Wolter K, Ji J, Ma C, Yevsa T, Klotz S, Medina-Echeverz J, Longerich T, Forgues M, Reisinger F, Heikenwalder M, Wang XW, Zender L, Greten TF (2016) Distinct Functions of Senescence-Associated Immune Responses in Liver Tumor Surveillance and Tumor Progression. *Cancer Cell* **30**, 533-547.
[228] Kang T-W, Yevsa T, Woller N, Hoenicke L, Wuestefeld T, Dauch D, Hohmeyer A, Gereke M, Rudalska R, Potapova A, Iken M, Vucur M, Weiss S, Heikenwalder M, Khan S, Gil J, Bruder D, Manns M, Schirmacher P, Tacke F, Ott M, Luedde T, Longerich T, Kubicka S, Zender L (2011) Senescence surveillance of pre-malignant hepatocytes limits liver cancer development. *Nature* **479**, 547-551.
[229] Freund A, Orjalo AV, Desprez P-Y, Campisi J (2010) Inflammatory networks during cellular senescence: causes and consequences. *Trends Mol Med* **16**, 238-246.
[230] Franceschi C, Campisi J (2014) Chronic inflammation (inflammaging) and its potential contribution to age-associated diseases. *J Gerontol A Biol Sci Med Sci* **69**, S4-9.
[231] Wu Z-H, Shi Y, Tibbetts RS, Miyamoto S (2006) Molecular linkage between the kinase ATM and NF-κB signaling in response to genotoxic stimuli. *Science* **311**, 1141-1146.
[232] Chien Y, Scuoppo C, Wang X, Fang X, Balgley B, Bolden JE, Premsrirut P, Luo W, Chicas A, Lee CS, Kogan SC, Lowe SW (2011) Control of the senescence-associated secretory phenotype by NF-κB promotes senescence and enhances chemosensitivity. *Genes Dev* **25**, 2125-2136.
[233] Adler AS, Sinha S, Kawahara TLA, Zhang JY, Segal E, Chang HY (2007) Motif module map reveals enforcement of aging by continual NF-κB activity. *Genes Dev* **21**, 3244-3257.
[234] Salminen A, Kauppinen A, Kaarniranta K (2012) Emerging role of NF-κB signaling in the induction of senescence-associated secretory phenotype (SASP). *Cell Signal* **24**, 835-845.

[235] Hayden MS, Ghosh S (2008) Shared Principles in NF-κB Signaling. *Cell* **132**, 344-362.
[236] Wan F, Lenardo MJ (2010) The nuclear signaling of NF-kappaB: current knowledge, new insights, and future perspectives. *Cell Res* **20**, 24-33.
[237] Ghosh S, Karin M (2002) Missing pieces in the NF-κB puzzle. *Cell* **109**, S81-S96.
[238] Jacobs MD, Harrison SC (1998) Structure of an IκBα/NF-κB Complex. *Cell* **95**, 749-758.
[239] Rice NR, MacKichan ML, Israel A (1992) The precursor of NF-kappa B p50 has I kappa B-like functions. *Cell* **71**, 243-253.
[240] Henkel T, Zabel U, van Zee K, Muller JM, Fanning E, Baeuerle PA (1992) Intramolecular masking of the nuclear location signal and dimerization domain in the precursor for the p50 NF-kappa B subunit. *Cell* **68**, 1121-1133.
[241] Savinova OV, Hoffmann A, Ghosh G (2009) The Nfkb1 and Nfkb2 Proteins p105 and p100 Function as the Core of High-Molecular-Weight Heterogeneous Complexes. *Mol Cell* **34**, 591-602.
[242] Tilstra JS, Robinson AR, Wang J, Gregg SQ, Clauson CL, Reay DP, Nasto LA, St Croix CM, Usas A, Vo N, Huard J, Clemens PR, Stolz DB, Guttridge DC, Watkins SC, Garinis GA, Wang Y, Niedernhofer LJ, Robbins PD (2012) NF-κB inhibition delays DNA damage–induced senescence and aging in mice. *J Clin Invest* **122**, 2601-2612.
[243] Sun SC (2017) The non-canonical NF-kappaB pathway in immunity and inflammation. *Nat Rev Immunol* **17**, 545-558.
[244] Senftleben U, Cao Y, Xiao G, Greten FR, Krahn G, Bonizzi G, Chen Y, Hu Y, Fong A, Sun SC, Karin M (2001) Activation by IKKalpha of a second, evolutionary conserved, NF-kappa B signaling pathway. *Science* **293**, 1495-1499.
[245] Iannetti A, Ledoux AC, Tudhope SJ, Sellier H, Zhao B, Mowla S, Moore A, Hummerich H, Gewurz BE, Cockell SJ, Jat PS, Willmore E, Perkins ND (2014) Regulation of p53 and Rb Links the Alternative NF-κB Pathway to EZH2 Expression and Cell Senescence. *PLoS Genet* **10**, e1004642.
[246] Rocha S, Martin AM, Meek DW, Perkins ND (2003) p53 Represses Cyclin D1 Transcription through Down Regulation of Bcl-3 and Inducing Increased Association of the p52 NF-κB Subunit with Histone Deacetylase 1. *Mol Cell Biol* **23**, 4713-4727.
[247] Seluanov A, Gorbunova V, Falcovitz A, Sigal A, Milyavsky M, Zurer I, Shohat G, Goldfinger N, Rotter V (2001) Change of the death pathway in senescent human fibroblasts in response to DNA damage is caused by an inability to stabilize p53. *Mol Cell Biol* **21**, 1552-1564.
[248] Sanders YY, Liu H, Zhang X, Hecker L, Bernard K, Desai L, Liu G, Thannickal VJ (2013) Histone modifications in senescence-associated resistance to apoptosis by oxidative stress. *Redox Biol* **1**, 8-16.
[249] Juping LIU, Merrett JB (2000) Apoptosis or senescence-like growth arrest: influence of cell-cycle position, p53, p21 and bax in H2O2 response of normal human fibroblasts. *Biochem J* **347**, 543-551.
[250] Chen QM, Liu J, Merrett JB (2000) Apoptosis or senescence-like growth arrest: influence of cell-cycle position, p53, p21 and bax in H2O2 response of normal human fibroblasts. *Biochem J* **347**, 543-551.
[251] Marcotte R, Lacelle C, Wang E (2004) Senescent fibroblasts resist apoptosis by downregulating caspase-3. *Mech Ageing Dev* **125**, 777-783.
[252] Baar MP, Brandt RM, Putavet DA, Klein JD, Derks KW, Bourgeois BR, Stryeck S, Rijksen Y, van Willigenburg H, Feijtel DA, van der Pluijm I, Essers J, van Cappellen WA, van IWF, Houtsmuller AB, Pothof J, de Bruin RW, Madl T, Hoeijmakers JH, Campisi J, de Keizer PL (2017) Targeted Apoptosis of Senescent Cells Restores Tissue Homeostasis in Response to Chemotoxicity and Aging. *Cell* **169**, 132-147.e116.
[253] Wang E (1995) Senescent human fibroblasts resist programmed cell death, and failure to suppress bcl2 is involved. *Cancer Res* **55**, 2284-2292.

[254] Villunger A, Michalak EM, Coultas L, Müllauer F, Böck G, Ausserlechner MJ, Adams JM, Strasser A (2003) p53-and drug-induced apoptotic responses mediated by BH3-only proteins puma and noxa. *Science* **302**, 1036-1038.
[255] Cory S, Huang DCS, Adams JM (2003) The Bcl-2 family: roles in cell survival and oncogenesis. *Oncogene* **22**, 8590-8607.
[256] Antignani A, Youle RJ (2006) How do Bax and Bak lead to permeabilization of the outer mitochondrial membrane? *Curr Opin Cell Biol* **18**, 685-689.
[257] Yosef R, Pilpel N, Tokarsky-Amiel R, Biran A, Ovadya Y, Cohen S, Vadai E, Dassa L, Shahar E, Condiotti R, Ben-Porath I, Krizhanovsky V (2016) Directed elimination of senescent cells by inhibition of BCL-W and BCL-XL. **7**, 11190.
[258] Gartel AL, Tyner AL (2002) The role of the cyclin-dependent kinase inhibitor p21 in apoptosis. *Mol Cancer Ther* **1**, 639-649.
[259] Xia M, Knezevic D, Vassilev LT (2011) p21 does not protect cancer cells from apoptosis induced by nongenotoxic p53 activation. *Oncogene* **30**, 346-355.
[260] Harvey KJ, Lukovic D, Ucker DS (2000) Caspase-dependent Cdk activity is a requisite effector of apoptotic death events. *J Cell Biol* **148**, 59-72.
[261] Zhang Y, Fujita N, Tsuruo T (1999) Caspase-mediated cleavage of p21 Waf1/Cip1 converts cancer cells from growth arrest to undergoing apoptosis. *Oncogene* **18**, 1131-1138.
[262] Xu S-Q, El-Deiry WS (2000) p21 WAF1/CIP1 inhibits initiator caspase cleavage by TRAIL death receptor DR4. *Biochem Biophys Res Commun* **269**, 179-190.
[263] Adachi S, Ito H, Tamamori-Adachi M, Ono Y, Nozato T, Abe S, Ikeda M-a, Marumo F, Hiroe M (2001) Cyclin A/cdk2 activation is involved in hypoxia-induced apoptosis in cardiomyocytes. *Circul Res* **88**, 408-414.
[264] Yonish-Rouach E, Resnftzky D, Lotem J, Sachs L, Kimchi A, Oren M (1991) Wild-type p53 induces apoptosis of myeloid leukaemic cells that is inhibited by interleukin-6. *Nature* **352**, 345-347.
[265] Coppé J-P, Patil CK, Rodier F, Sun Y, Muñoz DP, Goldstein J, Nelson PS, Desprez P-Y, Campisi J (2008) Senescence-associated secretory phenotypes reveal cell-nonautonomous functions of oncogenic RAS and the p53 tumor suppressor. *PLoS Biol* **6**, e301.
[266] Lotem J, Gal H, Kama R, Amariglio N, Rechavi G, Domany E, Sachs L, Givol D (2003) Inhibition of p53-induced apoptosis without affecting expression of p53-regulated genes. *Proc Natl Acad Sci U S A* **100**, 6718-6723.
[267] Miyashita T, Krajewski S, Krajewska M, Wang HG, Lin H-K, Liebermann DA, Hoffman B, Reed JC (1994) Tumor suppressor p53 is a regulator of bcl-2 and bax gene expression in vitro and in vivo. *Oncogene* **9**, 1799-1805.
[268] Lotem J, Sachs L (1999) Cytokines as suppressors of apoptosis. *Apoptosis* **4**, 187-196.
[269] Beg AA, Baltimore D (1996) An essential role for NF-kB in preventing TNF-alpha-induced cell death. *Science* **274**, 782-784.
[270] Mayo MW, Wang C-Y, Cogswell PC, Rogers-Graham KS, Lowe SW, Der CJ, Baldwin AS (1997) Requirement of NF-κB activation to suppress p53-independent apoptosis induced by oncogenic Ras. *Science* **278**, 1812-1815.
[271] Geng YQ, Guan JT, Xu XH, Fu YC (2010) Senescence-associated beta-galactosidase activity expression in aging hippocampal neurons. *Biochem Biophys Res Commun* **396**, 866-869.
[272] Hans VH, Kossmann T, Lenzlinger PM, Probstmeier R, Imhof HG, Trentz O, Morganti-Kossmann MC (1999) Experimental axonal injury triggers interleukin-6 mRNA, protein synthesis and release into cerebrospinal fluid. *J Cereb Blood Flow Metab* **19**, 184-194.
[273] Sallmann S, Jüttler E, Prinz S, Petersen N, Knopf U, Weiser T, Schwaninger M (2000) Induction of Interleukin-6 by Depolarization of Neurons. *J Neurosci* **20**, 8637-8642.
[274] Erta M, Quintana A, Hidalgo J (2012) Interleukin-6, a Major Cytokine in the Central Nervous System. *Int J Biol Sci* **8**, 1254-1266.

[275] Wei H, Chadman KK, McCloskey DP, Sheikh AM, Malik M, Brown WT, Li X (2012) Brain IL-6 elevation causes neuronal circuitry imbalances and mediates autism-like behaviors. *Biochim Biophys Acta* **1822**, 831-842.
[276] Hooper C, Meimaridou E, Tavassoli M, Melino G, Lovestone S, Killick R (2007) p53 is upregulated in Alzheimer's disease and induces tau phosphorylation in HEK293a cells. *Neurosci Lett* **418**, 34-37.
[277] Arendt T, Rodel L, Gartner U, Holzer M (1996) Expression of the cyclin-dependent kinase inhibitor p16 in Alzheimer's disease. *Neuroreport* **7**, 3047-3049.
[278] Ring RH, Valo Z, Gao C, Barish ME, Singer-Sam J (2003) The Cdkn1a gene (p21Waf1/Cip1) is an inflammatory response gene in the mouse central nervous system. *Neurosci Lett* **350**, 73-76.
[279] Lüth HJ, Holzer M, Gertz HJ, Arendt TH (2000) Aberrant expression of nNOS in pyramidal neurons in Alzheimer's disease is highly co-localized with p21 ras and p16 INK4a. *Brain Res* **852**, 45-55.
[280] Harms C, Albrecht K, Harms U, Seidel K, Hauck L, Baldinger T, Hubner D, Kronenberg G, An J, Ruscher K, Meisel A, Dirnagl U, von Harsdorf R, Endres M, Hortnagl H (2007) Phosphatidylinositol 3-Akt-kinase-dependent phosphorylation of p21(Waf1/Cip1) as a novel mechanism of neuroprotection by glucocorticoids. *J Neurosci* **27**, 4562-4571.
[281] Tomashevski A, Webster DR, Grammas P, Gorospe M, Kruman, II (2010) Cyclin-C-dependent cell-cycle entry is required for activation of non-homologous end joining DNA repair in postmitotic neurons. *Cell Death Differ* **17**, 1189-1198.
[282] Zonis S, Ljubimov VA, Mahgerefteh M, Pechnick RN, Wawrowsky K, Chesnokova V (2013) p21Cip restrains hippocampal neurogenesis and protects neuronal progenitors from apoptosis during acute systemic inflammation. *Hippocampus* **23**, 1383-1394.
[283] Simpson JE, Ince PG, Minett T, Matthews FE, Heath PR, Shaw PJ, Goodall E, Garwood CJ, Ratcliffe LE, Brayne C (2015) Neuronal DNA damage response-associated dysregulation of signalling pathways and cholesterol metabolism at the earliest stages of Alzheimer-type pathology. *Neuropathol Appl Neurobiol* **42**, 167-179.
[284] Simpson JE, Ince PG, Matthews FE, Shaw PJ, Heath PR, Brayne C, Garwood C, Higginbottom A, Wharton SB (2015) A neuronal DNA damage response is detected at the earliest stages of Alzheimer's neuropathology and correlates with cognitive impairment in the Medical Research Council's Cognitive Function and Ageing Study ageing brain cohort. *Neuropathol Appl Neurobiol* **41**, 483-496.
[285] Branzei D, Foiani M (2008) Regulation of DNA repair throughout the cell cycle. *Nat Rev Mol Cell Biol* **9**, 297-308.
[286] Herrup K, Yang Y (2007) Cell cycle regulation in the postmitotic neuron: oxymoron or new biology? *Nat Rev Neurosci* **8**, 368-378.
[287] Rashidian J, Iyirhiaro GO, Park DS (2007) Cell cycle machinery and stroke. *Biochim Biophys Acta* **1772**, 484-493.
[288] Rashidian J, Iyirhiaro G, Aleyasin H, Rios M, Vincent I, Callaghan S, Bland RJ, Slack RS, During MJ, Park DS (2005) Multiple cyclin-dependent kinases signals are critical mediators of ischemia/hypoxic neuronal death in vitro and in vivo. *Proc Natl Acad Sci U S A* **102**, 14080-14085.
[289] Di Giovanni S, Movsesyan V, Ahmed F, Cernak I, Schinelli S, Stoica B, Faden AI (2005) Cell cycle inhibition provides neuroprotection and reduces glial proliferation and scar formation after traumatic brain injury. *Proc Natl Acad Sci U S A* **102**, 8333-8338.
[290] Baumann K, Mandelkow EM, Biernat J, Piwnica-Worms H, Mandelkow E (1993) Abnormal Alzheimer-like phosphorylation of tau-protein by cyclin-dependent kinases cdk2 and cdk5. *FEBS Lett* **336**, 417-424.
[291] McShea A, Harris PL, Webster KR, Wahl AF, Smith MA (1997) Abnormal expression of the cell cycle regulators P16 and CDK4 in Alzheimer's disease. *Am J Pathol* **150**, 1933-1939.

[292] Busser J, Geldmacher DS, Herrup K (1998) Ectopic cell cycle proteins predict the sites of neuronal cell death in Alzheimer's disease brain. *J Neurosci* **18**, 2801-2807.
[293] Yang Y, Geldmacher DS, Herrup K (2001) DNA replication precedes neuronal cell death in Alzheimer's disease. *J Neurosci* **21**, 2661-2668.
[294] Yang Y, Mufson EJ, Herrup K (2003) Neuronal cell death is preceded by cell cycle events at all stages of Alzheimer's disease. *J Neurosci* **23**, 2557-2563.
[295] Vincent I, Jicha G, Rosado M, Dickson DW (1997) Aberrant expression of mitotic cdc2/cyclin B1 kinase in degenerating neurons of Alzheimer's disease brain. *J Neurosci* **17**, 3588-3598.
[296] Nagy ZS, Esiri MM, Cato AM, Smith AD (1997) Cell cycle markers in the hippocampus in Alzheimer's disease. *Acta Neuropathol* **94**, 6-15.
[297] Herrup K, Busser JC (1995) The induction of multiple cell cycle events precedes target-related neuronal death. *Development* **121**, 2385-2395.
[298] Herrup K, Neve R, Ackerman SL, Copani A (2004) Divide and die: cell cycle events as triggers of nerve cell death. *J Neurosci* **24**, 9232-9239.
[299] al-Ubaidi MR, Hollyfield JG, Overbeek PA, Baehr W (1992) Photoreceptor degeneration induced by the expression of simian virus 40 large tumor antigen in the retina of transgenic mice. *Proc Natl Acad Sci U S A* **89**, 1194-1198.
[300] Feddersen RM, Ehlenfeldt R, Yunis WS, Clark HB, Orr HT (1992) Disrupted cerebellar cortical development and progressive degeneration of Purkinje cells in SV40 T antigen transgenic mice. *Neuron* **9**, 955-966.
[301] Yang Y, Herrup K (2005) Loss of neuronal cell cycle control in ataxia-telangiectasia: a unified disease mechanism. *J Neurosci* **25**, 2522-2529.
[302] Gulbis JM, Kelman Z, Hurwitz J, O'Donnell M, Kuriyan J (1996) Structure of the C-Terminal Region of p21WAF1/CIP1 Complexed with Human PCNA. *Cell* **87**, 297-306.
[303] Shen X, Chen J, Li J, Kofler J, Herrup K (2016) Neurons in Vulnerable Regions of the Alzheimer's Disease Brain Display Reduced ATM Signaling. *eNeuro* **3**, ENEURO. 0124-0115.2016.
[304] Suberbielle E, Djukic B, Evans M, Kim DH, Taneja P, Wang X, Finucane M, Knox J, Ho K, Devidze N (2015) DNA repair factor BRCA1 depletion occurs in Alzheimer brains and impairs cognitive function in mice. *Nat Commun* **6**, 8897.
[305] Kruman II, Wersto RP, Cardozo-Pelaez F, Smilenov L, Chan SL, Chrest FJ, Emokpae Jr R, Gorospe M, Mattson MP (2004) Cell cycle activation linked to neuronal cell death initiated by DNA damage. *Neuron* **41**, 549-561.
[306] Khurana V, Merlo P, DuBoff B, Fulga TA, Sharp KA, Campbell SD, Götz J, Feany MB (2012) A neuroprotective role for the DNA damage checkpoint in tauopathy. *Aging Cell* **11**, 360-362.
[307] Park DS, Obeidat A, Giovanni A, Greene LA (2000) Cell cycle regulators in neuronal death evoked by excitotoxic stress: implications for neurodegeneration and its treatment. *Neurobiol Aging* **21**, 771-781.
[308] Schwartz EI, Smilenov LB, Price MA, Osredkar T, Baker RA, Ghosh S, Shi FD, Vollmer TL, Lencinas A, Stearns DM, Gorospe M, Kruman, II (2007) Cell cycle activation in postmitotic neurons is essential for DNA repair. *Cell Cycle* **6**, 318-329.
[309] Casafont I, Palanca A, Lafarga V, Berciano MT, Lafarga M (2011) Effect of ionizing radiation in sensory ganglion neurons: organization and dynamics of nuclear compartments of DNA damage/repair and their relationship with transcription and cell cycle. *Acta Neuropathol* **122**, 481-493.
[310] McShea A, Lee HG, Petersen RB, Casadesus G, Vincent I, Linford NJ, Funk J-O, Shapiro RA, Smith MA (2007) Neuronal cell cycle re-entry mediates Alzheimer disease-type changes. *Biochim Biophys Acta* **1772**, 467-472.
[311] Kingsbury MA, Friedman B, McConnell MJ, Rehen SK, Yang AH, Kaushal D, Chun J (2005) Aneuploid neurons are functionally active and integrated into brain circuitry. *Proc Natl Acad Sci U S A* **102**, 6143-6147.

[312] Hitomi M, Stacey DW (2010) The checkpoint kinase ATM protects against stress-induced elevation of cyclin D1 and potential cell death in neurons. *Cytometry A* **77**, 524-533.
[313] Li Y, Xiong H, Yang D-Q (2012) Functional switching of ATM: sensor of DNA damage in proliferating cells and mediator of Akt survival signal in post-mitotic human neuron-like cells. *Chin J Cancer* **31**, 364-372.
[314] Strosznajder RP, Jesko H, Banasik M, Tanaka S (2005) Effects of p53 inhibitor on survival and death of cells subjected to oxidative stress. *J Physiol Pharmacol* **56**, 215-221.
[315] Pallas M, Verdaguer E, Jorda EG, Jimenez A, Canudas AM, Camins A (2005) Flavopiridol: an antitumor drug with potential application in the treatment of neurodegenerative diseases. *Med Hypotheses* **64**, 120-123.
[316] Jorda EG, Verdaguer E, Canudas AM, Jiménez A, Bruna A, Caelles C, Bravo R, Escubedo E, Pubill D, Camarasa J (2003) Neuroprotective action of flavopiridol, a cyclin-dependent kinase inhibitor, in colchicine-induced apoptosis. *Neuropharmacol* **45**, 672-683.
[317] Kabadi SV, Faden AI (2014) Selective CDK inhibitors: promising candidates for future clinical traumatic brain injury trials. *Neural Regener Res* **9**, 1578–1580.
[318] Osuga H, Osuga S, Wang F, Fetni R, Hogan MJ, Slack RS, Hakim AM, Ikeda J-E, Park DS (2000) Cyclin-dependent kinases as a therapeutic target for stroke. *Proc Natl Acad Sci U S A* **97**, 10254-10259.
[319] Kabadi SV, Stoica BA, Loane DJ, Luo T, Faden AI (2014) CR8, a novel inhibitor of CDK, limits microglial activation, astrocytosis, neuronal loss, and neurologic dysfunction after experimental traumatic brain injury. *J Cereb Blood Flow Metab* **34**, 502-513.
[320] Wang F, Corbett D, Osuga H, Osuga S, Ikeda J-E, Slack RS, Hogan MJ, Hakim AM, Park DS (2002) Inhibition of cyclin-dependent kinases improves CA1 neuronal survival and behavioral performance after global ischemia in the rat. *J Cereb Blood Flow Metab* **22**, 171-182.
[321] Oumata N, Bettayeb K, Ferandin Y, Demange L, Lopez-Giral A, Goddard M-L, Myrianthopoulos V, Mikros E, Flajolet M, Greengard P (2008) Roscovitine-derived, dual-specificity inhibitors of cyclin-dependent kinases and casein kinases 1. *J Med Chem* **51**, 5229-5242.
[322] Oulès B, Del Prete D, Greco B, Zhang X, Lauritzen I, Sevalle J, Moreno S, Paterlini-Bréchot P, Trebak M, Checler F (2012) Ryanodine receptor blockade reduces amyloid-β load and memory impairments in Tg2576 mouse model of Alzheimer disease. *J Neurosci* **32**, 11820-11834.
[323] Acosta JC, Banito A, Wuestefeld T, Georgilis A, Janich P, Morton JP, Athineos D, Kang T-W, Lasitschka F, Andrulis M, Pascual G, Morris KJ, Khan S, Jin H, Dharmalingam G, Snijders AP, Carroll T, Capper D, Pritchard C, Inman GJ, Longerich T, Sansom OJ, Benitah SA, Zender L, Gil J (2013) A complex secretory program orchestrated by the inflammasome controls paracrine senescence. *Nat Cell Biol* **15**, 978-990.
[324] Coppé J-P, Rodier F, Patil CK, Freund A, Desprez P-Y, Campisi J (2011) Tumor suppressor and aging biomarker p16INK4a induces cellular senescence without the associated inflammatory secretory phenotype. *J Biol Chem* **286**, 36396-36403.
[325] Chien Y, Scuoppo C, Wang X, Fang X, Balgley B, Bolden JE, Premsrirut P, Luo W, Chicas A, Lee CS, Kogan SC, Lowe SW (2011) Control of the senescence-associated secretory phenotype by NF-kappaB promotes senescence and enhances chemosensitivity. *Genes Dev* **25**, 2125-2136.
[326] Baeuerle PA, Baichwal VR (1997) NF-κB as a frequent target for immunosuppressive and anti-inflammatory molecules. *Adv Immunol* **65**, 111-137.
[327] Medeiros R, Figueiredo CP, Pandolfo P, Duarte FS, Prediger RD, Passos GF, Calixto JB (2010) The role of TNF-alpha signaling pathway on COX-2 upregulation and cognitive decline induced by beta-amyloid peptide. *Behav Brain Res* **209**, 165-173.
[328] O'Banion MK (1998) Cyclooxygenase-2: molecular biology, pharmacology, and neurobiology. *Crit Rev Neurobiol* **13**, 45-82.

[329] Seibert K, Masferrer J, Zhang Y, Gregory S, Olson G, Hauser S, Leahy K, Perkins W, Isakson P (1994) Mediation of inflammation by cyclooxygenase-2. *Agents Actions Suppl* **46**, 41-50.
[330] Yang H, Chen C (2008) Cyclooxygenase-2 in synaptic signaling. *Curr Pharm Des* **14**, 1443-1451.
[331] Minghetti L (2004) Cyclooxygenase-2 (COX-2) in inflammatory and degenerative brain diseases. *J Neuropathol Exp Neurol* **63**, 901-910.
[332] Hoozemans JJM, Van Haastert ES, Veerhuis R, Arendt T, Scheper W, Eikelenboom P, Rozemuller AJM (2005) Maximal COX-2 and ppRb expression in neurons occurs during early Braak stages prior to the maximal activation of astrocytes and microglia in Alzheimer's disease. *J Neuroinflammation* **2**, 27.
[333] Hoozemans JJM, Veerhuis R, Rozemuller AJM, Arendt T, Eikelenboom P (2004) Neuronal COX-2 expression and phosphorylation of pRb precede p38 MAPK activation and neurofibrillary changes in AD temporal cortex. *Neurobiol Dis* **15**, 492-499.
[334] Hoozemans JJM, Brückner MK, Rozemuller AJM, Veerhuis R, Eikelenboom P, Arendt T (2002) Cyclin D1 and cyclin E are co-localized with cyclo-oxygenase 2 (COX-2) in pyramidal neurons in Alzheimer disease temporal cortex. *J Neuropathol Exp Neurol* **61**, 678-688.
[335] Nogawa S, Zhang F, Ross ME, Iadecola C (1997) Cyclo-oxygenase-2 gene expression in neurons contributes to ischemic brain damage. *J Neurosci* **17**, 2746-2755.
[336] Andreasson KI, Savonenko A, Vidensky S, Goellner JJ, Zhang Y, Shaffer A, Kaufmann WE, Worley PF, Isakson P, Markowska AL (2001) Age-dependent cognitive deficits and neuronal apoptosis in cyclooxygenase-2 transgenic mice. *J Neurosci* **21**, 8198-8209.
[337] Jiang J, Borisenko GG, Osipov A, Martin I, Chen R, Shvedova AA, Sorokin A, Tyurina YY, Potapovich A, Tyurin VA (2004) Arachidonic acid-induced carbon-centered radicals and phospholipid peroxidation in cyclo-oxygenase-2-transfected PC12 cells. *J Neurochem* **90**, 1036-1049.
[338] Teismann P, Tieu K, Choi D-K, Wu D-C, Naini A, Hunot S, Vila M, Jackson-Lewis V, Przedborski S (2003) Cyclooxygenase-2 is instrumental in Parkinson's disease neurodegeneration. *Proc Natl Acad Sci U S A* **100**, 5473-5478.
[339] Graham DG (1978) Oxidative pathways for catecholamines in the genesis of neuromelanin and cytotoxic quinones. *Mol Pharmacol* **14**, 633-643.
[340] McGeer PL, McGeer EG (2007) NSAIDs and Alzheimer disease: epidemiological, animal model and clinical studies. *Neurobiol Aging* **28**, 639-647.
[341] Vlad SC, Miller DR, Kowall NW, Felson DT (2008) Protective effects of NSAIDs on the development of Alzheimer disease. *Neurology* **70**, 1672-1677.
[342] Esposito E, Di Matteo V, Benigno A, Pierucci M, Crescimanno G, Di Giovanni G (2007) Non-steroidal anti-inflammatory drugs in Parkinson's disease. *Exp Neurol* **205**, 295-312.
[343] Chen H, Jacobs E, Schwarzschild MA, McCullough ML, Calle EE, Thun MJ, Ascherio A (2005) Nonsteroidal antiinflammatory drug use and the risk for Parkinson's disease. *Ann Neurol* **58**, 963-967.
[344] Hernán MA, Logroscino G, Rodríguez LAG (2006) Nonsteroidal anti-inflammatory drugs and the incidence of Parkinson disease. *Neurology* **66**, 1097-1099.
[345] Tchkonia T, Zhu Y, Van Deursen J, Campisi J, Kirkland JL (2013) Cellular senescence and the senescent secretory phenotype: therapeutic opportunities. *J Clin Invest* **123**, 966-972.
[346] Zhu Y, Tchkonia T, Pirtskhalava T, Gower AC, Ding H, Giorgadze N, Palmer AK, Ikeno Y, Hubbard GB, Lenburg M (2015) The Achilles' heel of senescent cells: from transcriptome to senolytic drugs. *Aging Cell* **14**, 644-658.
[347] Chinta SJ, Woods G, Rane A, Demaria M, Campisi J, Andersen JK (2015) Cellular senescence and the aging brain. *Exp Gerontol* **68**, 3-7.
[348] Farrall AJ, Wardlaw JM (2009) Blood-brain barrier: ageing and microvascular disease--systematic review and meta-analysis. *Neurobiol Aging* **30**, 337-352.

[349] Krishnamurthy J, Torrice C, Ramsey MR, Kovalev GI, Al-Regaiey K, Su L, Sharpless NE (2004) Ink4a/Arf expression is a biomarker of aging. *J Clin Invest* **114**, 1299-1307.
[350] Baker DJ, Jeganathan KB, Cameron JD, Thompson M, Juneja S, Kopecka A, Kumar R, Jenkins RB, de Groen PC, Roche P, van Deursen JM (2004) BubR1 insufficiency causes early onset of aging-associated phenotypes and infertility in mice. *Nat Genet* **36**, 744-749.
[351] Baker DJ, Perez-Terzic C, Jin F, Pitel KS, Niederländer NJ, Jeganathan K, Yamada S, Reyes S, Rowe L, Hiddinga HJ (2008) Opposing roles for p16Ink4a and p19Arf in senescence and ageing caused by BubR1 insufficiency. *Nat Cell Biol* **10**, 825-836.
[352] Montero JC, Seoane S, Ocana A, Pandiella A (2011) Inhibition of SRC family kinases and receptor tyrosine kinases by dasatinib: possible combinations in solid tumors. *Clin Cancer Res* **17**, 5546-5552.
[353] Bruning A (2013) Inhibition of mTOR signaling by quercetin in cancer treatment and prevention. *Anticancer Agents Med Chem* **13**, 1025-1031.
[354] Roos CM, Zhang B, Palmer AK, Ogrodnik MB, Pirtskhalava T, Thalji NM, Hagler M, Jurk D, Smith LA, Casaclang-Verzosa G, Zhu Y, Schafer MJ, Tchkonia T, Kirkland JL, Miller JD (2016) Chronic senolytic treatment alleviates established vasomotor dysfunction in aged or atherosclerotic mice. *Aging Cell* **15**, 973-977.
[355] Schafer MJ, White TA, Iijima K, Haak AJ, Ligresti G, Atkinson EJ, Oberg AL, Birch J, Salmonowicz H, Zhu Y, Mazula DL, Brooks RW, Fuhrmann-Stroissnigg H, Pirtskhalava T, Prakash YS, Tchkonia T, Robbins PD, Aubry MC, Passos JF, Kirkland JL, Tschumperlin DJ, Kita H, LeBrasseur NK (2017) Cellular senescence mediates fibrotic pulmonary disease. *Nat Commun* **8**, 14532.
[356] Zhu Y, Tchkonia T, Fuhrmann-Stroissnigg H, Dai HM, Ling YY, Stout MB, Pirtskhalava T, Giorgadze N, Johnson KO, Giles CB, Wren JD, Niedernhofer LJ, Robbins PD, Kirkland JL (2016) Identification of a novel senolytic agent, navitoclax, targeting the Bcl-2 family of anti-apoptotic factors. *Aging Cell* **15**, 428-435.
[357] Chang J, Wang Y, Shao L, Laberge R-M, Demaria M, Campisi J, Janakiraman K, Sharpless NE, Ding S, Feng W (2016) Clearance of senescent cells by ABT263 rejuvenates aged hematopoietic stem cells in mice. *Nat Med* **22**, 78-83.
[358] Childs BG, Baker DJ, Wijshake T, Conover CA, Campisi J, van Deursen JM (2016) Senescent intimal foam cells are deleterious at all stages of atherosclerosis. *Science* **354**, 472-477.
[359] Rödel TAL, Gärtner U, Holzer M (1996) Expression of the cyclin-dependent kinase inhibitor p16 in Alzheimer's disease. *Neuroreport* **7**, 3047-3050.
[360] Kranenburg O, van der Eb AJ, Zantema A (1996) Cyclin D1 is an essential mediator of apoptotic neuronal cell death. *EMBO J* **15**, 46-54.
[361] Harrison FE, Reiserer RS, Tomarken AJ, McDonald MP (2006) Spatial and nonspatial escape strategies in the Barnes maze. *Learn Mem* **13**, 809-819.
[362] Patil SS, Sunyer B, Hoger H, Lubec G (2009) Evaluation of spatial memory of C57BL/6J and CD1 mice in the Barnes maze, the Multiple T-maze and in the Morris water maze. *Behav Brain Res* **198**, 58-68.
[363] Fisahn A, Pike FG, Buhl EH, Paulsen O (1998) Cholinergic induction of network oscillations at 40 Hz in the hippocampus in vitro. *Nature* **394**, 186-189.
[364] Traub RD, Bibbig A, Fisahn A, LeBeau FEN, Whittington MA, Buhl EH (2000) A model of gamma-frequency network oscillations induced in the rat CA3 region by carbachol in vitro. *Eur J Neurosci* **12**, 4093-4106.
[365] Kaltschmidt C, Kaltschmidt B, Neumann H, Wekerle H, Baeuerle PA (1994) Constitutive NF-kappa B activity in neurons. *Mol Cell Biol* **14**, 3981-3992.
[366] Gupta SC, Sundaram C, Reuter S, Aggarwal BB (2010) Inhibiting NF-kappaB activation by small molecules as a therapeutic strategy. *Biochim Biophys Acta* **1799**, 775-787.
[367] Kaltschmidt B, Widera D, Kaltschmidt C (2005) Signaling via NF-kappaB in the nervous system. *Biochim Biophys Acta* **1745**, 287-299.

[368] Kaltschmidt C, Kaltschmidt B, Baeuerle PA (1993) Brain synapses contain inducible forms of the transcription factor NF-kappa B. *Mech Dev* **43**, 135-147.
[369] Wellmann H, Kaltschmidt B, Kaltschmidt C (2001) Retrograde transport of transcription factor NF-kappa B in living neurons. *J Biol Chem* **276**, 11821-11829.
[370] Bhakar AL, Tannis LL, Zeindler C, Russo MP, Jobin C, Park DS, MacPherson S, Barker PA (2002) Constitutive nuclear factor-kappa B activity is required for central neuron survival. *J Neurosci* **22**, 8466-8475.
[371] Bruce AJ, Boling W, Kindy MS, Peschon J, Kraemer PJ, Carpenter MK, Holtsberg FW, Mattson MP (1996) Altered neuronal and microglial responses to excitotoxic and ischemic brain injury in mice lacking TNF receptors. *Nat Med* **2**, 788-794.
[372] Sarnico I, Lanzillotta A, Boroni F, Benarese M, Alghisi M, Schwaninger M, Inta I, Battistin L, Spano P, Pizzi M (2009) NF-kappaB p50/RelA and c-Rel-containing dimers: opposite regulators of neuron vulnerability to ischaemia. *J Neurochem* **108**, 475-485.
[373] Lawrence T (2009) The Nuclear Factor NF-κB Pathway in Inflammation. *Cold Spring Harb Perspect Biol* **1**, a001651.
[374] Adler AS, Sinha S, Kawahara TL, Zhang JY, Segal E, Chang HY (2007) Motif module map reveals enforcement of aging by continual NF-kappaB activity. *Genes Dev* **21**, 3244-3257.
[375] Bonizzi G, Karin M (2004) The two NF-kappaB activation pathways and their role in innate and adaptive immunity. *Trends Immunol* **25**, 280-288.
[376] Elsharkawy AM, Oakley F, Lin F, Packham G, Mann DA, Mann J (2010) The NF-κB p50:p50:HDAC-1 repressor complex orchestrates transcriptional inhibition of multiple pro-inflammatory genes. *J Hepatol* **53**, 519-527.
[377] Kaltschmidt B, Linker RA, Deng J, Kaltschmidt C (2002) Cyclooxygenase-2 is a neuronal target gene of NF-κB. *BMC Mol Biol* **3**, 16-16.
[378] Vallabhapurapu S, Karin M (2009) Regulation and function of NF-kappaB transcription factors in the immune system. *Annu Rev Immunol* **27**, 693-733.
[379] Granic I, Dolga AM, Nijholt IM, van Dijk G, Eisel UL (2009) Inflammation and NF-kappaB in Alzheimer's disease and diabetes. *J Alzheimers Dis* **16**, 809-821.
[380] Lukiw WJ, Bazan NG (1998) Strong nuclear factor-kappaB-DNA binding parallels cyclooxygenase-2 gene transcription in aging and in sporadic Alzheimer's disease superior temporal lobe neocortex. *J Neurosci Res* **53**, 583-592.
[381] Niranjan R (2013) Molecular basis of etiological implications in Alzheimer's disease: focus on neuroinflammation. *Mol Neurobiol* **48**, 412-428.
[382] Ye SM, Johnson RW (2001) An age-related decline in interleukin-10 may contribute to the increased expression of interleukin-6 in brain of aged mice. *Neuroimmunomodulation* **9**, 183-192.
[383] Hunot S, Brugg B, Ricard D, Michel PP, Muriel M-P, Ruberg M, Faucheux BA, Agid Y, Hirsch EC (1997) Nuclear translocation of NF-κB is increased in dopaminergic neurons of patients with Parkinson disease. *Proc Natl Acad Sci U S A* **94**, 7531-7536.
[384] Kaltschmidt B, Kaltschmidt C (2009) NF-κB in the Nervous System. *Cold Spring Harb Perspect Biol* **1**, a001271.
[385] Khorooshi R, Babcock AA, Owens T (2008) NF-kappaB-driven STAT2 and CCL2 expression in astrocytes in response to brain injury. *J Immunol* **181**, 7284-7291.
[386] Block ML, Zecca L, Hong J-S (2007) Microglia-mediated neurotoxicity: uncovering the molecular mechanisms. *Nat Rev Neurosci* **8**, 57-69.
[387] Sha WC, Liou HC, Tuomanen EI, Baltimore D (1995) Targeted disruption of the p50 subunit of NF-kappa B leads to multifocal defects in immune responses. *Cell* **80**, 321-330.
[388] Bohuslav J, Kravchenko VV, Parry GC, Erlich JH, Gerondakis S, Mackman N, Ulevitch RJ (1998) Regulation of an essential innate immune response by the p50 subunit of NF-kappaB. *J Clin Invest* **102**, 1645-1652.

[389] Pereira SG, Oakley F (2008) Nuclear factor-κB1: Regulation and function. *The International Journal of Biochemistry & Cell Biology* **40**, 1425-1430.
[390] Oakley F, Mann J, Nailard S, Smart DE, Mungalsingh N, Constandinou C, Ali S, Wilson SJ, Millward-Sadler H, Iredale JP (2005) Nuclear factor-κB1 (p50) limits the inflammatory and fibrogenic responses to chronic injury. *Am J Pathol* **166**, 695-708.
[391] Schneider A, Martin-Villalba A, Weih F, Vogel J, Wirth T, Schwaninger M (1999) NF-kappaB is activated and promotes cell death in focal cerebral ischemia. *Nat Med* **5**, 554-559.
[392] Kassed CA, Willing AE, Garbuzova-Davis S, Sanberg PR, Pennypacker KR (2002) Lack of NF-κB p50 exacerbates degeneration of hippocampal neurons after chemical exposure and impairs learning. *Exp Neurol* **176**, 277-288.
[393] Yu Z, Zhou D, Bruce-Keller AJ, Kindy MS, Mattson MP (1999) Lack of the p50 subunit of nuclear factor-kappaB increases the vulnerability of hippocampal neurons to excitotoxic injury. *J Neurosci* **19**, 8856-8865.
[394] Haenold R, Weih F, Herrmann KH, Schmidt KF, Krempler K, Engelmann C, Nave KA, Reichenbach JR, Lowel S, Witte OW, Kretz A (2014) NF-kappaB controls axonal regeneration and degeneration through cell-specific balance of RelA and p50 in the adult CNS. *J Cell Sci* **127**, 3052-3065.
[395] Lu ZY, Yu SP, Wei JF, Wei L (2006) Age-related neural degeneration in nuclear-factor κB p50 knockout mice. *Neuroscience* **139**, 965-978.
[396] Kassed CA, Herkenham M (2004) NF-kappaB p50-deficient mice show reduced anxiety-like behaviors in tests of exploratory drive and anxiety. *Behav Brain Res* **154**, 577 - 584.
[397] Lehmann ML, Brachman RA, Listwak SJ, Herkenham M (2010) NF-κB activity affects learning in aversive tasks: possible actions via modulation of the stress axis. *Brain, Behav, Immun* **24**, 1008-1017.
[398] Oikawa K, Odero G, Platt E, Neuendorff M, Hatherell A, Bernstein M, Albensi B (2012) NF-kappaB p50 subunit knockout impairs late LTP and alters long term memory in the mouse hippocampus. *BMC Neurosci* **13**, 45.
[399] Denis-Donini S, Dellarole A, Crociara P, Francese MT, Bortolotto V, Quadrato G, Canonico PL, Orsetti M, Ghi P, Memo M (2008) Impaired adult neurogenesis associated with short-term memory defects in NF-kappaB p50-deficient mice. *J Neurosci* **28**, 3911 - 3919.
[400] Simen AA, Bordner KA, Martin MP, Moy LA, Barry LC (2011) Cognitive Dysfunction with Aging and the Role of Inflammation. *Ther Adv Chronic Dis* **2**, 175-195.
[401] Murray C, Sanderson DJ, Barkus C, Deacon RMJ, Rawlins JNP, Bannerman DM, Cunningham C (2012) Systemic inflammation induces acute working memory deficits in the primed brain: relevance for delirium. *Neurobiol Aging* **33**, 603-616.e603.
[402] Ito D, Imai Y, Ohsawa K, Nakajima K, Fukuuchi Y, Kohsaka S (1998) Microglia-specific localisation of a novel calcium binding protein, Iba1. *Mol Brain Res* **57**, 1-9.
[403] Nimmerjahn A, Kirchhoff F, Helmchen F (2005) Resting microglial cells are highly dynamic surveillants of brain parenchyma in vivo. *Science* **308**, 1314-1318.
[404] Davalos D, Grutzendler J, Yang G, Kim JV, Zuo Y, Jung S, Littman DR, Dustin ML, Gan WB (2005) ATP mediates rapid microglial response to local brain injury in vivo. *Nat Neurosci* **8**, 752-758.
[405] Morris GP, Clark IA, Zinn R, Vissel B (2013) Microglia: a new frontier for synaptic plasticity, learning and memory, and neurodegenerative disease research. *Neurobiol Learn Mem* **105**, 40-53.
[406] Ojo JO, Rezaie P, Gabbott PL, Stewart MG (2015) Impact of age-related neuroglial cell responses on hippocampal deterioration. *Front Aging Neurosci* **7**, 57.
[407] Gomez-Nicola D, Fransen NL, Suzzi S, Perry VH (2013) Regulation of microglial proliferation during chronic neurodegeneration. *J Neurosci* **33**, 2481-2493.

[408] Jinno S, Fleischer F, Eckel S, Schmidt V, Kosaka T (2007) Spatial arrangement of microglia in the mouse hippocampus: a stereological study in comparison with astrocytes. *Glia* **55**, 1334-1347.
[409] Kesner RP, Lee I, Gilbert P (2004) A behavioral assessment of hippocampal function based on a subregional analysis. *Rev Neurosci* **15**, 333-351.
[410] Kozlowski C, Weimer RM (2012) An automated method to quantify microglia morphology and application to monitor activation state longitudinally in vivo. *PLoS One* **7**, e31814.
[411] Clelland CD, Choi M, Romberg C, Clemenson GD, Fragniere A, Tyers P, Jessberger S, Saksida LM, Barker RA, Gage FH (2009) A functional role for adult hippocampal neurogenesis in spatial pattern separation. *Science* **325**, 210-213.
[412] Villeda SA, Luo J, Mosher KI, Zou B, Britschgi M, Bieri G, Stan TM, Fainberg N, Ding Z, Eggel A, Lucin KM, Czirr E, Park J-S, Couillard-Després S, Aigner L, Li G, Peskind ER, Kaye JA, Quinn JF, Galasko DR, Xie XS, Rando TA, Wyss-Coray T (2011) The aging systemic milieu negatively regulates neurogenesis and cognitive function. *Nature* **477**, 90-94.
[413] Couillard-Despres S, Winner B, Schaubeck S, Aigner R, Vroemen M, Weidner N, Bogdahn U, Winkler J, Kuhn HG, Aigner L (2005) Doublecortin expression levels in adult brain reflect neurogenesis. *Eur J Neurosci* **21**, 1-14.
[414] Brown JP, Couillard-Després S, Cooper-Kuhn CM, Winkler J, Aigner L, Kuhn HG (2003) Transient expression of doublecortin during adult neurogenesis. *J Comp Neurol* **467**, 1-10.
[415] Ek M, Engblom D, Saha S, Blomqvist A, Jakobsson P-J, Ericsson-Dahlstrand A (2001) Inflammatory response: Pathway across the blood-brain barrier. *Nature* **410**, 430-431.
[416] Banks WA (2008) Blood–Brain Barrier Transport of Cytokines In *NeuroImmune Biology* Elsevier, pp. 93-107.
[417] Lee SW, Haditsch U, Cord BJ, Guzman R, Kim SJ, Boettcher C, Priller J, Ormerod BK, Palmer TD (2013) Absence of CCL2 is sufficient to restore hippocampal neurogenesis following cranial irradiation. *Brain, Behav, Immun* **30**, 33-44.
[418] Henry CJ, Huang Y, Wynne AM, Godbout JP (2009) Peripheral Lipopolysaccharide (LPS) challenge promotes microglial hyperactivity in aged mice that is associated with exaggerated induction of both pro-inflammatory IL-1β and anti-inflammatory IL-10 cytokines. *Brain, Behav, Immun* **23**, 309-317.
[419] Rolova T, Puli L, Magga J, Dhungana H, Kanninen K, Wojciehowski S, Salminen A, Tanila H, Koistinaho J, Malm T (2014) Complex regulation of acute and chronic neuroinflammatory responses in mouse models deficient for nuclear factor kappa B p50 subunit. *Neurobiol Dis* **64**, 16-29.
[420] Taetzsch T, Levesque S, McGraw C, Brookins S, Luqa R, Bonini MG, Mason RP, Oh U, Block ML (2015) Redox Regulation of NF-κB p50 and M1 Polarization in Microglia. *Glia* **63**, 423-440.
[421] Rolova T, Dhungana H, Korhonen P, Valonen P, Kolosowska N, Konttinen H, Kanninen K, Tanila H, Malm T, Koistinaho J (2016) Deletion of Nuclear Factor kappa B p50 Subunit Decreases Inflammatory Response and Mildly Protects Neurons from Transient Forebrain Ischemia-induced Damage. *Aging Dis* **7**, 450-465.
[422] Takeuchi A, Miyaishi O, Kiuchi K, Isobe K (2001) Macrophage colony-stimulating factor is expressed in neuron and microglia after focal brain injury. *J Neurosci Res* **65**, 38-44.
[423] Yang G, Meng Y, Li W, Yong Y, Fan Z, Ding H, Wei Y, Luo J, Ke ZJ (2011) Neuronal MCP-1 mediates microglia recruitment and neurodegeneration induced by the mild impairment of oxidative metabolism. *Brain Pathol* **21**, 279-297.
[424] Raj DDA, Jaarsma D, Holtman IR, Olah M, Ferreira FM, Schaafsma W, Brouwer N, Meijer MM, de Waard MC, van der Pluijm I, Brandt R, Kreft KL, Laman JD, de Haan G, Biber KPH, Hoeijmakers JHJ, Eggen BJL, Boddeke HWGM (2014) Priming of microglia in a DNA-repair deficient model of accelerated aging. *Neurobiol Aging* **35**, 2147-2160.
[425] Parepally JM, Mandula H, Smith QR (2006) Brain uptake of nonsteroidal anti-inflammatory drugs: ibuprofen, flurbiprofen, and indomethacin. *Pharm Res* **23**, 873-881.

[426] Bauer MKA, Lieb K, Schulze-Osthoff K, Berger M, Gebicke-Haerter PJ, Bauer J, Fiebich BL (1997) Expression and regulation of cyclooxygenase-2 in rat microglia. *The FEBS Journal* **243**, 726-731.
[427] Elsisi NS, Darling-Reed S, Lee EY, Oriaku ET, Soliman KF (2005) Ibuprofen and apigenin induce apoptosis and cell cycle arrest in activated microglia. *Neurosci Lett* **375**, 91-96.
[428] Sekiyama K, Fujita M, Sekigawa A, Takamatsu Y, Waragai M, Takenouchi T, Sugama S, Hashimoto M (2012) Ibuprofen ameliorates protein aggregation and astrocytic gliosis, but not cognitive dysfunction, in a transgenic mouse expressing dementia with Lewy bodies-linked P123H beta-synuclein. *Neurosci Lett* **515**, 97-101.
[429] Teather LA, Packard MG, Bazan NG (2002) Post-training cyclooxygenase-2 (COX-2) inhibition impairs memory consolidation. *Learn Mem* **9**, 41-47.
[430] Lee YJ, Chuang YC (2010) Ibuprofen augments pro-inflammatory cytokine release in a mouse model of Vibrio vulnificus infection. *Microbiol Immunol* **54**, 542-550.
[431] Gebara E, Sultan S, Kocher-Braissant J, Toni N (2013) Adult hippocampal neurogenesis inversely correlates with microglia in conditions of voluntary running and aging. *Front Neurosci* **7**, 145.
[432] Imielski Y, Schwamborn JC, Lüningschrör P, Heimann P, Holzberg M, Werner H, Leske O, Püschel AW, Memet S, Heumann R, Israel A, Kaltschmidt C, Kaltschmidt B (2012) Regrowing the Adult Brain: NF-κB Controls Functional Circuit Formation and Tissue Homeostasis in the Dentate Gyrus. *PLoS One* **7**, e30838.
[433] Clark RE, Martin SJ (2005) Interrogating rodents regarding their object and spatial memory. *Curr Opin Neurobiol* **15**, 593-598.
[434] Fox GB, Fan L, LeVasseur RA, Faden AI (1998) Effect of traumatic brain injury on mouse spatial and nonspatial learning in the Barnes circular maze. *J Neurotrauma* **15**, 1037-1046.
[435] Seeger T, Fedorova I, Zheng F, Miyakawa T, Koustova E, Gomeza J, Basile AS, Alzheimer C, Wess J (2004) M2 muscarinic acetylcholine receptor knock-out mice show deficits in behavioral flexibility, working memory, and hippocampal plasticity. *J Neurosci* **24**, 10117-10127.
[436] Sunyer B, Patil S, Höger H, Lubec G (2007) Barnes maze, a useful task to assess spatial reference memory in the mice.
[437] Paylor R, Zhao Y, Libbey M, Westphal H, Crawley JN (2001) Learning impairments and motor dysfunctions in adult Lhx5-deficient mice displaying hippocampal disorganization. *Physiol Behav* **73**, 781-792.
[438] Pompl PN, Mullan MJ, Bjugstad K, Arendash GW (1999) Adaptation of the circular platform spatial memory task for mice: use in detecting cognitive impairment in the APP(SW) transgenic mouse model for Alzheimer's disease. *J Neurosci Methods* **87**, 87-95.
[439] Miyakawa T, Yared E, Pak JH, Huang FL, Huang KP, Crawley JN (2001) Neurogranin null mutant mice display performance deficits on spatial learning tasks with anxiety related components. *Hippocampus* **11**, 763-775.
[440] Albensi BC, Mattson MP (2000) Evidence for the involvement of TNF and NF-kappaB in hippocampal synaptic plasticity. *Synapse* **35**, 151 - 159.
[441] Schmeisser MJ, Baumann B, Johannsen S, Vindedal GF, Jensen V, Hvalby OC, Sprengel R, Seither J, Maqbool A, Magnutzki A, Lattke M, Oswald F, Boeckers TM, Wirth T (2012) IkappaB kinase/nuclear factor kappaB-dependent insulin-like growth factor 2 (Igf2) expression regulates synapse formation and spine maturation via Igf2 receptor signaling. *J Neurosci* **32**, 5688-5703.
[442] Boersma MC, Dresselhaus EC, De Biase LM, Mihalas AB, Bergles DE, Meffert MK (2011) A requirement for nuclear factor-kappaB in developmental and plasticity-associated synaptogenesis. *J Neurosci* **31**, 5414-5425.

[443] Groves JO, Leslie I, Huang G-J, McHugh SB, Taylor A, Mott R, Munafò M, Bannerman DM, Flint J (2013) Ablating adult neurogenesis in the rat has no effect on spatial processing: evidence from a novel pharmacogenetic model. *PLoS Genet* **9**, e1003718.
[444] Valero J, Mastrella G, Neiva I, Sanchez S, Malva JO (2014) Long-term effects of an acute and systemic administration of LPS on adult neurogenesis and spatial memory. *Front Neurosci* **8**, 83.
[445] Balschun D, Wetzel W, Del Rey A, Pitossi F, Schneider H, Zuschratter W, Besedovsky HO (2004) Interleukin-6: a cytokine to forget. *FASEB J* **18**, 1788-1790.
[446] Sparkman NL, Buchanan JB, Heyen JR, Chen J, Beverly JL, Johnson RW (2006) Interleukin-6 facilitates lipopolysaccharide-induced disruption in working memory and expression of other proinflammatory cytokines in hippocampal neuronal cell layers. *J Neurosci* **26**, 10709-10716.
[447] Gao HM, Jiang J, Wilson B, Zhang W, Hong JS, Liu B (2002) Microglial activation-mediated delayed and progressive degeneration of rat nigral dopaminergic neurons: relevance to Parkinson's disease. *J Neurochem* **81**, 1285-1297.
[448] Breder CD, Dewitt D, Kraig RP (1995) Characterization of inducible cyclooxygenase in rat brain. *J Comp Neurol* **355**, 296-315.
[449] Pardue S, Rapoport SI, Bosetti F (2003) Co-localization of cytosolic phospholipase A2 and cyclooxygenase-2 in Rhesus monkey cerebellum. *Brain Res Mol Brain Res* **116**, 106-114.
[450] Shaw KN, Commins S, O'Mara SM (2003) Deficits in spatial learning and synaptic plasticity induced by the rapid and competitive broad-spectrum cyclooxygenase inhibitor ibuprofen are reversed by increasing endogenous brain-derived neurotrophic factor. *Eur J Neurosci* **17**, 2438-2446.
[451] Sharifzadeh M, Naghdi N, Khosrovani S, Ostad SN, Sharifzadeh K, Roghani A (2005) Post-training intrahippocampal infusion of the COX-2 inhibitor celecoxib impaired spatial memory retention in rats. *Eur J Pharmacol* **511**, 159-166.
[452] Gray CM (1994) Synchronous oscillations in neuronal systems: mechanisms and functions. *J Comput Neurosci* **1**, 11-38.
[453] Singer W (1999) Neuronal synchrony: a versatile code for the definition of relations? *Neuron* **24**, 49-65.
[454] Axmacher N, Mormann F, Fernández G, Elger CE, Fell J (2006) Memory formation by neuronal synchronization. *Brain Res Rev* **52**, 170-182.
[455] Buzsaki G, Draguhn A (2004) Neuronal oscillations in cortical networks. *Science* **304**, 1926-1929.
[456] Colgin LL, Denninger T, Fyhn M, Hafting T, Bonnevie T, Jensen O, Moser M-B, Moser EI (2009) Frequency of gamma oscillations routes flow of information in the hippocampus. *Nature* **462**, 353-357.
[457] Lisman JE, Jensen O (2013) The theta-gamma neural code. *Neuron* **77**, 1002-1016.
[458] Leung L-WS, Da Silva FHL, Wadman WJ (1982) Spectral characteristics of the hippocampal EEG in the freely moving rat. *Electroencephalogr Clin Neurophysiol* **54**, 203-219.
[459] van Vugt MK, Schulze-Bonhage A, Litt B, Brandt A, Kahana MJ (2010) Hippocampal gamma oscillations increase with memory load. *J Neurosci* **30**, 2694-2699.
[460] Csicsvari J, Jamieson B, Wise KD, Buzsáki G (2003) Mechanisms of gamma oscillations in the hippocampus of the behaving rat. *Neuron* **37**, 311-322.
[461] Schmitz D, Schuchmann S, Fisahn A, Draguhn A, Buhl EH, Petrasch-Parwez E, Dermietzel R, Heinemann U, Traub RD (2001) Axo-axonal coupling. a novel mechanism for ultrafast neuronal communication. *Neuron* **31**, 831-840.
[462] Hájos N, Paulsen O (2009) Network mechanisms of gamma oscillations in the CA3 region of the hippocampus. *Neural Networks* **22**, 1113-1119.
[463] Traub RD, Whittington MA, Colling SB, Buzsaki G, Jefferys JG (1996) Analysis of gamma rhythms in the rat hippocampus in vitro and in vivo. *J Physiol* **493 (Pt 2)**, 471-484.

[464] Zemankovics R, Veres JM, Oren I, Hajos N (2013) Feedforward inhibition underlies the propagation of cholinergically induced gamma oscillations from hippocampal CA3 to CA1. *J Neurosci* **33**, 12337-12351.
[465] Driver JE, Racca C, Cunningham MO, Towers SK, Davies CH, Whittington MA, LeBeau FE (2007) Impairment of hippocampal gamma-frequency oscillations in vitro in mice overexpressing human amyloid precursor protein (APP). *Eur J Neurosci* **26**, 1280-1288.
[466] Vreugdenhil M, Toescu EC (2005) Age-dependent reduction of γ oscillations in the mouse hippocampus in vitro. *Neuroscience* **132**, 1151-1157.
[467] Herrmann CS, Demiralp T (2005) Human EEG gamma oscillations in neuropsychiatric disorders. *Clin Neurophysiol* **116**, 2719-2733.
[468] Uhlhaas PJ, Singer W (2006) Neural synchrony in brain disorders: relevance for cognitive dysfunctions and pathophysiology. *Neuron* **52**, 155-168.
[469] Rolls ET (1996) A theory of hippocampal function in memory. *Hippocampus* **6**, 601-620.
[470] Steffenach HA, Sloviter RS, Moser EI, Moser MB (2002) Impaired retention of spatial memory after transection of longitudinally oriented axons of hippocampal CA3 pyramidal cells. *Proc Natl Acad Sci U S A* **99**, 3194-3198.
[471] Johnson A, Redish AD (2007) Neural ensembles in CA3 transiently encode paths forward of the animal at a decision point. *J Neurosci* **27**, 12176-12189.
[472] Yamamoto J, Suh J, Takeuchi D, Tonegawa S (2014) Successful execution of working memory linked to synchronized high-frequency gamma oscillations. *Cell* **157**, 845-857.
[473] Bartos M, Vida I, Jonas P (2007) Synaptic mechanisms of synchronized gamma oscillations in inhibitory interneuron networks. *Nat Rev Neurosci* **8**, 45-56.
[474] Freund TF, Buzsaki G (1996) Interneurons of the hippocampus. *Hippocampus* **6**, 347-470.
[475] Chard PS, Bleakman D, Christakos S, Fullmer CS, Miller RJ (1993) Calcium buffering properties of calbindin D28k and parvalbumin in rat sensory neurones. *J Physiol* **472**, 341-357.
[476] Vela J, Gutierrez A, Vitorica J, Ruano D (2003) Rat hippocampal GABAergic molecular markers are differentially affected by ageing. *J Neurochem* **85**, 368-377.
[477] Honeycutt JA, Keary Iii KM, Kania VM, Chrobak JJ (2016) Developmental Age Differentially Mediates the Calcium-Binding Protein Parvalbumin in the Rat: Evidence for a Selective Decrease in Hippocampal Parvalbumin Cell Counts. *Dev Neurosci* **38**, 105-114.
[478] Brady DR, Mufson EJ (1997) Parvalbumin-immunoreactive neurons in the hippocampal formation of Alzheimer's diseased brain. *Neuroscience* **80**, 1113-1125.
[479] Lewis DA, Curley AA, Glausier JR, Volk DW (2012) Cortical parvalbumin interneurons and cognitive dysfunction in schizophrenia. *Trends Neurosci* **35**, 57-67.
[480] Filipovic D, Zlatkovic J, Gass P, Inta D (2013) The differential effects of acute vs. chronic stress and their combination on hippocampal parvalbumin and inducible heat shock protein 70 expression. *Neuroscience* **236**, 47-54.
[481] Collin T, Chat M, Lucas MG, Moreno H, Racay P, Schwaller B, Marty A, Llano I (2005) Developmental changes in parvalbumin regulate presynaptic Ca2+ signaling. *J Neurosci* **25**, 96-107.
[482] Padurariu M, Ciobica A, Mavroudis I, Fotiou D, Baloyannis S (2012) Hippocampal neuronal loss in the CA1 and CA3 areas of Alzheimer's disease patients. *Psychiatr Danub* **24**, 152-158.
[483] Kann O, Hollnagel J-O, Elzoheiry S, Schneider J (2016) Energy and Potassium Ion Homeostasis during Gamma Oscillations. *Front Mol Neurosci* **9**, 47.
[484] Dugan LL, Ali SS, Shekhtman G, Roberts AJ, Lucero J, Quick KL, Behrens MM (2009) IL-6 mediated degeneration of forebrain GABAergic interneurons and cognitive impairment in aged mice through activation of neuronal NADPH oxidase. *PLoS One* **4**, e5518.
[485] Steullet P, Cabungcal JH, Kulak A, Kraftsik R, Chen Y, Dalton TP, Cuenod M, Do KQ (2010) Redox dysregulation affects the ventral but not dorsal hippocampus: impairment of parvalbumin neurons, gamma oscillations, and related behaviors. *J Neurosci* **30**, 2547-2558.

[486] Chan F, Lax NZ, Davies CH, Turnbull DM, Cunningham MO (2016) Neuronal oscillations: A physiological correlate for targeting mitochondrial dysfunction in neurodegenerative diseases? *Neuropharmacol* **102**, 48-58.
[487] Qiu Z, Gruol DL (2003) Interleukin-6, beta-amyloid peptide and NMDA interactions in rat cortical neurons. *J Neuroimmunol* **139**, 51-57.
[488] Martin N, Bernard D (2017) Calcium signaling and cellular senescence. *Cell Calcium*.
[489] Pálmai-Pallag T, Bachrati CZ (2014) Inflammation-induced DNA damage and damage-induced inflammation: a vicious cycle. *Microb Infect* **16**, 822-832.
[490] Lonkar P, Dedon PC (2011) Reactive species and DNA damage in chronic inflammation: reconciling chemical mechanisms and biological fates. *Int J Cancer* **128**, 1999-2009.
[491] Davalos AR, Kawahara M, Malhotra GK, Schaum N, Huang J, Ved U, Beausejour CM, Coppe JP, Rodier F, Campisi J (2013) p53-dependent release of Alarmin HMGB1 is a central mediator of senescent phenotypes. *J Cell Biol* **201**, 613-629.
[492] von Zglinicki T, Nilsson E, Docke WD, Brunk UT (1995) Lipofuscin accumulation and ageing of fibroblasts. *Gerontology* **41 Suppl 2**, 95-108.
[493] Grosschedl R, Giese K, Pagel J (1994) HMG domain proteins: architectural elements in the assembly of nucleoprotein structures. *Trends Genet* **10**, 94-100.
[494] Klune JR, Dhupar R, Cardinal J, Billiar TR, Tsung A (2008) HMGB1: Endogenous Danger Signaling. *Mol Med* **14**, 476-484.
[495] Faraco G, Fossati S, Bianchi ME, Patrone M, Pedrazzi M, Sparatore B, Moroni F, Chiarugi A (2007) High mobility group box 1 protein is released by neural cells upon different stresses and worsens ischemic neurodegeneration in vitro and in vivo. *J Neurochem* **103**, 590-603.
[496] Gao H-M, Zhou H, Zhang F, Wilson BC, Kam W, Hong J-S (2011) HMGB1 acts on microglia Mac1 to mediate chronic neuroinflammation that drives progressive neurodegeneration. *The Journal of neuroscience : the official journal of the Society for Neuroscience* **31**, 1081-1092.
[497] Keller JN, Dimayuga E, Chen Q, Thorpe J, Gee J, Ding Q (2004) Autophagy, proteasomes, lipofuscin, and oxidative stress in the aging brain. *The international journal of biochemistry & cell biology* **36**, 2376-2391.
[498] Höhn A, Jung T, Grimm S, Grune T (2010) Lipofuscin-bound iron is a major intracellular source of oxidants: role in senescent cells. *Free Radic Biol Med* **48**, 1100-1108.
[499] Jolly RD, Douglas BV, Davey PM, Roiri JE (1995) Lipofuscin in bovine muscle and brain: a model for studying age pigment. *Gerontology* **41 Suppl 2**, 283-295.
[500] Jung T, Engels M, Kaiser B, Poppek D, Grune T (2006) Intracellular distribution of oxidized proteins and proteasome in HT22 cells during oxidative stress. *Free Radic Biol Med* **40**, 1303-1312.
[501] Yin D (1996) Biochemical basis of lipofuscin, ceroid, and age pigment-like fluorophores. *Free Radic Biol Med* **21**, 871-888.
[502] Rutten BPF, Schmitz C, Gerlach OHH, Oyen HM, de Mesquita EB, Steinbusch HWM, Korr H (2007) The aging brain: Accumulation of DNA damage or neuron loss? *Neurobiol Aging* **28**, 91-98.
[503] Birch J, Anderson RK, Correia-Melo C, Jurk D, Hewitt G, Marques FM, Green NJ, Moisey E, Birrell MA, Belvisi MG (2015) DNA damage response at telomeres contributes to lung aging and chronic obstructive pulmonary disease. *American Journal of Physiology-Lung Cellular and Molecular Physiology* **309**, L1124-L1137.
[504] Arnoult N, Karlseder J (2015) Complex interactions between the DNA-damage response and mammalian telomeres. *Nat Struct Mol Biol* **22**, 859-866.
[505] Qin L, Wu X, Block ML, Liu Y, Breese GR, Hong JS, Knapp DJ, Crews FT (2007) Systemic LPS causes chronic neuroinflammation and progressive neurodegeneration. *Glia* **55**, 453-462.

[506] Borgesius NZ, de Waard MC, van der Pluijm I, Omrani A, Zondag GC, van der Horst GT, Melton DW, Hoeijmakers JH, Jaarsma D, Elgersma Y (2011) Accelerated age-related cognitive decline and neurodegeneration, caused by deficient DNA repair. *J Neurosci* **31**, 12543-12553.
[507] Schneider L, Fumagalli M, d'Adda di Fagagna F (2012) Terminally differentiated astrocytes lack DNA damage response signaling and are radioresistant but retain DNA repair proficiency. *Cell Death Differ* **19**, 582-591.
[508] Mata-Garrido J, Casafont I, Tapia O, Berciano MT, Lafarga M (2016) Neuronal accumulation of unrepaired DNA in a novel specific chromatin domain: structural, molecular and transcriptional characterization. *Acta Neuropathol Commun* **4**, 41.
[509] Nelson G, Kucheryavenko O, Wordsworth J, von Zglinicki T (2017) The senescent bystander effect is caused by ROS-activated NF-κB signalling. *Mech Ageing Dev*.
[510] Frank MG, Weber MD, Fonken LK, Hershman SA, Watkins LR, Maier SF (2016) The redox state of the alarmin HMGB1 is a pivotal factor in neuroinflammatory and microglial priming: A role for the NLRP3 inflammasome. *Brain Behav Immun* **55**, 215-224.
[511] Kim JB, Sig Choi J, Yu YM, Nam K, Piao CS, Kim SW, Lee MH, Han PL, Park JS, Lee JK (2006) HMGB1, a novel cytokine-like mediator linking acute neuronal death and delayed neuroinflammation in the postischemic brain. *J Neurosci* **26**, 6413-6421.
[512] Fonken LK, Frank MG, Kitt MM, D'Angelo HM, Norden DM, Weber MD, Barrientos RM, Godbout JP, Watkins LR, Maier SF (2016) The Alarmin HMGB1 Mediates Age-Induced Neuroinflammatory Priming. *J Neurosci* **36**, 7946-7956.
[513] Scaffidi P, Misteli T, Bianchi ME (2002) Release of chromatin protein HMGB1 by necrotic cells triggers inflammation. *Nature* **418**, 191-195.
[514] Jortner BS (2006) The return of the dark neuron. A histological artifact complicating contemporary neurotoxicologic evaluation. *Neurotoxicology* **27**, 628-634.
[515] van Deursen JM (2014) The role of senescent cells in ageing. *Nature* **509**, 439-446.
[516] Ogrodnik M, Miwa S, Tchkonia T, Tiniakos D, Wilson CL, Lahat A, Day CP, Burt A, Palmer A, Anstee QM (2017) Cellular senescence drives age-dependent hepatic steatosis. *Nat Commun* **8**.
[517] Demaria M, Ohtani N, Youssef SA, Rodier F, Toussaint W, Mitchell JR, Laberge RM, Vijg J, Van Steeg H, Dolle ME, Hoeijmakers JH, de Bruin A, Hara E, Campisi J (2014) An essential role for senescent cells in optimal wound healing through secretion of PDGF-AA. *Dev Cell* **31**, 722-733.
[518] Krizhanovsky V, Yon M, Dickins RA, Hearn S, Simon J, Miething C, Yee H, Zender L, Lowe SW (2008) Senescence of activated stellate cells limits liver fibrosis. *Cell* **134**, 657-667.
[519] Collado M, Blasco MA, Serrano M (2007) Cellular senescence in cancer and aging. *Cell* **130**, 223-233.
[520] Pistell PJ, Spangler EL, Kelly-Bell B, Miller MG, de Cabo R, Ingram DK (2012) Age-Associated Learning and Memory Deficits in Two Mouse Versions of the Stone T-maze. *Neurobiol Aging* **33**, 2431-2439.
[521] Kametani H, Spangler EL, Bresnahan EL, Kobayashi S, Long JM, Ingram DK (1993) Impaired acquisition in a 14-unit T-maze following medial septal lesions in rats is correlated with lesion size and hippocampal acetylcholinesterase staining. *Physiol Behav* **53**, 221-228.
[522] Beauséjour CM, Krtolica A, Galimi F, Narita M, Lowe SW, Yaswen P, Campisi J (2003) Reversal of human cellular senescence: roles of the p53 and p16 pathways. *EMBO J* **22**, 4212-4222.
[523] Seluanov A, Gorbunova V, Falcovitz A, Sigal A, Milyavsky M, Zurer I, Shohat G, Goldfinger N, Rotter V (2001) Change of the death pathway in senescent human fibroblasts in response to DNA damage is caused by an inability to stabilize p53. *Mol Cell Biol* **21**, 1552-1564.
[524] Cohen SJ, Stackman RW, Jr. (2015) Assessing rodent hippocampal involvement in the novel object recognition task. A review. *Behav Brain Res* **285**, 105-117.
[525] Fahlström A, Zeberg H, Ulfhake B (2012) Changes in behaviors of male C57BL/6J mice across adult life span and effects of dietary restriction. *Age* **34**.

[526] Stein GH, Drullinger LF, Soulard A, Dulic V (1999) Differential roles for cyclin-dependent kinase inhibitors p21 and p16 in the mechanisms of senescence and differentiation in human fibroblasts. *Mol Cell Biol* **19**, 2109-2117.
[527] Wei Z, Chen X-C, Song Y, Pan X-D, Dai X-M, Zhang J, Cui X-L, Wu X-L, Zhu Y-G (2016) Amyloid β Protein Aggravates Neuronal Senescence and Cognitive Deficits in 5XFAD Mouse Model of Alzheimer's Disease. *Chin Med J* **129**, 1835.
[528] Gartner U, Holzer M, Heumann R, Arendt T (1995) Induction of p21ras in Alzheimer pathology. *Neuroreport* **6**, 1441-1444.
[529] Biber K, Neumann H, Inoue K, Boddeke HW (2007) Neuronal 'On' and 'Off' signals control microglia. *Trends Neurosci* **30**, 596-602.
[530] Lin W, Lin Y, Li J, Fenstermaker AG, Way SW, Clayton B, Jamison S, Harding HP, Ron D, Popko B (2013) Oligodendrocyte-specific activation of PERK signaling protects mice against experimental autoimmune encephalomyelitis. *J Neurosci* **33**, 5980-5991.
[531] Burnett SH, Beus BJ, Avdiushko R, Qualls J, Kaplan AM, Cohen DA (2006) Development of peritoneal adhesions in macrophage depleted mice. *J Surg Res* **131**, 296-301.
[532] Burnett SH, Kershen EJ, Zhang J, Zeng L, Straley SC, Kaplan AM, Cohen DA (2004) Conditional macrophage ablation in transgenic mice expressing a Fas-based suicide gene. *J Leukoc Biol* **75**, 612-623.
[533] Gabrusiewicz K, Hossain MB, Cortes-Santiago N, Fan X, Kaminska B, Marini FC, Fueyo J, Gomez-Manzano C (2015) Macrophage Ablation Reduces M2-Like Populations and Jeopardizes Tumor Growth in a MAFIA-Based Glioma Model()(). *Neoplasia (New York, N.Y.)* **17**, 374-384.
[534] Steel CD, Kim WK, Sanford LD, Wellman LL, Burnett S, Van Rooijen N, Ciavarra RP (2010) Distinct macrophage subpopulations regulate viral encephalitis but not viral clearance in the CNS. *J Neuroimmunol* **226**, 81-92.
[535] Wang NK, Lai CC, Liu CH, Yeh LK, Chou CL, Kong J, Nagasaki T, Tsang SH, Chien CL (2013) Origin of fundus hyperautofluorescent spots and their role in retinal degeneration in a mouse model of Goldmann-Favre syndrome. *Dis Model Mech* **6**, 1113-1122.
[536] Porkka K, Koskenvesa P, Lundan T, Rimpilainen J, Mustjoki S, Smykla R, Wild R, Luo R, Arnan M, Brethon B, Eccersley L, Hjorth-Hansen H, Hoglund M, Klamova H, Knutsen H, Parikh S, Raffoux E, Gruber F, Brito-Babapulle F, Dombret H, Duarte RF, Elonen E, Paquette R, Zwaan CM, Lee FY (2008) Dasatinib crosses the blood-brain barrier and is an efficient therapy for central nervous system Philadelphia chromosome-positive leukemia. *Blood* **112**, 1005-1012.
[537] Ishisaka A, Ichikawa S, Sakakibara H, Piskula MK, Nakamura T, Kato Y, Ito M, Miyamoto K, Tsuji A, Kawai Y, Terao J (2011) Accumulation of orally administered quercetin in brain tissue and its antioxidative effects in rats. *Free Radic Biol Med* **51**, 1329-1336.
[538] Elahy M, Jackaman C, Mamo JCL, Lam V, Dhaliwal SS, Giles C, Nelson D, Takechi R (2015) Blood–brain barrier dysfunction developed during normal aging is associated with inflammation and loss of tight junctions but not with leukocyte recruitment. *Immunity & Ageing : I & A* **12**, 2.
[539] Goodall EF, Wang C, Simpson JE (2017) Age-associated changes in the blood-brain barrier: comparative studies in human and mouse.
[540] Yamazaki Y, Baker DJ, Tachibana M, Liu CC, van Deursen JM, Brott TG, Bu G, Kanekiyo T (2016) Vascular Cell Senescence Contributes to Blood-Brain Barrier Breakdown. *Stroke* **47**, 1068-1077.
[541] Zhan Y, Krafft PR, Lekic T, Ma Q, Souvenir R, Zhang JH, Tang J (2015) Imatinib preserves blood-brain barrier integrity following experimental subarachnoid hemorrhage in rats. *J Neurosci Res* **93**, 94-103.
[542] Li Y, Zhou S, Li J, Sun Y, Hasimu H, Liu R, Zhang T (2015) Quercetin protects human brain microvascular endothelial cells from fibrillar β-amyloid1–40-induced toxicity. *Acta Pharmaceutica Sinica B* **5**, 47-54.

[543] Zou Y, Zhang N, Ellerby LM, Davalos AR, Zeng X, Campisi J, Desprez P-Y (2012) Responses of Human Embryonic Stem Cells and Their Differentiated Progeny to Ionizing Radiation. *Biochem Biophys Res Commun* **426**, 100-105.
[544] Bitto A, Sell C, Crowe E, Lorenzini A, Malaguti M, Hrelia S, Torres C (2010) Stress-induced senescence in human and rodent astrocytes. *Exp Cell Res* **316**, 2961-2968.
[545] Streit WJ, Sammons NW, Kuhns AJ, Sparks DL (2004) Dystrophic microglia in the aging human brain. *Glia* **45**, 208-212.
[546] Li MD, Burns TC, Kumar S, Morgan AA, Sloan SA, Palmer TD (2015) Aging-like changes in the transcriptome of irradiated microglia. *Glia* **63**, 754-767.
[547] Holtman IR, Raj DD, Miller JA, Schaafsma W, Yin Z, Brouwer N, Wes PD, Möller T, Orre M, Kamphuis W, Hol EM, Boddeke EWGM, Eggen BJL (2015) Induction of a common microglia gene expression signature by aging and neurodegenerative conditions: a co-expression meta-analysis. *Acta Neuropathologica Communications* **3**, 31.
[548] Villeda SA, Plambeck KE, Middeldorp J, Castellano JM, Mosher KI, Luo J, Smith LK, Bieri G, Lin K, Berdnik D, Wabl R, Udeochu J, Wheatley EG, Zou B, Simmons DA, Xie XS, Longo FM, Wyss-Coray T (2014) Young blood reverses age-related impairments in cognitive function and synaptic plasticity in mice. *Nat Med* **20**, 659-663.
[549] Castellano JM, Mosher KI, Abbey RJ, McBride AA, James ML, Berdnik D, Shen JC, Zou B, Xie XS, Tingle M, Hinkson IV, Angst MS, Wyss-Coray T (2017) Human umbilical cord plasma proteins revitalize hippocampal function in aged mice. *Nature* **544**, 488-492.
[550] Molofsky AV, Slutsky SG, Joseph NM, He S, Pardal R, Krishnamurthy J, Sharpless NE, Morrison SJ (2006) Increasing p16(INK4a) expression decreases forebrain progenitors and neurogenesis during ageing. *Nature* **443**, 448-452.